Charles University

Faculty of Science

Ph.D. study program: Cell and Developmental Biology

M.Sc. NGUYEN THI MINH XUAN

The study of *Xenopus tropicalis* testis-derived stem cells

Doctoral Dissertation

Supervisor:

Assoc.prof. RNDr. Ing. Vladimír Krylov, Ph.D.

Prague, 2019

Univerzite Karlova

Přírodovědecká fakulta

Doktorský studijní program: Buněčné a vývojové biologie

M.Sc. NGUYEN THI MINH XUAN

Studium kmenových buněk odvozených z varlat *Xenopus tropicalis*

Disertační práce

Školitel:

Assoc.prof. RNDr. Ing. Vladimír Krylov, Ph.D.

Praha, 2019

Declaration of Authorship

I, Nguyen Thi Minh Xuan, declare that this dissertation titled, “The study of *Xenopus tropicalis* testis-derived stem cells” and the work presented in it are my own. All the literature is properly cited, and I have not been yet awarded any other academic degree or diploma for this thesis or its substantial part.

Signed: 

Date: 08.03.2019

"Enjoy climbing the mountain"

"*Enjoy climbing the mountain*" because of no one at the destination after all,
they all went to sleep. Six years for Ph.D. is hard but leaving Prague is harder.
And to whom it may concern,
I have not mentioned your particular names on the paper
because you stay deeply in my heart.

Acknowledgments

My Ph.D. life for nearly 6 years in Czech Republic has been filled with full of fun, depression and hangovers. In some days I was a walking dead person and in others, microscope images induced me reprograming back to an enthusiastic girl-like person. I would not say doing Ph.D. here is my best thing but I can not imagine how I would live with this such colorful life elsewhere. My Ph.D. journey wouldn't have been accomplished without lovely companions. I would like to express my grateful acknowledgment to all of you.

Foremost, I would like to say "Thank you very much from bottom of my heart" to my supervisor Ass. Prof. Vladimir Krylov for giving me a chance to join our group. I have been impressed by his patience for students, immense knowledge, and his attitude for working. I have never expected he spent a whole weekend to revise this thesis and sometimes received his emails at midnight. Once again, thank him for his kind support, helpful advice, encouragement, and understanding not only with my study but also with my difficult personal life.

Besides my advisor, I would like to thank the rest of my thesis committee members for their insightful comments and the hard questions which encouraged me to widen my research from various perspectives.

My sincere thanks also go to Dr. Tereza Tlapakova, Marketa Vegrichtova, Dr. Magdalena Krulova, Dr. Lenka Doubravska, Jiri Vavra and other staff of Department of Cell Biology, Charles University for kindly helping and supporting me. Especially I would like to express my respectfulness to my beloved friend in Czech Republic, Andrea Mancikova. Life can go up and down, but that wonderful person always keeps me in a line of wonderful friendship.

I would like to acknowledge the STARS program and Charles University Grant Agency (GAUK) No. 2598461 for financial support of my Ph.D. study.

I would like to thank my parents and my younger sister who are physically and mentally taking care of my little treasure, my daughter. Their unconditional love gives me the courage to never surrender in front of challenges. In addition, many thanks to my friends for supporting me spiritually throughout writing this thesis and my life in general with cooking, traveling, shopping, drinking, dancing, laughing and fighting altogether. Last but not least, I would like to thank my husband, who immediately moved to Milano after his Ph.D. completion in Chemical Department. He has given me motivation towards obtaining a Dr. title, so I will not be only a M.S cleaner in my family. Finally, all loves to my gifts from God, my little daughter and two adorable twins, this thesis is my gift for them. Hopefully someday all of my efforts here can motivate my girls to achieve their accomplishment.

Prague, March 6th, 2019

Abstract

The substances secreted by Sertoli cells (SCs) are crucial to determine male sex characteristics in embryos and regulate spermatogenesis in adulthood. The failure in SC maturation can cause sterility in men. Before puberty, SCs keep the ability to proliferate and have been considered as immature cells. They differ remarkably from mature cells in connection with their morphology and biochemical activity and thus they probably play a part in maintaining spermatogonia stem cells in an undifferentiated stage. The transient presence of cytokeratin in immature SCs has been reported in many species, but not in *Xenopus* yet. We investigated which molecules are expressing only in immature Sertoli cells of *X. tropicalis* testes. The regulation of cytokeratin and β-catenin was revealed by fluorescent immunostaining. Cytokeratin and membrane β-catenin co-expressed in *X.tropicalis* juvenile testes and in cultured SC progenitors, called XtiSCs, but they were absent in adulthood. There was no signal of cytokeratin in migrating SCs (pre-SCs) located outside the seminiferous tubules. The suppression of cytokeratin along with the breakdown of β-catenin-based cell contacts have been observed in XtiSCs after the treatment with a small molecule drug, CHIR99021 and led to their dedifferentiation back to stem cell-like state. These findings confirm the expression of cytokeratin and a novel molecule, β-catenin along with Sox9 in SCs as markers indicating their immature state.

However, the function of CK in SC development is poorly understood. We examined interconnection between CK and β-catenin-based cell junctions in immature SCs. Reversible dissociation of CK by acrylamide in XtiSCs induced breakdown of membrane-bound β-catenin but had no effect on F-actin and β-tubulin or cell adhesion proteins (focal adhesion kinase and integrin β1). On the contrary, disruption of membrane β-catenin via uncoupling of cadherins with Ca2+ by chelator EGTA didn't show any influence on the cytokeratin stability. The results suggest a new role of CK in the retention of β-catenin-based junctions in immature Sertoli cells, and thus serving as structural support for arrested germ cells and for the formation of proper seminiferous tubules.

Epithelial-mesenchymal transition (EMT) and mesenchymal-epithelial transition (MET) are fundamental processes in embryonic development. In general, EMT is characterized by the conversion of sessile epithelial cells into mesenchymal cells with the migratory potential, whereas MET activates a reverse process. A mesenchymal phenotype of pre-Sertoli cells has been observed suggesting that pre-SCs must undergo a MET to differentiate into mature cells. Our laboratory has been successful in the establishment of *Xenopus tropicalis* somatic cell line from testes of juvenile frogs, called XtTSCs. The isolated cells possessed characteristics of Sertoli cells with expression of immature markers including Sox9, vimentin, cytokeratin and β-catenin, so latter called XtiSCs. The main aim of my Ph.D. project was the determination of factors responsible for the induction of EMT, a reverse differentiation process of SCs, and identification of a stemness window where cells possess the greatest differentiation potential in XtiSCs. GSK-3 inhibitor (CHIR99021), FGF2 and/or TGF-β1 ligands were employed in XtiSCs culture to induce EMT. Our results showed that XtiSCs underwent full EMT after 3-day treatment with GSK-3 inhibitor and partial EMT with FGF2, but not with TGF-beta 1. The morphology change of CHIR-treated XtiSCs to the typical spindle-like cell shape was associated with the upregulation of mesenchymal proteins (fibronectin, integrin α5β1, Snai1 and Zeb1) and low expression of the epithelial marker, cytokeratin. Moreover, this inhibitor also promoted stem cells markers (Sox2, *cd44*) and the efficient derivation of stem cells from *Xenopus* testes. CHIR-treated, but not FGF2-treated or vehicle XtiSCs can differentiate into chondrocytes *in vitro* and cardiomyocytes *in vivo* after their microinjection into the peritoneal cavity of *X. tropicalis* tadpoles. Interestingly, the EMT-shifted cells could migrate toward cervical cancer cells *in vitro* (HeLa cells) and to the injury site *in vivo*. In general, our results provide a better understanding of signaling pathways underlying the generation of testis-derived stem cells. Moreover, XtiSCs could represent a novel model for the study of the EMT process and SC maturation.

Abstrakt

Sertoliho buňky (SCs) produkují celou řadu molekul klíčových pro determinaci samčího pohlaví a pro regulaci spermatogeneze v dospělosti. Poruchy diferenciace Sertoliho buněk vedou u člověka ke sterilitě. Před nástupem puberty hrají důležitou roli v udržení spermatogoniálních buněk v kmenovém stavu a zajišťují tak jejich dostatečný počet. Zajímavým znakem odlišujícím nezralé a zralé Sertoliho buňky je dočasná přítomnost cytokeratinu, který byl u těchto buněk popsán u celé řady modelových organismů. V rámci této disertační práce jsme se zabývali rozdílnou genovou expresí proteinů spojených s regulací cytokeratinu u nezralých a zralých Sertoliho buněk odvozených z varlat Drápatky tropické (*Xenopus tropicalis*). Imunohistochemické řezy varlat z juvenilních jedinců a imunocytochemická analýza buněčné kultury odvozené ze stejného zdroje, obsahující nezralé progenitory Sertoliho a peritubulárních myoidních buněk (XtiSC) ukázaly na společnou expresi cytokeratinu a membránového β-kateninu. V případě vzorku z dospělých jedinců nebyla detekována přítomnost ani jednoho z nich. Dále pak podobný fenotyp vykazovaly i migrující Sertoliho buňky (pre-SCs), které se nacházely mimo semenotvorné kanálky. I zde byla exprese obou proteinů potlačena. Přidání inhibitoru glykogen syntázy kinázy 3, CHIR99021, k buněčné kultuře XtiSC vedlo k dediferenciaci přítomných buněk do kmenového stavu a k rozšíření jejich diferenciačního potenciálu.

Role cytokeratinu a dalších proteinů zahrnujících β-katenin a Sox9, marker Sertoliho buněk, na diferenciaci Sertoliho buněk nebyla dosud prozkoumána. V rámci předložené disertační práce jsme se zabývali vztahem mezi cytokeratinem a membránovým β-kateninem včetně příslušných mezibuněčných spojů (cell junctions) u nezralých Sertoliho buněk. Reverzibilní destrukce cytokeratinové sítě pomocí akrylamidu vedla u XtiSC buněk ke ztrátě membránového β-kateninu. F-aktin, β-tubulin nebo proteiny buněčné adheze (kináza fokálních adhezí - FAK a integrin β1) nebyly akrylamidem ovlivněny. Na druhou stranu narušení membránového β-kateninu pomocí Ca^{2+} chelatačního činidla EGTA nezpůsobilo vážnější dezintegraci cytokeratinové sítě. Výsledky ukazují na novou roli cytokeratinu pro stabilizaci

mezibuněčných spojů závislých na β-kateninu v nezralých Sertoliho buňkách. Tato stabilizace je klíčová pro udržení spermatogonií ve stavu dělících se buněk bez meiotického zrání v rámci pre-pubertálních varlat a dále pak pro správné formování semenotvorných kanálků.

Epitelo-mezenchymální tranzice (EMT) a mezenchymo-epiteliální tranzice (MET) patří mezi základní buněčné procesy v zárodečném vývoji. EMT je charakterizovaná jako přeměna adhezivních buněk epiteliálního typu na mezenchymální typ schopný migrace. MET pak představuje obrácený proces. Nezralé Sertoliho buňky (XtiSC) vykazují mezenchymální fenotyp. Za fyziologických *in vivo* podmínek musí tyto buňky podstoupit MET a diferencovat se ve zralé Sertoliho buňky. V laboratoři školitele se podařilo založit dlouhodobou buněčnou kulturu odvozenou z varlat juvenilních jedinců *X. tropicalis*. Expresní profil buněk obsahoval markery nezralých Sertoliho buněk jako Sox9, vimentin, cytokeratin a β-katenin. V první publikaci, která je součástí disertační práce byly tyto buňky zkracovány jako XtTSC (Xenopus tropicalis Testicular Somatic Cells). V dalších dvou rukopisech jsou popisovány jako nezralé Sertoliho buňky, XtiSC (Xenopus tropicalis immature Sertoli Cells). Cílem předložené disertační práce byla identifikace faktorů odpovědných za indukci epitelo-mezenchymální tranzice u XtiSC a nalezení tzv. "kmenového okna" (stemness window), ve kterém buňky vykazují nejširší diferenciační potenciál. K tomuto účelu jsme zvolili GSK-3 inhibitor (CHIR99021) a dále pak FGF2 a/nebo TGF-β1 ligandy. Třídenní ošetření XtiSC buněčné kultury GSK-3 inhibitorem vedlo ke kompletní EMT. FGF2 vedl pouze k částečné tranzici do mezenchymálního fenotypu. Na druhou stranu TGF-β1 měl vliv na senescenci nikoliv na EMT. Působení CHIR99021 bylo patrné jak na úrovni změny buněčné morfologie (vřetenovitý tvar buněk), ale také na zvýšené expresi mezenchymálních proteinů jako je fibronektin, integrin α5β1, Snai1 a Zeb1 a na snížené expresi epiteliálního markeru, cytokeratinu. Navíc ošetření buněk GSK-3 inhibitorem vedlo ke zvýšení markerů typických pro kmenové buňky, jako např. Sox2 a *cd44*. To mělo za následek schopnost XtiSC diferencovat do chondrocytů *in vitro* a kardiomyocytů *in vivo* po jejich mikroinjekci do peritoneálního prostoru pulců *X. tropicalis.* XtiSC buňky po EMT tranzici migrovaly k nádorovým buňkám cervikálního karcinomu a do místa po

indukovaném poranění. Výsledky této disertační práce umožní lepší pochopení mezibuněčné signalizace, která stojí za přípravou kmenových buněk odvozených z varlat. Navíc XtiSC buňky představují nový model pro studium epitelo-mezenchymální tranzice v rámci zrání Sertoliho buněk a spermatogeneze.

Contents

List of figures

List of tables

Abbreviations

01.	AMH	anti-Mullerian hormone
02.	BTB	Blood-testis barrier
03.	CK	Cytokeratin
04.	ECM	Extracellular matrix
05.	EMT	Epithelial-mesenchymal transition
06.	FBS	Fetal bovine serum
07.	FSH	Follicle-stimulating hormone
08.	GnRH	Gonadotropin-releasing hormone
09.	H&E staining	Haematoxylin-Eosin staining
10.	hCG	Human chorionic gonadotropin
11.	HGF	Hepatocyte growth factor
12.	IF	Intermediate filament
13.	LH	Luteinizing hormone
14.	MET	Mesenchymal-epithelial transition
15.	MDIF	Mullerian duct inhibitory factor
16.	MMP	Matrix metalloproteinases
17.	MSCs	Mesenchymal stem cells
18.	PBS	Phosphate buffer saline
19.	PBSTr	PBS+0.1% Triton-X 100
20.	PGCs	Primordial germ cells
21.	PMCs	Peritubular myoid cells
22.	qRT-PCR	quantitative Reverse transcription-polymerase chain reaction
23.	RFP	Red fluorescent protein
24.	RT-PCR	Reverse transcription-polymerase chain reaction
25.	SCs	Sertoli cells
26.	Sma/Acta2	Smooth muscle actin
27.	Snai1/SNAI1	Snail family zinc finger 1
28.	Sox9	(Sex-determining region Y)-box 9
29.	SRY	Sex-determining region Y
30.	SSCs	Spermatogonial stem cells
31.	TNF	Tumor necrosis factor
32.	TSCs	Testis-derived stem cells
33.	Twist	Twist-family bHLH transcription factor 1
34.	XtiSCs	*Xenopus tropicalis* immature Sertoli cells
35.	XtTSCs	*Xenopus tropicalis* testicular somatic cells
36.	Zeb1	Zinc finger E-box-binding homeobox 1

Chapter 1

INTRODUCTION

A series of conversion between epithelial and mesenchymal phenotype of embryonic cells through the epithelial-mesenchymal transition (EMT), and its reverse process mesenchymal-epithelial transition (MET) contribute to the morphogenesis of many tissues. During the gastrulation, cells break the basal membrane to migrate from primitive streak, resulting in mesoderm formation under the control of EMT signaling. This key process ensures both 1) a high migratory capacity and 2) the stemness maintenance of embryonic cells (Nakaya et al. 2008). The primary EMT is followed by the condensation of mesodermal cells into transient epithelial structures through a MET process, such as the notochord, somites and precursors of the urogenital system (Nakaya et al. 2004). These epithelial cells continue to undergo secondary or even more EMT and MET rounds to generate different cell types. Notably, EMT is triggered by the same signaling pathway in both physiological and pathological processes. The key transcription factor, Snail is evolutionarily conserved inducers of EMT (Seidel and Look 2001).

Recently, mesenchymal stem cell (MSC)-like cells have been generated by activating EMT in cultured epithelial cells. Indeed, non-tumorigenic immortalized mouse or human mammary epithelial cells were transduced with vectors expressing SNAI1 or TWIST, both of which are capable of inducing EMT in epithelial cells (Mani et al. 2008). Subsequently, the transformed cells acquired the mesenchymal traits and the expression of stem cell marker (CD44). In the agreement, Battula et. al. induced EMT by ectopic expression of TWIST, SNAI1, or incubation with TGF-β in the same cell line. The induced cells exhibited the characteristics of MSCs, including specific antigenic profile, the capacity to differentiate into mesodermal cell types and direct migration ability towards cancer cells and wounds (Battula et al. 2010).

Sertoli cells (SCs) play a central role in testis morphogenesis during embryonic development and spermatogenesis in adulthood. They are epithelial supporting cells which extend from basal membrane to lumen. They nurture germ cells, regulate

spermatogenesis and maintain spermatogonial stem cells (SSCs) in adult testes (Handelsman, Spaliviero, and Phippard 1990; de Winter 1993). Moreover, the blood-testis barrier and immunosuppressive molecules produced by SCs protect sperm cells from attacks of the immune system and pathological factors (Setchell 2009; Mital, Kaur, and Dufour 2010). SCs have been considered to be terminally differentiated once spermatogenesis has begun, and not capable to proliferate at this stage (R. M. Sharpe et al. 2003). However, recently, the generation of juvenile proliferative SCs outside the body by using activin A has been reported bringing new hope for male infertility (Nicholls et al. 2012).

The connection of EMT and MET to testis morphogenesis has also been reported elsewhere. The proper formation of testicular seminiferous tubules requires migration of pre-Sertoli cells (SCs) along with PGCs (primordial germ cells) into the testis cords. Mesenchymal morphology of pre-SCs has been revealed by using transgenic mice with EGFP (enhanced green fluorescent protein) or Myc-tags inserted into *Sry* gene which exclusively expresses in pre-SCs (Albrecht and Eicher 2001; Sekido et al. 2004). In spite of intensive researches, there is not a direct shred of evidence for SCs' origin. However, pre-SCs derived from coelomic epithelium migrating into testicles has been widely believed (Karl and Capel 1998; Schmahl et al. 2000; Albrecht and Eicher 2001). Indeed, Schmahl et al. showed that cells beneath the coelomic epithelium resettled in XY and XX/SRY gonads as visualized by labeling the cells with 5′-bromo-2′-deoxyuridine (BrdU). Later on, these migrated cells had positive staining with SF1 which regulates the SRY and SOX9 expression in SCs (Sekido and Lovell-Badge 2008), indicating their differentiation into SCs (Schmahl et al. 2000). Taking together, these results reveal **mesenchymal phenotype of pre-Sertoli cells**, and **pre-SCs** must undergo a **mesenchymal-epithelial transition** (MET) to become mature cells. Therefore, we assume that the reverse process, **EMT**, could convert **Sertoli cell precursors** or **immature Sertoli cells** back to their **stem cell-like stage** with expected broader differentiation potential.

The aim of my Ph.D. research is to answer two big scientific questions:

- Could EMT reprogram immature Sertoli cells back to their stem cell stage at which their differentiation potential increases?

- And what molecules are involved in the maintenance of immature SC phenotype?

To answer these questions, our laboratory has been established a cell line of ***X**enopus **t**ropicalis* **t**esticular **s**omatic cells (XtTSCs) in long-term culture (Tlapakova et al. 2016). Their characteristics have been described in detail in our article (Tlapakova et al. 2016) and the main findings are going to be mentioned in the result part. Co-expression of Sox9, vimentin and cytokeratin indicates XtTSCs are immature Sertoli cells (Paranko et al. 1986; Rogatsch et al. 1996), so-called ***X**enopus **t**ropicalis* **i**mmature **S**ertoli **c**ells (XtiSCs).

In this study, three common EMT inducers (TGF-β1, FGF2, and GSK-3 inhibitor) have been employed in XtiSCs culture. Subsequently, evaluation of cell morphology and changes in a gene expression profile has been conducted by RT-PCR, immunostaining and flow cytometry. We investigated their differentiation potential and migration capacity both *in vitro* and *in vivo,* as well.

Our results also showed that XtiSCs underwent EMT by pharmacological inhibition of GSK-3 (CHIR99021). EMT-shifted XtiSCs possessed the broader differentiation potential and directed migration capacity both *in vitro* and *in vivo*. The results bring a better understanding of signaling pathways underlying the generation of testis-derived stem cells and Sertoli cell differentiation. XtiSCs represent as a good model for EMT study. These findings provide insight into gonadal development confirming the mesenchymal origin of SCs.

Moreover, SCs with cytokeratin (CK) expression have been considered as immature cells, however, its function in SC development is still a question. Our study evidenced the interconnection between CK network and β-catenin-based cell junction in immature SCs which probably provide structural support to maintain undifferentiation SSCs until the appropriate time point.

The work reported in this thesis has resulted so far in one paper in Biology Open and two manuscripts; these paper and manuscripts are part of this thesis and they are given at Attachments.

This thesis is organized as follows: a general background of testicular structure and development, inserting epithelial-mesenchymal transition, are given in Section 2. Section 3 presents materials and methods which were applied in this work. Results and Discussion are presented in Section 4 and 5 those are the most comprehensive part of the thesis and are divided into several subsections: (i) The dynamic of cytokeratin during Sertoli cell development, (ii) Characteristics of *Xenopus tropicalis* testicular somatic cells, (iii) EMT promoted differentiation potential of immature Sertoli cells, (iv) The role of cytokeratin in Sertoli cell junctions in immature *Xenopus tropicalis* testicles. Finally, Conclusions are settled in Section 6.

Chapter 2

GENERAL BACKGROUND

2.1 Testicle

2.1.1 Testicular structure

2.1.1.1 Male reproductive organ

The testis (or testicle) is the primary male reproductive organ which produces gametes (spermatozoa) and hormones, particularly the male hormone testosterone. A typical man has two oval testes in a skin pouch called scrotum, which is an extension of the abdominal wall. Unlike most mammals, some of them such as elephant, whale, seal, and numerous families of rodents don't have the external scrotum, and their testicles are located inside their bodies (Lovegrove 2014). In *Xenopus*, each testis is 5x10 mm, pale ivory internal structure lying near the posterior dorsal surface of the abdominal cavity. The temperature of the testes is slightly less than the core body temperature to enhance spermatogenesis (Kandeel and Swerdloff 1988). Each testis seats inside a thick connective tissue called tunica albuginea that consists of myofibroblasts, rhythmically contractile cells and the tunica vasculosa, a highly vascular region. A testis is divided into lobules by thin septa. Each of these lobules encompasses from one to four seminiferous tubules, which are the site of sperm production.

Other tissue outside testis including rete testis, efferent ductules, epididymis and vas deferens serve for the transportation, storage and maturation of sperm cells. The rete testis carries the mixture of sperm and Sertoli cell secretions as they leave the seminiferous tubules to efferent ductules. The efferent ductules absorb about 95% of the fluid, which increases the sperm concentration before entering the epididymis. During the transit in the epididymis, spermatozoa undergo a maturation process to acquire motility and fertility by the time they come to the vas deferens. Besides, the epididymis protects sperm cells from fertility inside the male tract by blocking receptors on the plasma membrane of the sperm head. Because of its long track, the sperms are stored in the epididymis for 2–3 months. The vas deferens transport sperms from the epididymis to the ejaculatory ducts in anticipation of ejaculation. Sperms are mixed with the diluting

fluids of the seminal vesicles and other accessory glands before ejaculation (forming semen).

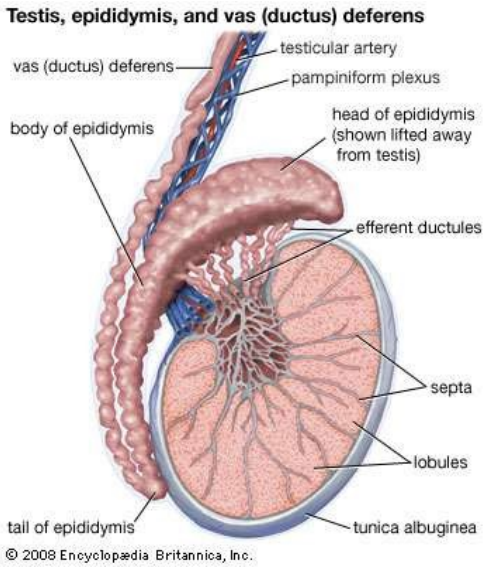

Figure 1: Human male testis, epididymis, and ductus deferens.
Credit: Encyclopædia Britannica, Inc.

2.1.1.2 Internal structure of testes

Seminiferous tubules

Seminiferous tubules lie within the testes, house germ cells and in general, they are the place of spermatogenesis (sperm production). The tubules are tightly coiled with the length up to 800 m. Each seminiferous tubule is covered by a layer of germinal epithelium which contains germ cells and Sertoli-supporting cells. In the center of the tubule, there is a lumen, or cavity, which is connected to the epididymis and spermatic duct (ductus deferens) to release spermatozoa (Fig. 2).

Germ cells: germ cells are the only ones whose genome pass through the next generation. In many animals, the germ cells separate from the primitive streak at the early stage of development and migrate to the developing gonads. There, they proliferate, enter to the meiosis and stop the maturation in diplotene stage after birth until puberty. In puberty, the meiosis resumption occurs and primary spermatocytes or oocytes reinitiate the maturation and become mature gametes, either sperms or eggs. These mature germ cells have reduced the number of chromosomes by half. Continuous differentiation of germ cells takes place in the seminiferous tubules throughout the whole life of a healthy male. The term spermatogenesis refers to the entire process of differentiation from stem cell to released spermatozoa. Based on their differentiation

stages, germ cells are classified into four categories - spermatogonia, spermatocytes, spermatids, and spermatozoa. Spermatogonia are pre-meiotic cells. With the commencement of meiosis, germ cells are called spermatocytes and after meiosis, four haploid cells called spermatids are formed from each spermatocyte. Finally, germ cells with the mature morphology are called spermatozoa or, more simply just sperms which are released into the central lumen of seminiferous tubules.

Sertoli cells are epithelial supporting cells (sustentacular cells) lying along with the wall of seminiferous tubules. They are tall, pyramid-shaped cells extending from the basement membrane to the lumen. Unlike Leydig cells, Sertoli cells proliferate before puberty and stop the division at the onset of puberty (R. Sharpe 2003). Sertoli cells have numerous vital functions in testis formation and spermatogenesis. In the early development, anti-Müllerian hormone (AMH) is secreted by SCs to regress Müllerian tract contributing to male sex characterization and testis morphogenesis (C. H. Lee and Taketo 1994; Appert et al. 1998; Barrionuevo, Burgos, and Jiménez 2011). Their primary function in adults is to provide support and nutrient for germ cells, control the microenvironment within the seminiferous tubule, and facilitate the differentiation of germ cells to spermatozoa. Under the influence of FSH and testosterone, Sertoli cells secrete androgen-binding proteins which bind to and transport testosterone and other androgen hormones into seminiferous tubules to stimulate spermatogenesis (Handelsman, Spaliviero, and Phippard 1990; de Winter 1993). A nutritious protein-rich fluid which sustains the germ cells and assists in their transport is also secreted by Sertoli cells. Moreover, the tight junctions between adjacent Sertoli cells form blood-testis barrier serving as a “gatekeeper” to isolate developing germ cells but to allow them to pass through the barrier. Moreover, this barrier and immunosuppressive molecules produced by SCs protect sperm cells from attacks of the immune system and pathological factors and establish stem cell niches for the maturation of SSCs (Setchell 2009; Mital, Kaur, and Dufour 2010). Sertoli cell differentiation and proliferation are under the regulation of Sex-determining region Y (SRY) gene which activates SOX9 and FGF9. Any misregulation of these genes affects the Sertoli cell differentiation, can lead to the female development (Moniot et al. 2009) or results in male infertility due to reduced production of spermatozoa (Nistal et al. 1982; Myers et al. 2005).

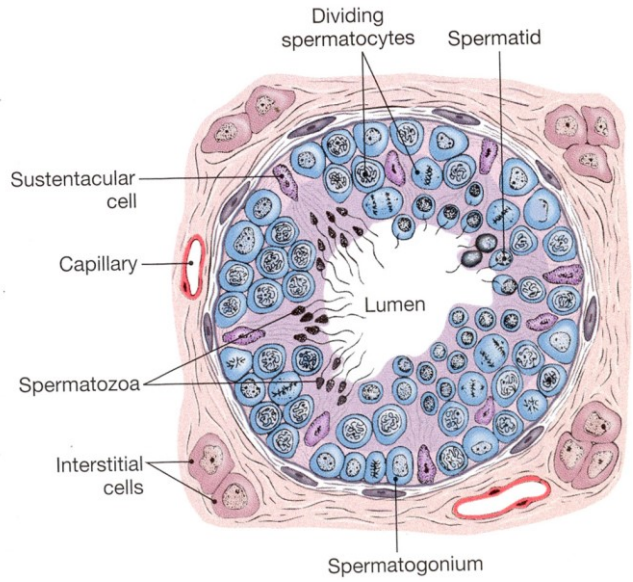

Figure 2: The depiction of cross section of testis
Credit*: https://os1-prod.amc.nl/celbiologie/20162017/2.1/mannelijk/php/22.php*

Blood-testis barrier

Neighboring Sertoli cells develop tight junctions between them to form a blood-testis barrier (BTB) in an adult male, so also called "Sertoli cell barrier" (Fig. 3). Besides the tight junctions, this barrier is composed of actin-based junctions (gap junctions) and intermediate filament-based junctions, desmosomes. This barrier functions for the isolation of developing germ cells from the circulatory system, thus preventing blood and other body fluids from the contact with the center of seminiferous tubules. Only Sertoli cell secretion is allowed to come to the lumen of the tubules. A BTB separates the basal compartment of seminiferous tubule from the apical part. In doing so, developing germ cells, spermatids are restricted inside the apical part and thus protected against the immune system or pathological factors (Mital, Kaur, and Dufour 2010; Setchell 2009). If the barrier is compromised, sperm-specific antigens are able to induce an autoimmune response, leading to male infertility. However, during germ cell maturation this barrier is not completely closed and spermatocytes must traverse across the BTB to the apical compartment. When preleptotene spermatocytes leave off the basement membrane, adjacent Sertoli cells form new tight junctions under the basal side of the spermatocyte, while the original BTB is disrupted above the cell (Pelletier 2011). Some studies suggested that the BTB serves as a "gate", with the tightly regulated opening and closing by the cell signaling. TGF-β2/-β3 via the p38 MAP kinase pathway has been shown to be involved in BTB dynamics. The transient induction of TGF-β2/-

β3 resulted in the disruption of the blood-testis barrier, accompanying the loss of occludin and ZO-1 (Wong 2004). Moreover, the knockdown of focal adhesion kinase in cultured Sertoli cells reduced occludin phosphorylation and induced its translocation from the cell membrane into cell cytoplasm, thereby led to the disruption of BTB (Siu et al. 2009; Lie et al. 2012). In contrast, the Arp2/3 complex, a primary nucleator of branched-actin arrays in eukaryotic cells was reported to participate in resembling BTB (Lie et al. 2010; Xiao et al. 2014).

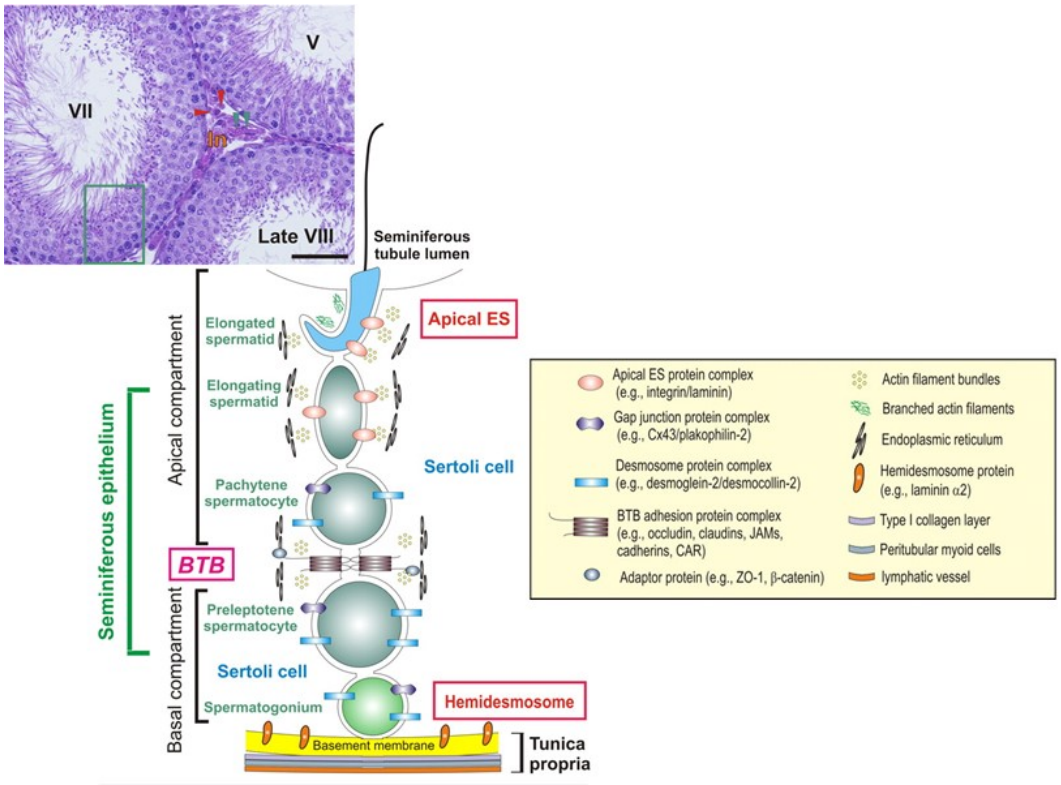

Figure 3: Sertoli and germ cells and the relative location of the BTB
Credit: *(Cheng and Mruk 2011)*

Peritubular myoid cells

Peritubular myoid cells (PMCs) surround seminiferous tubule to form an outer layer (Fig. 2). Some studies suggested PMCs originated from mesonephric cells (Buehr, Gu, and McLaren 1993; Merchant-Larios, Moreno-Mendoza, and Buehr 1993), however, their origin is still under debate. The lack of a molecular marker specific to PMCs in the early stage of differentiation is the main obstacle in studying their development. Like other smooth muscle cells, they contract by sliding of myosin and actin filaments over each other and transport spermatozoa within seminiferous tubules (Maekawa, Kamimura, and Nagano 1996; Catizone et al. 2015). Oxytocin produced by Leydig cells, transforming growth factor β, prostaglandins and hepatocyte growth factor are

suggested to be involved in the PMCs contractions (Maekawa, Kamimura, and Nagano 1996; Tripiciano et al. 1998; Catizone et al. 2015). However, the full mechanism of the contraction is still not fully understood yet. PMCs have also been shown to contact with Sertoli cells to lay down a basement membrane around the seminiferous tubule, and thus providing the structural integrity (Richardson, Kleinman, and Dym 1995). Besides Sertoli cells, PMCs also secrete growth factors to maintain spermatogonia stemness (L.-Y. Chen et al. 2014).

The connective tissue

Leydig (*interstitial*) cells are localized in the *connective tissue* among seminiferous tubules (Fig. 3). They have a large prominent nucleus, eosinophilic cytoplasm, and numerous lipid droplets inside the cytoplasm. There are two different populations—fetal and adult Leydig cells which have been observed in rodents. They are different in ultrastructure, lifespan, and capacity for androgen synthesis. The fetal Leydig cells synthesize only androstenedione and fetal Sertoli cells convert androstenedione to testosterone that is required for male genital differentiation and brain masculinization (Shima et al. 2013). In the perinatal period, the fetal Leydig cells undergo apoptosis accompanied the decreased production of testosterone (Yokoi et al. 1998). At the post-puberty, adult Leydig cells develop from stem cells of the neonatal testis and commence to synthesize testosterone once they are stimulated by Luteinizing hormone (LH). Even though LH is required for the activation of adult Leydig cells, development of fetal Leydig cells or their initial production of testosterone does not rely on the presence of Luteinizing hormone. The primary function of testosterone from Leydig cells is to induce spermatogenesis and support the development of immature germ cells. The capillary system of testis keeps Leydig cells floating around the tubules, and thus ensures that produced hormones immediately affect the germinal epithelium. Leydig cells are the primary source of testosterone in the male post-pubertal body.

2.1.2 Regulation of testicular function

Spermatogenesis in testis is directed by the central nervous system and pituitary gland via secreted hormones (Figure 4). Luteinizing hormone (LH) from anterior part binds to receptors on the surface of adult Leydig cells and activates a cascade of events via the G protein signaling. In response to LH, the various cytochrome P450 enzymes and

dehydrogenases are upregulated to convert cholesterol to testosterone, a male sex hormone. The secretion of LH is stimulated by gonadotropin-releasing hormone (GnRH) from the hypothalamus. In contrast, testosterone inhibits the activity and the secretion of GnRH. This endocrine feedback loop regulates the testosterone concentration in serum within the narrow range. When serum testosterone concentrations decrease, the secretion of GnRH and LH increase and vice versa. Besides of that, several factors may reduce testosterone level in male, including age, vitamin A deficiency (Livera et al. 2002), Zn deficiency (Prasad et al. 1996), and overweight (Håkonsen et al. 2011). In older man, testicular production of testosterone and spermatogenesis decrease but very slowly if compared to the ovarian function of women which ceases abruptly at the time of menopause.

Moreover, the GnRH also controls the synthesis of another hormone from the anterior pituitary gland, follicle-stimulating hormone (FSH). FSH interacts with follicle-stimulating hormone receptor on the plasma membrane of Sertoli cells. FSH stimulates Sertoli cells to release androgen-binding protein which binds to testosterone and transport it into seminiferous tubules to regulate spermatogenesis. Testosterone stimulates several kinases in Sertoli cells again to activate germ cell differentiation and proliferation, to increase the attachment between Sertoli cells and germ cells, and to promote germ cell migration (Walker 2011). When the sperm count is too high, Sertoli cells produce inhibin, an FSH inhibitor, thus locally regulate spermatogenesis. The inhibin hormone released into serum also suppresses FSH and GnRH production, which will cause spermatogenesis to slow down. Using the GnRH antagonist plus testosterone as male contraceptives have been conducted in human trials with a promising result (Pavlou et al. 1991; Tom et al. 1992).

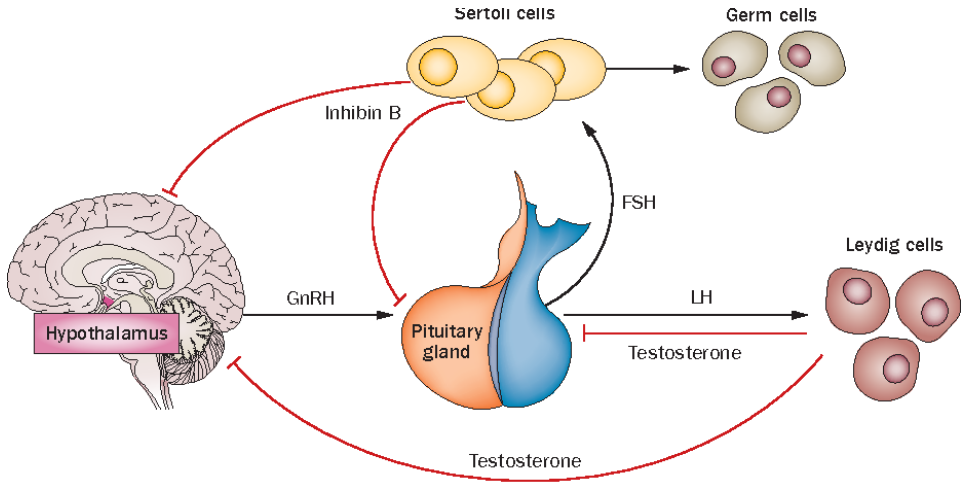

Figure 4: The hormonal regulation of testicular function in male
Credit: (Valenti et al. 2013)

2.1.3 Testicular development

2.1.3.1 At embryonic development

The testis is formed from the mesothelium and as well as from the mesonephros. Its earliest structure, called gonadal ridge consists of a central mass covered by a surface epithelium. The central mass arranges into a series of cords which are the precursors of most testicular tissues. During early embryonic development, primordial germ cells (PGCs) from the dorsal endoderm of the yolk sac migrate along the hindgut to the gonadal ridge. Once they have reached there, they attempt to associate with the other somatic cells (Sertoli cells) to form gonadal cords, a transient embryonic structure of seminiferous tubules. Until this stage, gonads are identical between both sexes (male and female).

Sex-determining region Y (SRY) protein is a driver gene to trigger the differentiation of Sertoli cells surrounding the PGCs. Following that, Sertoli cells of the developing testis secrete Mullerian duct inhibitory factor (MDIF) which causes regression of paramesonephric duct. Simultaneously, cells come from the mesonephros accumulating on the outer side of gonadal cords to differentiate into peritubular myocytes. These smooth muscle cells communicate with Sertoli cells to produce extracellular matrix to maintain the structure of seminiferous tubules and regulate spermatogenesis (Maekawa, Kamimura, and Nagano 1996; Potter and DeFalco 2017) in adulthood. Specific mesenchymal cells in the testicular cord develop into Leydig cells, which produce testosterone to retain mesonephric duct. Epididymis, vas deferens,

and seminal vesicles of a mature testis are differentiated from this duct. While the testicular cords separate from the overlying layer of epithelium, the tunica albuginea develops from a dense layer of fibroblastic cells. At the same time, the primordial germ cells continue to proliferate and differentiate into spermatogonial stem cells within the testicular cords.

2.1.3.2 Testicular descent

Concurrently with testicular maturation, the fetal testis undergoes anatomic changes in its position from abdominal cavity to a scrotum, called testicular descent. The testis movement differs among species in timing, final testis position and hormone regulation, for example, it occurs during late gestation in human, but at puberty in rodents. During development, undescended testes are anchored to abdominal wall by the cranial suspensory ligament and caudally by the gubernaculum. Later on, androgen from testes degenerates cranial suspensory ligament, but insulin-like factor 3 (INSL3) from Leydig cells promotes the gubernaculum to enlarge (Hutson et al. 2013). By that, the testis is still attached on the abdominal wall. Lengthening of gubernaculum and protruding of peritoneum through the developing scrotal sac facilitate the testes to slide through the abdominal wall on inguinal canal. The testes still stay in the inguinal canal and reach their final position by shortening of the gubernaculum under influences of androgen. In androgen insensitivity syndrome, the human testes cannot move to the scrotum, they are found either in the inguinal region or midway down the abdomen (Barthold et al. 2000).

2.1.3.3 At the onset of puberty

In male, puberty is a period when a male has achieved a full sexual maturity and is able to reproduce. The puberty is initiated by the onset of nocturnal pulses of GnRH which activate the pulses secretion of sex hormones, FSH and LH. Leptin, a hormone produced by adipose cells and acting on receptors in the hypothalamus, has been thought to cause GnRH synthesis and commence the puberty. In human leptin-deficiency inhibits the initiation of puberty (Clayton 2000). However, the cause of GnRH rise is still under debate. The increase of hormone concentration induces morphological changes within the gonad and also other secondary sex characteristics. Within the testis, SCs mature and cease the proliferation and differentiation at the onset of puberty. Under the control of hormone, SCs start to secret androgen-binding proteins and inhibin responsible for

the regulation of spermatogenesis. On the other hand, the number of Leydig cells increases altogether with a higher production of testosterone which then triggers the germ cell proliferation and maturation. Spermatogonial stem cells mature from primordial germ cells at an early stage after birth, but they commence differentiation into spermatozoa only at the puberty. The secondary functions of testosterone in male include the regulation in the development of the central nervous system influencing sexual behavior; muscle growth stimulation and the development of reproduction glands and organs. During this period, testes enlarge the volume up to 4 times. The reason is the increasing diameter of the seminiferous tubules due to spermatogonial proliferation and the expansion of meiotic and haploid germ cells (Koskenniemi, Virtanen, and Toppari 2017) (Fig. 5). In human, this process begins at 11 or 12 years of age and is complete between ages 16 and 18.

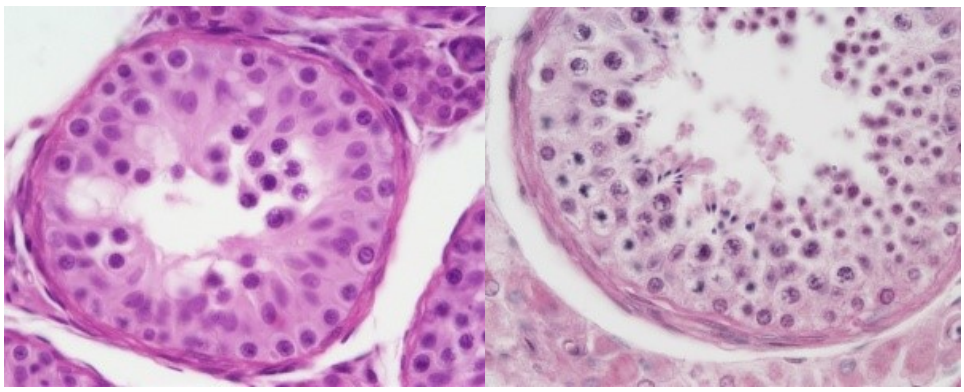

Figure 5: A cross-sectional view of the seminiferous tubule histology before and after puberty.
Credit: Hill, M.A. (2018, April 25) **Embryology** *Testis histology 006.jpg*

2.2 Epithelial-mesenchymal transition (EMT)

2.2.1 What is EMT?

The “epithelial-mesenchymal transformation” was firstly used by Elizabeth Hay in her research about the formation of a chicken primitive streak (Hay 1995). However, the initial report about inter-conversion between an epithelial and mesenchymal phase of cells appeared in the research of Frank Lillie in 1908 (Lillie 1908). The term “transformation” has been replaced with “transition” in the later reports to avoid the confusion with neoplastic transformation. This term also reflects the reversibility of the EMT process via mesenchymal-epithelial transition (MET) mechanism which induces

the conversion of mesenchymal cells to epithelial cells. EMT is an essentially biological process of embryogenesis. EMT is observed in the formation of various tissues such as mesoderm and neural crest (Richter et al. 2014; Kalcheim 2015). EMT is also associated with wound healing, tissue repair and cancer cell metastasis (Kalluri and Weinberg 2009).

In epithelial tissues, polarized cells are anchored to the basement membrane and tightly connected to each other via cell junctions. EMT allows polarized epithelial cells to undergo multiple biochemical and morphological changes to finally escape from surrounding cells and extracellular matrix (ECM). They give rise to mesenchymal cells able to migrate away from their origin tissue. During embryonic development, EMT increases the cells migratory capacity, however without altering their stemness characteristics. EMT is activated by EMT-activating signals and/or microenvironmental signals to induce changes in epithelial cells which include the following: (1) inhibition of epithelial gene expression and upregulation of mesenchymal genes; (2) a shift from cell-cell junction proteins and cytokeratin intermediate filaments in epithelial cells to cell-ECM interactions and vimentin intermediate filaments in mesenchymal cells; (3) finally morphological change from cobblestone-like cell shape with apical-basal polarity to spindle-shaped mesenchymal cells with a migratory pseudopodium (Puisieux, Brabletz, and Caramel 2014; Kim et al. 2017).

Depending on signals and tissue context, EMT-activated epithelial cells may lose only some of their traits and show the properties of both mesenchymal and epithelial cells. This process is considered as a “partial” EMT by which cells express hybrid epithelial/mesenchymal phenotype. Due to the weak cell-cell adhesion, the hybrid cells are characterized by collective cell migration, compared to individual, high motile migration of “full” EMT-underwent cells. The partial EMT is found in the wound healing in which epithelial cells at the edge of wound migrate into the injury site to re-establish normal tissue architecture (Fustaino et al. 2017).

2.2.2 The role of EMT in embryogenesis

During development, the embryonic cells must undergo consecutive rounds of EMT and MET to differentiate into specialized cell types and to form the three-dimensional structure of internal organs. These rounds are divided into primary EMT, secondary EMT and tertiary EMT (Thiery et al. 2009; Kim et al. 2017). A primary EMT occurs in

the formation of mesoderm and neural crest. After gastrulation, mesodermal cells subdivide and then condense into transient epithelial structures through the MET process, thereby forming the notochord, somites, precursors of the urogenital system and the somatopleure and splanchnopleure. The secondary EMT process is induced in these transient tissues (except for the notochord) to generate mesenchymal cells which possess more restricted differentiation potential. Moreover, in endoderm tissues such as the pancreas bud and the liver diverticulum, the secondary EMT induce the dissociation of endocrine cells and hepatoblasts from their respective epithelial primordia. A tertiary EMT is observed in heart formation with three rounds of EMT and MET (Fig. 6).

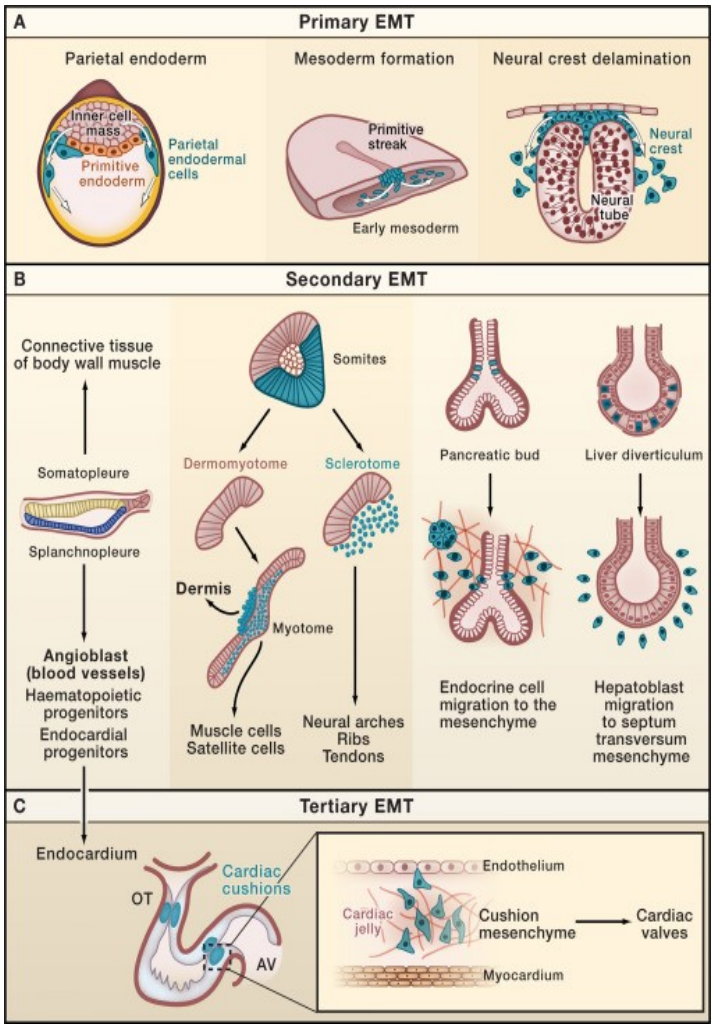

Figure 6: Successive EMT during Embryonic Development
Credit: (Thiery et al. 2009)

2.2.3 EMT signaling pathway and molecular mechanism

Multiple signaling pathways participate in the initiation and maintenance of EMT process. The PI3K–AKT pathway and the ERK MAPK, p38 MAPK are activated by growth factors through transmembrane RTK to stimulate cell proliferation. RTK signaling also increases TGFβ1 expression, thus enhancing the EMT induction of TGFβ signaling (Nyati et al. 2011). Hepatocyte growth factor (HGF) /Scatter factor is observed in converting kidney epithelial cells into migratory fibroblast-like cells (Stoker and Perryman 1985). Moreover, HGF signaling interacts with TGFβ2 to promote the formation of somites and the endocardial cushion via EMT (Romano and Runyan 2000). FGF signaling is necessary for cell migration away from primitive streak to form mesoderm and from neural crest (Sun et al. 1999; Sauka-Spengler and Bronner-Fraser 2008). TGF-β family proteins are the best-known EMT inducers, both in embryonic development and cancer. In response to TGFβ, the expression of SMAD complex is upregulated which then activate the expression and activity of EMT transcription factors and other mesenchymal genes as well (Yang et al. 2003; Vincent et al. 2009). Different pathways including RHO-like GTPases, PI3K and MAPK which contribute to EMT are also activated by TGFβ signaling (Derynck and Zhang 2003).

The stimulation of above-mentioned pathways often leads to the activation of EMT inducing transcription factors, such as Snail1/2, Twist and Zeb1/2. They serve as EMT master regulators which control the expression of each other and cooperate in the suppression of epithelial genes and/or activation of mesenchymal genes. SNAIL1 (also called SNAI1) and SNAIL2 (also known as SLUG) bind to E-box DNA sequences on the promoter of epithelial genes such as E-cadherin and suppress their expression (Peinado et al. 2004). SNAI1 also increases the expression of mesenchymal genes such as fibronectin, collagen, and MMP (Jorda 2005). In addition, SNAI1 cooperates with MAPKs to upregulate and stabilize TWIST in the nucleus, thus promoting EMT (Hong et al. 2011). TWIST1 and SNAI1 regulate ZEB1 expression during EMT (Dave et al. 2011). SNAI1 is inactivated by the phosphorylation of Glycogen synthase kinase-3β (GSK3β) which results in the degradation of SNAI1 via the ubiquitin-proteasome pathway. SNAI1 can be protected by several pathways which influence the activity of GSK3β. The disruption of GSK3β–SNAI1 interactions by Notch and nuclear factor-κB (NF-κB) signaling and the inhibition of GSK3β phosphorylation by the WNT and

PI3K–AKT pathways can retain SNAI1 activity (B. P. Zhou et al. 2004; Yook et al. 2006; Y. Wu et al. 2009).

2.2.4 The molecular changes during EMT

A hallmark of EMT is destabilization of cell-cell contacts by disrupting adherens junctions, tight junctions, and desmosomes, thus losing epithelial barrier function. Genes encoding cell junction proteins including E-cadherin, claudins and occludin, desmoplakin and plakophilin are repressed to prevent the *de novo* formation of epithelial cell-cell junctions (Huang, Guilford, and Thiery 2012). The upregulation of matrix metalloproteinases (MMP2 and MMP9) enhances the degradation of cell junction proteins on a basement membrane. Epithelial cells then escape from their niche and change the cell shape from cobblestone to fibroblast-like type. (Nisticò, Bissell, and Radisky 2012). Simultaneously, transiting epithelial cells increase the interaction with ECM by the downregulation of some epithelial integrins such as α6β4, and activation of α5β1 (fibronectin receptor), α1β1 or α2β1 integrins (Maschler et al. 2005). Remodeling of the ECM by increasing the expression of fibronectin and type I collagen also promotes the communication between transiting cells and ECM (Koenig et al. 2006; Mise et al. 2012). Alterations in the composition of intermediate filaments also contribute to EMT. During EMT, cytokeratin is repressed and vimentin expression is activated (Huang, Guilford, and Thiery 2012). These changes involve differences in the trafficking of different organelles and membrane-associated proteins via these cytoskeletal proteins. Moreover, vimentin shows the interaction with motor proteins which may enable cell motility (Mendez, Kojima, and Goldman 2010). EMT transcription factors, including SNAIL, ZEB and TWIST play an important role in regulating the expression of the proteins mentioned above (Fig. 7).

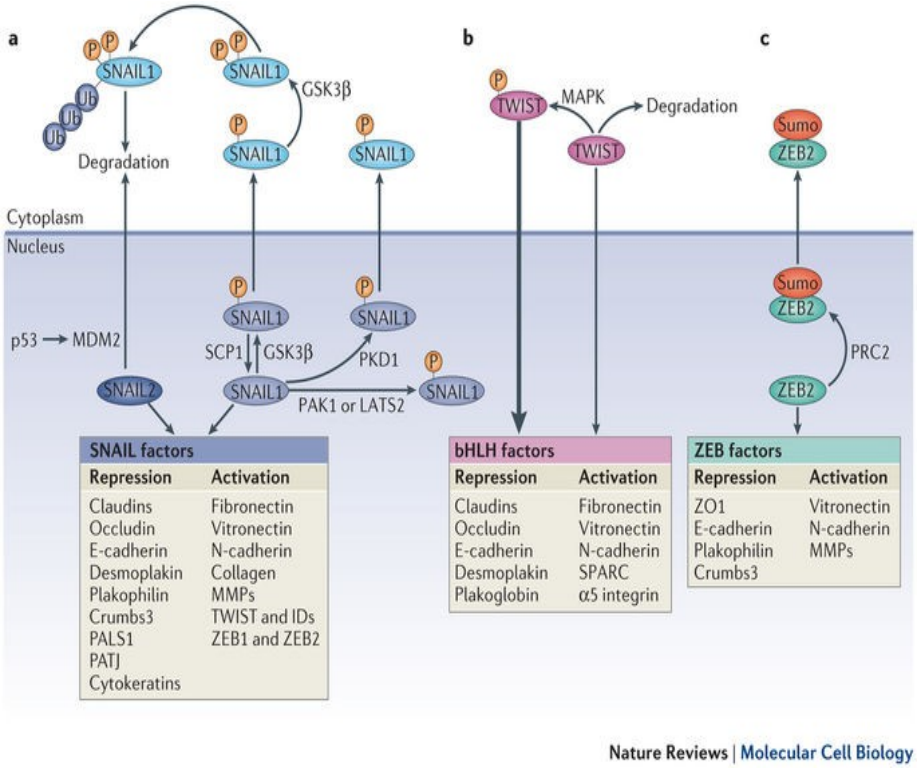

Figure 7: Roles and regulation of major EMT transcription factors.
Credit: (Lamouille, Xu, and Derynck 2014).

2.2.5 EMT and stem cell acquisition in vitro

EMT can be induced *in vitro* by TGF-β, FGF2, Wnt, or by a combination of several cytokines (Nieto, Angela Nieto, and Amparo 2012). Cancer cells could acquire stemness properties along with the ability to self-renew, migrate to distant sites and regrow the tumor after undergoing EMT (Hollier et al. 2013; P. Li et al. 2014; Q. Li et al. 2016). Moreover, efforts to transdifferentiate epithelial cells to mesenchymal stem cells (MSCs) via EMT has been performed in several groups. In order to induce EMT, immortalized human epithelial cells from mammalian gland were treated with recombinant TGF-β1 or transduced with vectors expressing EMT key transcriptional factors, SNAIL and TWIST. These EMT-derived cells have exhibited similar properties to MSCs, including antigenic profile, the capacity to differentiate into mesodermal cell types, migrate towards cancer cells and wound injury sites (Mani et al. 2008).

Recently, the mathematical model supported with experimental data was established concerning the molecules relevant to the EMT and the acquisition of stem cell features (Jia et al. 2015; Jolly et al. 2015). The EMT and stemness of epithelial cells were induced by miR-200/LIN28/ZEB/let-7 feedback circuit in that miR-200 inhibits LIN28 which inhibits let-7. ZEB actively inhibits miR-200 previously inhibited by let-

7. This circuit was driven by transcription factors SNAIL, OVOL and NF-kB as described in Fig. 8. Experiments showed that too high or too low OCT4 level which was activated by LIN28 (Qiu et al. 2010) could force cells to differentiate (Niwa, Miyazaki, and Smith 2000; Karwacki-Neisius et al. 2013). Thus, the relative OCT4 or LIN28 level is important for the stemness maintenance so-called stemness window. The epithelial (E), mesenchymal (M) or hybrid E/M phenotype(s) in which transited cells acquire stemness can be determined by SNAIL and endogenous OVOL expression level. In the presence of OVOL and absence of SNAIL, the 'stemness window' shifts more to E phenotype. On the other hand, in the case of higher levels of SNAIL, and the absence of OVOL mesenchymal (M) phenotype is involved in the stemness window. The intermediate state with high SNAIL and OVOL is typical for the hybrid E/M phenotype.

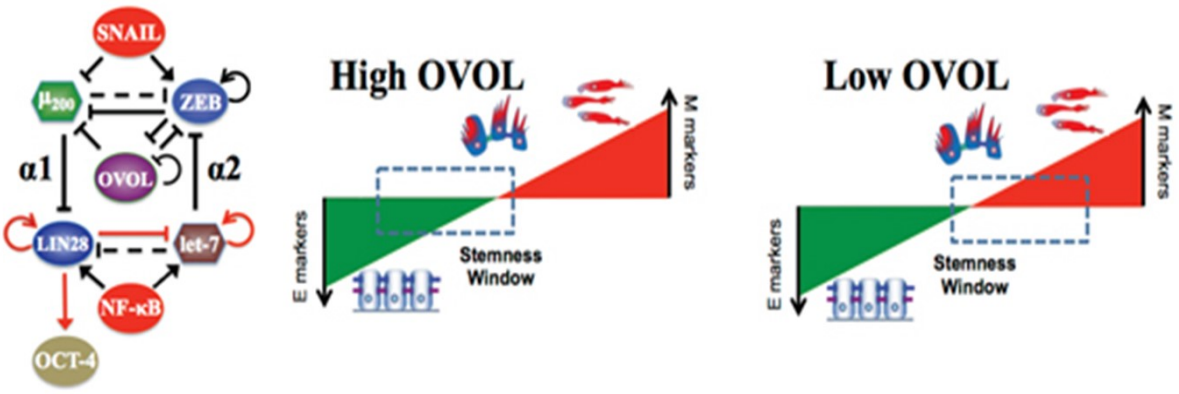

Figure 8: Phase diagram of the circuit for which different phenotypes can attain stemness or lie in the 'stemness window'.
Credit: (Jolly et al. 2015)

Chapter 3

MATERIALS AND METHODS

All material was purchased from Sigma, except as stated.

3.1 Ethical statement

This study was carried out in strict accordance with the Act No. 246/1992 Coll., on the protection of animals against cruelty. Official permission was issued to the Faculty of Science, Charles University in Prague by the Ministry of Education, Youth and Sports of the Czech Republic (No. MSMT-37376/2014-4, date of expiry 03.03. 2019).

3.2 *X. tropicalis* testicular somatic cell isolation and culture

The *X. tropicalis* **t**esticular **s**omatic **c**ells (XtTSCs) or later called *X. tropicalis* **i**mmature **S**ertoli **c**ell**s** (XtiSCs) were isolated from juvenile testes of 5 – 6-month old male (Ivory Coast strain). Because of the difference in cell osmolarity between amphibian and mammalian cells, phosphate-buffered saline (PBS) was diluted to ⅔ (91.33 mM NaCl, 1.8 mM KCl, 6.7 mM Na_2HPO_4, and 1.2 mM KH_2PO_4) in deionized H_2O before using as a basic buffer.

The collected testicles were thoroughly rinsed with ⅔ PBS, disrupted by needles, and then nurtured in medium (33.3% L-15 and 33.3% RPMI 1640 HEPES modification medium, 10% FBS (Life Technologies), 1.33 mg/ml sodium bicarbonate, 2 mM L-glutamine, and 50 µg/ml gentamicin) at 29.5°C with 5.5% CO_2 for 5 days without any interference. Following, adherent cells were harvested and cultured in growth medium (the isolating medium above supplemented with 1 mM sodium pyruvate, 0.1 mM 2-mercaptoethanol and 1000 U/ml recombinant mouse LIF (ESGRO; Millipore)) according to (Chowdhury et al. 2010). After 1.5-2 months, cell colonies have been visible in the growth medium. Primary culture of testicular explants was successfully done three times with different frogs from various breedings. All three isolated cell lines displayed the same morphology, gene expression profile and behavior during long-term culture.

The growth medium was exchanged every three days and cells were passaged every 10 days in culture. The colonies couldn´t be dissociated completely by

AccutaseTM (Thermo Electron Corporation), Biotase or trypsin-EDTA solutions, except papain solution (all of three enzymes from Biochrom AG), probably due to extracellular matrix covering the colonies. Because of that, we harvested the colonies by using 0.025% trypsin-EDTA solutions, then filtered the suspension with 40 μm cell strainer (Fisher Scientific). Subsequently, the colonies were obtained by upside down the strainer and washing with medium. The single cell suspension was then collected by pipetting the colonies in papain solution (61.25 mg/l).

To induce epithelial-mesenchymal transition (EMT), the colony-forming cells were collected and cultured in growth medium overnight before treatment with CHIR99021 (CHIR) (3 μM) (GSK-3 inhibitor), LiCl (10-40 mM), IWP2 (2 μM), mFGF2 (25 ng/ml), or hTGF-β1 (2.5, 5 or 10 ng/ml) (all growth factors from Peprotech) for 3-4 days before using for further experiments. CHIR99021, FGF2 and TGF-β1 solution was prepared according to the manufacturer's instructions. CHIR and IWP2 were dissolved in DMSO at 3 mM and 2 mM stock solution, respectively. The same amount of DMSO (0.1%) was added in the growth medium as a vehicle control. All cell media contained 10% fetal bovine serum (FBS), except medium supplemented with TGF-β1 (only 0.5% FBS).

3.3 Fluorescent immunostaining

For immunofluorescence, 20 μl drop of 10 000 cells were plated on Ø12 mm coverslip glasses coated with collagen type I (2.5 μg/cm^2) or poly-(L) Lysine (4 μg/cm^2) in 24-well plates. Cells were kept in the drop for 20 minutes allowing them to adhere on the glass surface, and then 0.5 ml of the growth medium were added to culture cells overnight before exchanging into the indicated medium for the indicated time. Cells were then fixed with 2% formaldehyde for 20 minutes at RT or Dent's fixative (methanol: DMSO = 4:1) overnight at 4^{o}C, permeabilized with 0.1% Triton-X 100 for 20 minutes or omitted in the case of Dent's fixing. Excess formaldehyde was quenched by 125 mM glycine. 5% bovine serum albumin (BSA) was used for blocking for 45 minutes at RT before incubating with primary antibodies (list and dilution in Table 1) diluted in 1% BSA and 0.05% Triton X-100 overnight at 4^{o}C. Following, the secondary antibodies conjugated with Alexa Fluor -488 (anti-mouse) or -594 (anti-rabbit) were employed for 1.5 hours at RT. For F-actin staining, fixed cells were incubated with

Alexa Fluor 568- conjugated phalloidin for 1 hour at RT. In the final step, the coverslips were mounted in the mounting media with DAPI to visualized cell nuclei. ⅔ PBS with pH=7.4 was used as a washing solution and a basic buffer in all solution. Between all steps, samples were rinsed thoroughly 3 times for 5 minutes each.

Table 1: Antibodies used in fluorescent immunostaining

Antigen	Species	Provider	Cat./Clone No.	Reference/ Certificate No.	Dilution
Cytokeratin	Mouse	Developmental Studies Hybridoma Bank	1h5	(Klymkowsky, Maynell, and Polson 1987)	2 µg/ml
Fibronectin	Mouse	Developmental Studies Hybridoma Bank	MT4	(Nace and Tassava 1995)	2 µg/ml
Beta- catenin	Rabbit	Sigma-Aldrich	C2206		1:500
Integrin alpha 5 beta 1 (fibronectin receptor)	Mouse	Developmental Studies Hybridoma Bank	P8D4	9/26/16	2 µg/ml
Integrin beta 1 (CD29)	Mouse	Developmental Studies Hybridoma Bank	8C8	3/14/13	2 µg/ml
Snai1	Mouse	Santa Cruz Biotechnology	sc271977	E2716	1:100
Snai1	Mouse	St John's Laboratory	STJ95716		2 µg/ml
Zeb1	Mouse	Novus Biologicals	2A8A6	NBP2-23484SS A-1	1:100
Sox2	Mouse	Santa Cruz	sc-365823	E2716	1:100
Cardiac troponin T	Mouse	Developmental Studies Hybridoma Bank	CT3	(Dagle et al. 2003)	2 µg/ml
STAT3	Mouse	Developmental Studies Hybridoma Bank	PCRP-STAT3-2F12	11/5/15	2 µg/ml
Vimentin	Mouse	Developmental Studies Hybridoma Bank	14h7	(Dent, Polson, and Klymkowsky 1989)	1 µg/ml
alpha-smooth muscle actin	Mouse	Sigma-Aldrich	A2547	Validate by staining on testis sections	1:400
Phalloidin (F-actin)		Thermo Fisher Scientific		1668974	1:100
Sox9	Rabbit	Sigma-Aldrich	HPA001758		1:300
E-cadherin	Mouse	Invitrogen	33-4000		1:150
β-tubulin	Mouse	Sigma-Aldrich			1:500
Red fluorescence	Rabbit	Evrogen	AB233	23301291014	1:5000

protein					
Red fluorescence protein	Mouse	Thermo Fisher Scientific	MA5-15257	QB205317	1:500
Mouse IgG-Alexa Fluor® 488 conjugate	Goat	Thermo Fisher Scientific	A11001	1664729	1:500
Rabbit IgG-Alexa Fluor® 594 conjugate	Goat	Thermo Fisher Scientific	A11012	1678830	1:500
Mouse IgG-Alexa Fluor® 594 conjugate	Goat	Thermo Fisher Scientific	A11032	419361	1:500
Rabbit IgG-Alexa Fluor®488 conjugate	Goat	Thermo Fisher Scientific	A11034	870976	1:500

3.4 Preparation of transgenic Katushka RFP testicular cell culture

Preparation of transgenic Katushka RFP testicular cell culture was described in (Tlapakova et al. 2016). Testicular cells were electroporated with 6 µg of ISpBSIISK-CAG-Katushka RFP vector (Shcherbo et al., 2007) using Nucleofector™ 2b Device (Lonza), program T-020 and nucleofection solution (5 mM KCl, 15 mM $MgCl_2$, 50 mM Na_2HPO_4, 100 mM NaCl). One month after nucleofection, transfected cells were separated on the basis of Katushka RFP signal by a fluorescence-activated cell sorting (FACS) using the inFlux v7 Sorter (BD Bioscience).

3.5 RT-PCR and qRT-PCR

Total RNA isolated from XtTSCs by RNeasy Plus Mini Kit (Quiagen) following the manufacturer‘s instructions. This process included an on-column DNase treatment step. The quality of isolated RNA was assessed by denaturing gel electrophoresis. Reverse transcription was performed with the same amount of total RNA (200 ng) by the RevertAid H Minus First Strand cDNA Synthesis Kit (Thermo Scientific). Target cDNA levels were analyzed by semiquantitative RT-PCR in quadruplicates in 25 µl reactions containing 500 nM each forward and reverse primers, and 0.5 µl of the cDNA reaction. PCR was conducted over 30 cycles of 94°C for 1 min, 60°C for 1 min, 72ºC for 1 min 30 s in a thermal cycle, preceded by an initial 1 min step at 94°C to activate the Taq DNA polymerase (Promega). The reaction was ended at 72ºC for 5 min. The final product was kept at 4ºC until analyzing by electrophoresis. The relative expression of

desired transcription genes was normalized by *odc1* or *β-actin*. ImageJ program was used to measure the intensity of the PCR product on photographs of the electrophoresis gel.

Quantitative RT-PCR (qRT-PCR) was performed with a real-time CFX384 cycler system (BioRad) using iQTM SYBR® Green Supermix (BioRad). An RNA spike (TATAA Biocenter) was used to validate the reverse transcription and the quantitative PCR reactions. The detailed protocol of cDNA synthesis and qPCR reaction was already described (Flachsova et al., 2013; Sidova et al., 2015). Primer sequences are shown in Table 2.

Table 2: Primer sequences for RT-PCR and qRT-PCR of *X. tropicalis* transcripts

X. tropicalis gene symbol	Gene transcript	Primer F Primer R	Size (bp)
acta2	ENSXETT00000020391	ACTGCTGAGCGTGAAATCGT GCCAGCAGATTCCATACCAA	213
cd44	ENSXETT00000016456	CCCTGGGCAATAACGATTCC ATCGGTGACCTCTCCTGGAT	572
cyp11a1	ENSXETT00000011263	GTCACCGGATTGCCCTAAAT CCTTTCCAGAGGCATCTCGT	645
cyp17a1	ENSXETT00000033323	TGCTCTTCTGAAAGCGAAGC TTTGGGAGGGGGTGTAGAG	497
dazl	NM_203748	CAAGCTTTTGTGTTGCCAGA AATGCCATGATCCCAAAGAG	1114
ddx4	ENSXETT00000066339	TGCATGCAATGAGGGATGTTG AGATGAAGGAGCACTGACGTA	899
ddx25	ENSXETT00000064463	AAACGCATCCCAAGCGGAA CGACTCAGCATAGCCAGGAC	435
itgb1	ENSXETT00000048743	CAACTGACGCAGGATTCCATT TCCCCAGTTCCCTTGACTC	400
kitlg	NM_001045596	ACTGAAGGAGGACCATACCCA GGGAGGGATTTGTGGCTGAA	789
klf4	ENSXETT00000012646	TTCCTCACCTCCACCTCCT ACAGTCTCTGCCCATCAGC	556
lif	ENSXETT00000053337	TGTGCAACTGCTGATTCTCC CATTGACTGCTTGGTGGATG	581
myc	ENSXETT00000054171	TGACCCTTCGGTGGTTTTCC CCGCCTCTTGTCGTTCTCTT	454
odc1	ENSXETT00000007603	GCTGCACTGATCCTCAGAC CAAGCTCAATGCCACTCTCC	744
pou5f3.1	NM_001285474	GCAAACAAGAGACGAGCAGG GTGGGCAAAGGAAGGGTAGG	281
pou5f3.2	NM_001129934	ACTCCGACTTATTTGGGTGGAA TCCCTTGTTGGTTGGTCTCC	464
pou5f3.3	NM_001130364	CACTTGCTGGTTTAGGGGGT GGAGGGGGCATTGTAGTTCC	264
sox2	ENSXETT00000004031	GGGCTCCAACAACCAGAGT TAGTGTTGGGACATGTGCAGT	804
sox9	ENSXETT00000048344	AACTCCTCCAACTACCCCC CCTCACTGCTCAGTTCACC	143
tert	ENSXETT00000034113	TGACCAGCCAAAACGGGATG TCGTAGACGAATCCAAGAGCA	484
thy1	ENSXETT00000046686	AAGCCTCACTGCCTGTCTGA AAAGACTGACTCCGCCACAG	350
vim	ENSXETT00000016267	CCTCTTTGGCACGTATTGACTT TCTCCTCCATTTCTCGCATTTG	464
cd44	ENSXETT00000016456	CCCTGGGCAATAACGATTCC ATCGGTGACCTCTCCTGGAT	572
twist1	ENSXETT00000054522	TCTCCCCAGTAGACAGTCTAA AGACCTGGCAGAGAAAGTCG	351
actb	ENSXETT00000006761	CCAAGCTGTGTTGTCCCTGT GCTGTGGTGGTGAAGCTGTA	235

3.6 Immunoblotting

Cells were cultured in the indicated medium as mentioned above before collecting by papain for nuclear extraction. The cell pellet was gently resuspended in frog hypotonic solution (0.038 M KCl, 1.9 mM HEPES, 0.038 mM EGTA, pH = 7.3) with 15 minutes on ice before adding Triton X-100 to a final concentration of 1% and then vortexing for

10 seconds at the highest setting. The homogenate was centrifuged to separate the nuclear fraction from the supernatant containing the cytoplasmic fraction. The nuclear pellets or whole cells were immersed into RIPA lysis buffer containing protease inhibitor cocktail (1:100, Promega) for 30 minutes on ice with vortexing at 10 minutes intervals, followed by sonication (cycles 60s, amplitude at 0.75, 11 times). The lysate was centrifuged for 30 minutes at 14,000 x g at 4^{o}C to remove the insoluble compartments. Protein concentration was determined by Bradford assay. 10 µg of total protein was loaded into each well of 10% acrylamide gel for immunoblotting analysis following the standard protocol as described (Towbin, Staehelin, and Gordon 1992). Protein was transferred to PVDF membrane and then blocked with 5% of non-fat milk for 45 minutes at RT. Primary antibodies were used including β-tubulin (1:2000, T8328), β-catenin (1:5000, C2206), Sox9 (0.4 µg/ml, HPA001758) overnight at 4^{o}C, following the secondary antibody conjugated with HRP for 1 hour at RT. For Western blot detection, Pierce ECL Plus Substrate (Thermo Scientific), an acridan-based chemiluminescent HRP substrate was used with X-ray film.

3.7 Cell transformation assessment

3.7.1 Chromosome analysis

Cells at the exponential growth phase (around 70% of confluency) were kept arresting at metaphase by adding 0.02 µg/ml colchicine into the culture medium for 4.5 hours in culture incubator. Then, cells were harvested by trypsin, gently dispersed in frog hypotonic solution (0.038 M KCl, 1.9 mM HEPES, 0.038 mM EGTA, pH = 7.3), followed by fixing in Carnoy's fixative (methanol: acetic acid ratio 3:1) for 15 mins. The fresh fixative was replaced for three times by centrifuging at low speed of 100 g for 5 min, and cells were suspended in a small volume of fixative in the last step. The cell suspension was dropped on a clean glass slide to spread out chromosome. Cell membrane and protein were washed off by 50% acetic acid before staining with Giemsa and observing under a microscope.

3.7.2 Soft agar colony formation assay

Anchorage-independent growth has been considered as one of the hallmarks for malignant transformation in cells. The soft agar colony formation assay allows for *in vitro* evaluation of this capability of cells. Cells at passage 5 and 12 were harvested by

papain to get single cell suspension, counted using cell counter (Thermo Fisher Scientific), and resuspended in growth medium. The bottom layer of the soft agar plate was made with 0.6% agar by mixing equal parts of 1.2% agar with 2X growth medium, poured in a six-well plate, and allowed to solidify completely. 24,000 harvested cells/well were mixed with medium containing 0.3% agar and overlaid above the bottom agar in triplicates. The plates were replenished with fresh medium at an interval of two or three days. Colonies were observed under a dissecting microscope after 3 weeks, and as a positive control, HeLa cells were cultured simultaneously. Colonies of sizes greater than 100 μm were considered transformed. Three independent assays were done.

3.8 Cell viability assay

5,000 or 10,000 cells were plated in each well of a 96-well plate and incubated with the appropriate stimulus for the desired time (3 days). Cells were then washed with PBS ⅔ and incubated with medium (no phenol red) containing 1.2 mM 3-(4,5-dimethylthiazol-2-yl)-2,5-diphenyltetrazolium bromide (or MTT) (ThermoFisher Scientific) overnight in cell culture incubator. NAD(P)H-dependent cellular oxidoreductase enzymes in viable cells will converse water-soluble yellow MTT to insoluble violet crystals. The crystals were then dissolved by 10% of SDS in 0.01 M HCl at 37ºC for 4 hours in a humidified chamber before absorbance reading at 570 nm. Three independent assays were done.

3.9 X-gal staining assay

Senescent cells, which are permanently arrested with G1 DNA content, express a high activity of lysosomal β-galactosidase, which is histochemically detectable at pH 6.0 instead of at pH 4.0 in normal cells (Dimri et al. 1995). Cells at passage 3-5 were used for TGF-β1 treatment and for X-gal staining assay. After 3 days of treatment, cells were fixed with 4% formaldehyde for 5 minutes at room temperature, and then incubated with 0.1 % X-gal (Fermentas) in staining solution (5 mM potassium ferrocyanide, 5 mM potassium ferricyanide, 150 mM NaCl, 2 mM MgCl2, 40 mM citric acid in sodium phosphate solution, pH 6.0) at 37ºC for 12 hours. Stained (senescent) cells with blue color were imaged under an inverted microscope (Olympus).

3.10 Transplantation of testicular somatic cells into tadpole´s peritoneal cavity

X. tropicalis embryos were produced by the standard *in vitro* fertilization procedure (Geach and Zimmerman, 2011). Briefly, 2 female frogs were injected with hormone hCG (Pregnyl) at 15 IU/frog 18 hours before stimulating again with 150 IU/frog. The frogs started to lay out eggs 6 hours after the second dose. The suspension of *X. tropicalis* testes homogenized by tissue grinder (Fisher Scientific) in L-15 medium supplemented with 10% FBS was used for the fertilization of laid eggs. Embryos were selected and cultivated in 0.05x MMR (5 mM NaCl, 0.1 mM KCl, 0.05 mM $MgCl_2$, 0.25 mM HEPES, pH 7.5) with gentamicin (50 µg/ml) for two days (stage 41) before transferring to tanks containing salted water without antibiotics. The developmental stage was determined according to Nieuwkoop and Faber (1994).

Katushka RFP positive testicular cells were detached from the bottom of the cultivation flask by trypsin. Single cell suspension from cell colonies was prepared as described above. 40 nL containing 1,000 Katushka RFP positive cells were microinjected into each peritoneal cavity of tadpoles at stage 41 using a thin glass capillary (Drummond, type 1-000-0500) and the Narishige IM-300 pneumatic microinjector. To prevent movements, tadpoles were anesthetized by 0.02% MS222 (tricaine, Sigma) in 0.05x MMR medium. After transplantation, the tadpoles were cultivated for up to one month and the distribution of RFP positive cells was observed under a fluorescence stereomicroscope (Olympus). Non-injected tadpoles were used as controls.

3.11 Immunohistochemistry of vibratome sections

Transplanted tadpoles at 2 hours after injection (day 0, stage 41), stage 45 (day 1) and 55 (day 30) were fixed overnight in MEMFA (0.1 M MOPS, 2 mM EGTA, 1 mM MgSO4, and 3.7% formaldehyde) at 4ºC, following by 3 times washing with PBS 1X. The fixed tadpoles were kept in methanol at -20ºC at least overnight for permeabilization or no longer than 3 months for long-term storage. Then, tadpoles were rehydrated using 90, 75, 50, and 25% methanol diluted by PBSTr (PBS 1X plus 0.1% Triton-X 100) and 3 times washing with PBS 1X. Tadpoles were then immersed into 3% agarose in PBS overnight at 48.5 °C and cooled down. Agarose blocks with fixed tadpoles were then cut into 30-40 µm sections on a vibratome (Leica 1200) in cold PBS.

The sections were permeabilized with 0.25% Triton X-100 in PBS for 1 hour and blocked with TNB (0.1M Tris-HCl, 0.15M NaCl, 0.5% Blocking Reagent (Boehringer Mannheim GmbH) for the same time. Incubation with primary antibody in TNB was done at 4ºC for 3 days. The dilution of primary antibodies against vimentin, Sox9 and Sma were 1:40, 1:300 and 1:400 respectively or 1:5000 for anti-tRFP (rabbit, Evrogen). An appropriate secondary antibody (Life Technology) was applied for 2 hours at room temperature. At the end of each step, 5 times washing with PBSTr for 2 hours was applied. Individual sections were mounted on slides with Mowiol/DAPI mounting medium and observed under fluorescence microscopy (Olympus Cell-R). Z-stack images for every single layer have been acquired and presented to avoid mixing flourescent signals of cells in different optical layer.

3.12 *In vitro* differentiation

For chondrogenesis differentiation of XtiSCs, the micromass culture technique as described by (Greco et al. 2011) was employed. Briefly, treated-XtiSCs in the indicated medium were harvested and re-suspended in growth medium at a density of 2.5×10^7 viable cells/mL. 20 µL of cell suspension was dropped into an individual well of 24-well plates and left them resting for 3 hours. Following, the warmed chondrogenesis media from StemPro™ Chondrogenesis Differentiation Kit (Thermo Fisher Scientific) was added gently to culture vessels. The cell pellets were cultivated in an incubator at 29.5°C with 5.5% CO2. The half of differentiation medium was exchanged every 2–3 days. Cells in growth medium were used as a control. After 10 days, the pellets were fixed and embedded in OCT for cryostat sectioning. Alcian blue staining was used to assess the formation of extracellular matrix, a hallmark of chondrogenic differentiation. The expression of a chondrogenic marker (collagen type II) was also analyzed by immunofluorescent staining.

To differentiate XtiSCs into osteocytes, StemPro™ Osteogenesis Differentiation Kit (Thermo Fisher Scientific) was used. The single XtiSC suspension was seed into 6-well plate at 5×10^3 cells/cm^2 in growth medium (without phenol red) for 24 hours, then replaced with Complete Osteogenesis Differentiation Medium as the manufacturer's instruction. Only half of the medium was changed each 3-4 days. Control cells were cultured in standard growth medium. After 21 days the cells were stained with Alizarin

Red and quantitation of Alizarin Red staining was done by The Osteogenesis Quantitation Kit (Millipore). Cells were fixed with 10% formaldehyde at room temperature for 15 min., rinsed thoroughly, and Alizarin Red Stain Solution was added into each well for at least 20 min. The excess dye was removed by washing 4 times with deionized water. Differentiated cells containing mineral deposits are stained bright red by the Alizarin red solution. The cells were imaged under microscopy before extracting the dye from stained monolayer at low pH with 10% acetic acid at 85°C for 10 min. The supernatant was neutralized by 10% ammonium hydroxide to pH 4.1-4.5 and quantified directly by colorimetric method.

Adipogenic differentiation of XtiSCs was performed by adding 1 μM dexamethasone, 0.2 mM indomethacin, 0.1 mg/ml insulin, 1 mM 3-isobutyl-1-methylxanthine to 33.3% L-15 and 33.3% RPMI 1640 with 10% FBS to a confluent cell culture as described elsewhere (L. Wu et al. 2009). The medium was changed every 2 days. After 21 days, Oil Red-O staining was used to assess adipogenic differentiation. XtiSCs were fixed in a 10% formaldehyde solution for 1 hr, washed with 60% isopropanol and stained with Oil Red O solution (in 60% isopropanol) for 5 mins. Following, the excess dye was washed out with PBS repeatedly until the solution was colorless. The oil drops of differentiated cells were stained with bright red and imaged under microscope.

3.13 *In vitro* migration assay

Another feature of EMT-shifted cells, directed migration ability towards cancer cells, was examined in XtiSCs. HeLa cells, a cervical cancer cell line, and HEK cells, a human embryonic kidney cell line, were chosen as an attractant and negative control for *in vitro* migration test, respectively because of their different cell shape from XtiSCs. Paraffin wax was used to fix a collagen-coating cover glass on a Superfrost plus slide and to make a narrow slot between them for cell culture (ThermoFisher Scientific). The slot was filled with 100 μl suspension of $1.3x10^5$ XtiSCs. This chamber was cultured vertically using the indicated medium until reaching confluency (3-4 days). The induction medium was then replaced with 120 μl of low FBS medium (with 0.5% FBS) plus 10% PL-matrix (PL BioScience, Aachen, Germany) to make a detection zone above the cell layer (Fig. 25A). The backside of the cell growth area was covered with a white

adhesive label to distinguish it from the detection zone. HeLa cell suspension of 10^5 cells was then added after the complete solidification of PL-matrix (about 1 hour in an incubator), in the control group HEK cell suspension was used alternatively. After 2 days, the number of cells migrating into the detection zone was counted based on at least five microscope pictures per experimental group. The average of the number of cells per mm^2 is depicted in the result part below.

3.14 *In vivo* wound assay

To investigate wound homing capacity of XtiSCs wound assay was conducted as described in a previous study (Paredes et al. 2015) with some modifications. Briefly, stage 51 or elder (around 3-week old) *X. tropicalis* larvae were anesthetized with 0.01% tricaine (MS-222) and immersed in 6% Ficoll, 0.1 x MMR, and 0.1% BSA to prevent the leakage of injected cells. Two hundred Katushka RFP positive XtiSCs (40 nL) treated or untreated with CHIR99021 had been microinjected into larvae through blood vessels near the abdomen. Immediately after microinjection, the distal third of the tail with 6 mm distance from the injection site was wounded by #55 Forceps (Fine Scientific Tool). Transplanted *X. tropicalis* larvae without injury were used as a control. The injected tadpoles were transferred and kept in the 3% Ficoll solution for at least 30 minutes, and then exchanged to low salted water until imaging. The tadpoles were imaged after 6 hours under the fluorescence stereomicroscope (Olympus). Two days later, the wounded tadpoles were collected, fixed, and sectioned for immunohistochemistry employing antibody against fibronectin.

3.15 Dissociation of tadpoles and flow cytometry analysis

The tadpoles at an indicated time point were collected and sacrificed by 0.4% tricaine. Intestines were removed to avoid autofluorescence from intestinal bacteria before immersing small pieces of tadpoles in 0.05% collagenase type 1A in 0.036 mM $CaCl_2$ for 1 hour at RT. The collagenase was inhibited by adding EDTA to 5 mM final concentration. The supernatant was removed by centrifugation and then exchanged for 0.025% trypsin-EDTA solution overnight at 4°C. In the next day, trypsin was activated at 37°C for 20-30 minutes to dissociate tadpoles completely by pipetting several times and then filtering through 20 μm. Cells were collected by centrifuge at 1200 rpm for 5

minutes and suspended in PBS for flow cytometry analysis. Tadpoles without injected RFP- positive cells was as a negative control.

Cells were washed with PBS, collected by scrapers, fixed with 4% formaldehyde for 10 minutes, rinsed and incubated with primary antibodies for 1 hour at room temperature, following staining with Alexa488- conjugated secondary antibodies (Life Technologies, 1:500) for 30 minutes. Cells incubated with only secondary antibodies were used as a control. Stained cells or dissociated tadpoles were analyzed by flow cytometer (BD LSR II) accompanied by BD FACSDIVA™ software for data analysis.

3.16 Statistical analysis

All assays were repeated at least in three independent experiments. All the data were expressed as mean ± standard deviation (SD). For evaluation of group differences, the unpaired Student's *t*-test was used assuming equal variance. A P value of <0.05 was accepted as significant.

Chapter 4

RESULTS

4.1 The dynamic of Cytokeratin during Sertoli cell development

The testes of juvenile (5-month old) and adult (3-year old) male *X. tropicalis* were collected and sectioned to visualize Sertoli cells (SCs) at different stages of testicular development. H&E staining of paraffin sections from juvenile testes showed well-organized seminiferous tubules. However, most tubules were small and narrow due to the incomplete development of tubular lumen compared to ones from 3-years old individuals (Fig. 9). On the contrary, the expanded lumens in the center of seminiferous tubules filled with spermatozoa were observed in the mature sexual frogs. Therefore, the germinal epithelium of young testes lying on the basal membrane was thicker than in older individuals.

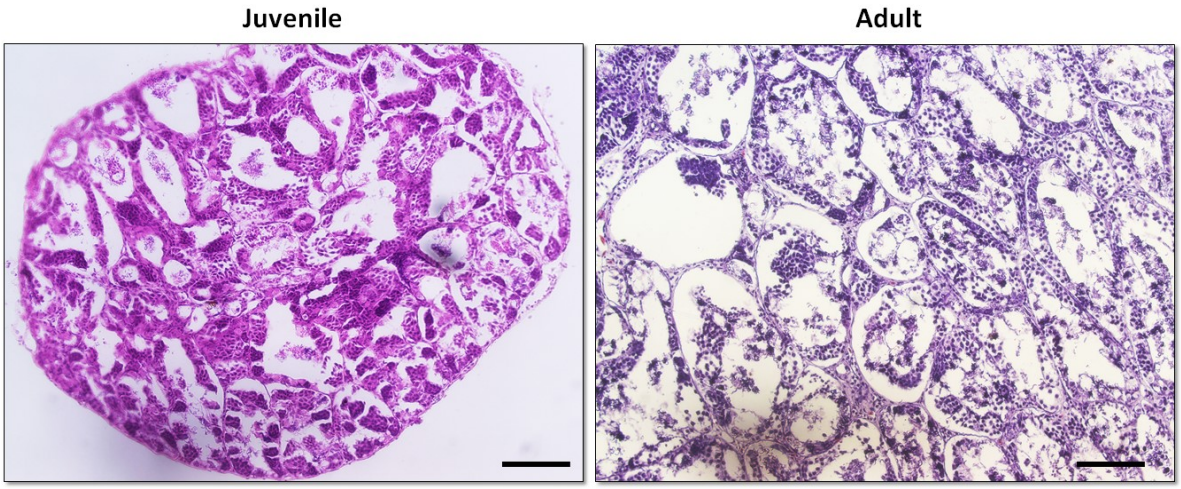

Figure 9: H&E staining of 5-month and 3-year old *X. tropicalis* testes.
Scale bar: 100 µm.

The dynamics of CK in Sertoli cells was verified by double staining of testicular sections from juvenile and adult *X. tropicalis* with two antibodies against cytokeratin/Sox9 or vimentin/Sox9 (Sox9, a Sertoli cell marker). In the young testes, SCs positively stained with Sox9 antibody in their nuclei were detected both, sitting inside seminiferous tubules and migrating outside the tubules (SC progenitors) (Fig. 10A). On the contrary, most of SCs were localized only inside the tubules in adult frogs (Fig. 10B). Although intermediate filament, vimentin is visible consistently in SCs, the

expression of CK changed regarding their developmental state. Immunostaining showed that there was little to no CK in migrating and adult Sertoli cells (Fig. 10, A&B), however the tubular SCs of premature testicles strongly expressed this IF (Fig. 10A&B).

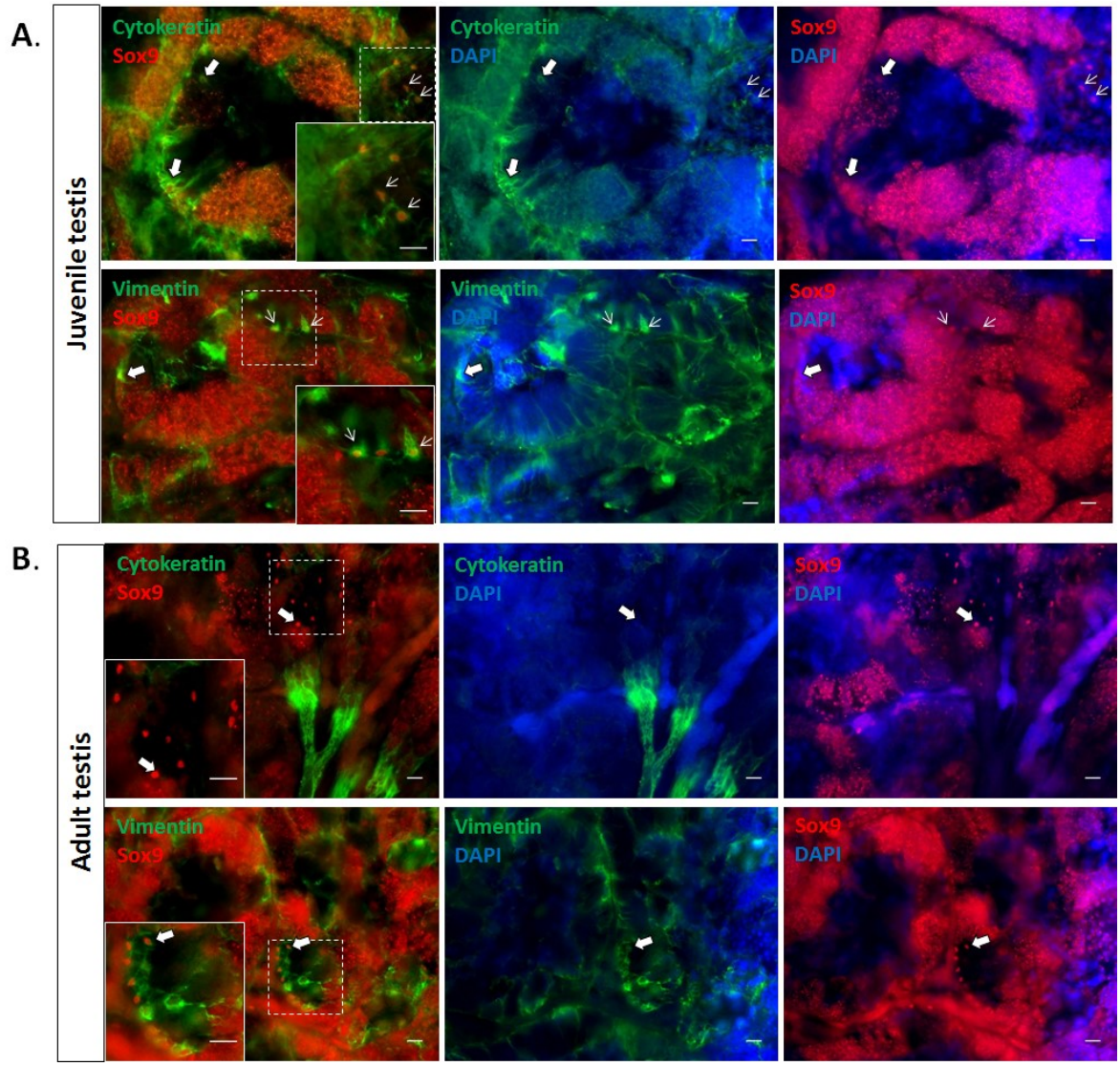

Figure 10: Immunohistochemistry of testicular cross-sections of juvenile and adult *Xenopus tropicalis.*
(A) Testicular cross-sections from juvenile *Xenopus tropicalis* stained with two antibodies, cytokeratin (green)/Sox9 (red, SC marker) or vimentin (green)/Sox9 (Sox9, a Sertoli cell marker). Thin arrows show Sox9-positive migrating cells (SCs) or pre-SCs outside the seminiferous tubules. Thick arrows indicate Sox9-positive SCs inside the tubules. Cytokeratin is absent in pre-SCs, in contrast to tubular SCs. On the other hand, vimentin is present in both types, migrating and tubular SCs. (B) Double staining of testicular cross-sections with two antibodies, cytokeratin (green)/Sox9 (red) or vimentin (green)/Sox9 from adult *Xenopus tropicalis.* The only vimentin is observed in SCs

Interestingly, we also observed another protein, β-catenin which expressed along with CK in juvenile testes, but both proteins were suppressed in the adult ones. Here, β-catenin was found mainly on the cell membrane and in the cytoplasm, however, some CK-positive SCs showed weak nuclear staining as well (Fig. 11). Taking together, these

results indicate that CK and β-catenin accompanied by Sox9 can be used as markers of immature Sertoli cells**.**

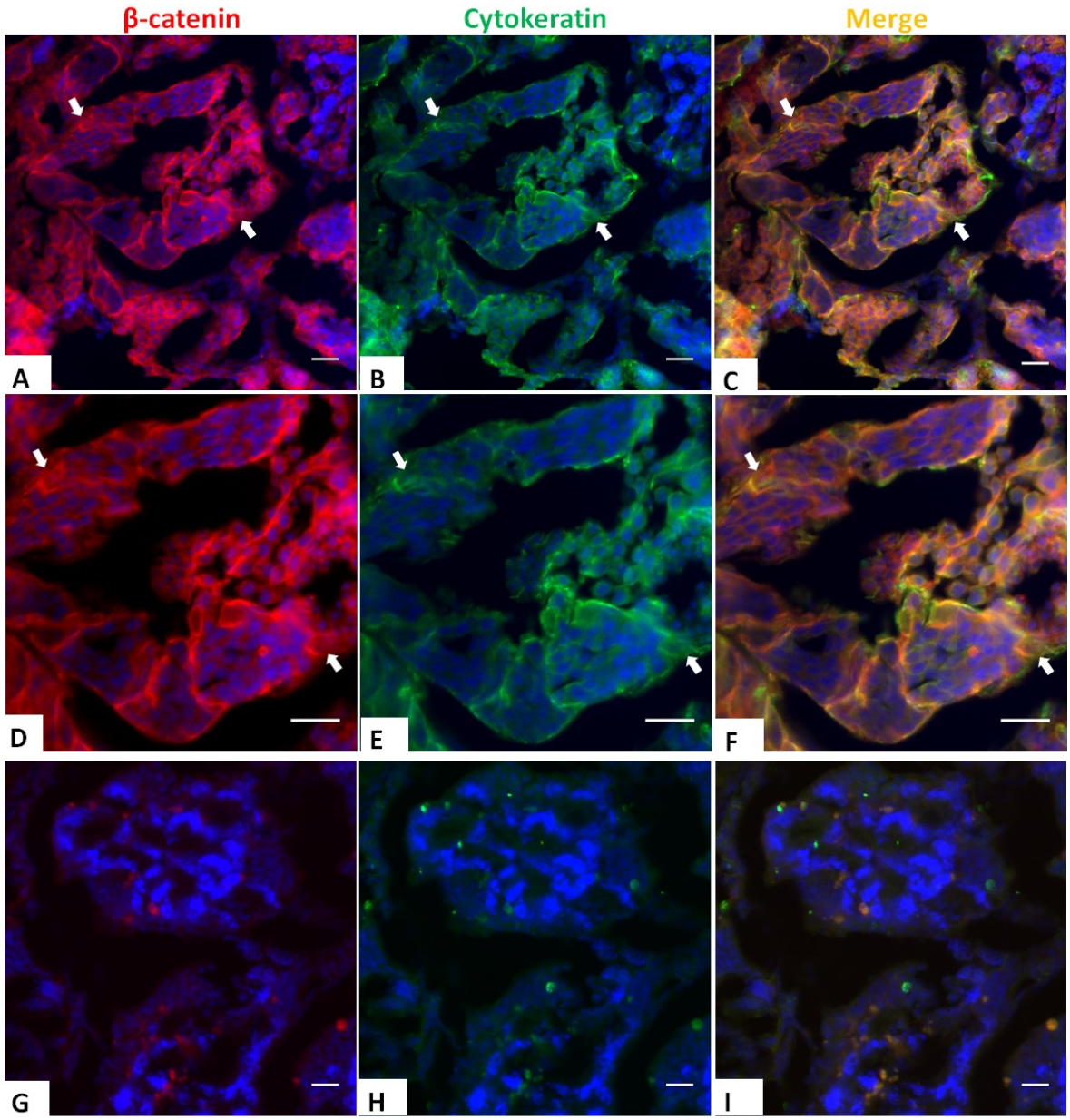

Figure 11: CK and β-catenin staining on testicular sections of juvenile and adult frogs Double staining on testicular sections of juvenile (A-F) and adult frogs (G-I) with CK (mouse, green) and β-catenin (rabbit, red) antibodies; (D-F) show higher magnification of young testes' staining. Nuclei were stained with DAPI (blue). Scale bar: 20 µm. Both proteins are presented in the immature testes, but not in adulthood.

4.2 Characterization of *Xenopus tropicalis* testicular somatic cells

4.2.1 Morphological and gene expression characterization of X. tropicalis testicular cell culture

The cell culture of *Xenopus tropicalis* testicular somatic cells (XtTSCs) was established from juvenile *X. tropicalis* testicles (6-month old) by mechanical dissociation and plating in plastic vessels containing the growth medium supplemented with LIF. After 1.5 months, cells from the testicles adhered on a plastic surface and formed compact colonies with multiple layers (Fig. 12, A&B). Transmission electron microscopy (TEM) was used to visualize their structure. Two or three tight layers of cells were observed in colonies (Fig. 12, E&F). Their shape and size differed from the surrounding feeder cells (Fig. 12E). However, few feeder cells were detected inside the colonies as well (Fig. 12F). In addition, TEM showed also an extensive production of extracellular matrix covering the colonies (Fig. 12F). For the easier cell tracking in transplantation experiments, DNA vector containing the gene encoding Katushka red fluorescent protein under the control of CAG promoter was introduced via nucleofection.

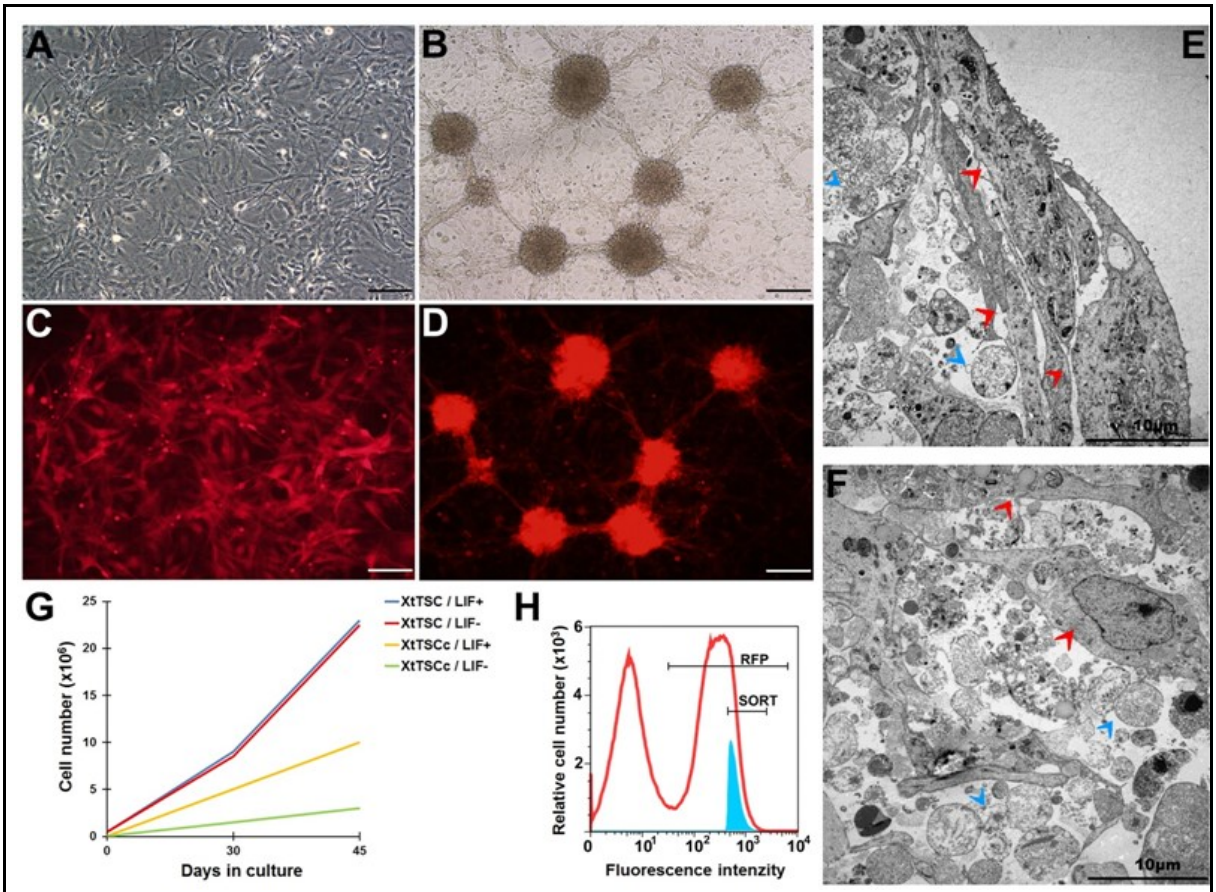

Figure 12: *In vitro* characterization of *XtTSCs*.
(A) The testicular somatic cell culture of the adherent layer (XtTSC) and colonies (XtTSCc) after long-term cultivation (B). (C) *X. tropicalis* transgenic XtTSC expressing Katushka RFP under CAG promoter (XtTSC-RFP). (D) Transgenic Katushka RFP expressing XtTSCs in colonies (XtTSCc-RFP). (E-F) Structure of *in vitro* testicular cell colony visualized by TEM. In the colony, the cells are placed in an extensive amount of extracellular matrix with two or three tight layers of XtTSCs surrounding the colony at the edge (E). Both XtTSCs and XtTSCcs are present in the center of the colony (F). Red arrowheads = XtTSC, blue arrowheads = XtTSCc. (G) *X. tropicalis* cell culture proliferation during long-term cultivation in medium with or without recombinant mouse LIF. (H) FACS sorting after nucleofection. Only about 15% of living transgenic cells with the highest intensity of the fluorescent signal was sorted (blue area). Scale bar in A and C = 100 µm, scale bar in B and D = 200 µm, scale bar in E and F = 10 µm. *Credit: Tereza.T*

Colony-forming and feeder cells were separated and collected for RT-PCR and RT-qPCR analysis to reveal their gene expression profile. Both cell types expressed neither germ cell markers such as *dazl, ddx4 and ddx25* nor markers of Leydig cells *(cyp11a1* and *cyp17a1)*. Despite that, transcript expression of other testicular somatic cell markers, comprising Sertoli cells *(sox9, kitlg, vim and lif),* peritubular myoid cells *(acta2 and lif)* and markers of mesenchymal cells *(itgb1-cd29, cd44 and thy1-cd90)* were detected in both cell types. RT-qPCR analysis of 6 genes in two groups of germ cell and testis associated markers was conducted to confirm RT-PCR data. In consistent with RT-PCR results, the hierarchical clustering showed transcripts of *dazl, ddx25* and

ddx4 were exclusively expressed in testes, whereas expression of *lif* was substantially reduced in comparison with XtTSCs (Fig. 13). These results confirm the somatic origin of isolated testicular cells.

Notably, transcripts of some pluripotency markers, including *klf4 (kruppel-like factor 4)*, *c-myc* and *telomerase reverse transcriptase* (*tert*) were detected in both, colony-forming and feeder XtTSCs (Fig. 13A). However, neither the key pluripotency gene POU5F1 (in *Xenopus tropicalis* p*ou5f3.1, pou5f3.2 and pou5f3.3*) (Morrison and Brickman 2006) nor *sox2 (sex determining region Y box 2)* were found suggesting that XtTSCs are not pluripotent as defined in the mouse model. Unfortunately, since no homolog of *nanog* gene, another key transcriptional factor in pluripotency acquisition (Silva et al. 2009), has been described in *Xenopus* yet, its expression couldn't be determined.

Immunocytochemistry on XtTSCs employing antibodies against markers of Sertoli cells, Sox9 and vimentin revealed their coexpression on more than 90% of the cell population (Fig. 14A). Taken together, we conclude that *X. tropicalis* testicular cell culture represents a population of Sertoli cells. However, they also expressed immature SC proteins, cytokeratin and β-catenin (Fig. 14, B&C). These data indicate that XtTSCs are SCs but not fully mature. There was no different staining between colony-forming and feeder XtTSCs populations. Interestingly, XtTSCs also expressed Sma, a specific protein found in peritubular myoid cells in testis (Fig. 16, A-C). Based on that, to identify the presence of these population cells in adult individuals, agarose-embedded sections of *X. tropicalis* and mouse testes were prepared for double staining with Sox9 and Sma antibodies. We observed few cells expressing both antigens in the interstitial space attached to seminiferous tubules in *X. tropicalis* and even in mouse testis (Fig.16).

A

X. tropicalis gene symbol	Gene name	Gene transcript	Gene expression: testes	XtTSC	XtTSCc	XtTSC-RFP	XtTSCc-RFP
Pluripotent cell markers							
klf4	Kruppel-like factor 4	ENSXETT00000012646					
myc	v-myc avian myelocytomatosis viral oncogene homolog	ENSXETT00000054171					
pou5f3.1	POU class 5 homeobox 3, gene 1	NM_001285474					
pou5f3.2	POU class 5 homeobox 3, gene 2	NM_001129934					
pou5f3.3	POU class 5 homeobox 3, gene 3	NM_001130364					
sox2	SRY (sex determining region Y) - box 2	ENSXETT00000004031					
tert	telomerase reverse transcriptase	ENSXETT00000034113					
Germ cell markers							
dazl	deleted in azoospermia-like	NM_203748					
ddx4	DEAD (Asp-Glu-Ala-Asp) box polypeptide 4	ENSXETT00000066339					
ddx25	DEAD (Asp-Glu-Ala-Asp) box polypeptide 25	ENSXETT00000064463					
Mesenchymal stem cell surface markers							
itgb1	integrin, beta 1 (antigen CD29 includes MDF2)	ENSXETT00000048743					
cd44	CD44 molecule (Indian blood group)	ENSXETT00000016456					
thy1	Thy-1 cell surface antigen	ENSXETT00000046686					
Testis associated markers							
acta2	actin, alpha 2, smooth muscle, aorta	ENSXETT00000020391					
cyp11a1	cytochrome P450, family 11, subfamily A, polypeptide 1	ENSXETT00000011263					
cyp17a1	cytochrome P450, family 17, subfamily A, polypeptide 1	ENSXETT00000033323					
kitlg	KIT ligand ~ Stem Cell Factor	NM_001045596					
lif	leukemia inhibitory factor	ENSXETT00000053337					
sox9	SRY (sex determining region Y) - box 9	ENSXETT00000048344					
vim	vimentin	ENSXETT00000016267					
Housekeeping gene							
odc1	ornithine decarboxylase 1	ENSXETT00000007603					

B

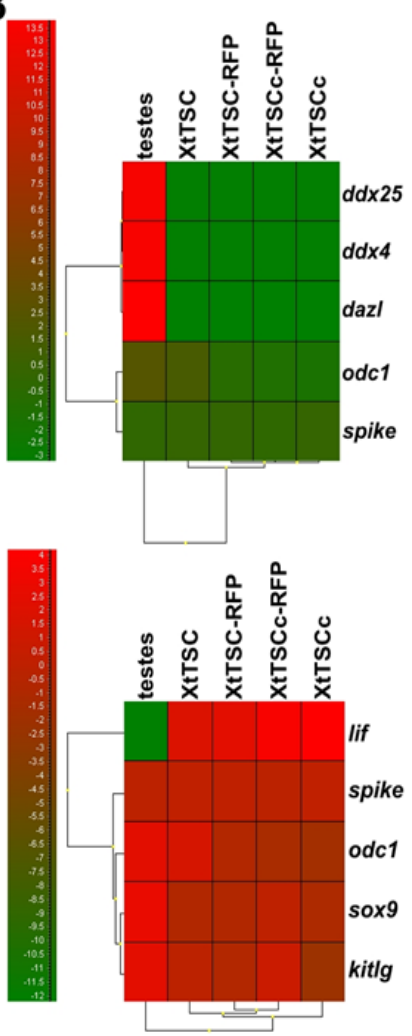

Figure 13: Expression analysis of XtTSCs.
(A) RT-PCR analysis of *X. tropicalis testis*, XtTSC, XtTSCc, XtTSC-RFP and XtTSCc-RFP. (B) Hierarchical clustering presented as qPCR heatmaps of germ cell markers and selected testis associated markers. A scale of colors indicates the level of expression (the highest expression is shown by bright red, whereas the lowest expression is shown by bright green). The similarity between cell types/genes is indicated by the height at which the dendrograms are joined. The RNA spike represents a highly stable transcript across the cell types and odc1 represents housekeeping gene. *Credit: Tereza.T*

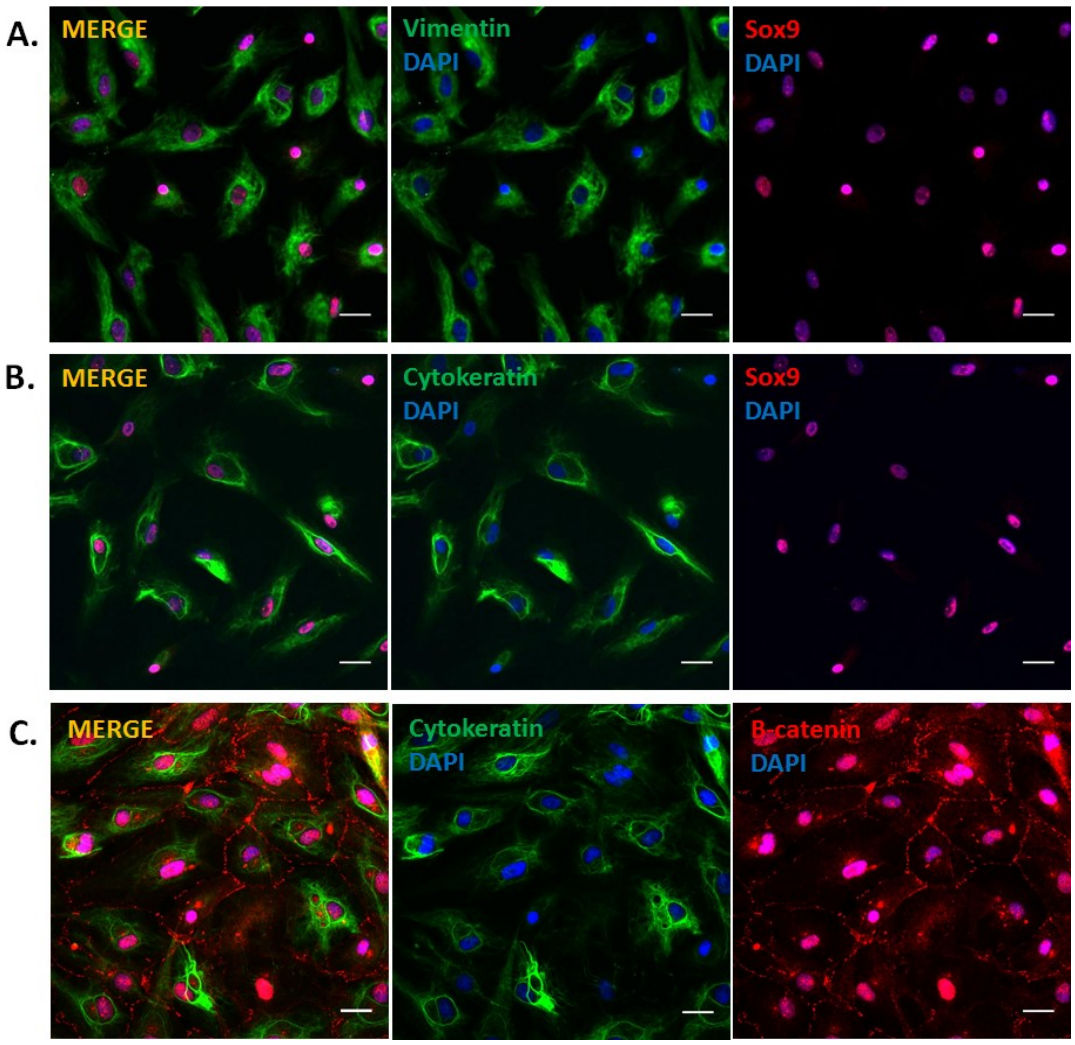

Figure 14: Immunocytochemistry of XtTSCs.
(A) Positive staining of XtTSCs for vimentin, cytokeratin (green), Sox9, and β-catenin (red). Nuclei were counterstained with DAPI (blue). (A) Double staining with vimentin (green) and Sox9 (red) antibodies. (B) Double staining with Cytokeratin (green) and Sox9 (red) antibodies. (C) Double staining with Cytokeratin (green) and β-catenin (red). Scale bar = 20 μm.

Abnormal chromosome and anchorage-independent growth are the hallmarks of malignant cell transformation. After 12 passages, XtTSCs still had normal karyotype consisting of 20 chromosomes in a diploid set (Fig. 15A) and they didn't form colonies in soft agar (Fig. 15B). Other work revealed that XtTSCs kept the same characteristics even after 48 passages (data not showed).

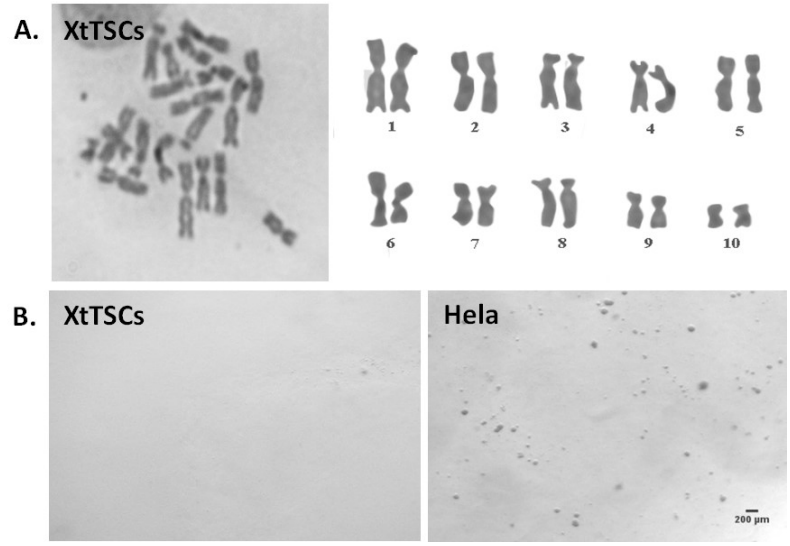

Figure 15: Chromosome analysis (A) and soft agar assay (B)
The data show XtTSCs as non-transformed cells.

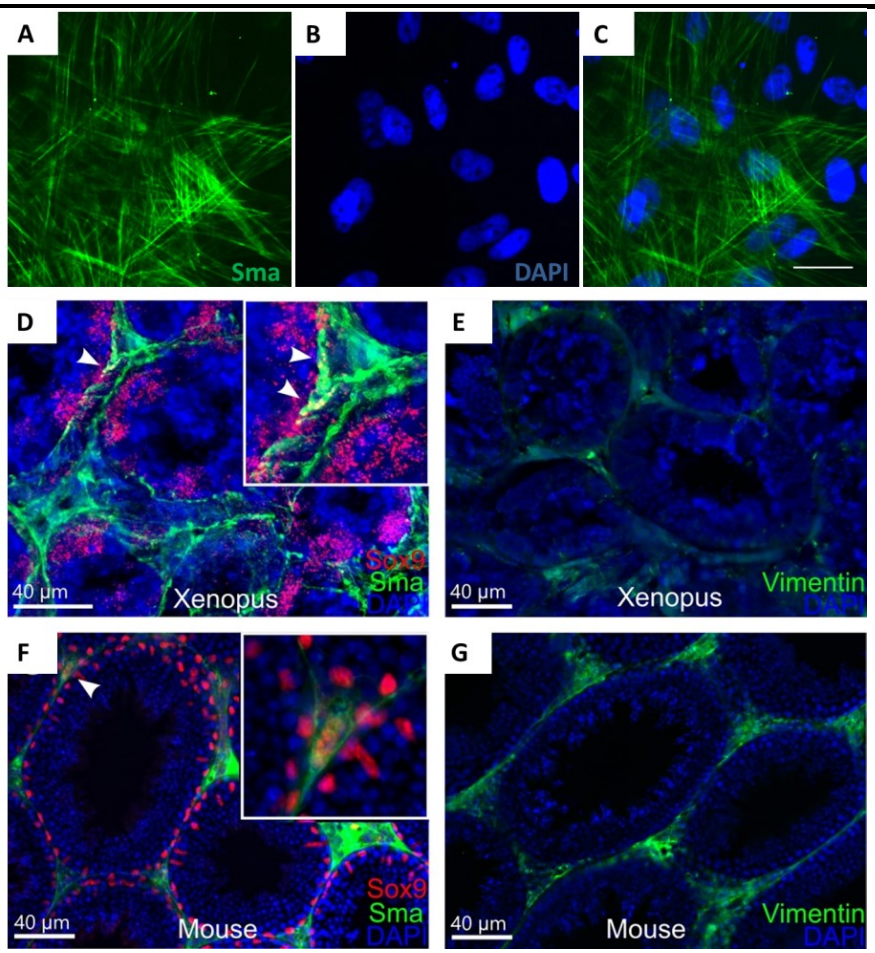

Figure 16: Immunohistochemistry of Sma and Sox9 on testicular section of *X. tropicalis* (D-E) and mouse (F-G).
(A-C) XtTSCs show positive staining with antibody against Sma. (D+F) Double staining with Sox9 (red, rabbit) and Sma (green, mouse) antibodies. White arrow caps refer the potential XtTSCs in testes which expressing both antigens in X. tropicalis (D) and mouse (F). (E+G) Staining with vimentin (green) antibody on X. tropicalis (E) and mouse (G). Nuclei were counterstained with DAPI (blue). Scale bar in (A-C) = 20 µm and in (D-G) = 40 µm.

4.2.2 In vivo characteristics of Xenopus tropicalis testicular somatic cells

Transgenic XtTSC-expressing Katushka under ubiquitous CAG promoter were established to reveal *in vivo* behavior of isolated cells. The characteristics, gene profile and protein expression of transgenic XtTSCs were examined as displayed in (Fig. 12, 13 & 17). The results showed no significant difference between transgenic and normal XtTSCs. Tadpoles at stage 41 which have a clear peritoneal cavity, soft muscle, and immature immune system were used for transplantation. 1000 transgenic colony-forming XtTSCs with strong RFP signal after FACS sorting (Fig. 12H) were microinjected into the peritoneum of the tadpoles through the dorsal side as depicted in (Fig. 18A). Tadpoles containing RPF-positive cells were selected and observed under a fluorescent stereomicroscope at the indicated time points. Most of the transplanted cells accumulated nearby the injection site right after that (2 hours). On the contrary, during the two following weeks, these cells were found scattered inside the tadpoles, mostly in heart and pronephros (Fig. 18, B-E). After 4 weeks of transplantation, injected cells formed dense cell to cell connecting net without serious impact on the tadpole survival (Fig. 18, F&G).

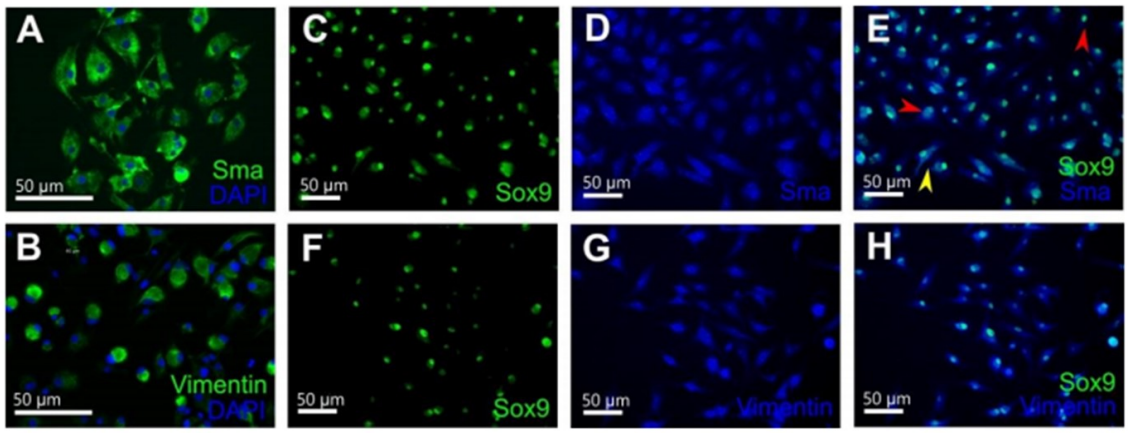

Figure 17: Immunocytochemistry of *X. tropicalis* testicular cell culture expressing Katushka RFP.
Positive staining for Sma (green) (A) and Vimentin (green) (B). Nuclei were counterstained with DAPI (blue). (C-E) Double staining with Sox9 (green) (C) and Sma (blue) (D) antibodies. (E) Merge of C and D. Yellow arrowhead - cell expressing both antigens, red arrowheads - cells expressing only Sox9 or only Sma. (F-H) Double staining with Sox9 (green) (F) and vimentin (blue) (G) antibodies. (H) - merge of F and G. Scale bar = 50 µm.

To reveal *in vivo* expression and behavior of XtTSCs, immunohistochemical analysis of agarose-embedded sections of tadpoles 0, 1 and 30 days after transplantation was performed (Fig. 18H). In spite of the fact that the transgenic XtTSCs expressed

Sox9, Sma and vimentin prior to microinjection (Fig. 17), only a strong vimentin expression but not Sox9 and Sma was observed in the RFP-positive cells even only 2 hours (group ‘day 0’) after transplantation. Notably, 30 days after microinjection Sox9 expression was detected in a few transplanted cells. Since feeder XtTSCs showed a similar migration and expression pattern as colony-forming cells, here we presented only data concerning transplantation of testicular somatic cell derived from colonies (XtTSCc).

Fluorescent immunostaining on the injected-tadpole sections with antibodies against specific tissue markers, including cardiac troponin T (cardiomyocyte marker), zn12 (specific neuronal surface marker), tropomyosin (skeletal muscle marker) was also conducted. However, no positive staining of XtTSCs was observed with all antibodies mentioned above, indicating restricted *in vivo* differentiation potential of XtTSCs.

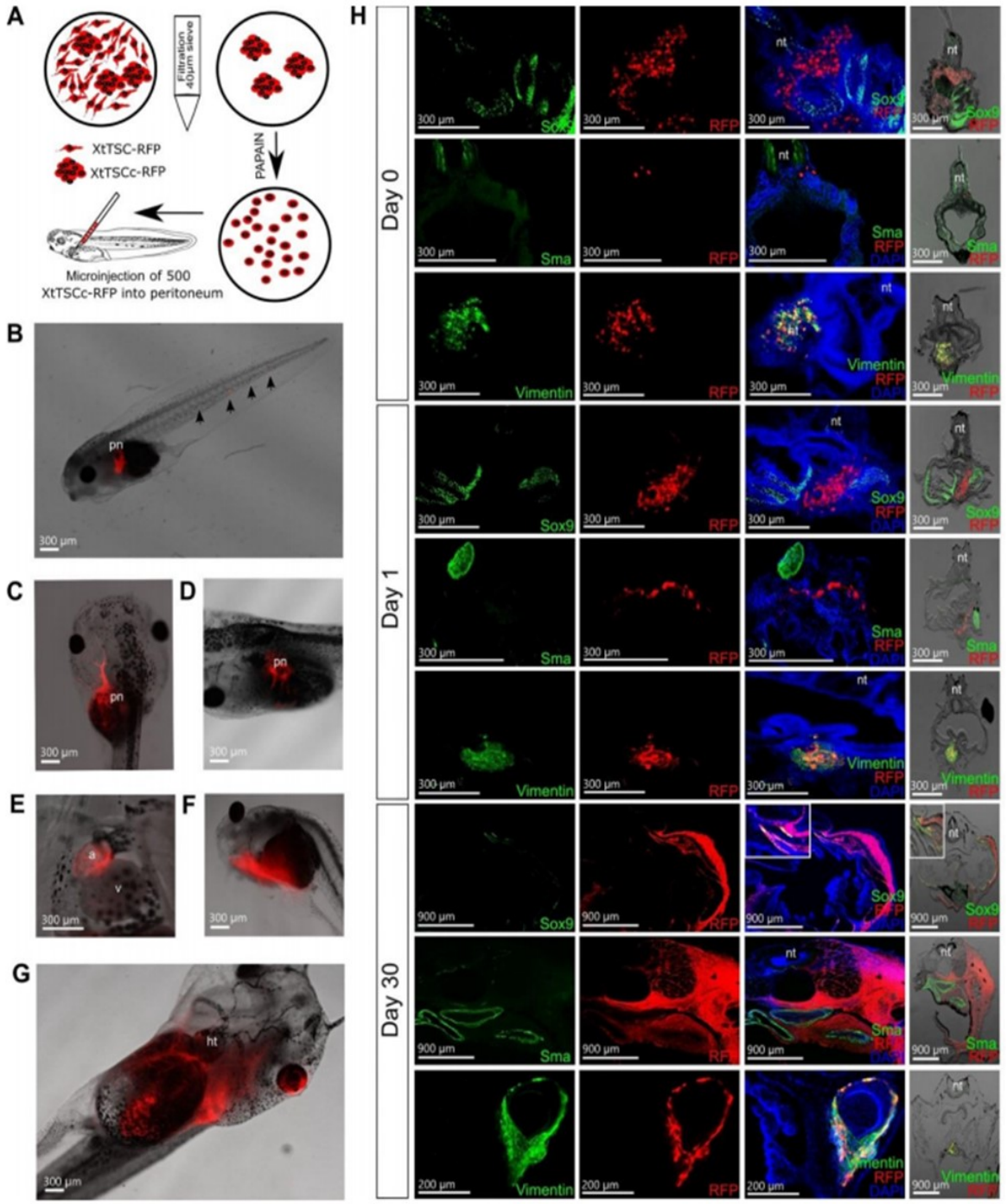

Figure 18: Migration potential of *X. tropicalis* testicular somatic cells
Allogeneic transplantation into the peritoneal cavity of tadpoles in st. 41. (A) Scheme of XtTSCc-RFP preparation prior to transplantation. (B-G) Observation of RFP positive cells in transplanted tadpoles under stereo microscopy. (B) Cell deposit in pronephros and tail 1 day after microinjection. (C-D) Cell deposits in pronephros 13 days after microinjection. (E) Migration of RFP positive cells into heart atrium 15 days after transplantation. (F-G) Cell to cell net growing through the tadpole body observable 30 days after microinjection. (H) Immunohistochemistry of agarose-embedded sections of transplanted tadpoles using antibodies against Sox9, Sma and vimentin (green) and Katushka RFP (red) at 0, 1 and 30 days after transplantation. RFP positive cells were stained with vimentin antibody but not Sox9 or Sma even 2 hours after transplantation. 30 days after microinjection few cells start to express Sox9 indicating potential redifferentiation into Sertoli cells or chondrocytes where Sox9 is considered as a specific marker. The figures in each line were taken under

fluorescence microscopy. The figures on the right side were taken under fluorescence stereomicroscope. Nuclei were counterstained with DAPI (blue). Scale bars in B-G and in H (0 and 1 day) = 300 μm. Scale bars in H (30 days, staining with Sox9 and Sma antibodies) = 900 μm. Scale bar in H (30 days, staining with vimentin antibody) = 200 μm.

4.3 EMT promoted differentiation potential of immature Sertoli cells

EMT and MET in developing gonad have also been observed. The proper formation of testicular seminiferous tubules depends on the migration of Sertoli cell precursors altogether with PGCs (primordial germ cells). However, later on, the key event is their aggregation and differentiation of Sertoli cells to an epithelial polarized cell type via MET in the seminiferous cord (Kanai et al. 1991). A number of morphological changes correlate with differentiation of Sertoli cells including the upregulation of epithelial cell markers (for example CK) which is then no longer expressed around prepuberty (Paranko et al. 1986). Interestingly, the mesenchymal intermediate filament, vimentin is still expressed in fully matured Sertoli cells indicating their mesenchymal origin. Therefore, co-expression of CK and Vimentin has been considered as a marker of "dedifferentiated" or "trans-differentiated" Sertoli cells in the early stage of gonad development (Paranko et al. 1986; Rogatsch et al. 1996).

As mentioned in two previous parts, in contrast to their mesenchymal phenotype XtTSCs have still expressed epithelial intermediate filament, cytokeratin. The co-expression of vimentin and cytokeratin (Fig. 15) may indicate their transdifferentiation state, in other words, they are the immature Sertoli cells. For this reason, from now the isolated testicular somatic cells are called "***X**enopus **t**ropicalis* **i**mmature **S**ertoli **c**ells" (XtiSCs).

The negative results from immunohistochemistry on tadpole sections with tissue-specific markers suggest that XtiSCs are not in "stemness window" as defined in (Jolly et al. 2015). Thus, EMT would be beneficial for getting them back to a stem cell phenotype.

In the next part, we are going to investigate the EMT activation of XtiSCs and their stemness features. GSK-3 inhibitors (CHIR99021 and LiCl), FGF2 and/or TGF-β1 ligands were used in XtiSCs culture to induce EMT.

4.3.1 Pharmacological inhibition of GSK-3 by CHIR99021 induced EMT in XtiSCs

Expression of the key EMT transcription factors such as Snai1, Zeb1 and *twist* transcript was upregulated after three-day incubation of XtiSCs with 3 μM CHIR99021 as revealed by immunofluorescent staining (Fig. 19D, 23A) and by RT-PCR analysis (Fig. 19B). The downregulation of cytokeratin (Fig. 19C) was also observed in cells treated with the GSK-3 inhibitor. On the other hand, cell-cell junctions were disrupted as evidenced by the disappearance of β-catenin on the cell membrane (Fig. 19C), inducing the change in cell morphology to spindle-like cell shape (Fig. 19A). Alternatively, cell-matrix adhesions, fibronectin and its receptor, α5β1 integrin were produced (Fig. 19D) to attach the CHIR-treated cells on hydrophilic plastic or collagen-coated surface, but not on poly-Lysine-coated nor glass surface (Fig. 20). On the other hand, CHIR99021 is responsible for Stat3 suppression (Fig. 21).

FGF2 upregulated the Zeb1 and Stat3 expression in XtiSCs (Fig. 21, 23A) but not other mesenchymal markers. The epithelial markers, such as CK (Fig. 19) were still presented in FGF2-treated cells.

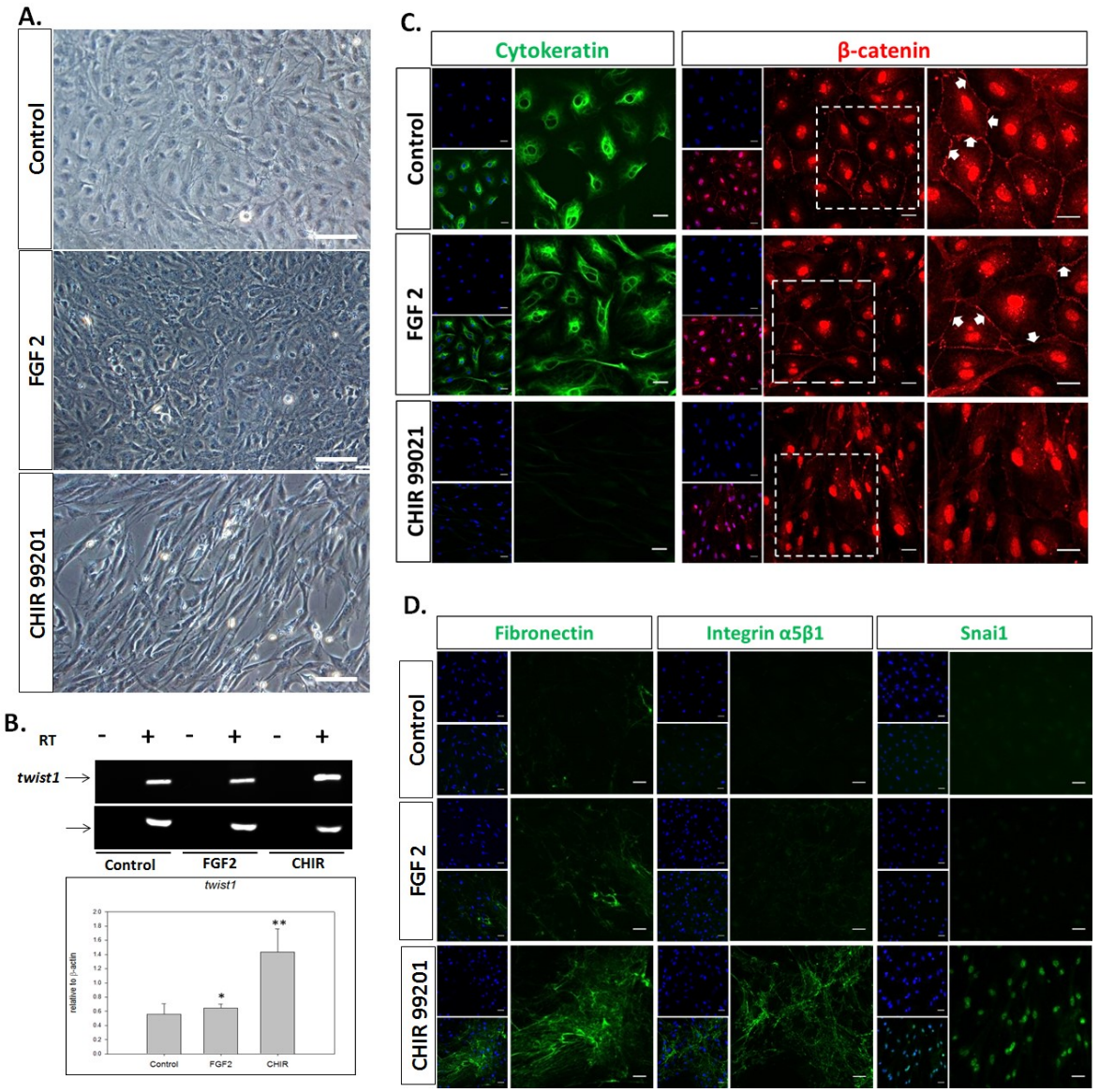

Figure 19: GSK3 inhibitor (CHIR99021) stimulates EMT in XtiSCs cell culture. XtiSCs were cultured in growth medium supplemented with 25 ng/ml FGF2 or 3 µM CHIR99021, or 0.1% DMSO as a control. (A) After three-day treatment, the morphological change of XtiSCs from cobblestone shape to a long-rod shape in medium with CHIR99021 was observed. Scale bar: 100 µm. (B-D) RT-PCR analysis and immunofluorescent staining showed the downregulation of epithelial markers (Cytokeratin, β-catenin at plasma cell membrane) (C), and the increase of mesenchymal markers (Fibronectin, Integrin α5β1, Snai1, and *twist1*) (B, D). Arrows show the expression of β-catenin at the plasma cell membrane. Nuclei stained with DAPI. Scale bar: 20 µm. Results are representative of three biological replicates. *p<0.5, **p<0.001.

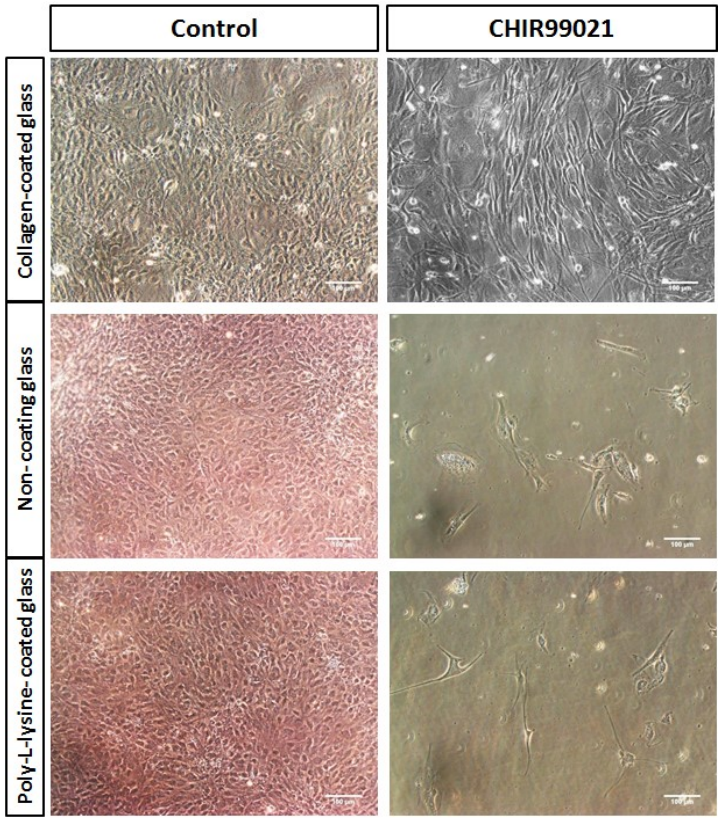

Figure 20: XtiSCs on microscopic glass coated with various materials.
CHIR99021- treated XtiSCs were able to grow only on the collagen type I- coated glass, but not on the non-coated or poly-L-lysine coated glass. In contrary, cells with 0.1% DMSO (control) were not affected by the coating materials. Scale bar: 100 µm.

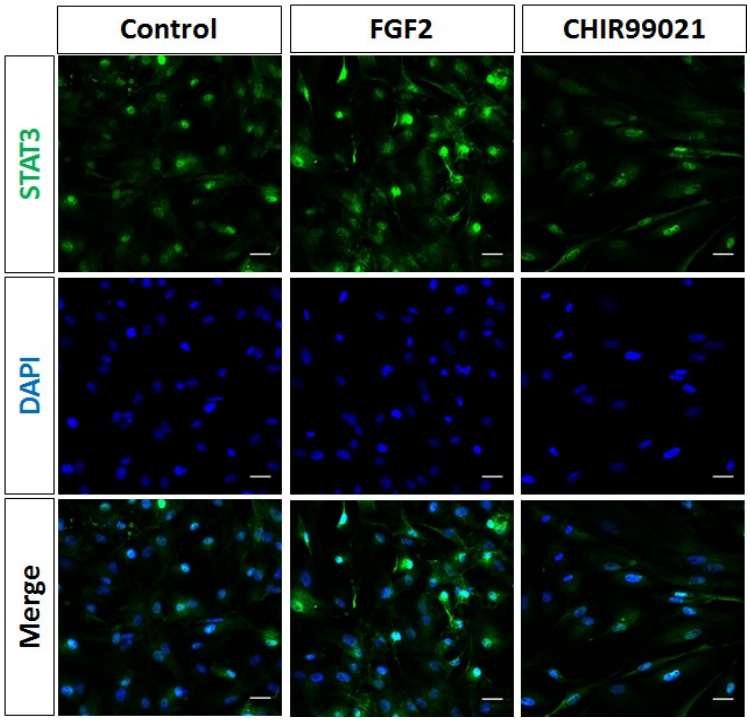

Figure 21: The representative fluorescent images of Stat3 expression
Stat3 expression in XtiSCs in different medium culture. Nuclei were stained with DAPI. Scale bar: 20 µm.

XtiSCs didn't respond to 10 mM LiCl after 3-day treatment. At 20 mM solution, cells died after 24 hours. 40 mM concentration led to cell death even after 6 hours (data not shown).

Even though TGF- β1 is a common EMT inducer, this growth factor has another effect on XtiSCs rather than EMT induction. At the concentration of 2.5 ng/ml or 5 ng/ml, TGF- β1 triggered the higher activity of β-galactosidase at pH 6.0 (positive staining of senescent cells using X-gal) (Fig. 22B) in XtiSCs which became bigger and flatter cells after 3 days as well (Fig. 22A). The thick and parallel stress fibers were also observed in TGF-β1-treated XtiSCs as visualized by F-actin staining with Alexa-594-conjugated phalloidin. All groups of cells expressed cytokeratin (Fig. 22C). These results indicated that TGF-β1 induced senescence in XtiSCs and eventual cell death after 24-hour treatment with TGF- β1 at the concentration of 10 ng/ml (data not shown). The same results were observed in cells treated with TGF-β1 at different time-courses (5 days and 7 days) (data not shown). Therefore, all results presented in the following parts include only experiments employing FGF2 and CHIR99021.

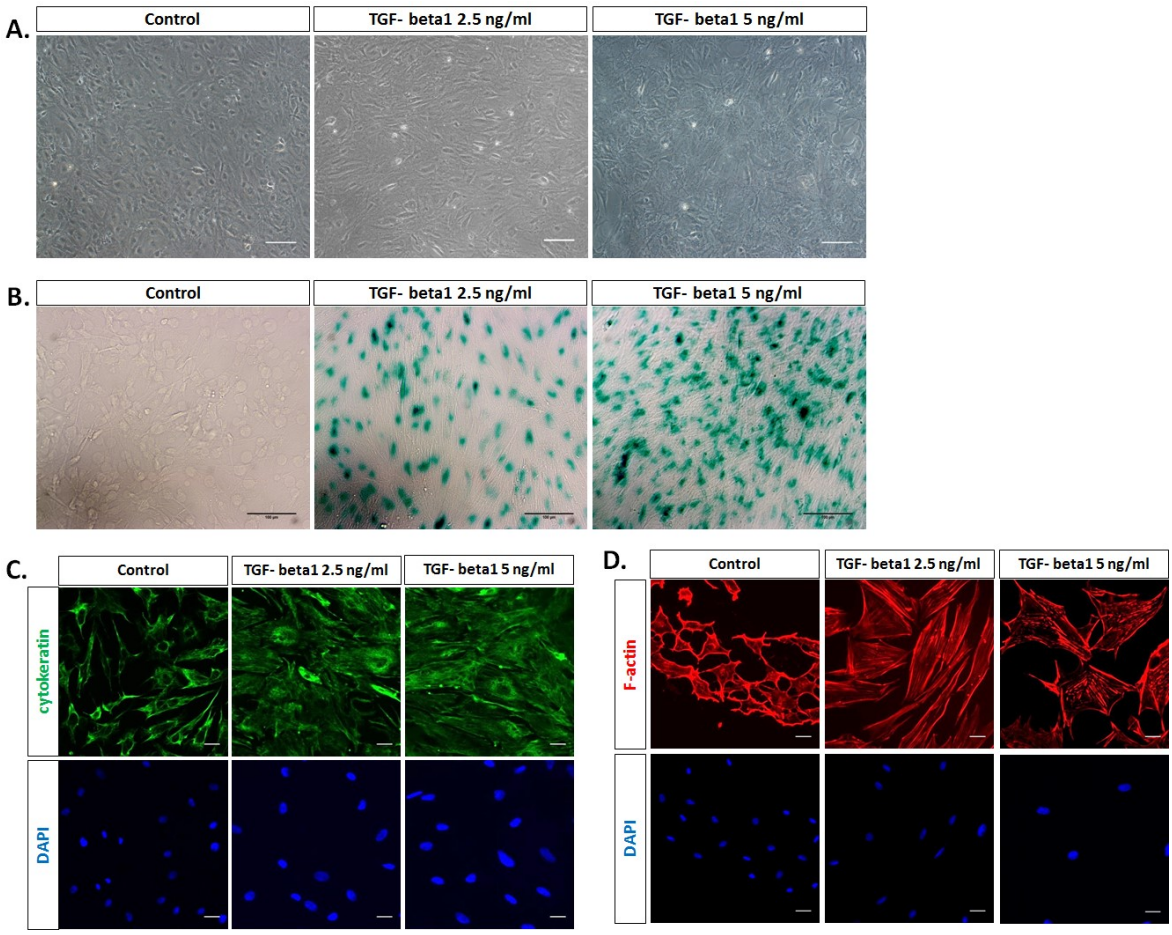

Figure 22: XtiSCs became senescent after 3 days treatment with TGF-β1.
Phase-contrast images (A), X-gal (B) and Phalloidin (F-actin) staining (C) showed the XtiSCs change of shape into bigger and flat cells, and the increase of galactosidase activity, a senescent marker after TGF-β1 treatment. XtiSCs untreated or treated with TGF-β1 still expressed the epithelial interfilament, cytokeratin (D). Phase- contrast images with scale bar: 100 µm. Nuclei were stained with DAPI. Immunofluorescent images with scale bar: 20 µm.

Taking together, GSK-3 inhibitor (CHIR99021) stimulated XtiSCs undergoing full EMT by up-regulation of mesenchymal and down-regulation of epithelial proteins. Whereas, only partial EMT accompanied by the upregulation of Zeb1 and Stat3 was observed in FGF2-treated cells.

4.3.2 EMT promoted the XtiSCs stemness and migration potential in vitro.

Next, we investigated the stemness of vehicle and treated XtiSCs *in vitro*. The expression of stem cell marker Sox2 was observed in either full EMT (CHIR99021) or partial EMT (FGF2) XtiSCs as revealed by immunocytochemistry staining (Fig. 23A). Transcript of mesenchymal stem cell surface marker *cd44* was increased 56-fold (0.53±0.048) and 44-fold (0.44±0.026) in both, FGF2 and CHIR99021 treated groups, respectively if compared with the vehicle (Fig. 23B). However, Smooth muscle actin (Acta2), the earliest marker of mural cells was suppressed in XtiSCs only by

CHIR99021 (Fig. 23A). The data suggest that the GSK3 inhibitor has induced XtiSCs reprogramming.

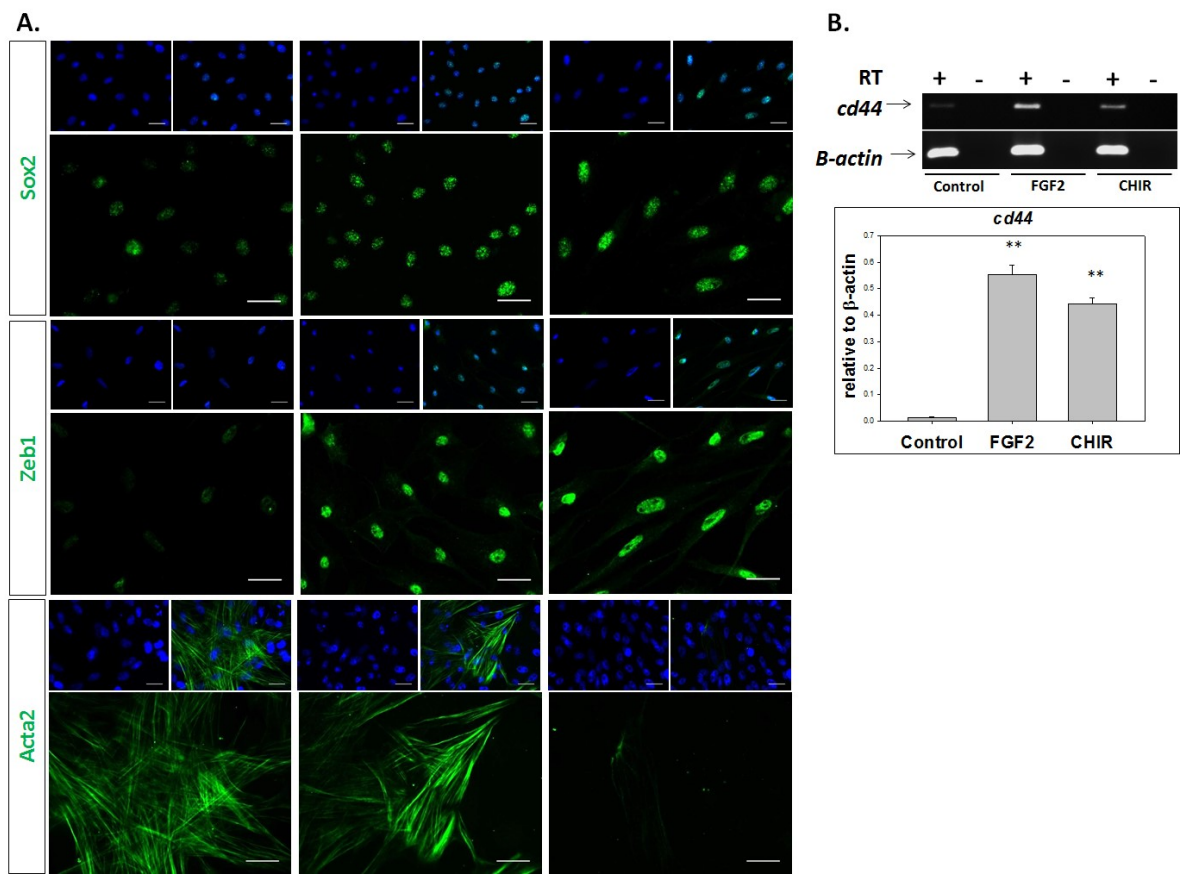

Figure 23: The expression of mesenchymal stem cell markers in FGF2 and CHIR99021- treated XtiSCs.
Immunofluorescent staining (A) and RT-PCR (B) show the increased expression of stem cell marker Sox2, *cd44* and Zeb1 after FGF2 and CHIR99021 treatment. However, only CHIR-treated XtiSCs suppressed Acta2, the earliest marker of mural cell progenitors. RT, reverse transcriptase. Scale bar: 20 µm. Nuclei stained with DAPI. Results are representative of three biological replicates. **p<0.01.

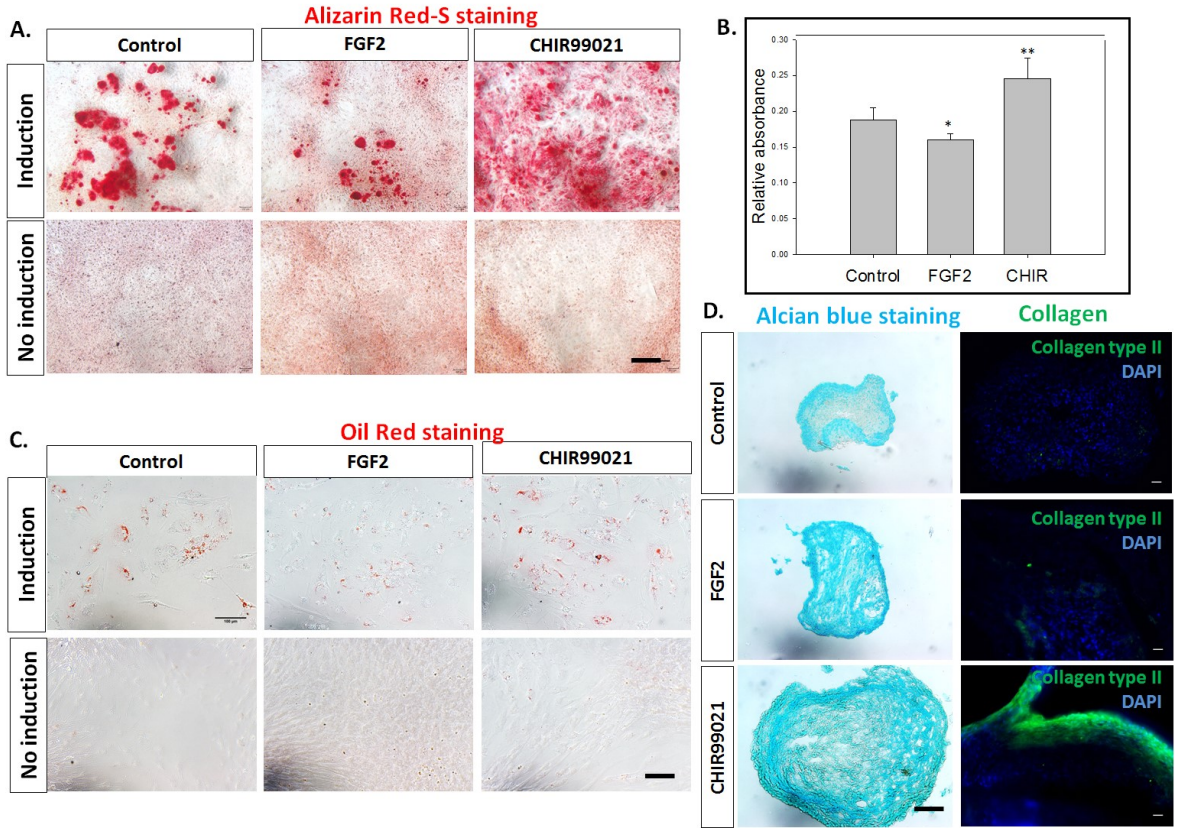

Figure 24: *In vitro* differentiation of XtiSCs.
(A, B) Osteogenesis induction. Cells were immersed into Osteogenesis medium for 14 days, then stained with Alizarin red-S for examining Calcium deposit (A). Lower panels are cells in the growth medium as a negative control. Alizarin red-S-stained cells were lysed and measured absorbance at 420 nm. The relative absorbance was reduced to a respective negative control (B). Data are expressed as the mean (n= 4) with error bars representing standard deviations. **p<0.01. (C) Microscope images were taken to visualize red *oil droplets* staining in Oil red of XtiSCs in adipogenesis medium. Scale bar: 100 µm. (D) A drop of treated or untreated XtiSCs was seeded into plastic plate overnight before being induced with chondrogenesis medium. XtiSCs in growth medium didn't form pellets. XtiSC pellets were sectioned and stained with Alcian blue or the antibody against Collagen type II, a maker of chondrocytes. Microscope images show the sections in the middle of pellets.

Following, we examined the differentiation potential of XtiSCs into three typical mesenchymal cell lineages *in vitro*. Although osteocytes and adipocytes could be induced in all groups of cells, CHIR-treated cells showed higher efficiency in comparison to the vehicle or FGF2 cells (Fig. 24, A-C). After 14 days in the osteogenic induction medium, calcium deposit was determined by alizarin red staining followed by colorimetric analysis of cell lysate. Relative absorbance of the lysate from cells pretreated with CHIR99021 (0.2457±0.026) was significantly higher than vehicle (0.1879±0.015) and FGF2- treated cells (0.1607±0.004) (Fig. 24, A&B). Micromass culture technique was used to induce chondrocyte differentiation in XtiSCs, and only cells in the induction medium, but not in the growth medium, could form cell pellets.

Two weeks after induction, alcian blue staining and immunofluorescence analysis were employed on cryostat sections of the cell pellets. The size and shape of pellets differed among experimental groups. The biggest and round shaped spheres were characterized for pellets from CHIR-treated cells. Moreover, collagen type II, a cartilage-specific marker was expressed on the outside surface of pellets formed by cells pretreated with CHIR99021 (Fig. 24D). These data confirm the mesenchymal origin of XtiSCs, and their reprogramming to stem cell-like cells using GSK3 inhibitor.

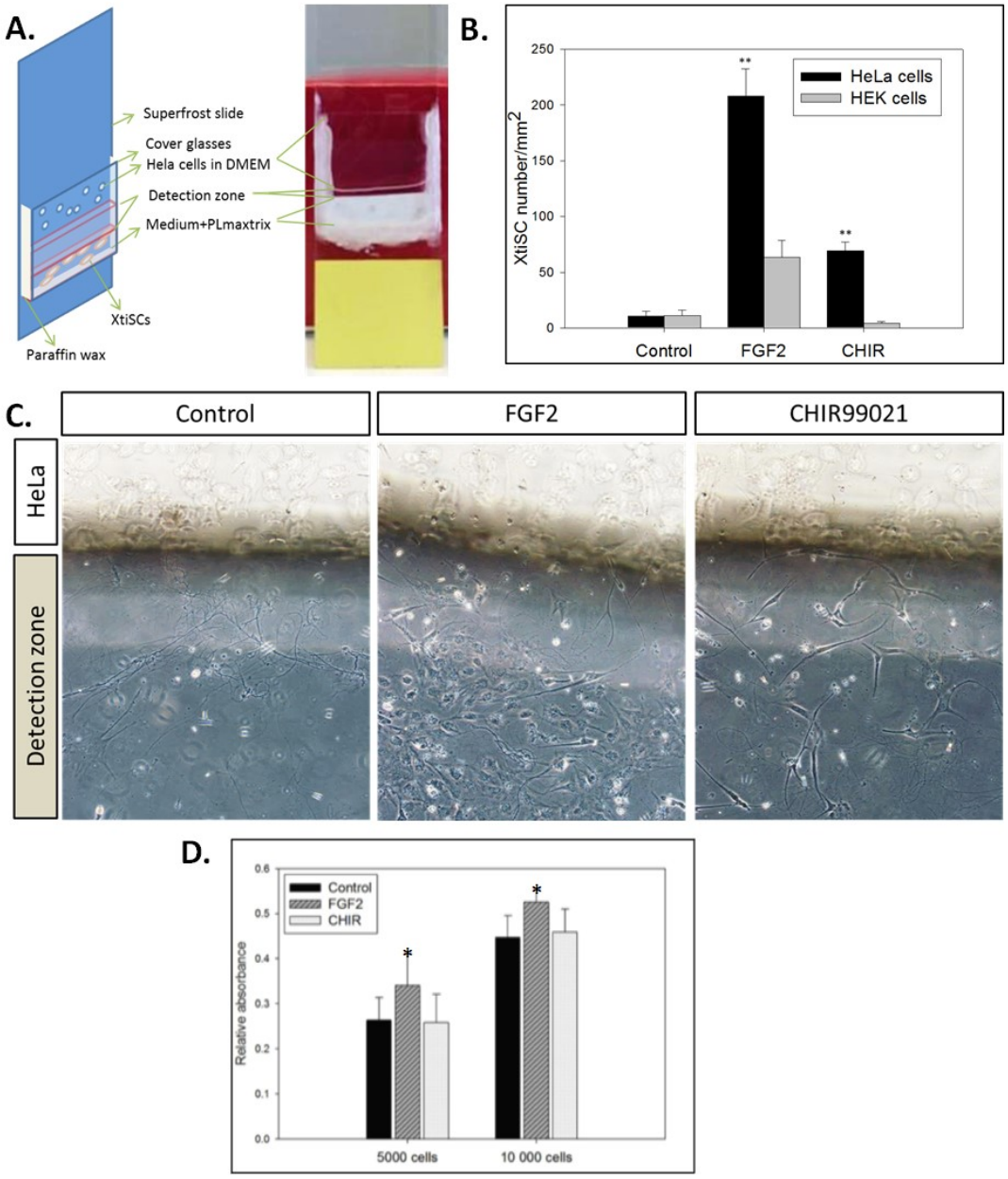

Figure 25: Directed migration of XtiSCs toward cervical cancer cells (HeLa). Scheme (A) illustrates the directed migration assay with XtiSCs in the lower part of incubation chamber containing 100 µl of FGF2, CHIR99021 or 0.1% DMSO enriched media. After three-day treatment, inducing or control (0,1% DMSO) medium was replaced by 120 µl of standard cultivation medium supplemented with PL-matrix. HeLa or HEK cells suspension (control) was added to the upper part after the solidifying of PL-matrix. Cervical cancer cells are separated from XtiSCs by the detection zone. After 36-48 hours, the number of cells in the detection zone was counted and expressed in the chart (B-C). (D) shows the cell viability of XtiSCs after 3-day treatment with FGF2 and CHIR99021. The results are representative of five biological replicates. **p<0.01, *p<0.05.

Eventually, to analyze the XtiSCs migration capacity toward cancer cells *in vitro*, another prominent feature of mesenchymal stem cells (MSCs) and EMT-shifted cells, human cervical cancer cells (HeLa) as an attractant and HEK cells as a negative control were employed. Boyden chambers in which cells are plated on the membrane of the

upper insert to be kept separated from their attractant in the bottom layer are a commercial and common technique to study cell migration. However, there are several limitations in this method, including cell leakage, high cost and difficulty to identify the migrated cells due to the mixing of both cell types (experimental and their attractant cells) in the bottom compartment. In order to overcome these disadvantages of Boyden chambers, we designed *in vitro* migration assay by using vertical cell culture. XtiSCs were seeded into the lower part and cultured until reaching confluence, subsequently, migration inducer (HeLa cell suspension) was placed in the upper layer. XtiSCs and the attractant were separated from each other by the "detection zone" based on a semi-solid cultivation medium containing human platelet lysate matrix (Fig. 25A). HeLa cells had higher affinity to either FGF2 (207.8±24.3) or CHIR99021 (69.1±8.1) pre-treated XtiSCs than HEK cells as revealed by the number of cells with 63.4±15.2 (FGF2) and 4.4±1.7 (CHIR) in the detection zone during 2-day assay (Fig. 25B). Whereas no to little untreated cells in the zone were observed neither with HeLa cells (10.4±4.4) or HEK cells (11.3±4.9) cultured in the upper part. Interestingly, collective migration of FGF2-treated cells enhanced their cell number in the detection zone in comparison with the individually migrated cells pretreated with CHIR99021 (Fig. 25, B&C). To eliminate the effect of proliferation on the number of cells, medium with low FBS concentration (0.5%) was used to culture XtiSCs in the migration assay. In addition, MTT assay was also conducted to test the cell proliferation in the different media. No significant difference was observed in CHIR-treated and vehicle group, only FGF2 induced cells to divide a bit faster than both other groups.

4.3.3 EMT promoted the XtiSCs stemness and migration potential in vivo

Approximately 1000 untreated or treated (FGF2 or CHIR99021) RFP expressing XtiSCs were microinjected into the peritoneal cavity of 2-day old *X. tropicalis* tadpoles (stage 41) (Fig. 26A). Two weeks after injection, 900-1500 transplanted cells were detected in each individual using flow cytometry (Fig. 26A), indicating their high survival rate.

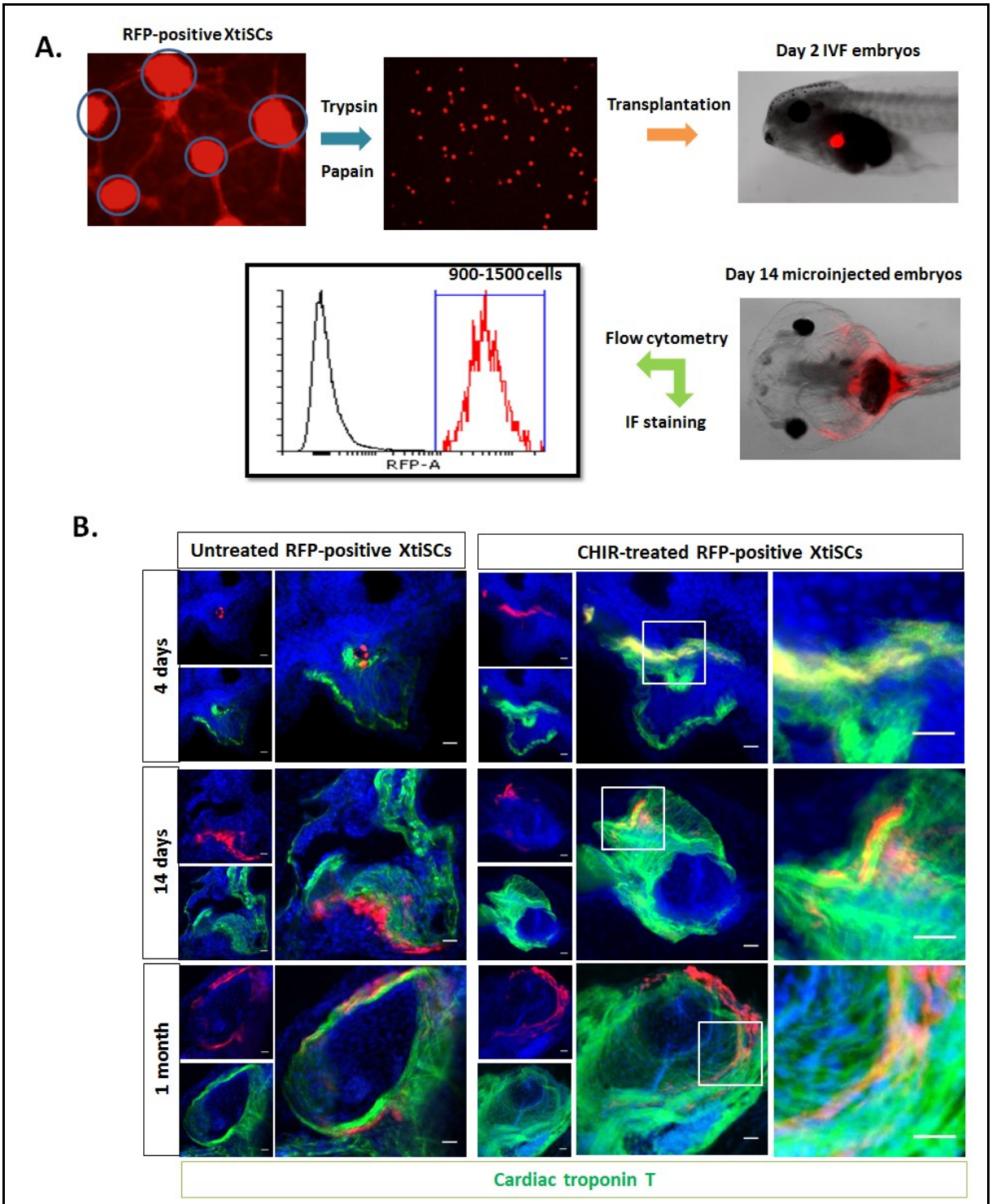

Figure 26: *In vivo* differentiation of EMT- induced XtiSCs into cardiomyocytes.
(A) Experimental scheme. RFP- positive XtiSCs were cultured in growth medium supplemented with 3 µM CHIR99021, or 0.1% DMSO as a control for 3-4 days before transplantation into 2 days old tadpoles. (B) At 4, 14 or 30th-day post-injection (dpi), tadpoles were fixed and sectioned for double staining with antibodies against red fluorescent protein and cardiac troponin T labeling cardiomyocytes in the heart. Scale bar: 20 µm. Nuclei stained with DAPI. Results are representative of four biological replicates.

CHIR-treated XtiSCs showed their capacity to *in vivo* differentiate into cardiomyocytes after allotransplantation. Vibratome sections of transplanted tadpoles at 4, 14 or 30th-day post-injection (dpi) were double-stained with antibodies against rabbit

RFP and mouse cardiac troponin T. Staining of XtiSCs prior to microinjection was negative for cardiomyocyte marker, cardiac troponin T (data not shown). 30 days after transplantation, 15% tadpoles (3/20) contained CHIR99021-treated cells which expressed cardiac troponin T and were infiltrated in the myocardium (Fig. 26B). Vehicle XtiSCs were found around the aorta and outside of heart only and their staining with cardiac troponin T was negative (Fig. 26B). Markers of other cell types, including chondrocytes, skeletal and smooth muscle cells, and neurons were examined on transplanted cells as well, however, no positive staining of XtiSCs was observed. As for the FGF2 experimental group, there was no difference between treated and untreated cells (data not shown).

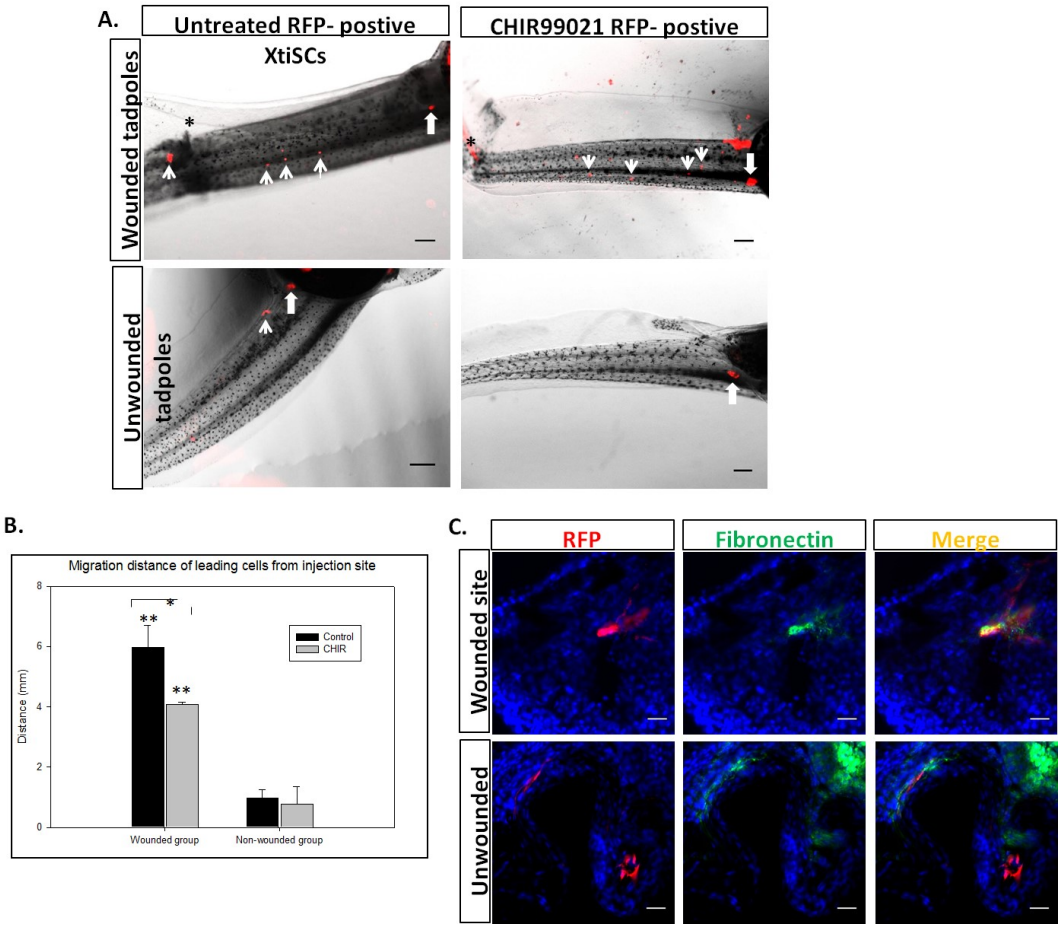

Figure 27: *In vivo* migration of untreated or CHIR99021 treated XtiSCs
Cells were transplanted into the peritoneal cavity of two days old tadpoles toward skin injury. (A) Differential migration behavior of untreated and treated RFP expressing XtiSCs inside wounded or unwounded tadpoles. Arrows show the migrating RFP positive XtiSCs, thick arrows indicate the injection sites. The injury site is marked by a black asterisk. Scale bar: 500 µm. (B) the distance of leading cells from the injection site was measured 6 hours after transplantation by ImageJ and expressed in the chart. (C) Two days after transplantation, fibronectin was detected in untreated XtiSCs at injury site only, but not in cells outside wounded areas in both groups. Nuclei were stained with DAPI. Scale bar: 20 µm. *p<0.05, **p<0.01.

Directed migration of XtiSCs was evaluated by transplanting transgenic cells into 3-week old tadpoles, following a wound in a distal part of the tail at 6 mm distance from the injection site using fine forceps. Control group was non-wounded tadpoles with transplanted cells (Fig. 27A). 6 hours after the transplantation, RFP cells migrated toward the injury site, whereas transgenic XtiSCs were found only around the injection sites in non-wounded tadpoles (Fig. 27A). Unexpectedly, untreated XtiSCs migrated significantly faster than CHIR99021 treated cells, and their accumulation at the injury site was also observed (Fig. 27, A&B) by which the distance of leading cells from injection site was 5.98±0.72 mm (untreated) and 4.075±0.078 mm (CHIR-treated cells). 2 days post-injury, the expression of fibronectin was also examined. Only XtiSCs

aggregated at the injury site were positive but not cells migrated elsewhere (Fig. 27C). This means that XtiSCs have responded to injury signals and contributed to a wound healing by expressing fibronectin, an essential component of the extracellular matrix to recover the epidermal layer.

4.3.4 CHIR99021 inhibited testicular development in vivo

The above results show that CHIR99021 reprogrammed XtiSCs and reversed them back to the stem cell stage, in other words, the inhibition of GSK3 dedifferentiated immature Sertoli cells. To examine the role of GSK3 *in vivo* SC development, we injected CHIR99021 with different concentration (0, 0.6, 1 and 1.5 μM) into a dorsal sac of juvenile (5-month old) frogs.

All of the treated frogs looked healthy after 2 months of injection, however, testicles of the male animals injected with 1.5 μM CHIR99021 have vanished (Fig. 28A). Testicles of other experimental frogs were collected and embedded into paraffin or agarose for sectioning. Impaired morphology and structure of seminiferous tubules in CHIR-treated animals were revealed by H&E staining on testicular sections. Injection with 1 μM concentration of CHIR99021 caused the most serious damage to the germinal epithelium didn't attach to the basement membrane and the outer myoid layer (Fig. 28C). At 0.6 μM concentration, CHIR99021 was responsible for the disorganization of seminiferous tubules in treated frogs. In contrast to vehicle individuals, Sox9 protein, a specific maker of Sertoli cells, wasn't detected in testes isolated from CHIR-injected frogs as analyzed by Western blot (Fig. 28B). The data suggest the importance of GSK3 in SC differentiation via inhibition of mesenchymal proteins and consequently, the mesenchymal-epithelial transition is activated to allow the complete maturation of SCs. Suppression of GSK3 by CHIR99021 inhibited the maturation of SCs resulting in testicular failure.

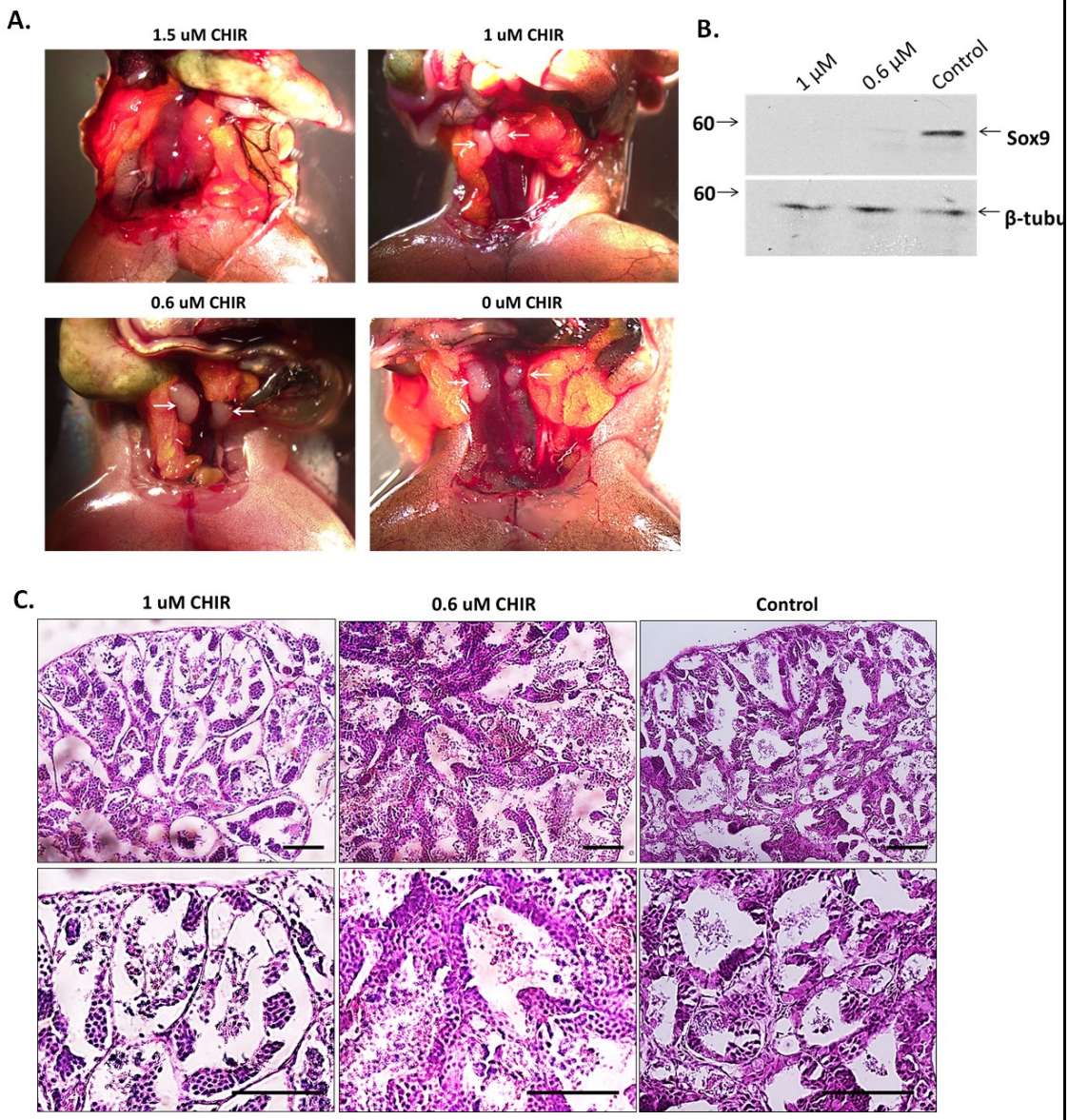

Figure 28: *In vivo* treatment of CHIR99021 in young *X. tropicalis* testes
The CHIR treatment led to the failure in testes development. (A) 2.5 months after CHIR99021 injected into the dorsal sac, no testicles were observed in 1.5 μM injected frogs. Arrows indicate testes. (B)Immunoblotting of testicular extract from 1, 0.6, 0 μM CHIR-injected *X.tropicalis* with the antibody against Sox9 (Sertoli cell marker). β-tubulin is as a loading control. (C) H&E staining of testicular sections from 1, 0.6, 0 μM CHIR-injected *X.tropicalis* showed the serious damage with the detachment of germinal epithelium from tubules in 1 μM group. Testes with 0.6 μM CHIR had no clear seminiferous tubules' structure. Scale bar: 100 μm.

4.4 The interconnection between cytokeratin and cell-cell junctions in immature Sertoli cells of *X. tropicalis*

β-catenin possesses multiple biological functions and is present in various cell compartments. On the plasma membrane, it serves as a component of adherens junction and in cell nuclei, it acts as a transcription factor involving in the most well-studied Wnt signaling (Daugherty and Gottardi 2007). Co-expression of β-catenin and E-cadherin

surrounding SCs of young *Xenopus* testes (Fig. 29, A-C) confirmed the role of β-catenin in immature SCs as a component of adherens junction complex. The downregulation of β-catenin in matured testes was observed suggesting the change in cell-cell junctions of fully functional SCs to provide structural support for spermatogenesis, even though E-cadherin continued to be present mainly in the basal compartment of the matured cells (Fig. 29, D-F). Moreover, even though CK has been considered as a marker of immature Sertoli cells (Rogatsch et al. 1996), its role in SC development is still poorly understood. In this chapter, I would like to describe our results concerning the role of CK in SC development in association with β-catenin-based cell junctions on the *Xenopus* model.

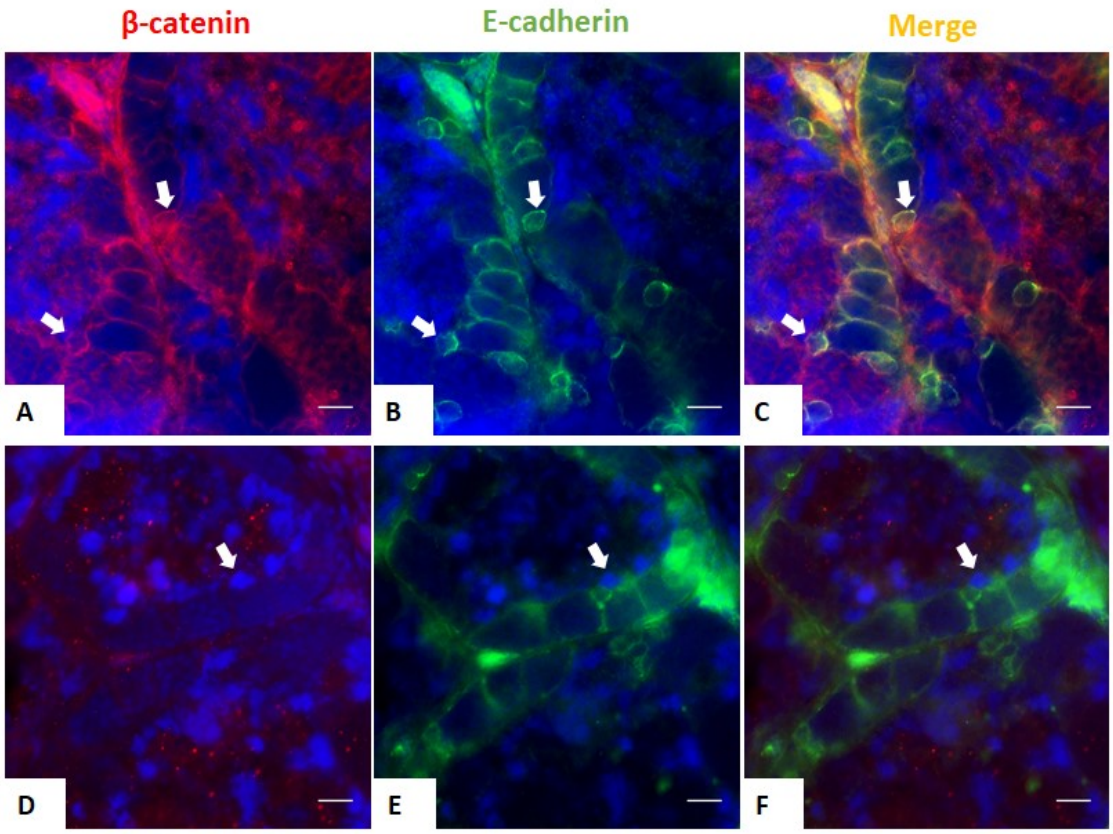

Figure 29: Expression of E-cadherin and β-catenin in Sertoli cells during testicular development.
Double staining on testicular sections of juvenile (A-C) and adult frogs (D-F) with E-cadherin (mouse, green) and β-catenin (rabbit, red) antibodies. Nuclei were stained with DAPI (blue). Scale bar: 20 µm. Both proteins surrounded the Sertoli cells of juvenile testes, but only E-cadherin is expressed in adulthood. Arrows represent Sertoli cells.

Firstly, we investigate the regulatory effect of CK on membrane-bound β-catenin by disrupting CK network in XtiSCs. The transient negative impact of acrylamide (unpolymerized form) on CK integrity has been well-described in *Xenopus* and

mammals as well (Shabana, Oboeuf, and Forest 1994; Duncan et al. 2009; Sonavane et al. 2017). After 75 minutes of incubation, 10 mM acrylamide caused the serious disruption of CK in XtiSCs (Fig. 30B1), subsequently, the breakdown of β-catenin on the cell membrane was observed (Fig. 30B2). Washing out the acrylamide from the culture medium led to the gradual recovery of membrane β-catenin after 90 minutes coincidentally with the cytokeratin re-organization (Fig. 30C). Adherens complex on plasma membrane comprises β-catenin binding to a transmembrane protein, Ca2+-dependent cadherin. Thus, a Ca2+ chelator, EGTA is a common chemical used for the induction of reversible dissociation of cell-cell adherens junctions, and subsequent destabilization of β-catenin on the plasma membrane. To examine an effect of membrane β-catenin downregulation on the stability of CK, 2 mM EGTA was added to XtiSC culture. The disruption of β-catenin was obtained after 15 minutes treatment with EGTA, consequently, the morphology of XtiSCs changed into fibroblast-like cell shape probably due to the loss of cell-cell interaction (Fig. 30D). However, expression and structure of CK weren't influenced by EGTA leading to complete recovery of β-catenin on the plasma membrane after 90 minutes EGTA washed out from XtiSCs' culture. (Fig. 30, D2&E).

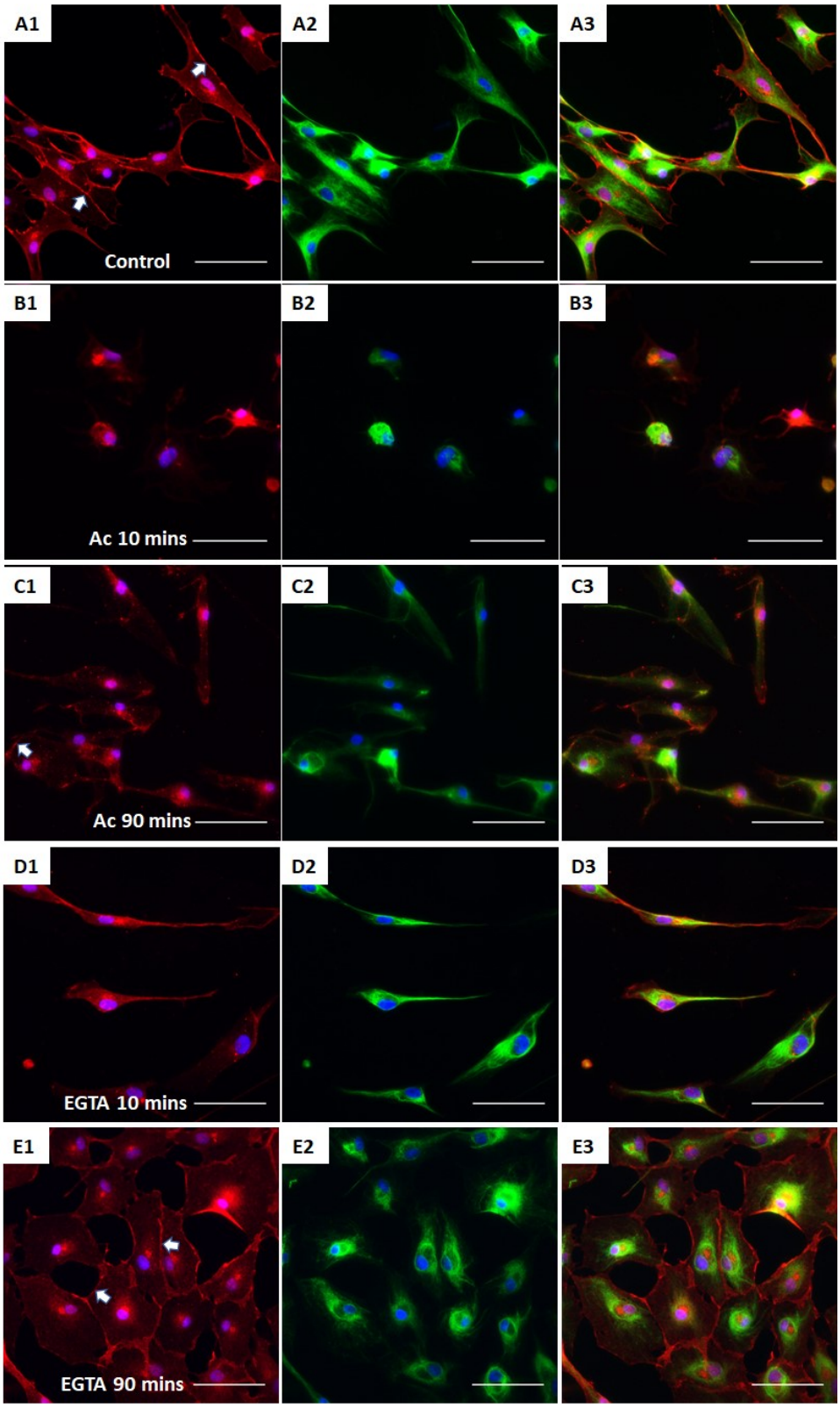

Figure 30: The effect of CK network on the β-catenin-based cell junctions.
XtiSCs were treated with vehicles (Control, A) or 10 mM acrylamide (Ac, B&C) or 2 mM EGTA (EGTA, D&E). After treatment, cells were washed and exchange to the fresh medium, and then collected at indicated time points, 10 minutes (B&D) or 90 minutes (C&E) for immunofluorescent staining with antibodies against β-catenin (red, A1-E1), CK (green, A2-E2), and merge (A3-E3). Arrows show membrane β-catenin. Nuclei were stained with DAPI (blue). Scale bar: 50 μm.

Effect of acrylamide and EGTA on expression and structure of F-actin, β-tubulin and cell adhesion proteins was also examined by immunohistochemistry staining. Cell-matrix adhesion molecules (FAK and integrin β1) weren't influenced (Fig. 31), whereas cortical actin filaments of treated cells became predominant to probably recruit β-catenin-based cell-cell adhesions dissociated by acrylamide and EGTA (Fig. 32, B1&C1) (Engl et al. 2014; S. K. Wu et al. 2014). While no change in β-tubulin was induced by acrylamide (Fig. 32B2), it formed aggregates after EGTA treatment (Fig. 32C2). Taken together, the data indicate that retainment of the β-catenin-based cell junctions in XtiSCs required the stability of CK network, however, membrane β-catenin wasn't necessary for the CK stability.

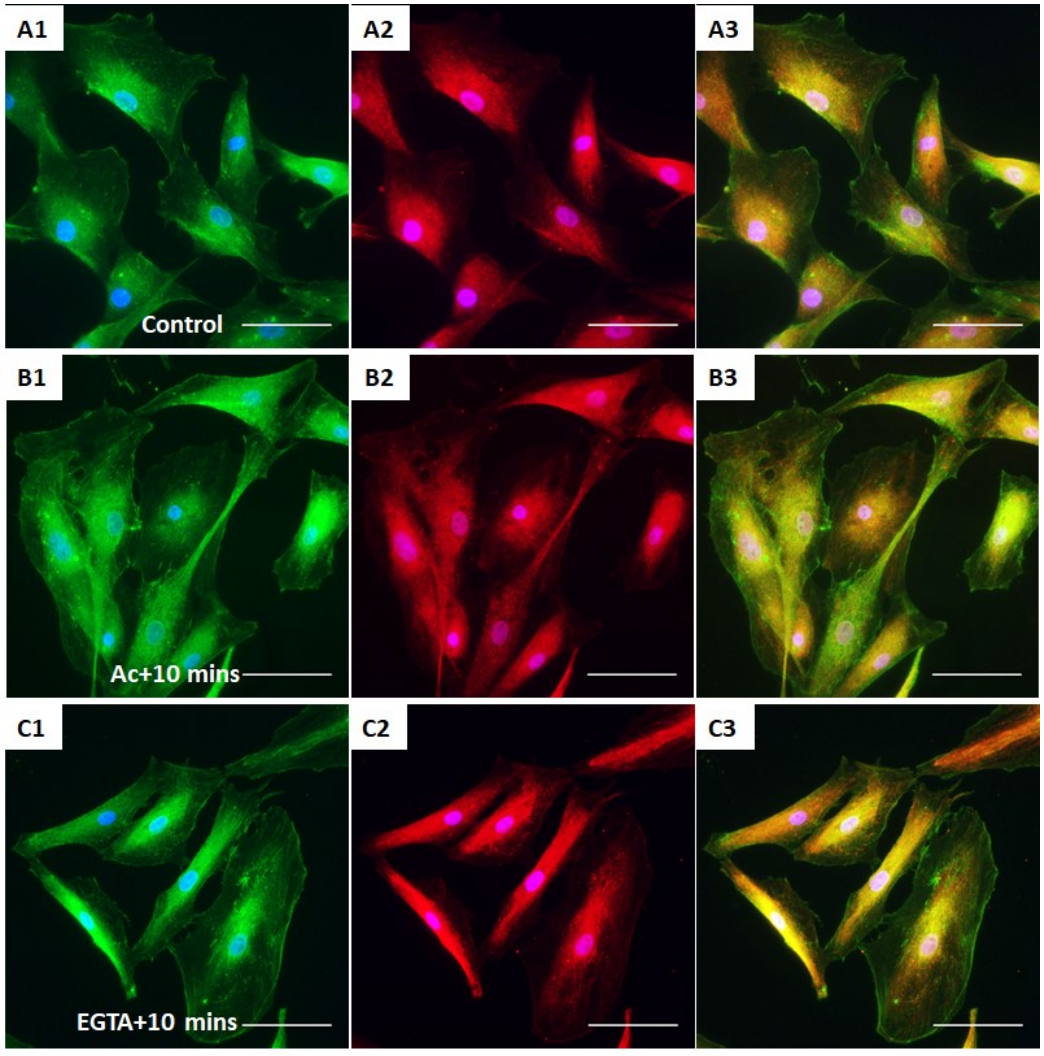

Figure 31: The effect of acrylamide and EGTA on cell adhesions.
Immunofluorescent images of XtiSCs 10 minutes after washing out the acrylamide (B) or EGTA (C) staining with antibodies against integrin β1 (CD29, green, A1-C1), Focal adhesion kinase (Fak, red, A2-C2), and merge (A3-C3). Nuclei were stained with DAPI (blue). Scale bar: 50 μm.

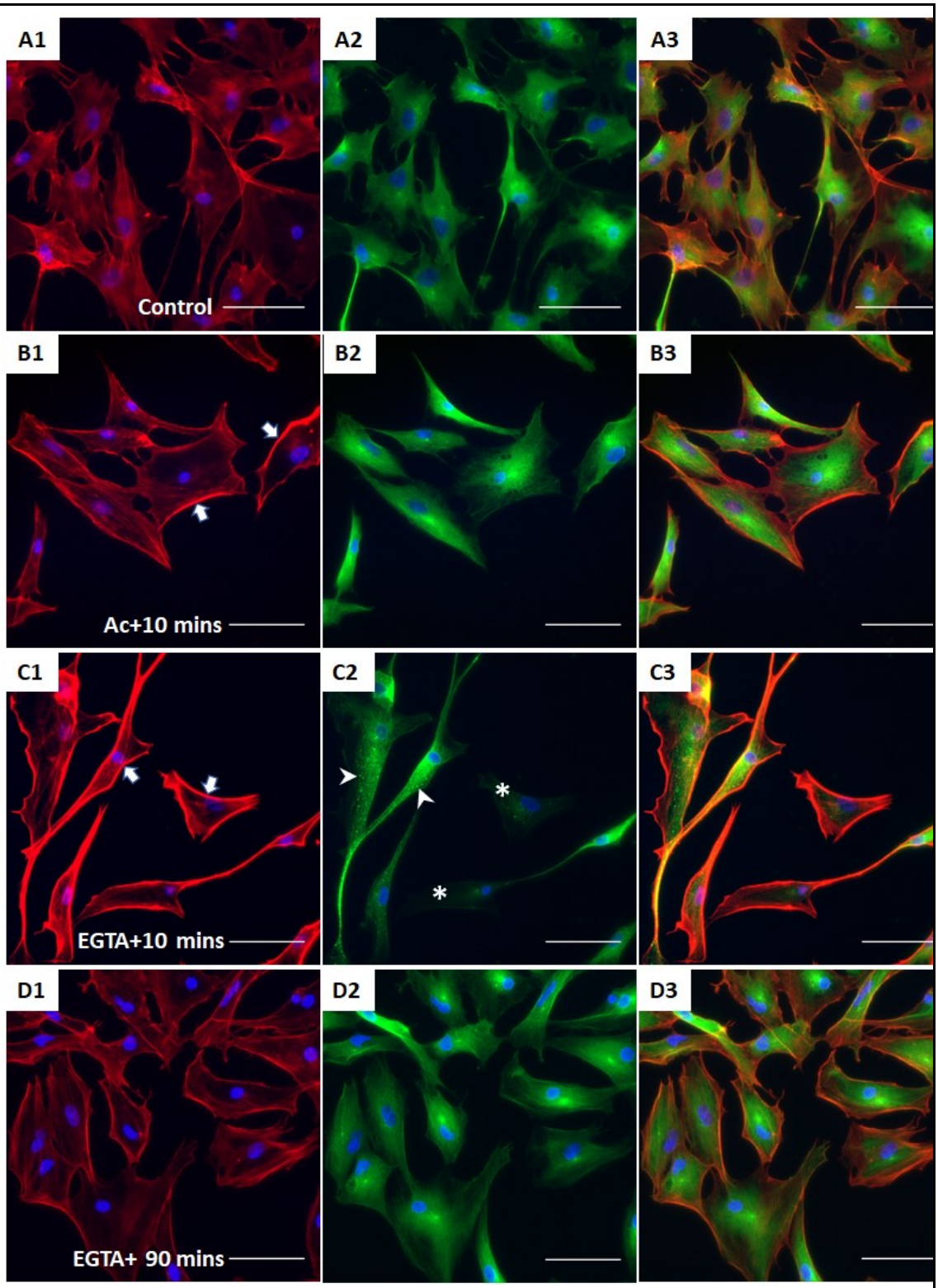

Figure 32: The effect of acrylamide and EGTA on F-actin and tubulin.
After treatment, XtiSCs were collected at indicated time points for immunofluorescent staining with antibodies against F-actin (red, A1-D1), β-tubulin (green, A2-D2), and merge (A3-D3). Arrows show thick membrane F-actin in figure C1 and D1. The aggregates of β-tubulin are marked by arrowheads and asterisks indicate the cells without β-tubulin in figure C2. Nuclei were stained with DAPI (blue). Scale bar: 50 μm.

β-catenin phosphorylation by GSK-3 results in its proteasomal degradation. Interestingly, in the results mentioned above, we observed the suppression of CK in

XtiSCs by CHIR99021, a GSK-3 inhibitor. Thus, to determine the relationship between CK expression and β-catenin we added CHIR99021 to XtiSC culture. Reactivation of GSK-3 was achieved by the IWP2 which blocks the secretion of Wnt ligands (García-Reyes et al. 2018).

Little bit higher accumulation of β-catenin in cell nuclei after 3-day treatment with 3 μM CHIR was revealed by immunoblotting analysis. Concerning whole cell lysate, we observed no significant difference in the β-catenin level between control and CHIR-treated cells (Fig. 33G). Substantial degradation of β-catenin in the nuclear fraction was obtained after 3 days treated with 2 μM IWP2 (Fig. 33G). Immunocytochemistry was also used to examine expression level as well as the distribution of CK and β-catenin in XtiSCs (Fig. 33, D-F). While membrane β-catenin in cells treated with CHIR99021 was disrupted, their strong signal in cell nuclei was still observed. Incubation of XtiSC with IWP2 resulted in the downregulation of nuclear β-catenin consistently with the immunoblotting analysis. Staining intensity of membrane β-catenin was similar in control and IWP2-treated cells (Fig. 33C). Interestingly, the expression of CK was detected only along with the presence of membrane β-catenin in control cells and XtiSCs cultivated with IWP2 (Fig. 33C). This result supports the positive role of CK in the retention of β-catenin in the plasma membrane hence the stabilization of adherens junctions in immature SCs.

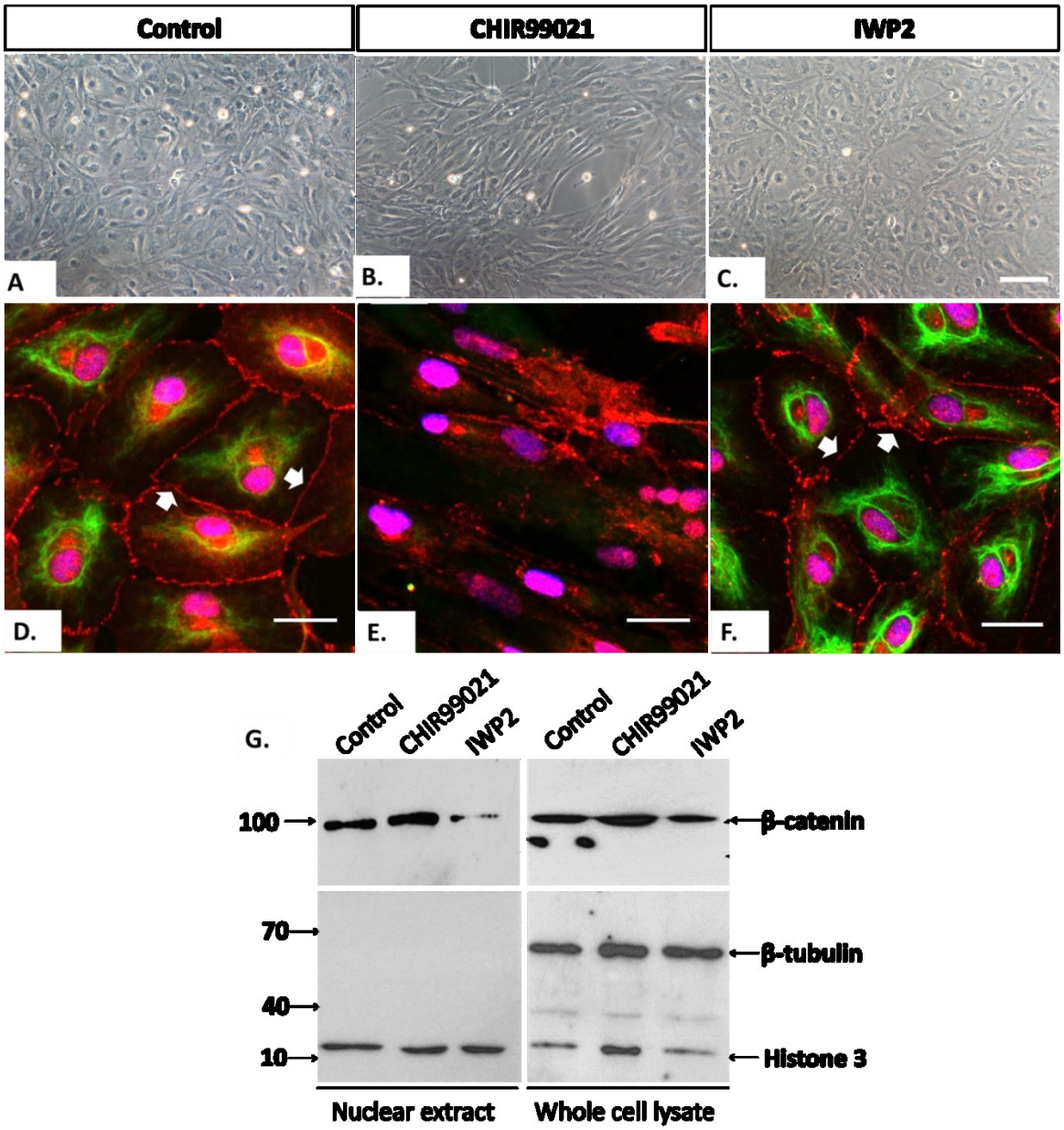

Figure 33: XtiSC after treatment with CHIR99021 and IWP2.
(A-C) Phase-contrast images of XtiSC after treatment with CHIR99021 and IWP2 for 3 days showed the morphological change in CHIR99021-treated cells. XtiSCs were collected for immunofluorescent (D-F) or blotting analysis (G). Nuclear β-catenin was downregulated in media supplemented with IWP2. Immunostaining of CHIR99021-treated XtiSCs against CK (green) and β-catenin (red) revealed the disruption of cytokeratin network and cell-to-cell contact altogether with the disappearance of membrane β-catenin. Arrows in (D-F) show the membrane β-catenin. Nuclei were stained with DAPI (blue). Scale bar: in (A-C) 100 μm and in (D-F) 20 μm.

Chapter 5

DISCUSSION

5.1 Sertoli cell origin of testis-derived stem cells

Stem cells isolated from testicular explants of human, monkey, mouse and rat have been reported (Kanatsu-Shinohara et al. 2004; Guan et al. 2006; Seandel et al. 2007). Stem cell colonies have formed in media supplemented with various growth factors and small drugs for an extended time (around 2 months). The colony-forming cells have shown stemness features with the expression of stem cell markers, potential to differentiate into many cell types and long-term survival in culture, promising a novel source of adult stem cells. However, their origin and cellular signaling underlying their formation are still questioning. Nevertheless, human **t**estis-derived **s**tem **c**ells (TSCs) have not expressed the *VASA* gene, a most conserved marker of germline cells (Golestaneh et al. 2009). Subsequently, employing different isolation methods to sort out a mixed cell culture into defined cell types, Chikhovskaya et al. (2013) retrieved that no human testis-derived stem cells were produced in the absence of somatic cells. These results verify the somatic origin of human TSCs. The similar results were obtained using primate monkey TSCs (Eildermann, Gromoll, and Behr 2012).

We have been successful in establishing a cell line of *Xenopus tropicalis* testicular stem cell (XtiSCs) in long-term culture (Tlapakova et al. 2016) with LIF and CHIR99021. XtiSCs have showed similar features to testis-derived stem cells of other species, they formed the compact colonies after 2 months in the culture (Fig. 12). XtiSCs did not express any germ-cell line markers (such as *dazl* or *vasa*), but testis associated somatic markers (Acta2, Sox9, *lif, kitlg,* vimentin, cytokeratin) (Fig. 13&14), confirming their somatic origin. They also exhibited stemness features correlated with the capacity of differentiation towards mesodermal lineage both *in vitro* and *in vivo* (Fig. 24&26) and the ability to keep their characteristics even after 48 passages.

A Sox9 gene indispensable for the initiation and sustenance of SC differentiation in all vertebrates is activated early in pre-SCs (Kent et al. 1996; Kanai 2005; Kidokoro et al. 2005). Unlike SRY is expressed transiently in pre-SCs until 12.5 d.p.c, Sox9 exists exclusively in SCs for a whole life, implying the importance of this protein in the

maintenance of SC function (Hemendinger et al. 2002; Sekido et al. 2004). Moreover, vimentin expression is also stable in SCs during their maturation (Rogatsch et al. 1996). In agreement with previous studies performed in mammals, double immunofluorescence staining on young and adult *X. tropicalis* testicular sections with antibodies against vimentin/Sox9 revealed stable expression of vimentin in Sox9-positive SCs (Fig. 10A&B). Positive immunofluorescent staining for Sox9 and vimentin (Fig.14) in addition to the presence of relevant transcripts (Fig. 13) confirmed Sertoli cell origin of XtiSCs.

Locally produced soluble factors in testicles are important for the regulation of germ cell survival and differentiation. One of them, the leukemia inhibitory factor (LIF) mainly produced by the peritubular myoid (PTM) cells (Piquet-Pellorce et al. 2000) is a key paracrine regulator of testicular function via the leukemia inhibitory factor receptor (LIFR). Sertoli cells have been thought to be one of the main targets of LIFR signaling as revealed by *in vitro* binding assays with biotinylated LIF and immunohistochemical detection of LIFR in testis sections (Dorval-Coiffec et al. 2005). Moreover, another research showed a degenerative phenotype of SCs lacking LIFR which led to the loss of germ cells, and abnormal structure of seminiferous tubules (Curley et al. 2018). In this study, the addition of recombinant mouse LIF into culture medium enhanced XtiSC survival and colony-forming activity. However, a total proliferation rate was unaffected by LIF, since experimental groups (+LIF and -LIF) revealed the same growth curves as depicted in Fig. 12G.

5.2 Pharmacological GSK-3β inhibitor induce EMT in XtiSCs

The presence of GSK-3β inhibitor, CHIR99021 in culture medium has promoted the efficient derivation of stem cells from mouse and human testes (Chikhovskaya et al. 2011; Moraveji et al. 2012). By testing several small molecules in mouse testis explant culture, Moraveji et al. (2012) determined that CHIR99021 has been able to induce testicular cells reprogramming to stem cell-like cells. CHIR99021-treated cells could differentiate toward cardiac and neural lineages. Chikhovskaya et al. (2011) showed that human TSCs cultured in CHIR99021-supplemented medium have possessed features of multipotent MSCs with the expression of MSC markers and typical tri-lineage *in vitro* differentiation. However, the mechanism underlying the effect of GSK-3β inhibitor on

testicular cell reprogramming is understood only partly. Basically, the relevance between GSK-3β inhibition and EMT activation by stabilizing Snail expression has been reported elsewhere (Bachelder et al. 2005; Hao Wang et al. 2013; Zheng et al. 2013).

The regulatory role of signal transducer and activator of transcription 3 (STAT3), a transcription factor, in the EMT process is heterogeneous. STAT3 overexpression enhanced colorectal carcinoma undergoing EMT, characterized by the downregulation of E-cadherin and subsequently, the increase of invasion and metastasis (Xiong et al. 2012). However, proteasomal degradation of SNAI1, a key transcription factor of EMT progress was increased by STAT3 in metastatic colorectal cancer cells via promoting GSK3β-mediated phosphorylation of SNAI1 and consequently, EMT was suppressed (J. Lee et al. 2012). Moreover, GSK3β has been reported to regulate the DNA binding activity of STAT3 as well. Mouse primary astrocytes and microglia cells with GSK3β-knockdown or/and GSK3β inhibitor-treatment showed reduced STAT3 activation and STAT3-induced GFAP and Bcl-3 expression (Beurel and Jope 2008). Taking together, STAT3 differentially regulates an EMT, firstly as an activator during the initiation and as an inhibitor for EMT completion. Our study revealed that XtiSCs possessed characteristics of both, mesenchymal and epithelial cells. Indeed, vimentin and alpha-smooth muscle actin, mesenchymal proteins were found in XtiSCs which showed migration capacity after transplantation into *X. tropicalis* tadpoles (Tlapakova et al. 2016). Moreover, epithelial markers, such as cytokeratin and β-catenin on the plasma membrane (cell-cell adhesions) (Fig. 14C) were detected in XtiSCs as well, indicating their hybrid epithelial/mesenchymal phenotype. In agreement with (Beurel and Jope 2008) and (J. Lee et al. 2012), GSK3 inhibitor (CHIR99021) reduced Stat3 activity in XtiSCs (Fig. 21); consequently, Snai1 expression was upregulated (Fig. 19) to allow XtiSCs to achieve a full mesenchymal state. On the other hand, Stat3 signal was stable in FGF2-treated XtiSCs (Fig. 21), resulting in their hybrid phenotype. In addition, the differentiation potential of EMT-shifted XtiSCs was broadened as evidenced by their higher efficiency in osteogenic and chondrogenic induction *in vitro* and into cardiomyocytes *in vivo* (Fig. 24&26). To our knowledge, this is the first study that reveals the EMT program as a primary cellular mechanism driving the formation of testis-derived stem cells by CHIR99021.

Furthermore, we observed that EMT-shifted cells could grow only on collagen type 1-coated slides or on the gamma-irradiated plastic surface, but not on the non-coated or poly-(L) lysine-coated slides (Fig. 20). This may correlate with the increase of ECM-cell interaction through the deposition of fibronectin and their receptor on the selective surface. Our results are in agreement with previous studies performed on human cell lines. Collagen type I accompanied with fibronectin-coated surface induced EMT more effectively than the poly-lysine layer in human epithelial cells, alveolar type II A549s and human bronchial cells (Câmara and Jarai 2010). In addition, the motility of EMT-induced HT29 cells seeded on collagen type 1 or fibronectin-coated surface was promoted compared to poly-(L) lysine coating (Przygodzka et al. 2016).

Depending on the signaling and cell context, partial EMT, where both epithelial and mesenchymal phenotypes are exhibited, or full EMT, in which only mesenchymal features are found, can be achieved in EMT-shifted epithelial cells. Cells undergoing a partial EMT are able to migrate collectively (as a cell sheet or a chain) and maintain a dynamic equilibrium among two phenotypes. In addition, the full mesenchymal state doesn't assure the stemness acquisition in EMT-shifted cells, instead, a hybrid phenotype is closer to the "stemness window" as defined by (Jolly et al. 2014). Using mathematical model supported with experimental data, authors demonstrated a distinctive stemness window with various shifts toward to as mesenchymal so as epithelial phenotype. Among four key regulators of EMT, upregulated ZEB1 has been thought to gain and maintain stemness of EMT-shifted cells via inhibiting miRNA such as miR-200 (Brabletz et al. 2011; C. Zhou et al. 2017) which its downregulated expression was observed in both normal mammary stem cells and breast cancer stem cells (Shimono et al. 2009). The interconnection between EMT phenotypes and stemness has been well-studied in cancer cells. However, regarding physiological condition, researches focusing on this relationship are quite restricted, having only a few available epithelial cell lines able to undergo EMT under *in vitro* treatment. By this time, only two non-transformed cell lines, mouse mammary epithelial (NMuMG) and mouse cortical tubule (MCT) cells which are able to undergo EMT *in vitro* (Brown et al. 2004) have been identified. However, their EMT activation is quite restricted only on the TGF-β signaling pathway. This is disadvantageous to the study of other EMT signaling pathways in normal epithelial cells.

Notably, XtiSCs which achieved various EMT phenotypes by different EMT inducers represents a suitable model to identify the signaling pathway underlying EMT activation. Indeed, XtiSCs are in the hybrid (more epithelial) state or hold the partial EMT characteristics close to the mesenchymal phenotype in response to FGF2 stimulation and promote the complete mesenchymal phenotype by GSK-3 inhibitor. Particularly, XtiSCs have displayed similar changes in gene expression to gain mesenchymal features, e.g morphology and migration potential during the EMT process to mammary cells (Fig. 19&23A). Moreover, the pharmacological inhibitor, CHIR99021 upregulated stem cell markers (Sox2, *cd44*) (Fig. 23, A&B), adhesions protein integrin α5β1 (Fig. 19C) which is absent in SCs (Lustig et al. 1998) but present in mesenchymal stem cells (Veevers-Lowe et al. 2011), and suppressed an earliest marker of mural cells, Acta2. These data have evidenced for the reprogramming of XtiSCs back to stem cell state by CHIR99021. We found out that hybrid cells, XtiSCs, could differentiate into osteocytes and adipocytes (Fig. 24) *in vitro*. However, this potential was broadened into chondrocytes *in vitro* (Fig. 24) as well as cardiac myocytes *in vivo* (Fig. 26) at the mesenchymal state by CHIR99021 which increased Zeb1 expression (Fig. 23) in agreement with the previous studies on mammals. Therefore, XtiSCs provide a novel model for the investigation of EMT signaling and the stemness acquisition of EMT-shifted cells.

The loss of epithelial features consisting of the breakdown of cell-cell junctions and the increase of extracellular matrix adhesions enhances the migration capacity of EMT-shifted cells. Unexpectedly, CHIR-treated XtiSCs (full EMT phenotype) migrated *in vitro* slower than cells in the hybrid state (FGF2 treatment) (Fig. 25) which have shown the significant upregulation of *cd44* transcript, a cell-surface glycoprotein involved in cell adhesion and migration. Relative *cd44* mRNA expression of FGF2-treated XtiSCs is 56-fold higher than in control and 1.27-fold higher than in CHIR-treated cells (Fig. 23B). Increased directed migration in connection with the upregulation of CD44 after FGF2 treatment has also been reported in several cell types, including periodontal ligament cells (Shimabukuro et al. 2011), endothelial cells and melanoma cells (Baljinnyam et al. 2014).

Furthermore, a re-epithelialization process during wound healing has been thought to induce EMT in primary keratinocytes by which epithelial sheets are able to migrate to the injury site and form a new epidermal layer (Ben Amar and Wu 2014). This indicates that healing signaling induces the keratinocytes to undergo partial and reversible EMT in a response to inflammatory cytokines such as tumor necrosis factor (TNF)- alpha (Yan et al. 2010). Moreover, the partial EMT cells are characterized by a collective migration as a sheet of cells moving together in high number thus promoting the wound healing process faster. Nevertheless, the role of mesenchymal stem cells (MSCs) in the wound healing process is quite complex. Firstly, MSCs are activated by injury signals such as TNF- alpha (Kwon et al. 2013; H. Chen et al. 2015) to secrete paracrine factors which trigger a homing and angiogenesis process in endothelial progenitors. Later on, MSCs migrate directly to the injury site and their differentiation was induced into neural fate or osteogenic lineage by proinflammatory mediators, e.g. TNF- alpha (Egea et al. 2011; Croes et al. 2015). This study revealed that a hybrid phenotype of XtiSCs (untreated cells) showed potentiated tropism towards injured skin faster and more effectively with the expression of fibronectin at the injury site than full mesenchymal state XtiSCs induced by CHIR99021 (Fig. 27).

5.3 The interconnection between cytokeratin and cell-cell junction in immature SCs

In human and mouse, expression of cytokeratin in SCs is detected only in a short period of time as revealed by immunohistochemistry and immunoblotting. Cytokeratin is observed in basal part of SCs from E12.5 with well-differentiated testicular cords up to an early postnatal period, however, it hasn't been found in pre-SCs or fully developed SCs (Stosiek, Kasper, and Karsten 1990). Thus, SCs with the expression of CK have been considered as immature cells (Rogatsch et al. 1996). In consistent with studies on mammals, double immunofluorescent staining on juvenile and mature *X. tropicalis* testicular sections with antibodies against cytokeratin/Sox9 revealed the transient expression of CK in Sox9-positive tubular SCs only in young testes (Fig. 10A). These data indicate the evolutionary conservation between *Xenopus* and human regarding testicular development.

Because of the lack of plus and minus ends, CK and other members of IFs have been thought not to be involved in intracellular transport. However, the key role of IF and CK in vesicular trafficking has been recently reported. Indeed, vesicle transport towards the plasma membrane in astrocytes was strongly inhibited in association with depolymerization of IF (Potokar et al. 2007). SNARE proteins are a large protein complex which forms a coat on the cytosolic surface of vesicles and is crucial for docking and fusion of vesicles in the proper membrane position. In CK 8-deficient mice, impaired delivery of SNARE protein Syntaxin 3 and mistargeted trafficking of a number of apical proteins has been observed (Ameen, Figueroa, and Salas 2001), implying the importance of CK in organizing the apical pole of epithelial cells. In agreement with these results, GLUT -1 and -3 mislocalized from the apical compartment in embryonic epithelia of CK-null mice (Vijayaraj et al. 2009). Moreover, CK has been reported to be essential for the retention of proteins at their proper positions. Knockdown of CK caused the miss-targeting of Core 2 N-acetylglucosaminyltransferase 2/M (C2GnT-M), an enzyme in the Golgi apparatus to endoplasmic reticulum with subsequent ubiquitination and degradation by proteasomes (Petrosyan, Ali, and Cheng 2015).

In epithelial cells, β-catenin conjugates with cadherins forming adherens junctions on the plasma membrane to maintain cell integrity or accumulates in the nucleus to act as a key mediator of Wnt signaling. High turnover rate of β-catenin between the nucleus and the plasma membrane has been observed in NIH 3T3 cells employing GFP-tagged β-catenin and photobleaching assay (Johnson et al. 2009). The vesicle-associated intracellular trafficking is used to transport β-catenin and maintain the balance between Wnt signaling and cell-to-cell contacts (Chairoungdua et al. 2010). Moreover, disruption of CK network in transfected cultured cells with CK mutant (GFP-CK18 R89C) led to the detachment of several junction-associated proteins, including β-catenin from the cell membrane and their colocalization with CK aggregates (Hanada et al. 2005). Our study reveals the connection between β-catenin retention at the plasma membrane and CK expression in immature SCs. Co-expression of both proteins has been observed in juvenile testes and *in vitro* cultured immature SCs as visualized by double immunofluorescence staining (Fig. 10&30). The transient disruption of CK network in XtiSCs by acrylamide could be linked to its interaction with Epidermal Growth Factor Receptor and thus blocking EGF signaling (Smaill et al. 1999). EGF has

been reported to regulate keratin phosphorylation inducing the reorganization of keratin filaments (Ku and Omary 1997; Makarova et al. 2013). Subsequently, the breakdown of membrane-bound β-catenin was obtained (Fig. 30) but not in the opposite manner. EGTA treatment caused the loss of β-catenin-based adherens junctions but didn't affect the structure and expression of CK network (Fig. 30). Moreover, observation of CK loss caused by CHIR99021 in primary kidney cells and bladder cancer organoids has been reported previously (Francipane and Lagasse 2015; Yoshida et al. 2018). In agreement with the previous studies, CK suppressed by CHIR99021 was observed in XtiSCs (immature SCs) as well (Fig. 33E). Simultaneously the absence of membrane β-catenin was also observed. CHIR99021 was responsible for the failure in testis development as a consequence of the dedifferentiation of immature Sertoli cells (Fig. 28). In spite of no direct evidence of CK interaction with β-catenin in immature SC, our experimental data suggest that functional CK network is necessary for the retention of β-catenin-based junctions, and thus for the proper maturation of male sex organ.

5.4 The role of GSK3 and Wnt/β-catenin signaling in SC maturation

Glycogen synthase kinase 3 (GSK3), a serine/threonine protein kinase, participates in a number of intracellular signaling pathways, e.g. in the innate immune response, glucose regulation, and apoptosis (Ali, Hoeflich, and Woodgett 2001; Huizhi Wang, Brown, and Martin 2011). In mammals, GSK-3 is encoded by two known genes, GSK-3 alpha (GSK3α) and GSK-3 beta (GSK3β). β-catenin and Snai1 are two of more than 40 known substrates of GSK3 phosphorylating and targeting them for the proteasomal degradation. Regarding the role of GSK3 in testis function and development, down-regulation of GSK3β in testicles of non-obstructive azoospermic men has been observed (Nazarian et al. 2014). Another research showed that GSK3α- KO mice displayed lower sperm motility (Bhattacharjee et al. 2015). Our study revealed that pharmacological GSK3 inhibitor, CHIR99021 could dedifferentiate cultured immature Sertoli cells derived from the testes of juvenile *X. tropicalis* male back to their stem cell-like stage (Fig. 23, 24&26). Injection of this inhibitor into the 4-5-month old male frogs caused failure in testis development (Fig. 28), indicating the regulatory function of GSK3 in SC maturation. Interestingly, GSK3 inhibition didn't significantly increase the accumulation of β-catenin in XtiSCs nuclei (Fig. 33G). On the other hand, we observed stabilization of another nuclear GSK3 substrate, Snai1 (Fig. 19), a key migratory

transcription factor. These data suggest that the activity of GSK3 inhibits Snai1 expression resulting in the immobilization of SCs in seminiferous cords which provide the structural support for the formation of appropriate seminiferous tubules. Nevertheless, indirect upregulation of GSK3 activity in XtiSCs by IWP2 led to the downregulation of nuclear β-catenin (Fig. 33, D-G). However, membrane β-catenin and CK were not affected by IWP2 evidencing they were still in immature stage (Fig. 33, D-G). These data suggest that GSK-3 doesn't stimulate the complete maturation of SCs but maintains them in an immature stage.

Wnt/β-catenin signaling pathway is activated by binding a Wnt-protein ligand to a Frizzled family receptor, followed by the translocation of β-catenin into the nucleus as a transcription factor. This signaling pathway is highly evolutionarily conserved in animals. It controls a number of processes during embryonic development including cell fate specification axis patterning. However, its role in Sertoli cell and testis development is still a matter under debate. Pharmacological activator of Wnt/β-catenin signaling triggered the proliferation of adult human Sertoli cells *in vitro* culture by upregulating *c-myc* expression (Y. Li et al. 2012). SCs containing activated allele of *β-catenin* gene showed continuous proliferation, but impaired maturation with high expression of embryonic SC proteins, AMH and GDNF (Tanwar et al. 2010). Constitutive activation of the Wnt signaling effector β-catenin resulted in the loss of SSC activity and infertility in the mutant mice (Tanwar et al. 2010; Boyer et al. 2012). These data suggest the role of Wnt/β-catenin signaling in the regulation of immature SC division. On the other hand, its inhibition is necessary for SC differentiation and germ cell development. XtiSCs, *Xenopus* SC precursors displayed high activity of nuclear β-catenin and proliferation (Fig. 14C, 25D & 33E) which may inhibit their maturation in culture. However, the inhibition of Wnt/β-catenin signaling by IWP2 wasn't sufficient for completing SCs differentiation since the CK expression was still visible (Fig. 33).

Chapter 6

CONCLUSION

The data suggest the association of EMT with generating testis-derived stem cells. EMT-shifted XtiSCs have brought the similar characteristics of mesenchymal stem cells including the capacity to differentiate to the chondrocytes, osteocytes, and adipocytes *in vitro* and cardiomyocytes *in vivo*, directed migration towards cervical cancer cells *in vitro* and injury site *in vivo*. XtiSCs can become a potential model for studying EMT signaling. Sertoli cell origin of XtiSCs is confirmed by their expression profile. The XtiSCs represent a good model for the identification of key molecules involving Sertoli cell maturation. This study revealed a potential role of CK in maintaining immature SC junctions via retention of plasma membrane β-catenin, contributing to proper testicular development and spermatogenesis. This study brings the evidence for the role of GSK3 as a differentiation inducer of SCs to immobilize them into seminiferous tubules. A further experiment should be conducted to confirm and specify the role of GSK3 during SC maturation and testis development.

REFERENCE

Albrecht, K. H., and E. M. Eicher. 2001. “Evidence That Sry Is Expressed in Pre-Sertoli Cells and Sertoli and Granulosa Cells Have a Common Precursor.” *Developmental Biology* 240 (1): 92–107.

Ali, A., K. P. Hoeflich, and J. R. Woodgett. 2001. “Glycogen Synthase Kinase-3: Properties, Functions, and Regulation.” *Chemical Reviews* 101 (8): 2527–40.

Ameen, N. A., Y. Figueroa, and P. J. Salas. 2001. “Anomalous Apical Plasma Membrane Phenotype in CK8-Deficient Mice Indicates a Novel Role for Intermediate Filaments in the Polarization of Simple Epithelia.” *Journal of Cell Science* 114 (Pt 3): 563–75.

Appert, Alexandre, Valérie Fridmacher, Odette Locquet, and S. Magre. 1998. “Patterns of Keratins 8, 18 and 19 during Gonadal Differentiation in the Mouse: Sex- and Time-Dependent Expression of Keratin 19.” *Differentiation; Research in Biological Diversity* 63 (5): 273.

Bachelder, Robin E., Sang-Oh Yoon, Clara Franci, Antonio García de Herreros, and Arthur M. Mercurio. 2005. “Glycogen Synthase Kinase-3 Is an Endogenous Inhibitor of Snail Transcription: Implications for the Epithelial-Mesenchymal Transition.” *The Journal of Cell Biology* 168 (1): 29–33.

Baljinnyam, Erdene, Masanari Umemura, Christine Chuang, Mariana S. De Lorenzo, Mizuka Iwatsubo, Suzie Chen, James S. Goydos, Yoshihiro Ishikawa, John M. Whitelock, and Kousaku Iwatsubo. 2014. “Epac1 Increases Migration of Endothelial Cells and Melanoma Cells via FGF2-Mediated Paracrine Signaling.” *Pigment Cell & Melanoma Research* 27 (4): 611–20.

Barrionuevo, Francisco, Miguel Burgos, and Rafael Jiménez. 2011. “Origin and Function of Embryonic Sertoli Cells.” *Biomolecular Concepts* 2 (6): 537–47.

Barthold, J. S., K. Kumasi-Rivers, J. Upadhyay, B. Shekarriz, and J. Imperato-Mcginley. 2000. “Testicular Position in the Androgen Insensitivity Syndrome: Implications for the Role of Androgens in Testicular Descent.” *The Journal of Urology* 164 (2): 497–501.

Battula, Venkata Lokesh, Kurt William Evans, Brett George Hollier, Yuexi Shi, Frank C. Marini, Ayyakkannu Ayyanan, Rui-Yu Wang, et al. 2010. “Epithelial-Mesenchymal Transition-Derived Cells Exhibit Multilineage Differentiation Potential Similar to Mesenchymal Stem Cells.” *Stem Cells* 28 (8): 1435–45.

Ben Amar, M., and M. Wu. 2014. “Re-Epithelialization: Advancing Epithelium Frontier during Wound Healing.” *Journal of the Royal Society, Interface / the Royal Society* 11 (93): 20131038.

Beurel, Eléonore, and Richard S. Jope. 2008. “Differential Regulation of STAT Family Members by Glycogen Synthase Kinase-3.” *The Journal of Biological Chemistry* 283 (32): 21934–44.

Bhattacharjee, Rahul, Suranjana Goswami, Tejasvi Dudiki, Anthony P. Popkie, Christopher J. Phiel, Douglas Kline, and Srinivasan Vijayaraghavan. 2015. “Targeted Disruption of Glycogen Synthase Kinase 3A (GSK3A) in Mice Affects Sperm Motility Resulting in Male Infertility.” *Biology of Reproduction* 92 (3): 65.

Boyer, Alexandre, Jonathan R. Yeh, Xiangfan Zhang, Marilène Paquet, Aurore Gaudin, Makoto C. Nagano, and Derek Boerboom. 2012. “CTNNB1 Signaling in Sertoli Cells Downregulates Spermatogonial Stem Cell Activity via WNT4.” *PloS One* 7 (1): e29764.

Brabletz, Simone, Karolina Bajdak, Simone Meidhof, Ulrike Burk, Gabriele Niedermann, Elke Firat, Ulrich Wellner, et al. 2011. “The ZEB1/miR-200 Feedback Loop Controls Notch Signalling in Cancer Cells.” *The EMBO Journal* 30 (4): 770–82.

Brown, Kimberly A., Mary E. Aakre, Agnieska E. Gorska, James O. Price, Sakina E. Eltom, Jennifer A. Pietenpol, and Harold L. Moses. 2004. “Induction by Transforming Growth

Factor-β1 of Epithelial to Mesenchymal Transition Is a Rare Event in Vitro." *Breast Cancer Research: BCR* 6 (3). https://doi.org/10.1186/bcr778.

Buehr, M., S. Gu, and A. McLaren. 1993. "Mesonephric Contribution to Testis Differentiation in the Fetal Mouse." *Development* 117 (1): 273–81.

Câmara, Joana, and Gabor Jarai. 2010. "Epithelial-Mesenchymal Transition in Primary Human Bronchial Epithelial Cells Is Smad-Dependent and Enhanced by Fibronectin and TNF-α." *Fibrogenesis & Tissue Repair* 3 (1): 2.

Catizone, Angela, Giulia Ricci, Maria Caruso, Michela Galdieri, Katia Corano Scheri, Virginia Di Paolo, and Rita Canipari. 2015. "HGF Modulates Actin Cytoskeleton Remodeling and Contraction in Testicular Myoid Cells." *Biomedicines* 3 (1): 89–109.

Chairoungdua, Arthit, Danielle L. Smith, Pierre Pochard, Michael Hull, and Michael J. Caplan. 2010. "Exosome Release of β-Catenin: A Novel Mechanism That Antagonizes Wnt Signaling." *The Journal of Cell Biology* 190 (6): 1079–91.

Cheng, C. Y., and D. D. Mruk. 2011. "The Blood-Testis Barrier and Its Implications for Male Contraception." *Pharmacological Reviews* 64 (1): 16–64.

Chen, Hao, Xiao-Hui Min, Qi-Yi Wang, Felix W. Leung, Liu Shi, Yu Zhou, Tao Yu, et al. 2015. "Pre-Activation of Mesenchymal Stem Cells with TNF-α, IL-1β and Nitric Oxide Enhances Its Paracrine Effects on Radiation-Induced Intestinal Injury." *Scientific Reports* 5 (March): 8718.

Chen, Liang-Yu, Paula R. Brown, William B. Willis, and Edward M. Eddy. 2014. "Peritubular Myoid Cells Participate in Male Mouse Spermatogonial Stem Cell Maintenance." *Endocrinology* 155 (12): 4964–74.

Chikhovskaya, J. V., M. J. Jonker, A. Meissner, T. M. Breit, S. Repping, and A. M. M. van Pelt. 2011. "Human Testis-Derived Embryonic Stem Cell-like Cells Are Not Pluripotent, but Possess Potential of Mesenchymal Progenitors." *Human Reproduction* 27 (1): 210–21.

Chowdhury, Farhan, Yanzhen Li, Yeh-Chuin Poh, Tamaki Yokohama-Tamaki, Ning Wang, and Tetsuya S. Tanaka. 2010. "Soft Substrates Promote Homogeneous Self-Renewal of Embryonic Stem Cells via Downregulating Cell-Matrix Tractions." *PloS One* 5 (12): e15655.

Clayton, P. E. 2000. "Leptin and Puberty." *Archives of Disease in Childhood* 83 (1): 1–4.

Croes, Michiel, F. Cumhur Oner, Moyo C. Kruyt, Taco J. Blokhuis, Okan Bastian, Wouter J. A. Dhert, and Jacqueline Alblas. 2015. "Proinflammatory Mediators Enhance the Osteogenesis of Human Mesenchymal Stem Cells after Lineage Commitment." *PloS One* 10 (7): e0132781.

Curley, Michael, Laura Milne, Sarah Smith, Nina Atanassova, Diane Rebourcet, Annalucia Darbey, Patrick W. F. Hadoke, Sara Wells, and Lee B. Smith. 2018. "Leukemia Inhibitory Factor-Receptor Is Dispensable for Prenatal Testis Development but Is Required in Sertoli Cells for Normal Spermatogenesis in Mice." *Scientific Reports* 8 (1): 11532.

Dagle, John M., Jaime L. Sabel, Jennifer L. Littig, Lillian B. Sutherland, Sandra J. Kolker, and Daniel L. Weeks. 2003. "Pitx2c Attenuation Results in Cardiac Defects and Abnormalities of Intestinal Orientation in Developing Xenopus Laevis." *Developmental Biology* 262 (2): 268–81.

Daugherty, Rebecca Leadem, and Cara J. Gottardi. 2007. "Phospho-Regulation of β-Catenin Adhesion and Signaling Functions." *Physiology* 22 (5): 303–9.

Dave, Natàlia, Sandra Guaita-Esteruelas, Susana Gutarra, Àlex Frias, Manuel Beltran, Sandra Peiró, and Antonio García de Herreros. 2011. "Functional Cooperation between Snail1 and Twist in the Regulation of ZEB1 Expression during Epithelial to Mesenchymal Transition." *The Journal of Biological Chemistry* 286 (14): 12024–32.

Dent, J. A., A. G. Polson, and M. W. Klymkowsky. 1989. "A Whole-Mount Immunocytochemical Analysis of the Expression of the Intermediate Filament Protein

Vimentin in Xenopus." *Development* 105 (1): 61–74.
Derynck, Rik, and Ying E. Zhang. 2003. "Smad-Dependent and Smad-Independent Pathways in TGF-β Family Signalling." *Nature* 425 (6958): 577–84.
Dimri, G. P., X. Lee, G. Basile, M. Acosta, G. Scott, C. Roskelley, E. E. Medrano, M. Linskens, I. Rubelj, and O. Pereira-Smith. 1995. "A Biomarker That Identifies Senescent Human Cells in Culture and in Aging Skin in Vivo." *Proceedings of the National Academy of Sciences* 92 (20): 9363–67.
Dorval-Coiffec, Isabelle, Jean-Guy Delcros, Harri Hakovirta, Jorma Toppari, Bernard Jégou, and Claire Piquet-Pellorce. 2005. "Identification of the Leukemia Inhibitory Factor Cell Targets within the Rat Testis." *Biology of Reproduction* 72 (3): 602–11.
Duncan, Alice R., Jennifer J. Forcina, Paul C. W. Tsang, and David H. Townson. 2009. "Disruption of Cytokeratin 18-Containing Intermediate Filaments in Bovine Luteal Cells: Effects of Acrylamide on Progesterone Secretion, Fas Expression, and FasL-Induced Apoptosis." *Biology of Reproduction* 81 (Suppl_1): 558–558.
Egea, V., L. von Baumgarten, C. Schichor, B. Berninger, T. Popp, P. Neth, R. Goldbrunner, et al. 2011. "TNF-α Respecifies Human Mesenchymal Stem Cells to a Neural Fate and Promotes Migration toward Experimental Glioma." *Cell Death and Differentiation* 18 (5): 853–63.
Eildermann, K., J. Gromoll, and R. Behr. 2012. "Misleading and Reliable Markers to Differentiate between Primate Testis-Derived Multipotent Stromal Cells and Spermatogonia in Culture." *Human Reproduction* 27 (6): 1754–67.
Engl, W., B. Arasi, L. L. Yap, J. P. Thiery, and V. Viasnoff. 2014. "Actin Dynamics Modulate Mechanosensitive Immobilization of E-Cadherin at Adherens Junctions." *Nature Cell Biology* 16 (6): 587–94.
Francipane, Maria Giovanna, and Eric Lagasse. 2015. "The Lymph Node as a New Site for Kidney Organogenesis." *Stem Cells Translational Medicine* 4 (3): 295–307.
Fustaino, Valentina, Dario Presutti, Teresa Colombo, Beatrice Cardinali, Giuliana Papoff, Rossella Brandi, Paola Bertolazzi, Giovanni Felici, and Giovina Ruberti. 2017. "Characterization of Epithelial-Mesenchymal Transition Intermediate/hybrid Phenotypes Associated to Resistance to EGFR Inhibitors in Non-Small Cell Lung Cancer Cell Lines." *Oncotarget* 8 (61): 103340–63.
García-Reyes, Balbina, Lydia Witt, Björn Jansen, Ebru Karasu, Tanja Gehring, Johann Leban, Doris Henne-Bruns, et al. 2018. "Discovery of Inhibitor of Wnt Production 2 (IWP-2) and Related Compounds As Selective ATP-Competitive Inhibitors of Casein Kinase 1 (CK1) δ/ε." *Journal of Medicinal Chemistry* 61 (9): 4087–4102.
Golestaneh, Nady, Golestaneh Nady, Kokkinaki Maria, Pant Disha, Jiang Jiji, Destefano David, Fernandez-Bueno Carlos, et al. 2009. "Pluripotent Stem Cells Derived From Adult Human Testes." *Stem Cells and Development* 18 (8): 1115–25.
Greco, K. V., A. J. Iqbal, L. Rattazzi, G. Nalesso, N. Moradi-Bidhendi, A. R. Moore, M. B. Goldring, F. Dell'Accio, and M. Perretti. 2011. "High Density Micromass Cultures of a Human Chondrocyte Cell Line: A Reliable Assay System to Reveal the Modulatory Functions of Pharmacological Agents." *Biochemical Pharmacology* 82 (12): 1919–29.
Guan, Kaomei, Guan Kaomei, Nayernia Karim, Lars S. Maier, Wagner Stefan, Dressel Ralf, Jae Ho Lee, et al. 2006. "Pluripotency of Spermatogonial Stem Cells from Adult Mouse Testis." *Nature* 440 (7088): 1199–1203.
Håkonsen, Linn Berger, Ane Marie Thulstrup, Anette Skærbech Aggerholm, Jørn Olsen, Jens Peter Bonde, Claus Yding Andersen, Mona Bungum, et al. 2011. "Does Weight Loss Improve Semen Quality and Reproductive Hormones? Results from a Cohort of Severely Obese Men." *Reproductive Health* 8 (1). https://doi.org/10.1186/1742-4755-8-24.
Hanada, Shinichiro, Masaru Harada, Hiroto Kumemura, M. Bishr Omary, Takumi Kawaguchi, Eitaro Taniguchi, Hironori Koga, et al. 2005. "Keratin-Containing

Inclusions Affect Cell Morphology and Distribution of Cytosolic Cellular Components." *Experimental Cell Research* 304 (2): 471–82.

Handelsman, David J., Jennifer A. Spaliviero, and Andrew F. Phippard. 1990. "Highly Vectorial Secretion of Inhibin by Primate Sertoli Cellsin Vitro*." *The Journal of Clinical Endocrinology and Metabolism* 71 (5): 1235–38.

Hay, E. D. 1995. "An Overview of Epithelio-Mesenchymal Transformation." *Acta Anatomica* 154 (1): 8–20.

Hemendinger, R. A., P. Gores, L. Blacksten, V. Harley, and C. Halberstadt. 2002. "Identification of a Specific Sertoli Cell Marker, Sox9, for Use in Transplantation." *Cell Transplantation* 11 (6): 499–505.

Hollier, Brett G., Agata A. Tinnirello, Steven J. Werden, Kurt W. Evans, Joseph H. Taube, Tapasree Roy Sarkar, Nathalie Sphyris, et al. 2013. "FOXC2 Expression Links Epithelial-Mesenchymal Transition and Stem Cell Properties in Breast Cancer." *Cancer Research* 73 (6): 1981–92.

Hong, Jun, Jian Zhou, Junjiang Fu, Tao He, Jun Qin, Li Wang, Lan Liao, and Jianming Xu. 2011. "Phosphorylation of Serine 68 of Twist1 by MAPKs Stabilizes Twist1 Protein and Promotes Breast Cancer Cell Invasiveness." *Cancer Research* 71 (11): 3980–90.

Huang, Ruby Yun-Ju, Parry Guilford, and Jean Paul Thiery. 2012. "Early Events in Cell Adhesion and Polarity during Epithelial-Mesenchymal Transition." *Journal of Cell Science* 125 (Pt 19): 4417–22.

Hutson, John M., Bridget R. Southwell, Ruili Li, Gabrielle Lie, Khairul Ismail, George Harisis, and Nan Chen. 2013. "The Regulation of Testicular Descent and the Effects of Cryptorchidism." *Endocrine Reviews* 34 (5): 725–52.

Jia, Dongya, Mohit Kumar Jolly, Marcelo Boareto, Princy Parsana, Steven M. Mooney, Kenneth J. Pienta, Herbert Levine, and Eshel Ben-Jacob. 2015. "OVOL Guides the Epithelial-Hybrid-Mesenchymal Transition." *Oncotarget* 6 (17): 15436–48.

Johnson, Michael, Manisha Sharma, Cara Jamieson, Jasmine M. Henderson, Myth T. S. Mok, Linda Bendall, and Beric R. Henderson. 2009. "Regulation of β-Catenin Trafficking to the Membrane in Living Cells." *Cellular Signalling* 21 (2): 339–48.

Jolly, Mohit Kumar, Bin Huang, Mingyang Lu, Sendurai A. Mani, Herbert Levine, and Eshel Ben-Jacob. 2014. "Towards Elucidating the Connection between Epithelial-Mesenchymal Transitions and Stemness." *Journal of the Royal Society, Interface / the Royal Society* 11 (101): 20140962.

Jolly, Mohit Kumar, Dongya Jia, Marcelo Boareto, Sendurai A. Mani, Kenneth J. Pienta, Eshel Ben-Jacob, and Herbert Levine. 2015. "Coupling the Modules of EMT and Stemness: A Tunable 'Stemness Window' Model." *Oncotarget* 6 (28): 25161–74.

Jorda, M. 2005. "Upregulation of MMP-9 in MDCK Epithelial Cell Line in Response to Expression of the Snail Transcription Factor." *Journal of Cell Science* 118 (15): 3371–85.

Kalcheim, Chaya. 2015. "Epithelial–Mesenchymal Transitions during Neural Crest and Somite Development." *Journal of Clinical Medicine Research* 5 (1): 1.

Kalluri, Raghu, and Robert A. Weinberg. 2009. "The Basics of Epithelial-Mesenchymal Transition." *The Journal of Clinical Investigation* 119 (6): 1420–28.

Kanai, Y. 2005. "From SRY to SOX9: Mammalian Testis Differentiation." *Journal of Biochemistry* 138 (1): 13–19.

Kanai, Y., Y. Hayashi, H. Kawakami, K. Takata, M. Kurohmaru, H. Hirano, and T. Nishida. 1991. "Effect of Tunicamycin, an Inhibitor of Protein Glycosylation, on Testicular Cord Organization in Fetal Mouse Gonadal Explants in Vitro." *The Anatomical Record* 230 (2): 199–208.

Kanai, Y., H. Kawakami, K. Takata, M. Kurohmaru, H. Hirano, and Y. Hayashi. 1992. "Involvement of Actin Filaments in Mouse Testicular Cord Organization in Vivo and in Vitro." *Biology of Reproduction* 46 (2): 233–45.

Kanatsu-Shinohara, Mito, Kanatsu-Shinohara Mito, Inoue Kimiko, Lee Jiyoung, Yoshimoto Momoko, Ogonuki Narumi, Miki Hiromi, et al. 2004. “Generation of Pluripotent Stem Cells from Neonatal Mouse Testis.” *Cell* 119 (7): 1001–12.

Kandeel, F. R., and R. S. Swerdloff. 1988. “Role of Temperature in Regulation of Spermatogenesis and the Use of Heating as a Method for Contraception.” *Fertility and Sterility* 49 (1): 1–23.

Karl, J., and B. Capel. 1998. “Sertoli Cells of the Mouse Testis Originate from the Coelomic Epithelium.” *Developmental Biology* 203 (2): 323–33.

Karwacki-Neisius, Violetta, Jonathan Göke, Rodrigo Osorno, Florian Halbritter, Jia Hui Ng, Andrea Y. Weiße, Frederick C. K. Wong, et al. 2013. “Reduced Oct4 Expression Directs a Robust Pluripotent State with Distinct Signaling Activity and Increased Enhancer Occupancy by Oct4 and Nanog.” *Cell Stem Cell* 12 (5): 531–45.

Kent, J., S. C. Wheatley, J. E. Andrews, A. H. Sinclair, and P. Koopman. 1996. “A Male-Specific Role for SOX9 in Vertebrate Sex Determination.” *Development* 122 (9): 2813–22.

Kidokoro, Tomohide, Shogo Matoba, Ryuji Hiramatsu, Masahiko Fujisawa, Masami Kanai-Azuma, Choji Taya, Masamichi Kurohmaru, et al. 2005. “Influence on Spatiotemporal Patterns of a Male-Specific Sox9 Activation by Ectopic Sry Expression during Early Phases of Testis Differentiation in Mice.” *Developmental Biology* 278 (2): 511–25.

Kim, Do, Tiaosi Xing, Zhibin Yang, Ronald Dudek, Qun Lu, and Yan-Hua Chen. 2017. “Epithelial Mesenchymal Transition in Embryonic Development, Tissue Repair and Cancer: A Comprehensive Overview.” *Journal of Clinical Medicine Research* 7 (1): 1.

Klymkowsky, M. W., L. A. Maynell, and A. G. Polson. 1987. “Polar Asymmetry in the Organization of the Cortical Cytokeratin System of Xenopus Laevis Oocytes and Embryos.” *Development* 100 (3): 543–57.

Koenig, Alexander, Claudia Mueller, Cornelia Hasel, Guido Adler, and Andre Menke. 2006. “Collagen Type I Induces Disruption of E-Cadherin-Mediated Cell-Cell Contacts and Promotes Proliferation of Pancreatic Carcinoma Cells.” *Cancer Research* 66 (9): 4662–71.

Koskenniemi, Jaakko J., Helena E. Virtanen, and Jorma Toppari. 2017. “Testicular Growth and Development in Puberty.” *Current Opinion in Endocrinology, Diabetes, and Obesity* 24 (3): 215–24.

Ku, N. O., and M. B. Omary. 1997. “Phosphorylation of Human Keratin 8 in Vivo at Conserved Head Domain Serine 23 and at Epidermal Growth Factor-Stimulated Tail Domain Serine 431.” *The Journal of Biological Chemistry* 272 (11): 7556–64.

Kwon, Yang Woo, Soon Chul Heo, Geun Ok Jeong, Jung Won Yoon, Won Min Mo, Mi Jeong Lee, Il-Ho Jang, Sang Mo Kwon, Jung Sub Lee, and Jae Ho Kim. 2013. “Tumor Necrosis Factor-α-Activated Mesenchymal Stem Cells Promote Endothelial Progenitor Cell Homing and Angiogenesis.” *Biochimica et Biophysica Acta* 1832 (12): 2136–44.

Lamouille, Samy, Jian Xu, and Rik Derynck. 2014. “Molecular Mechanisms of Epithelial–mesenchymal Transition.” *Nature Reviews. Molecular Cell Biology* 15 (3): 178–96.

Lee, C. H., and T. Taketo. 1994. “Normal Onset, but Prolonged Expression, of Sry Gene in the B6.YDOM Sex-Reversed Mouse Gonad.” *Developmental Biology* 165 (2): 442–52.

Lee, Jongdae, Joanna C. K. Kim, Shee-Eun Lee, Christine Quinley, Hyeri Kim, Scott Herdman, Maripat Corr, and Eyal Raz. 2012. “Signal Transducer and Activator of Transcription 3 (STAT3) Protein Suppresses Adenoma-to-Carcinoma Transition in Apcmin/+ Mice via Regulation of Snail-1 (SNAI) Protein Stability.” *The Journal of Biological Chemistry* 287 (22): 18182–89.

Lie, Pearl P. Y., Apple Y. N. Chan, Dolores D. Mruk, Will M. Lee, and C. Yan Cheng. 2010. “Restricted Arp3 Expression in the Testis Prevents Blood-Testis Barrier Disruption during Junction Restructuring at Spermatogenesis.” *Proceedings of the National Academy of Sciences of the United States of America* 107 (25): 11411–16.

Lie, Pearl P. Y., Dolores D. Mruk, Ka Wai Mok, Linlin Su, Will M. Lee, and C. Yan Cheng. 2012. "Focal Adhesion Kinase-Tyr407 and -Tyr397 Exhibit Antagonistic Effects on Blood-Testis Barrier Dynamics in the Rat." *Proceedings of the National Academy of Sciences of the United States of America* 109 (31): 12562–67.

Lillie, Frank Rattray. 1908. *The Development of the Chick; an Introduction to Embryology*. Holt, Rinehart and Winston.

Li, Ping, Li Ping, Yang Ru, and Gao Wei-Qiang. 2014. "Contributions of Epithelial-Mesenchymal Transition and Cancer Stem Cells to the Development of Castration Resistance of Prostate Cancer." *Molecular Cancer* 13 (1): 55.

Li, Qingguo, Li Qingguo, Wei Ping, Huang Ben, Xu Ye, Li Xinxiang, Li Yaqi, Cai Sanjun, and Li Dawei. 2016. "MAEL Expression Links Epithelial-Mesenchymal Transition and Stem Cell Properties in Colorectal Cancer." *International Journal of Cancer* 139 (11): 2502–11.

Livera, Gabriel, Virginie Rouiller-Fabre, Catherine Pairault, Christine Levacher, and René Habert. 2002. "Regulation and Perturbation of Testicular Functions by Vitamin A." *Reproduction* 124 (2): 173–80.

Li, Yi, Qing Gao, Gang Yin, Xiangyun Ding, and Jing Hao. 2012. "WNT/β-Catenin-Signaling Pathway Stimulates the Proliferation of Cultured Adult Human Sertoli Cells via Upregulation of C-Myc Expression." *Reproductive Sciences* 19 (11): 1232–40.

Lovegrove, B. G. 2014. "Cool Sperm: Why Some Placental Mammals Have a Scrotum." *Journal of Evolutionary Biology* 27 (5): 801–14.

Lustig, L., S. Meroni, S. Cigorraga, M. B. Casanova, S. E. Vianello, and B. Denduchis. 1998. "Immunodetection of Cell Adhesion Molecules in Rat Sertoli Cell Cultures." *American Journal of Reproductive Immunology* 39 (6): 399–405.

Maekawa, M., K. Kamimura, and T. Nagano. 1996. "Peritubular Myoid Cells in the Testis: Their Structure and Function." *Archives of Histology and Cytology* 59 (1): 1–13.

Makarova, Galina, Michael Bette, Ansgar Schmidt, Ralf Jacob, Chengzhong Cai, Fiona Rodepeter, Thomas Betz, et al. 2013. "Epidermal Growth Factor-Induced Modulation of Cytokeratin Expression Levels Influences the Morphological Phenotype of Head and Neck Squamous Cell Carcinoma Cells." *Cell and Tissue Research* 351 (1): 59–72.

Mani, Sendurai A., Guo Wenjun, Liao Mai-Jing, Elinor Ng Eaton, Ayyanan Ayyakkannu, Alicia Y. Zhou, Brooks Mary, et al. 2008a. "The Epithelial-Mesenchymal Transition Generates Cells with Properties of Stem Cells." *Cell* 133 (4): 704–15.

Maschler, Sabine, Gerhard Wirl, Herbert Spring, Dorothea V. Bredow, Isabelle Sordat, Hartmut Beug, and Ernst Reichmann. 2005. "Tumor Cell Invasiveness Correlates with Changes in Integrin Expression and Localization." *Oncogene* 24 (12): 2032–41.

Mendez, Melissa G., Shin-Ichiro Kojima, and Robert D. Goldman. 2010. "Vimentin Induces Changes in Cell Shape, Motility, and Adhesion during the Epithelial to Mesenchymal Transition." *FASEB Journal: Official Publication of the Federation of American Societies for Experimental Biology* 24 (6): 1838–51.

Merchant-Larios, H., N. Moreno-Mendoza, and M. Buehr. 1993. "The Role of the Mesonephros in Cell Differentiation and Morphogenesis of the Mouse Fetal Testis." *The International Journal of Developmental Biology* 37 (3): 407–15.

Mise, Nikica, Rajkumar Savai, Haiying Yu, Johannes Schwarz, Naftali Kaminski, and Oliver Eickelberg. 2012. "Zyxin Is a Transforming Growth Factor-β (TGF-β)/Smad3 Target Gene That Regulates Lung Cancer Cell Motility via Integrin α5β1." *The Journal of Biological Chemistry* 287 (37): 31393–405.

Mital, Payal, Gurvinder Kaur, and Jannette M. Dufour. 2010. "Immunoprotective Sertoli Cells: Making Allogeneic and Xenogeneic Transplantation Feasible." *Reproduction* 139 (3): 495–504.

Moniot, Brigitte, Faustine Declosmenil, Francisco Barrionuevo, Gerd Scherer, Kosuke Aritake, Safia Malki, Laetitia Marzi, et al. 2009. "The PGD2 Pathway, Independently of

FGF9, Amplifies SOX9 Activity in Sertoli Cells during Male Sexual Differentiation." *Development* 136 (11): 1813–21.

Moraveji, Seyedeh-Faezeh, Farnoosh Attari, Abdolhossein Shahverdi, Houri Sepehri, Ali Farrokhi, Seyedeh-Nafiseh Hassani, Hananeh Fonoudi, Nasser Aghdami, and Hossein Baharvand. 2012. "Inhibition of Glycogen Synthase Kinase-3 Promotes Efficient Derivation of Pluripotent Stem Cells from Neonatal Mouse Testis." *Human Reproduction* 27 (8): 2312–24.

Morrison, Gillian M., and Joshua M. Brickman. 2006. "Conserved Roles for Oct4 Homologues in Maintaining Multipotency during Early Vertebrate Development." *Development* 133 (10): 2011–22.

Myers, M., F. J. P. Ebling, M. Nwagwu, R. Boulton, K. Wadhwa, J. Stewart, and J. B. Kerr. 2005. "Atypical Development of Sertoli Cells and Impairment of Spermatogenesis in the Hypogonadal (hpg) Mouse." *Journal of Anatomy* 207 (6): 797–811.

Nace, J. D., and R. A. Tassava. 1995. "Examination of Fibronectin Distribution and Its Sources in the Regenerating Newt Limb by Immunocytochemistry and in Situ Hybridization." *Developmental Dynamics: An Official Publication of the American Association of Anatomists* 202 (2): 153–64.

Nakaya, Yukiko, Shinya Kuroda, Yuji T. Katagiri, Kozo Kaibuchi, and Yoshiko Takahashi. 2004. "Mesenchymal-Epithelial Transition during Somitic Segmentation Is Regulated by Differential Roles of Cdc42 and Rac1." *Developmental Cell* 7 (3): 425–38.

Nakaya, Yukiko, Erike W. Sukowati, Yuping Wu, and Guojun Sheng. 2008. "RhoA and Microtubule Dynamics Control Cell-Basement Membrane Interaction in EMT during Gastrulation." *Nature Cell Biology* 10 (7): 765–75.

Nazarian, Hamid, Marefat Ghaffari Novin, Mohammad Reza Jalili, Reza Mirfakhraie, Mohammad Hassan Heidari, Seyed Jalil Hosseini, Mohsen Norouzian, and Nahid Ehsani. 2014. "Expression of Glycogen Synthase Kinase 3-β (GSK3-β) Gene in Azoospermic Men." *Iranian Journal of Reproductive Medicine* 12 (5): 313–20.

Nicholls, Peter K., Peter G. Stanton, Justin L. Chen, Justine S. Olcorn, Jenna T. Haverfield, Hongwei Qian, Kelly L. Walton, Paul Gregorevic, and Craig A. Harrison. 2012. "Activin Signaling Regulates Sertoli Cell Differentiation and Function." *Endocrinology* 153 (12): 6065–77.

Nieto, M. Angela, M. Angela Nieto, and Cano Amparo. 2012. "The Epithelial–mesenchymal Transition under Control: Global Programs to Regulate Epithelial Plasticity." *Seminars in Cancer Biology* 22 (5-6): 361–68.

Nistal, M., R. Paniagua, M. A. Abaurrea, and L. Santamaría. 1982. "Hyperplasia and the Immature Appearance of Sertoli Cells in Primary Testicular Disorders." *Human Pathology* 13 (1): 3–12.

Nisticò, Paola, Mina J. Bissell, and Derek C. Radisky. 2012. "Epithelial-Mesenchymal Transition: General Principles and Pathological Relevance with Special Emphasis on the Role of Matrix Metalloproteinases." *Cold Spring Harbor Perspectives in Biology* 4 (2). https://doi.org/10.1101/cshperspect.a011908.

Niwa, Hitoshi, Jun-Ichi Miyazaki, and Austin G. Smith. 2000. "Quantitative Expression of Oct-3/4 Defines Differentiation, Dedifferentiation or Self-Renewal of ES Cells." *Nature Genetics* 24 (4): 372–76.

Nyati, Shyam, Katrina Schinske, Dipankar Ray, Mukesh K. Nyati, Mukesh Nyati, Brian Dale Ross, and Alnawaz Rehemtulla. 2011. "Molecular Imaging of TGFβ-Induced Smad2/3 Phosphorylation Reveals a Role for Receptor Tyrosine Kinases in Modulating TGFβ Signaling." *Clinical Cancer Research: An Official Journal of the American Association for Cancer Research* 17 (23): 7424–39.

Paranko, J., M. Kallajoki, L. J. Pelliniemi, V. P. Lehto, and I. Virtanen. 1986. "Transient Coexpression of Cytokeratin and Vimentin in Differentiating Rat Sertoli Cells." *Developmental Biology* 117 (1): 35–44.

Paredes, Roberto, Shoko Ishibashi, Roisin Borrill, Jacques Robert, and Enrique Amaya. 2015. "Xenopus: An in Vivo Model for Imaging the Inflammatory Response Following Injury and Bacterial Infection." *Developmental Biology* 408 (2): 213–28.

Pavlou, S. N., K. Brewer, M. G. Farley, J. Lindner, M. C. Bastias, B. J. Rogers, L. L. Swift, J. E. Rivier, W. W. Vale, and P. M. Conn. 1991. "Combined Administration of a Gonadotropin-Releasing Hormone Antagonist and Testosterone in Men Induces Reversible Azoospermia without Loss of Libido." *The Journal of Clinical Endocrinology and Metabolism* 73 (6): 1360–69.

Peinado, Hector, Esteban Ballestar, Manel Esteller, and Amparo Cano. 2004. "Snail Mediates E-Cadherin Repression by the Recruitment of the Sin3A/histone Deacetylase 1 (HDAC1)/HDAC2 Complex." *Molecular and Cellular Biology* 24 (1): 306–19.

Pelletier, R-Marc. 2011. "The Blood-Testis Barrier: The Junctional Permeability, the Proteins and the Lipids." *Progress in Histochemistry and Cytochemistry* 46 (2): 49–127.

Petrosyan, Armen, Mohamed F. Ali, and Pi-Wan Cheng. 2015. "Keratin 1 Plays a Critical Role in Golgi Localization of Core 2N-Acetylglucosaminyltransferase M via Interaction with Its Cytoplasmic Tail." *The Journal of Biological Chemistry* 290 (10): 6256–69.

Piquet-Pellorce, C., I. Dorval-Coiffec, M. D. Pham, and B. Jégou. 2000. "Leukemia Inhibitory Factor Expression and Regulation within the Testis." *Endocrinology* 141 (3): 1136–41.

Potokar, Maja, Marko Kreft, Lizhen Li, J. Daniel Andersson, Tina Pangrsic, Helena H. Chowdhury, Milos Pekny, and Robert Zorec. 2007. "Cytoskeleton and Vesicle Mobility in Astrocytes." *Traffic* 8 (1): 12–20.

Potter, Sarah J., and Tony DeFalco. 2017. "Role of the Testis Interstitial Compartment in Spermatogonial Stem Cell Function." *Reproduction* 153 (4): R151–62.

Prasad, A. S., C. S. Mantzoros, F. W. Beck, J. W. Hess, and G. J. Brewer. 1996. "Zinc Status and Serum Testosterone Levels of Healthy Adults." *Nutrition* 12 (5): 344–48.

Przygodzka, Patrycja, Izabela Papiewska-Pajak, Helena Bogusz, Jakub Kryczka, Katarzyna Sobierajska, M. Anna Kowalska, and Joanna Boncela. 2016. "Neuromedin U Is Upregulated by Snail at Early Stages of EMT in HT29 Colon Cancer Cells." *Biochimica et Biophysica Acta* 1860 (11 Pt A): 2445–53.

Puisieux, Alain, Thomas Brabletz, and Julie Caramel. 2014. "Oncogenic Roles of EMT-Inducing Transcription Factors." *Nature Cell Biology* 16 (6): 488–94.

Qiu, Caihong, Yinghong Ma, Jianquan Wang, Shuping Peng, and Yingqun Huang. 2010. "Lin28-Mediated Post-Transcriptional Regulation of Oct4 Expression in Human Embryonic Stem Cells." *Nucleic Acids Research* 38 (4): 1240–48.

Richardson, L. L., H. K. Kleinman, and M. Dym. 1995. "Basement Membrane Gene Expression by Sertoli and Peritubular Myoid Cells in Vitro in the Rat." *Biology of Reproduction* 52 (2): 320–30.

Richter, Anne, Richter Anne, Valdimarsdottir Lena, Helga Eyja Hrafnkelsdottir, Johann Frimann Runarsson, Arna Run Omarsdottir, Dorien Ward-van Oostwaard, Mummery Christine, and Valdimarsdottir Gudrun. 2014. "BMP4 Promotes EMT and Mesodermal Commitment in Human Embryonic Stem Cells via SLUG and MSX2." *Stem Cells* 32 (3): 636–48.

Rogatsch, H., A. Hittmair, G. Mikuz, H. Feichtinger, and D. Jezek. 1996. "Expression of Vimentin, Cytokeratin, and Desmin in Sertoli Cells of Human Fetal, Cryptorchid, and Tumour-Adjacent Testicular Tissue." *Virchows Archiv: An International Journal of Pathology* 427 (5). https://doi.org/10.1007/bf00199510.

Romano, Laura A., and Raymond B. Runyan. 2000. "Slug Is an Essential Target of TGFβ2 Signaling in the Developing Chicken Heart." *Developmental Biology* 223 (1): 91–102.

Sauka-Spengler, Tatjana, and Marianne Bronner-Fraser. 2008. "A Gene Regulatory Network Orchestrates Neural Crest Formation." *Nature Reviews. Molecular Cell Biology* 9 (7): 557–68.

Schmahl, J., E. M. Eicher, L. L. Washburn, and B. Capel. 2000. “Sry Induces Cell Proliferation in the Mouse Gonad.” *Development* 127 (1): 65–73.

Seandel, Marco, Daylon James, Sergey V. Shmelkov, Ilaria Falciatori, Jiyeon Kim, Sai Chavala, Douglas S. Scherr, et al. 2007. “Generation of Functional Multipotent Adult Stem Cells from GPR125+ Germline Progenitors.” *Nature* 449 (7160): 346–50.

Seidel, M. G., and A. T. Look. 2001. “E2A-HLF Usurps Control of Evolutionarily Conserved Survival Pathways.” *Oncogene* 20 (40): 5718–25.

Sekido, Ryohei, Isabelle Bar, Véronica Narváez, Graeme Penny, and Robin Lovell-Badge. 2004. “SOX9 Is up-Regulated by the Transient Expression of SRY Specifically in Sertoli Cell Precursors.” *Developmental Biology* 274 (2): 271–79.

Sekido, Ryohei, and Robin Lovell-Badge. 2008. “Sex Determination Involves Synergistic Action of SRY and SF1 on a Specific Sox9 Enhancer.” *Nature* 456 (7223): 824–824.

Setchell, Brian P. 2009a. “Blood-Testis Barrier, Junctional and Transport Proteins and Spermatogenesis.” In *Advances in Experimental Medicine and Biology*, 212–33.

Shabana, A. H., M. Oboeuf, and N. Forest. 1994. “Cytoplasmic Desmosomes and Intermediate Filament Disturbance Following Acrylamide Treatment in Cultured Rat Keratinocytes.” *Tissue & Cell* 26 (1): 43–55.

Sharpe, R. 2003. “Proliferation and Functional Maturation of Sertoli Cells, and Their Relevance to Disorders of Testis Function in Adulthood.” *Reproduction* 125 (6): 769–84.

Sharpe, Richard M., Chris McKinnell, Catrina Kivlin, and Jane S. Fisher. 2003. “Proliferation and Functional Maturation of Sertoli Cells, and Their Relevance to Disorders of Testis Function in Adulthood.” *Reproduction* 125 (6): 769–84.

Shimabukuro, Yoshio, Hiroaki Terashima, Masahide Takedachi, Kenichiro Maeda, Tomomi Nakamura, Keigo Sawada, Mariko Kobashi, et al. 2011. “Fibroblast Growth Factor-2 Stimulates Directed Migration of Periodontal Ligament Cells via PI3K/AKT Signaling and CD44/hyaluronan Interaction.” *Journal of Cellular Physiology* 226 (3): 809–21.

Shima, Yuichi, Kanako Miyabayashi, Shogo Haraguchi, Tatsuhiko Arakawa, Hiroyuki Otake, Takashi Baba, Sawako Matsuzaki, et al. 2013. “Contribution of Leydig and Sertoli Cells to Testosterone Production in Mouse Fetal Testes.” *Molecular Endocrinology* 27 (1): 63–73.

Shimono, Yohei, Maider Zabala, Robert W. Cho, Neethan Lobo, Piero Dalerba, Dalong Qian, Maximilian Diehn, et al. 2009. “Downregulation of miRNA-200c Links Breast Cancer Stem Cells with Normal Stem Cells.” *Cell* 138 (3): 592–603.

Silva, Jose, Jennifer Nichols, Thorold W. Theunissen, Ge Guo, Anouk L. van Oosten, Ornella Barrandon, Jason Wray, Shinya Yamanaka, Ian Chambers, and Austin Smith. 2009. “Nanog Is the Gateway to the Pluripotent Ground State.” *Cell* 138 (4): 722–37.

Siu, Erica R., Elissa W. P. Wong, Dolores D. Mruk, Catarina S. Porto, and C. Yan Cheng. 2009. “Focal Adhesion Kinase Is a Blood-Testis Barrier Regulator.” *Proceedings of the National Academy of Sciences of the United States of America* 106 (23): 9298–9303.

Smaill, J. B., B. D. Palmer, G. W. Rewcastle, W. A. Denny, D. J. McNamara, E. M. Dobrusin, A. J. Bridges, et al. 1999. “Tyrosine Kinase Inhibitors. 15. 4-(Phenylamino) quinazoline and 4-(phenylamino)pyrido[d]pyrimidine Acrylamides as Irreversible Inhibitors of the ATP Binding Site of the Epidermal Growth Factor Receptor.” *Journal of Medicinal Chemistry* 42 (10): 1803–15.

Sonavane, Pooja R., Chong Wang, Bette Dzamba, Gregory F. Weber, Ammasi Periasamy, and Douglas W. DeSimone. 2017. “Mechanical and Signaling Roles for Keratin Intermediate Filaments in the Assembly and Morphogenesis of Mesendoderm Tissue at Gastrulation.” *Development* 144 (23): 4363–76.

Stoker, M., and M. Perryman. 1985. “An Epithelial Scatter Factor Released by Embryo Fibroblasts.” *Journal of Cell Science* 77 (August): 209–23.

Stosiek, P., M. Kasper, and U. Karsten. 1990. “Expression of Cytokeratins 8 and 18 in

Human Sertoli Cells of Immature and Atrophic Seminiferous Tubules." *Differentiation; Research in Biological Diversity* 43 (1): 66–70.

Sun, X., E. N. Meyers, M. Lewandoski, and G. R. Martin. 1999. "Targeted Disruption of Fgf8 Causes Failure of Cell Migration in the Gastrulating Mouse Embryo." *Genes & Development* 13 (14): 1834–46.

Tanwar, Pradeep S., Tomoko Kaneko-Tarui, Lihua Zhang, Poonam Rani, Makoto M. Taketo, and Jose Teixeira. 2010. "Constitutive WNT/Beta-Catenin Signaling in Murine Sertoli Cells Disrupts Their Differentiation and Ability to Support Spermatogenesis1." *Biology of Reproduction* 82 (2): 422–32.

Thiery, Jean Paul, Hervé Acloque, Ruby Y. J. Huang, and M. Angela Nieto. 2009. "Epithelial-Mesenchymal Transitions in Development and Disease." *Cell* 139 (5): 871–90.

Tlapakova, Tereza, Thi Minh Xuan Nguyen, Marketa Vegrichtova, Monika Sidova, Karolina Strnadova, Monika Blahova, and Vladimir Krylov. 2016. "Identification and Characterization of Xenopus Tropicalis Common Progenitors of Sertoli and Peritubular Myoid Cell Lineages." *Biology Open* 5 (9): 1275–82.

Tom, L., S. Bhasin, W. Salameh, B. Steiner, M. Peterson, R. Z. Sokol, J. Rivier, W. Vale, and R. S. Swerdloff. 1992. "Induction of Azoospermia in Normal Men with Combined Nal-Glu Gonadotropin-Releasing Hormone Antagonist and Testosterone Enanthate." *The Journal of Clinical Endocrinology and Metabolism* 75 (2): 476–83.

Towbin, H., T. Staehelin, and J. Gordon. 1992. "Electrophoretic Transfer of Proteins from Polyacrylamide Gels to Nitrocellulose Sheets: Procedure and Some Applications. 1979." *Biotechnology* 24: 145–49.

Tripiciano, A., A. Filippini, F. Ballarini, and F. Palombi. 1998. "Contractile Response of Peritubular Myoid Cells to Prostaglandin F2alpha." *Molecular and Cellular Endocrinology* 138 (1-2): 143–50.

Valenti, Daniela, Sandro La Vignera, Rosita A. Condorelli, Rocco Rago, Nunziata Barone, Enzo Vicari, and Aldo E. Calogero. 2013. "Follicle-Stimulating Hormone Treatment in Normogonadotropic Infertile Men." *Nature Reviews. Urology* 10 (1): 55–62.

Veevers-Lowe, Jennifer, Stephen G. Ball, Adrian Shuttleworth, and Cay M. Kielty. 2011. "Mesenchymal Stem Cell Migration Is Regulated by Fibronectin through α5β1-Integrin-Mediated Activation of PDGFR-β and Potentiation of Growth Factor Signals." *Journal of Cell Science* 124 (Pt 8): 1288–1300.

Vijayaraj, Preethi, Cornelia Kröger, Ursula Reuter, Reinhard Windoffer, Rudolf E. Leube, and Thomas M. Magin. 2009. "Keratins Regulate Protein Biosynthesis through Localization of GLUT1 and -3 Upstream of AMP Kinase and Raptor." *The Journal of Cell Biology* 187 (2): 175–84.

Vincent, Theresa, Etienne P. A. Neve, Jill R. Johnson, Alexander Kukalev, Federico Rojo, Joan Albanell, Kristian Pietras, et al. 2009. "A SNAIL1-SMAD3/4 Transcriptional Repressor Complex Promotes TGF-Beta Mediated Epithelial-Mesenchymal Transition." *Nature Cell Biology* 11 (8): 943–50.

Walker, William H. 2011. "Testosterone Signaling and the Regulation of Spermatogenesis." *Spermatogenesis* 1 (2): 116–20.

Wang, Hao, Wang Hao, Wang Hong-Sheng, Zhou Bin-Hua, Li Cui-Lin, Zhang Fan, Wang Xian-Feng, et al. 2013. "Epithelial–Mesenchymal Transition (EMT) Induced by TNF-α Requires AKT/GSK-3β-Mediated Stabilization of Snail in Colorectal Cancer." *PloS One* 8 (2): e56664.

Wang, Huizhi, Jonathan Brown, and Michael Martin. 2011. "Glycogen Synthase Kinase 3: A Point of Convergence for the Host Inflammatory Response." *Cytokine* 53 (2): 130–40.

Winter, J. P. de. 1993. "Activin Is Produced by Rat Sertoli Cells in Vitro and Can Act as an Autocrine Regulator of Sertoli Cell Function." *Endocrinology* 132 (3): 975–82.

Wong, C-H. 2004. "Regulation of Blood-Testis Barrier Dynamics: An in Vivo Study."

Journal of Cell Science 117 (5): 783–98.

Wu, Ling, Xiaoxiao Cai, Hai Dong, Wei Jing, Yuanding Huang, Xingmei Yang, Yao Wu, and Yunfeng Lin. 2009. "Serum Regulates Adipogenesis of Mesenchymal Stem Cells via MEK/ERK-Dependent PPARγ Expression and Phosphorylation." *Journal of Cellular and Molecular Medicine* 14 (4): 922–32.

Wu, Selwin K., Guillermo A. Gomez, Magdalene Michael, Suzie Verma, Hayley L. Cox, James G. Lefevre, Robert G. Parton, Nicholas A. Hamilton, Zoltan Neufeld, and Alpha S. Yap. 2014. "Cortical F-Actin Stabilization Generates Apical–lateral Patterns of Junctional Contractility That Integrate Cells into Epithelia." *Nature Cell Biology* 16 (2): 167–78.

Wu, Yadi, Jiong Deng, Piotr G. Rychahou, Suimin Qiu, B. Mark Evers, and Binhua P. Zhou. 2009. "Stabilization of Snail by NF-κB Is Required for Inflammation-Induced Cell Migration and Invasion." *Cancer Cell* 15 (5): 416–28.

Xiao, Xiang, Dolores D. Mruk, Elizabeth I. Tang, R 'ada Massarwa, Ka Wai Mok, Nan Li, Chris K. C. Wong, et al. 2014. "N-Wasp Is Required for Structural Integrity of the Blood-Testis Barrier." *PLoS Genetics* 10 (6): e1004447.

Xiong, Hua, Jie Hong, Wan Du, Yan-Wei Lin, Lin-Lin Ren, Ying-Chao Wang, Wen-Yu Su, et al. 2012. "Roles of STAT3 and ZEB1 Proteins in E-Cadherin down-Regulation and Human Colorectal Cancer Epithelial-Mesenchymal Transition." *The Journal of Biological Chemistry* 287 (8): 5819–32.

Yan, Chunli, Wesley A. Grimm, Warren L. Garner, Lan Qin, Taryn Travis, Neiman Tan, and Yuan-Ping Han. 2010. "Epithelial to Mesenchymal Transition in Human Skin Wound Healing Is Induced by Tumor Necrosis Factor-α through Bone Morphogenic Protein-2." *The American Journal of Pathology* 176 (5): 2247–58.

Yang, Yaw-Ching, Ester Piek, Jiri Zavadil, Dan Liang, Donglu Xie, Joerg Heyer, Paul Pavlidis, Raju Kucherlapati, Anita B. Roberts, and Erwin P. Böttinger. 2003. "Hierarchical Model of Gene Regulation by Transforming Growth Factor Beta." *Proceedings of the National Academy of Sciences of the United States of America* 100 (18): 10269–74.

Yokoi, Hiromichi, Yoshihiro Yamama, Yoshihiro Tsuruo, Yoshihiko Kawarada, Naoyuki Miura, Toshihiro Sugiyama, and Kazunori Ishimura. 1998. "Leydig Cells Undergoing Apoptosis in the Perinatal Rat Testis." *Acta Histochemica et Cytochemica* 31 (4): 355–61.

Yook, Jong In, Xiao-Yan Li, Ichiro Ota, Casey Hu, Hyun Sil Kim, Nam Hee Kim, So Young Cha, et al. 2006. "A Wnt-Axin2-GSK3beta Cascade Regulates Snail1 Activity in Breast Cancer Cells." *Nature Cell Biology* 8 (12): 1398–1406.

Yoshida, Takahiro, Nikolai A. Sopko, Max Kates, Xiaopu Liu, Gregory Joice, David J. McConkey, and Trinity J. Bivalacqua. 2018. "Three-Dimensional Organoid Culture Reveals Involvement of Wnt/β-Catenin Pathway in Proliferation of Bladder Cancer Cells." *Oncotarget* 9 (13): 11060–70.

Zheng, Haoxuan, Wenjing Li, Yadong Wang, Zhizhong Liu, Yidong Cai, Tingting Xie, Meng Shi, Zhiqing Wang, and Bo Jiang. 2013. "Glycogen Synthase Kinase-3 Beta Regulates Snail and β-Catenin Expression during Fas-Induced Epithelial-Mesenchymal Transition in Gastrointestinal Cancer." *European Journal of Cancer* 49 (12): 2734–46.

Zhou, Binhua P., Jiong Deng, Weiya Xia, Jihong Xu, Yan M. Li, Mehmet Gunduz, and Mien-Chie Hung. 2004. "Dual Regulation of Snail by GSK-3beta-Mediated Phosphorylation in Control of Epithelial-Mesenchymal Transition." *Nature Cell Biology* 6 (10): 931–40.

Zhou, Chen, Huimin Jiang, Zhen Zhang, Guomin Zhang, Hang Wang, Quansheng Zhang, Peiqing Sun, Rong Xiang, and Shuang Yang. 2017. "ZEB1 Confers Stem Cell-like Properties in Breast Cancer by Targeting Neurogenin-3." *Oncotarget* 8 (33): 54388–401.

List of Attached Publications and Manuscripts

1. Tlapakova Tereza, **Thi Minh Xuan Nguyen**, Marketa Vegrichtova, Monika Sidova, Karolina Strnadova, Monika Blahova, and Vladimir Krylov. 2016. "Identification and Characterization of Xenopus Tropicalis Common Progenitors of Sertoli and Peritubular Myoid Cell Lineages." *Biology Open* 5 (9): 1275–82.

2. **Thi Minh Xuan Nguyen**, Marketa Vegrichtova, Tlapakova Tereza, Magdalena Krulova, and Vladimir Krylov. "Epithelial-mesenchymal transition promotes the differentiation potential of *Xenopus tropicalis* immature Sertoli cells". Submitted in: Stem Cell International Journal with minor revision.

3. **Thi Minh Xuan Nguyen**, Marketa Vegrichtova, Tlapakova Tereza, Magdalena Krulova, and Vladimir Krylov. "The interconnection between cytokeratin and cell-cell junctions in *Xenopus tropicalis* immature Sertoli cells". Submitted in: *Biology Open*.

Attached Publications

Title: Identification and characterization of *X. tropicalis* common progenitors of Sertoli and peritubular myoid cell lineages.

Authors: Tereza Tlapakova[a], Thi Minh Xuan Nguyen[a], Marketa Vegrichtova[a], Monika Sidova[a,b], Karolina Strnadova[a], Monika Blahova[a] and Vladimir Krylov[a*]

Tereza Tlapakova[a]

Email: tereza.tlapakova@natur.cuni.cz

Thi Minh Xuan Nguyen[a]

Email: ntmxuanbk@gmail.com

Marketa Vegrichtova[a]

Email: marketa.vegrichtova@natur.cuni.cz

Monika Sidova[a,b]

Email: monca-sidova@seznam.cz

Karolina Strnadova[a]

Email: karolina.strnadova5@gmail.com

Monika Blahova[a]

Email: blahovm5@natur.cuni.cz

Vladimir Krylov[a*]

* Corresponding author

Email: vkrylov@natur.cuni.cz

Affiliation:

[a] Charles University in Prague, Faculty of Science, Vinicna 7, 128 44, Prague 2, Czech Republic. [b] Laboratory of Gene Expression, Institute of Biotechnology, Academy of Sciences of the Czech Republic, Videnska 1083, 142 20 Prague 4, Czech Republic.

***Corresponding author:** tel: +420221951773, fax: +420221951758, E-mail: vkrylov@natur.cuni.cz

Keywords:

Testicular somatic cells, *Xenopus tropicalis*, migration potential, common progenitor

Summary statement:

We identified cells co-expressing differentiation markers of Sertoli and peritubular myoid cell lineages in *X. tropicalis* through the establishment and characterization of cell culture derived from juvenile testis.

ABSTRACT

The origin of somatic cell lineages during testicular development is controversial in mammals. Employing basal amphibian tetrapod, *Xenopus tropicalis*, we established a cell culture derived from testes of juvenile male. Expression analysis showed transcription of some pluripotency genes and Sertoli cell, peritubular myoid cell and mesenchymal cell markers. Transcription of germ line specific genes was downregulated. Immunocytochemistry revealed that majority of cells express vimentin and co-express Sox9 and smooth muscle α-actin (Sma) indicating the existence of common progenitor of Sertoli and peritubular myoid cell lineages. Microinjection of transgenic, red fluorescent protein (RFP) positive somatic testicular cells into peritoneal cavity of *X. tropicalis* tadpoles resulted in cell deposits in heart, pronephros and intestine and later in a strong proliferation and formation of cell to cell net growing through the tadpole body. Immunohistochemistry analysis of transplanted tadpoles showed a strong expression of vimentin in RFP positive cells. No co-localization of Sox9 and Sma signals was observed during the first three weeks indicating their dedifferentiation to a migratory active mesenchymal cells recently described in human testicular biopsies.

INTRODUCTION

The architecture of seminiferous tubules is tightly associated with the presence of peritubular myoid cells (PTMC) and Sertoli cells (SC) both forming basement membranes underlying the seminiferous epithelium (Skinner et al., 1985). Sertoli cells (SC) are also indispensable for germ cell maturation and differentiation (Berndtson and Thompson, 1990; Johnson et al., 1984). They stretch to the lumen and have an intimate contact with developing gametes ranging from spermatogonia located on the base to spermatids in the centre. Sertoli cells also provide the signaling niche via expression of several growth factors and cytokines (de Rooij, 2009). In addition, with PTMCs they participate on the formation of seminiferous cords and appropriate vascularization through the expression of Sry (Koopman et al., 1990) and downstream signaling cascades (Bott et al., 2006). Moreover, they function as an immunological barrier since testes are immunologically privileged organ (Dufour et al.,
2005). Leydig cells start to differentiate in the end of the proliferative phase of Sertoli cells

(Baker et al., 1999; Nef et al., 2000; O'Shaughnessy et al., 2008) and form the stable cell line indispensable for the production of male sex hormones.

The origin of individual testicular somatic cell lineages in mouse is still controversial. Precursors of Sertoli cells were detected in the population of coelomic epithelial cells migrated into the gonad 11.5 days post coitum (Karl and Capel, 1998). Later publications disproved these findings and showed that pre-Sertoli cells are already present in the developing gonad altogether with arrived germ cells and form Sertoli-Germ Cell Mass (SGCM) (reviewed in Cool et al., 2012). Based on the expression of the low affinity neurotrophin receptor p75, peritubular myoid cells were found as mesenchymal precursors migrated from an adjacent mesonephric tissue (Campagnolo et al., 2001). However, also this result was disproved and only endothelial cells, but not PTMCs were identified as a migrating population from mesonephros to the gonadal base (Combes et al., 2009). Authors performed *ex vivo* assay in which they co-cultured a wild type male genital ridge alongside mesonephroi constitutively expressing GFP (Nishino et al., 2000). They found that endothelial cells with VE-cadherin expression and not p75 positive PTMCs are the only migrating cells entering gonad. Furthermore, endothelial cells were identified indispensable for the establishing a proper seminiferous tubule architecture (Combes et al., 2009).

Regarding humans (Chikhovskaya et al., 2012) used frozen testicular biopsies for variable enzymatic digestions and subsequent cultivation *in vitro.* During 30-50 days ESC (embryonic stem cells) like colonies emerged. Gene expression analysis revealed a low level of pluripotency markers such as *POU5F1*, *NANOG* and *SOX2* which was in disagreement with similar studies performed on mouse where such colonies were found to be derived from dedifferentiated spermatogonial stem cells (SSCs) and showed the ability to form teratoma (Guan et al., 2006; Kanatsu-Shinohara et al., 2004, 2008; Ko et al., 2009). Human testicular cells expressed mesenchymal stem cells (MSC) markers and were able to differentiate to three mesodermal lineages (adipocytes, chondrocytes and osteocytes) indicating their multipotent but not pluripotent character (Chikhovskaya et al., 2014).

So far, the majority of experiments employing testicular cells have been conducted in mammalian models. However, studies of their migration and differentiation potential *in vivo* via transplantation into early embryos are hampered by the inner

embryonic development in the womb. In addition, Sertoli cells are able to survive after xenogeneic transplantation into the evolutionarily distant host. This feature is interesting as for the basic research in the field of evolutionary immunology so as for the potential utilization of xenogeneic Sertoli cells for co-transplantations with grafts without the need of immunosuppressive treatment. With this regard, well established non-mammalian vertebrate model organisms are desirable. The diploid amphibian *Xenopus tropicalis* suits these requirements well. *X. tropicalis* is highly valuable in the fields of early vertebrate development, cell biology, and genome evolution. Large oocytes and outer fecundation and embryonic development make it feasible for microinjection or transplantation experiments. *X. tropicalis* genome is fully sequenced and arranged into linkage groups (Hellsten et al., 2010; Wells et al., 2011). Compared to evolutionarily close fish model organisms (zebrafish, carp, trout etc.) the genome is diploid (Tymowska, 1973), and thus more suitable for a gene function studies (Geach and Zimmerman, 2011).

Here we present a successful establishment and *in vitro* and *in vivo* (allogeneic transplantation into the tadpole peritoneal cavity) characterization of a stable cell culture derived from mechanically disrupted testes of a juvenile *X. tropicalis* male three months after metamorphosis. The cell culture is composed of a proliferative testicular cell feeder layer (*Xenopus tropicalis* Testicular Somatic Cells - XtTSC) and testicular cell colonies (*Xenopus tropicalis* Testicular Somatic Cell colonies - XtTSCc). RT and quantitative PCR analysis revealed a strong expression of mesenchymal, Sertoli and peritubular myoid cell markers. On the other hand, germ cell markers were not detected which confirms their somatic origin.

Double immunocytochemical staining against Sox9 (SC marker) and Sma (smooth muscle αactin - marker of PTMC) clearly showed the presence of both antigens in approx. 80% of cells. This result indicates that at least in *Xenopus* there exist a common progenitor of Sertoli and PTM cell lineages emerging from mesenchymal cells present in developing testes.

RESULTS

Morphological and gene expression characterization of *X. tropicalis* testicular cell culture

After establishing a *X. tropicalis* testicular cell culture, the adherent cells formed feeder layer (XtTSC), with the morphological characteristics of Pre-Sertoli cells (Fig. 1A). Long-term cultivation enables the forming of colonies (XtTSCc) resembling embryonic stem cells (ESC) (Fig. 1B). The ultrastructure and cell arrangement within the colony were visualized via transmission electron microscopy (TEM). Sertoli cell-like cells surrounded the colony in two or three tight layers (Fig. 1E). Few of them were found inside. TEM showed that XtTSCs and XtTSCcs were arranged individually in an extensive amount of extracellular matrix (Fig. 1F).

Reverse transcription polymerase chain reaction (RT-PCR) analysis revealed a similar gene expression profile for both cell types. Feeder and colonies were positive for pluripotency markers *klf4* (kruppel-like factor 4), *c-myc* and telomerase reverse transcriptase (*tert*). On the other hand, the key pluripotency genes *POU5F1* (in *Xenopus tropicalis pou5f3.1*, *pou5f3.2* and *pou5f3.3*) (Morrison and Brickman, 2006; Frankenberg et al., 2014) or *sox2* (sex determining region Y box 2), were downregulated suggesting that our cells are not in pluripotent state as it has been defined in the mouse model.

Unfortunately, the expression of *nanog* gene, another key player in pluripotency acquisition (Silva et al., 2009), couldn't be determined since no homologue has been described in *Xenopus* yet. Germ cell markers such as *dazl, ddx4* and *ddx25* were not detected. This result confirmed the somatic origin of testicular cells. More detailed characterization was based on expression markers encompassing Sertoli cells (*sox9*, *kitlg, vim* and *lif*), peritubular myoid cells (*acta2* and *lif*), Leydig cells (*cyp11a1* and *cyp17a1*) and markers of mesenchymal cells (*itgb1*- *cd29*, *cd44* and *thy1*-*cd90*). Except Leydig cell markers, both cell types were positive for all above mentioned genes (Fig. 2A).

RT-PCR data was confirmed by qPCR analysis. The standard deviation of the RNA spike quantification across all samples was 0.2 cycles, which evidences minimum of technical variation and high reproducibility. The hierarchical clustering was performed according to the two groups of analyzed markers, germ cell markers and testis associated markers. Each heatmap includes RNA spike as a highly stable transcript across the cell types and housekeeping gene *odc1*. The result of the clustering indicated that the gene expression profile of testicular tissue is different from XtTSC and XtTSCc groups. Transcripts *dazl*, *ddx25* and *ddx4* are exclusively expressed in the testes, whereas expression of *lif* is substantially reduced in comparison with XtTSCs and XtTSCcs (Fig. 2B).

Immunocytochemistry on feeder cells and colonies employing Sox9, Sma (smooth muscle αactin) and vimentin antibodies revealed their colocalization on more than 80% of cells (Fig 3). Taken together, we concluded that *X. tropicalis* testicular cell culture represents a population of Sertoli cell and PTMC common progenitors. To test if these cells are also present in adult individuals we prepared agarose embedded sections of *X. tropicalis* and mouse testes. After double staining with Sox9 and Sma antibodies we found individual cells expressing both antigens in the interstitial space close to the seminiferous tubules in *X. tropicalis* and even in mouse testis (Fig. 4)

Sertoli cells produce many soluble factors necessary for germ cell survival and proliferation. One of them, the leukemia inhibitory factor (Lif), turned out to be crucial for *in vitro* enhanced XtTSC survival and colony forming activity. Although both the XtTSCs and XtTSCcs express their own *lif* (measured on the RNA level) (Fig. 2A), the addition of recombinant mouse LIF into the cultivation medium entailed a rapid formation and expansion of XtTSCc colonies. On the other hand, a total proliferation rate was unaffected by LIF, since experimental groups (+LIF and -LIF) revealed the same growth curves as depicted on Fig.
1G.

In vivo migration potential of testicular somatic cells

A peritoneal cavity of tadpoles at stage 41 was used for the transplantation of transgenic XtTSCc-RFP and XtTSC-RFP expressing Katushka RFP under ubiquitous CAG promotor (Fig. 1C, D). Cell microinjection of 500 cells per peritoneum was performed through the dorsal side as depicted in (Fig. 5A). One week after transplantation we observed cell deposits mostly in heart and pronephros (Fig. 5B-E). During three following weeks transplanted cells strongly proliferated and formed dense cell to cell connecting net growing through the tadpole's body (Fig. 5F, G). Immunohistochemical analysis of agarose embedded sections of tadpoles 0, 1 and 30 days after transplantation revealed a strong vimentin and RFP colocalization (Fig. 5H).

However, expression of Sox9 and Sma, found in testicular cells prior to microinjection was not detected even 2 hours after transplantation when tadpoles from group ´0 day´ were fixed. Interestingly, 30 days after microinjection we observed Sox9 expression in a few RFP positive cells indicating their potential differentiation into Sertoli cells or chondrocytes where this protein is also considered as a cell specific marker. Since both cell types (XtTSCc-RFP and XtTSC-RFP) showed the same migration and expression pattern, here we published only data concerning transplantation of testicular somatic cell colonies (XtTSCc).

DISCUSSION

In this study we characterized a newly established *X. tropicalis* testicular cell culture encompassing adherent feeder Sertoli-like cells (XtTSC) and cell colonies resembling ESC (XtTSCc). A long-term stem cell culture derived from testis was firstly described by KanatsuShinohara et al. (2003) in mouse. Testes from newborn males were enzymatically dispersed and transferred to gelatine-coated plates. Here, in the presence of the glial cell line-derived neurotrophic factor (GDNF), epidermal growth factor (EGF), fibroblast growth factor 2 (FGF2) and leukemia inhibitory factor (LIF) spermatogonia could be propagated as cell clumps. One year later the same team announced a conversion of germ cells (GS) to multipotent germ stem cells (mGSs) using standard ESC cultivation medium containing 15% fetal bovine serum (FBS) and LIF (Kanatsu-Shinohara et al., 2004). In humans the establishing of similar cell lines was found as a controversial. Four papers described the existence of ES-like cell colonies derived from testicular tissue (Conrad et al., 2008; Golestaneh et al., 2009; Kossack et al., 2009; Mizrak et al., 2010). However, in three of them (Golestaneh et al., 2009; Kossack et al., 2009; Mizrak et al., 2010) authors failed to induce teratoma after subcutaneous transplantation of testicular stem cells into immunodeficient mice. Chikhovskaya et al. (2012) revised previously published data of Mizrak et al. (2010) and performed an expanded study on human testis embryonic stem cell like cells (htES-like cells) derived from frozen testicular samples using different enzyme digestion and cultivation conditions. Gene expression analysis revealed an expression of *KLF4* and *MYC* but not *SOX2*, *NANOG* or key pluripotency marker *POU5FI* indicating their multipotent rather than pluripotent character. RT-PCR confirmed the presence of *CD73*, *CD90* and *CD150* and absence of *CD31*, *CD34* and *CD45* surface markers characteristic for the expression profile of mesenchymal stem cells. Repeated efforts to induce teratoma with htES-like cells in immunodeficient mouse failed. Chikhovskaya et al. (2014) differentiated htES-like cells *in vitro* into three mesodermal cell lineages typical for mesenchymal stem cells (adipocytes, chondrocytes and osteocytes). In our hands, up to five days after the mechanical disruption of *X. tropicalis* testis in the culture medium, adherent cells migrating from the organ were observed. Two months later small colonies of ES-like cells (XtTSCc) started to appear on the feeder layer (XtTSC). RT-PCR analysis showed the same expression profile as in the case of htES-like cells (Chikhovskaya et al., 2012). We detected only some pluripotency markers (*klf4* and *myc*) and markers of mesenchymal stem cells *cd29* (*itgb1*), *cd44* and *cd90* (*thy1*). Germ cell markers (*dazl*, *ddx4* and *ddx25*) were downregulated which further confirms the somatic rather than germ line origin of our testicular cells. Unlike Chikhovskaya et al., (2012) we performed gene expression analysis regarding testicular somatic lineages: Sertoli cells, peritubular myoid cells and

Leydig cells. Except for the Leydig cell markers (*cyp11a1 and cyp17a1*) we found positive reactions for both remaining cell types (*sox9*, *kitlg*, *lif*, *acta2* and *vim*). Immunocytochemistry revealed a colocalization of nuclear Sox9 and cytoplasmic Sma antigens. Together with previously published expression data in humans we concluded that in *Xenopus tropicalis* there exists a common progenitor of Sertoli and PTM cell lineages with morphological and expression characteristics of mesenchymal stem cells. Stem cell precursors for Leydig cells were already identified and characterized in interstitial space of rat testis close to seminiferous tubules (Inoue et al., 2016; Shan and Hardy, 1992; Stanley et al., 2011). We observed the same localization of cells double stained with Sox9 and Sma antibodies in *X. tropicalis* agarose embedded testicular sections and even in mouse samples.

Growth curve of our amphibian testicular cells showed a strong correlation between the addition of mouse leukemia inhibitory factor (mLIF) to the cultivation medium and cell colony forming activity. RT-PCR analysis revealed a relatively high *lif* transcription in both cell types (XtTSC and XtTSCc). In testis, a LIF production was determined in PTM cells located between the seminiferous tubules and the interstitium (Piquet-Pellorce et al., 2000) and also in remaining somatic cell types (Sertoli and Leydig cells) and spermatogonia (Jenab and Morris, 1998). LIF has an effect on spermatogonia proliferation and on the increased survival rate of Sertoli cells (De Miguel et al., 1996). We observed that for a successful establishment of amphibian testicular cell culture and also for the formation of colonies is indispensable at least the initial addition of mLIF to the cultivation medium. Further supplementation is important for the colony forming activity but not for the testicular cell proliferation and survival. It is possible that initial addition of mouse LIF triggers the production of *Xenopus* homolog by testicular cells which is sufficient for their maintenance in the cell culture but not for the formation of cell colonies.

The conservation of mammalian and non-mammalian Lif amino acid sequences is rather low (20%-40%). On the other hand, all orthologous proteins share a conserved threedimensional structure (Mathieu et al., 2012). As for lower vertebrates, *lif* cDNA was cloned in zebrafish, carp and goldfish (Fujiki et al., 2003; Abe et al., 2007; Hanington and Belosevic, 2007). Morpholino-based knockdown of *lif* in zebrafish revealed no obvious effect on early embryonic development. However, when its receptor (LIFR) had been targeted, effects on proper neural development were observed (Hanington et al., 2008). In chicken, LIF has been shown to function as an anti-differentiation factor for blastoderm cells (Horiuchi et al., 2006). In amphibians, its effect on early embryonic development is still unknown.

Unlike testicular cell culture, RT-PCR and quantitative PCR analysis showed a low expression of *lif* in adult testes. As mentioned above, in mouse, LIF is mostly produced by peritubular cells located on a periphery of seminiferous tubules (Piquet-Pellorce et al., 2000). It is possible, that in *Xenopus* testis Lif is expressed by scarce cells positively stained for Sox9 and Sma antigens. When transferred out of the testicular niche, these cells can proliferate *in vitro* and produce a higher amount of Lif.

El Jamil et al. (2008) studied the distribution of *sox9* mRNA and protein in *X. tropicalis* testicular and ovarian cryosections. In males, authors observed a Sox9 expression in nuclei of supporting (pre-Sertoli) cells located on the base of seminiferous tubules in the vicinity of germ cells. Unlike higher vertebrates, Sox9 is also expressed in

oocyte cytoplasm indicating its role in the testicular differentiation but not in the sex determination.

To study of migration potential of *X. tropicalis* testicular somatic cells we performed a series of transplantation experiments with transgenic cell culture expressing Katushka RFP (XtTSCc-RFP). Cells were microinjected into the peritoneal cavity of tadpoles at stage 41. During the first week after microinjection we observed migration of RFP positive cells into heart, pronephros (tadpole kidney) and intestine. The same organs are also major migratory targets for mouse mesenchymal stem cells intravenously injected into bloodstream (reviewed in Cornelissen et al., 2015). Strong expression of vimentin in transplanted cells observed even one month after microinjection is typical for migratory mesenchymal cells (reviewed in Kim et al., 2014). In addition, differentiation markers of Sertoli and PTM cells (Sox9 and Sma) were downregulated indicating dedifferentiation process towards to mesenchymal stem cells able to successfully proliferate and migrate through the tadpole body.

MATERIAL AND METHODS

Ethical statement

This study was carried out in strict accordance with the Act No. 246/1992 Coll., on the protection of animals against cruelty. An official permission was issued to the Faculty of Science, Charles University in Prague by the Ministry of Education, Youth and Sports of the Czech Republic (No. MSMT-37376/2014-4, date of expiry 3. 3. 2019).

X. tropicalis testicular somatic cell culture

The *X. tropicalis* testicular somatic cell culture was established from testes of juvenile male

(Ivory Coast strain) 6 months after metamorphosis. For wash steps, ⅔ diluted PBS (2:1 PBS/deionized H_2O) was used due to different cell osmolarity of amphibian contrary to mammalian cells. Testes were extensively washed with ⅔ PBS and disrupted with needles in cultivation medium consisting of 33.3% L-15 and 33.3% RPMI 1640 HEPES modification medium (both Sigma-Aldrich) supplemented with 10% FBS (Life Technologies), 1.33 mg/ml sodium bicarbonate, 2 mM L-glutamine and 50 µg/ml gentamicin (all Sigma-Aldrich). Testicular explants were cultivated at 29.5°C with 5.5% CO_2 for 5 days without any interference. Preparation of primary culture was successfully repeated three times with different *X. tropicalis* individuals originated from various breedings. All three lines exhibited the same morphology and behaviour during long term cultivation and subsequent experiments.

For XtTSCc cultivation, medium has been improved with 1 mM sodium pyruvate, 0.1 mM 2mercaptoethanol (both Sigma-Aldrich) and 1000 U/ml recombinant mouse LIF (ESGRO; Millipore) according to Chowdhury et al. (2010). The XtTSCc medium was changed every three days and cells were passaged every two weeks. To obtain a single cell suspension of XtTSCc, dissociation by a papain solution (61.25 mg/l papain, 0.5 mM EDTA and 1 mM Lcysteine in PBS without Ca2+, Mg2+; Biochrom AG) was only efficient. Disintegration of colonies using AccutaseTM (Thermo Electron Corporation), Biotase

(Biochrome AG) or trypsin-EDTA (0.5% trypsin-0.2% EDTA) was always incomplete. To measure growth, viable cells were seeded at a density of $1x10^5$ cells per flask (75 cm^2) and cultured in XtTSCc medium with and without recombinant mouse LIF for 45 days. During this time period cells were counted three times (15 days interval). Mean values were used to plot a growth curve for both cell types together and for XtTSCc separately.

Visualization of XtTSCc via transmission electron microscopy (TEM)

XtTSCc was separated from XtTSC feeder layer by trypsin-EDTA treatment and filtered through a 20 µm filter (CellTrics®, Partec). For TEM, colonies were fixed, dehydrated in a graded ethanol series and acetone, and embedded in Araldite 502/PolyBed 812 resin (Polyscience, Inc.) as previously described (Hylis et al., 2007). Ultrathin sections (70 µm) were stained with uranyl acetate and lead citrate and examined with the JOEL 1011 transmission electron microscope with a Veleta CCD camera and Olympus Soft Imaging Solution GmbH software.

Preparation of transgenic Katushka RFP testicular cell culture

Testicular cells were electroporated with 6 µg of ISpBSIISK-CAG-Katushka RFP vector

(Shcherbo et al., 2007) using Nucleofector™ 2b Device (Lonza), program T-020 and nucleofection solution (5 mM KCl, 15 mM $MgCl_2$, 50 mM Na_2HPO_4, 100 mM NaCl). One month after nucleofection, transfected cells were separated on the basis of Katushka RFP signal by a fluorescence-activated cell sorting (FACS) using the inFlux v7 Sorter (BD Bioscience) (Fig. 1H).

RT-PCR and qRT-PCR

Total RNA was isolated from the adult *X. tropicalis* testes, XtTSC, XtTSCc, XtTSC-RFP and

XtTSCc-RFP using RNeasy Mini Kit (Qiagen) according to the manufacturer's instructions. Reverse transcription was performed with the same amount of total RNA (200 ng) by the RevertAid H Minus First Strand cDNA Synthesis Kit (Thermo Scientific). The relative expression of target genes was determined by using *odc1* as a reference gene. Quantitative RT-PCR (qRT-PCR) was performed with a real-time CFX384 cycler system (BioRad) using iQTM SYBR® Green Supermix (BioRad). A RNA spike (TATAA Biocenter) was used to validate the reverse transcription and the quantitative PCR reactions. The detailed protocol of cDNA synthesis and qPCR reaction was already described (Flachsova et al., 2013; Sidova et al., 2015). For primer sequences and further details, see the supplementary material Table S1.

Transplantation of testicular somatic cells into tadpole´s peritoneal cavity

X. tropicalis embryos were produced by the standard *in vitro* fertilization procedure (Geach and Zimmerman, 2011). Embryos were cultivated in 0.05x MMR with gentamicin (50 µg/ml) for two days (stage 41). The developmental stage was determined according to Nieuwkoop and Faber (1994). Katushka RFP positive testicular cells were detached from the bottom of the cultivation flask by trypsin. XtTSCc were separated using 40 µm

sieve and colonies were then disintegrated to single cell suspension by papain. 40 nl containing 500 Katushka RFP positive cells was microinjected into each peritoneal cavity of tadpoles at stage 41 using a thin glass capillary (Drummond, type 1-000-0500) and the Narishige IM-300 pneumatic microinjector (Fig. 6A). To prevent tadpole movements, the microinjection experiments were performed in an agarose-coated Petri dish filled with 0.05x MMR containing few drops of 0.02% MS222 (Sigma-Aldrich). After transplantation, tadpoles were cultivated for up to one month and the distribution of RFP positive cells was observed under a fluorescence stereomicroscope (Olympus).

Immunohistochemistry of vibratome sections from transplanted tadpoles

Transplanted tadpoles at stage 41 (day 0), 45 (day 1) and 55 (day 30) were fixed overnight in

MEMFA (0.1 M MOPS, 2 mM EGTA, 1 mM MgSO4, and 3.7% formaldehyde) at 4°C. Agarose embedding was performed by gradual rehydration using 90, 75, 50 and 25% methanol diluted by PBST (PBS plus 0.1% Tween 20), following by 3 times washing with PBS. Tadpoles were then immersed into 3% agarose in PBS overnight at 48.5°C and cooled down. Agarose blocks with fixed tadpoles were then cut into 30-40 µm sections on vibratome (Leica 1200) in PBS. The sections were permeabilized with 0.1% Triton X-100 in PBS for 1 hour and blocked with TNB (0.1M Tris-HCl, 0.15M NaCl, 0.5% Blocking Reagent (Boehringer Mannheim GmbH)) for the same time. Incubation with primary antibody in TNB was done for 3 days at 4ºC. The dilution of primary antibodies against vimentin, Sox9 and Sma was 1:40, 1:300 and 1:400 respectively or 1:5000 for anti-tRFP (rabbit, Evrogen). Appropriate secondary antibody (Sigma) was applied for 2 hours at room temperature following 5 times washing with PBSTr. Individual sections were mounted on slides with Mowiol/DAPI mounting medium and observed under fluorescence microscopy. For details of antibodies used in immunofluorescence, see the supplementary material Table S2.

Acknowledgements

We thank Dr. Marcela Buchtova and Hana Dosedelova for the provision of Sox9 antibody.

Competing interests

The authors declare no competing financial interests.

Author contributions

Designing the experiments: T.T. and V.K. Experiments carrying out: T.T., T.M.X.N., M.V., M.S., K.S., M.B. and V.K. Writing the manuscript: V.K. and T.T.

Funding

The research was funded by the Charles University in Prague programs UNCE 204013, 20504151 PRVOUK P41 and SVV 260310 for T.T., V.K., M.V., T.M.X.N., K.S., M.B. and grant from the Charles University Grant Agency GAUK 1008314 for T.M.X.N. M.S. was

paid by grant AV0Z50520701 from the Ministry of Youth, Education and Sports of the Czech Republic, grant LK21305 and BIOCEV CZ.1.05/1.1.00/02.0109 from the ERDF.

Supplementary material

Supplementary material is available online.

References

Abe, T., Mikekado, T., Haga, S., Kisara, Y., Watanabe, K., Kurokawa, T. and Suzuki, T. (2007). Identification, cDNA cloning, and mRNA localization of a zebrafish ortholog of leukemia inhibitory factor. *Comp. Biochem. Physiol. B, Biochem. Mol. Biol.* **147**, 38–44.

Baker, P.J., Sha, J.A., McBride, M.W., Peng, L., Payne, A.H. and O'Shaughnessy, P.J. (1999). Expression of 3beta-hydroxysteroid dehydrogenase type I and type VI isoforms in the mouse testis during development. *Eur. J. Biochem*. **260**, 911–917.

Berndtson, W.E. and Thompson, T.L. (1990). Changing relationships between testis size, Sertoli cell number and spermatogenesis in Sprague-Dawley rats. *J. Androl.* **11**, 429–435.

Bott, R., McFee, R., Clopton, D., Toombs, C. and Cupp, A. (2006). Vascular endothelial growth factor and kinase domain region receptor are involved in both seminiferous cord formation and vascular development during testis morphogenesis in the rat. *Biol. Reprod.* **75**, 56–67.

Campagnolo, L., Russo, M.A., Puglianiello, A., Favale, A. and Siracusa, G. (2001). Mesenchymal cell precursors of peritubular smooth muscle cells of the mouse testis can be identified by the presence of the p75 neurotrophin receptor. *Biol. Reprod*. **64**, 464– 472.

Chikhovskaya, J.V., van Daalen, S.K., Korver, C.M., Repping, S. and van Pelt, A.M. (2014). Mesenchymal origin of multipotent human testis-derived stem cells in human testicular cell cultures. *Mol. Hum. Reprod.* **20**, 155–167.

Chikhovskaya, J.V., Jonker, M.J., Meissner, A., Breit, T.M., Repping, S. and van Pelt, A.M. (2012). Human testis-derived embryonic stem cell-like cells are not pluripotent, but possess potential of mesenchymal progenitors. *Hum. Reprod.* **27**, 210–221.

Chowdhury, F., Li, Y., Poh, Y.C., Yokohama-Tamaki, T., Wang, N. and Tanaka, T.S. (2010). Soft substrates promote homogeneous self-renewal of embryonic stem cells via downregulating cell-matrix tractions. *PLoS One* **5**, e15655.

Combes, A.N., Wilhelm, D., Davidson, T., Dejana, E., Harley, V., Sinclair, A. and Koopman, P. (2009). Endothelial cell migration directs testis cord formation. *Dev. Biol.* **326**, 112–120.

Conrad, S., Renninger, M., Hennenlotter, J., Weisner, T., Just, L., Bonin, M., Aicher, W., Buhring, H., Mattheus, U., Mack, A., et al. (2008). Generation of pluripotent stem cells from adult human testis. *Nature* **456**, 344–351.

Cool, J., DeFalco, T. and Capel, B. (2012). Testis formation in the fetal mouse: dynamic and complex de novo tubulogenesis. *Wiley Interdiscip Rev. Dev. Biol.* **1**, 847–859.

Cornelissen, A.S., Maijenburg, M.W., Nolte, M.A. and Voermans, C. (2015). Organspecific migration of mesenchymal stromal cells: Who, when, where and why? *Immunol. Lett.* **168**, 159–169.

Dufour, J., Hamilton, M., Rajotte, R. and Korbutt, G. (2005). Neonatal Porcine Sertoli Cells Inhibit Human Natural Antibody-Mediated Lysis. *Biol. Reprod.* **72**, 1224–1231.

El Jamil, A., Kanhoush, R., Magre, S., Boizet-Bonhoure, B. and Penrad-Mobayed, M. (2008). Sex-specific expression of SOX9 during gonadogenesis in the amphibian Xenopus tropicalis. *Dev. Dyn.* **237**, 2996–3005.

Flachsova, M., Sindelka, R. and Kubista, M. (2013). Single blastomere expression profiling of Xenopus laevis embryos of 8 to 32-cells reveals developmental asymmetry. *Sci Rep.* **3**, 2278.

Frankenberg, S.R., Frank, D., Harland, R., Johnson, A.D., Nichols, J., Niwa, H., Schöler, H.R., Tanaka, E., Wylie, C. and Brickman, J.M. (2014). The POU-er of gene nomenclature. *Development* **141**, 2921–2923.

Fujiki, K., Nakao, M. and Dixon, B. (2003). Molecular cloning and characterisation of a carp (Cyprinus carpio) cytokine-like cDNA that shares sequence similarity with IL-6 subfamily cytokines CNTF, OSM and LIF. *Dev. Comp. Immunol*. **27**, 127–136.

Geach, T. and Zimmerman, L. (2011). Developmental genetics in Xenopus tropicalis. *Methods Mol. Biol.* **770**, 77–117.

Golestaneh, N., Kokkinaki, M., Pant, D., Jiang, J., DeStefano, D., Fernandez-Bueno, C., Rone, J.D., Haddad, B.R., Gallicano, G.I. and Dym, M. (2009). Pluripotent stem cells derived from adult human testes. *Stem Cells Dev.* **18**, 1115–1126.

Guan, K., Nayernia, K., Maier, L., Wagner, S., Dressel, R., Lee, J., Nolte, J., Wolf, F., Li, M., Engel, W., et al. (2006). Pluripotency of spermatogonial stem cells from adult mouse testis. *Nature* **440**, 1199–1203.

Hanington, P.C. and Belosevic, M. (2007). Interleukin-6 family cytokine M17 induces differentiation and nitric oxide response of goldfish (Carassius auratus L.) macrophages.
Dev. Comp. Immunol. **31**, 817–829.

Hanington, P.C., Patten, S.A., Reaume, L.M., Waskiewicz, A.J., Belosevic, M. and Ali, D.W. (2008). Analysis of leukemia inhibitory factor and leukemia inhibitory factor receptor in embryonic and adult zebrafish (Danio rerio). *Dev. Biol*. **314**, 250–260.

Hellsten, U., Harland, R., Gilchrist, M., Hendrix, D., Jurka, J., Kapitonov, V., Ovcharenko, I., Putnam, N., Shu, S., Taher, L., et al. (2010). The genome of the Western clawed frog Xenopus tropicalis. *Science* **328**, 633–636.

Horiuchi, H., Furusawa, S. and Matsuda, H. (2006). Maintenance of chicken embryonic stem cells in vitro. *Methods Mol. Biol.* **329**, 17–34.

Hylis, M., Oborník, M., Nebesárová, J. and Vávra, J. (2007). Aquatic tetrasporoblastic microsporidia from caddis flies (Insecta, Trichoptera): characterisation, phylogeny and taxonomic reevaluation of the genera Episeptum Larsson, 1986, Pyrotheca Hesse, 1935 and Cougourdella Hesse, 1935. *Eur. J. Protistol.* **43**, 205–224.

Inoue, M., Shima, Y., Miyabayashi, K., Tokunaga, K., Sato, T., Baba, T., Ohkawa, Y., Akiyama, H., Suyama, M. and Morohashi, K.I. (2016). Isolation and Characterization of Fetal Leydig Progenitor Cells of Male Mice. *Endocrinology* **157**, 1222–1233.

Jenab, S. and Morris, P.L. (1998). Testicular leukemia inhibitory factor (LIF) and LIF receptor mediate phosphorylation of signal transducers and activators of transcription (STAT)-3 and STAT-1 and induce c-fos transcription and activator protein-1 activation in rat Sertoli but not germ cells. *Endocrinology* **139**, 1883–1890.

Johnson, L., Zane, R.S., Petty, C.S. and Neaves, W.B. (1984). Quantification of the human Sertoli cell population: its distribution, relation to germ cell numbers, and age-related decline. *Biol. Reprod.* **31**, 785–795.

Kanatsu-Shinohara, M., Inoue, K., Lee, J., Yoshimoto, M., Ogonuki, N., Miki, H., Baba, S., Kato, T., Kazuki, Y., Toyokuni, S., et al. (2004). Generation of pluripotent stem cells from neonatal mouse testis. *Cell* **119**, 1001–1012.

Kanatsu-Shinohara, M., Lee, J., Inoue, K., Ogonuki, N., Miki, H., Toyokuni, S., Ikawa, M., Nakamura, T., Ogura, A. and Shinohara, T. (2008). Pluripotency of a single spermatogonial stem cell in mice. *Biol. Reprod.* **78**, 681–687.

Kanatsu-Shinohara, M., Ogonuki, N., Inoue, K., Miki, H., Ogura, A., Toyokuni, S. and Shinohara, T. (2003). Long-term proliferation in culture and germline transmission of mouse male germline stem cells. *Biol. Reprod.* **69**, 612–616.

Karl, J. and Capel, B. (1998). Sertoli cells of the mouse testis originate from the coelomic epithelium. *Dev. Biol*. **203**, 323–333.

Kim, Y.S., Yi, B.R., Kim, N.H. and Choi, K.C. (2014). Role of the epithelial-mesenchymal transition and its effects on embryonic stem cells. *Exp. Mol. Med*. **46**, e108.

Ko, K., Tapia, N., Wu, G., Kim, J., Bravo, M., Sasse, P., Glaser, T., Ruau, D., Han, D., Greber, B., et al. (2009). Induction of pluripotency in adult unipotent germline stem cells. *Cell stem cell* **5**, 87–96.

Koopman, P., Münsterberg, A., Capel, B., Vivian, N. and Lovell-Badge, R. (1990). Expression of a candidate sex-determining gene during mouse testis differentiation. *Nature* **348**, 450–452.

Kossack, N., Meneses, J., Shefi, S., Nguyen, H.N., Chavez, S., Nicholas, C., Gromoll, J., Turek, P.J. and Reijo-Pera, R.A. (2009). Isolation and characterization of pluripotent human spermatogonial stem cell-derived cells. *Stem Cells* **27**, 138–149.

Mathieu, M.-E., Saucourt, C., Mournetas, V., Gauthereau, X., Thézé, N., Praloran, V., Thiébaud, P. and Boeuf, H. (2012). LIF-dependent signaling: new pieces in the Lego. *Stem Cell Rev.* **8**, 1–15.

De Miguel, M.P., De Boer-Brouwer, M., Paniagua, R., van den Hurk, R., de Rooij, D.G. and Van Dissel-Emiliani, F.M. (1996). Leukemia inhibitory factor and ciliary neurotropic factor promote the survival of Sertoli cells and gonocytes in coculture system. *Endocrinology* **137**, 1885–1893.

Mizrak, S.C., Chikhovskaya, J.V., Sadri-Ardekani, H., van Daalen, S., Korver, C.M., Hovingh, S.E., Roepers-Gajadien, H.L., Raya, A., Fluiter, K. and de Reijke, T.M.

(2010). Embryonic stem cell-like cells derived from adult human testis. *Hum. Reprod.* **25**, 158–167.

Morrison, G.M. and Brickman, J.M. (2006). Conserved roles for Oct4 homologues in maintaining multipotency during early vertebrate development. *Development* **133**, 2011– 2022.

Nef, S., Shipman, T. and Parada, L.F. (2000). A molecular basis for estrogen-induced cryptorchidism. *Dev. Biol*. **224**, 354–361.

Nieuwkoop, P.D. and Faber, J. (1994). *Normal Table of Xenopus laevis (Daudin).* Garland Publishing Inc, New York.

Nishino, K., Kato, M., Yokouchi, K., Yamanouchi, K., Naito, K. and Tojo, H. (2000). Establishment of fetal gonad/mesonephros coculture system using EGFP transgenic mice. *J. Exp. Zool.* **286**, 320–327.

O'Shaughnessy, P.J., Morris, I.D. and Baker P.J. (2008). Leydig cell re-generation and expression of cell signaling molecules in the germ cell-free testis. *Reproduction* **135**, 851–858.

Piquet-Pellorce, C., Dorval-Coiffec, I., Pham, M.D. and Jégou, B. (2000). Leukemia inhibitory factor expression and regulation within the testis. *Endocrinology* **141**, 1136–1141. **de Rooij, D.G.** (2009). The spermatogonial stem cell niche. *Microsc. Res. Tech.* **72**, 580– 585.

Shcherbo, D., Merzlyak, E.M., Chepurnykh, T.V., Fradkov, A.F., Ermakova, G.V., Solovieva, E.A., Lukyanov, K.A., Bogdanova, E.A., Zaraisky, A.G., Lukyanov, S. et al. (2007). Bright far-red fluorescent protein for whole-body imaging. *Nat. Methods* **4**, 741–746.

Shan, L.X. and Hardy, M.P. (1992). Developmental changes in levels of luteinizing hormone receptor and androgen receptor in rat Leydig cells. *Endocrinology* **131**, 1107– 1114.

Sidova, M., Sindelka, R., Castoldi, M., Benes, V. and Kubista, M. (2015). Intracellular microRNA profiles form in the Xenopus laevis oocyte that may contribute to asymmetric cell division. *Sci Rep.* **5,** 11157.

Silva, J., Nichols, J., Theunissen, T.W., Guo, G., Oosten, A.L. van Barrandon, O., Wray, J., Yamanaka, S., Chambers, I. and Smith, A. (2009). Nanog is the gateway to the pluripotent ground state. *Cell* **138**, 722–737.

Skinner, M.K., Tung, P.S. and Fritz, I.B. (1985). Cooperativity between Sertoli cells and testicular peritubular cells in the production and deposition of extracellular matrix components. *J. Cell Biol.* **100**, 1941–1947.

Stanley, E., Johnston, D., Fan, J., Papadopoulos, V., Chen, H., Ge, R.-S., Zirkin, B. and Jelinsky, S. (2011). Stem Leydig cell differentiation: gene expression during development of the adult rat population of Leydig cells. *Biol. Reprod.* **85**, 1161–1166.

Tymowska, J. (1973). Karyotype analysis of Xenopus tropicalis Gray, Pipidae. *Cytogenet. Cell Genet.* **12**, 297–304.

Wells, D.E., Gutierrez, L., Xu, Z., Krylov, V., Macha, J., Blankenburg, K.P., Hitchens, M., Bellot, L.J., Spivey, M., Stemple, D.L., et al. (2011). A Genetic Map of Xenopus tropicalis. *Dev Biol.* **354,** 1-8.

Figures

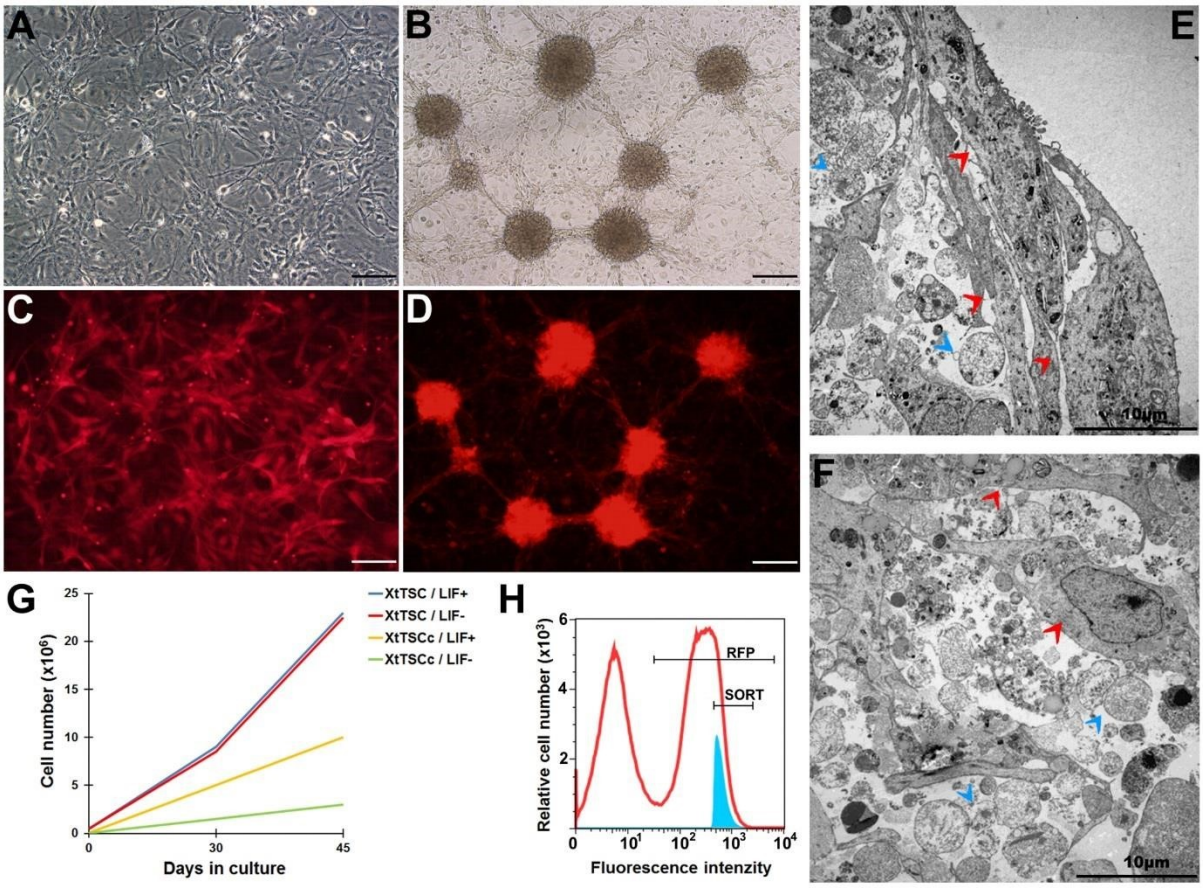

Fig. 1. *In vitro* characterization of *X. tropicalis* cell culture. (A) Testicular somatic cell culture in morphology of adherent feeder layer (XtTSC) and after long-term cultivation which enables the forming of colonies (XtTSCc) (B). (C) *X. tropicalis* transgenic XtTSC expressing Katushka RFP under CAG promotor (XtTSC-RFP). (D) Transgenic Katushka RFP expressing XtTSC in colonies (XtTSCc-RFP). (E-F) Structure of *in vitro* testicular cell colony visualized by TEM. In the colony the cells are placed in an extensive amount of extracellular matrix with two or three tight layers of XtTSCs surrounding the colony at the edge (E). Both XtTSC and XtTSCc are present in the centre of the colony (F). The XtTSCc are clearly several times smaller than the XtTSC. Red arrowheads = XtTSC, blue arrowheads = XtTSCc. (G) *X. tropicalis* cell culture proliferation during long-term cultivation in medium with or without recombinant mouse LIF. (H) Representative graph of FACS sorting after nucleofection. Only about 15% of living transgenic cells with the highest intensity of fluorescent signal were sorted (blue area). Scale bar in A and C = 100 µm, scale bar in B and

D = 200 µm, scale bar in E and F = 10 µm.

A

X. tropicalis gene symbol	Gene name	Gene transcript	Gene expression: testes	XtTSC	XtTSCc	XtTSC-RFP	XtTSCc-RFP
Pluripotent cell markers							
klf4	Kruppel-like factor 4	ENSXETT00000012646					
myc	v-myc avian myelocytomatosis viral oncogene homolog	ENSXETT00000054171					
pou5f3.1	POU class 5 homeobox 3, gene 1	NM_001285474					
pou5f3.2	POU class 5 homeobox 3, gene 2	NM_001129934					
pou5f3.3	POU class 5 homeobox 3, gene 3	NM_001130364					
sox2	SRY (sex determining region Y) - box 2	ENSXETT00000004031					
tert	telomerase reverse transcriptase	ENSXETT00000034113					
Germ cell markers							
dazl	deleted in azoospermia-like	NM_203748					
ddx4	DEAD (Asp-Glu-Ala-Asp) box polypeptide 4	ENSXETT00000066339					
ddx25	DEAD (Asp-Glu-Ala-Asp) box polypeptide 25	ENSXETT00000064463					
Mesenchymal stem cell surface markers							
itgb1	integrin, beta 1 (antigen CD29 includes MDF2)	ENSXETT00000048743					
cd44	CD44 molecule (Indian blood group)	ENSXETT00000016456					
thy1	Thy-1 cell surface antigen	ENSXETT00000046686					
Testis associated markers							
acta2	actin, alpha 2, smooth muscle, aorta	ENSXETT00000020391					
cyp11a1	cytochrome P450, family 11, subfamily A, polypeptide 1	ENSXETT00000011263					
cyp17a1	cytochrome P450, family 17, subfamily A, polypeptide 1	ENSXETT00000033323					
kitlg	KIT ligand ~ Stem Cell Factor	NM_001045596					
lif	leukemia inhibitory factor	ENSXETT00000053337					
sox9	SRY (sex determining region Y) - box 9	ENSXETT00000048344					
vim	vimentin	ENSXETT00000016267					
Housekeeping gene							
odc1	ornithine decarboxylase 1	ENSXETT00000007603					

B

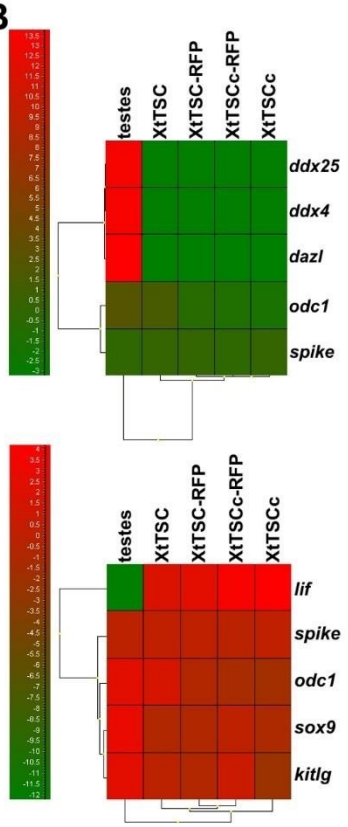

Fig. 2. Expression analysis of *X. tropicalis* testicular culture. (A) RT-PCR analysis of *X. tropicalis* testis, XtTSC, XtTSCc, XtTSC-RFP and XtTSCc-RFP. (B) Hierarchical clustering presented as a qPCR heatmaps of germ cell markers and selected testis associated markers. A scale of colours indicates level of expression (the highest expression is shown by bright red, whereas the lowest expression is shown by bright green). Similarity between cell types/genes is indicated by the height at which the dendrograms are joined. The RNA spike represents a highly stable transcript across the cell types and odc1 represents housekeeping gene.

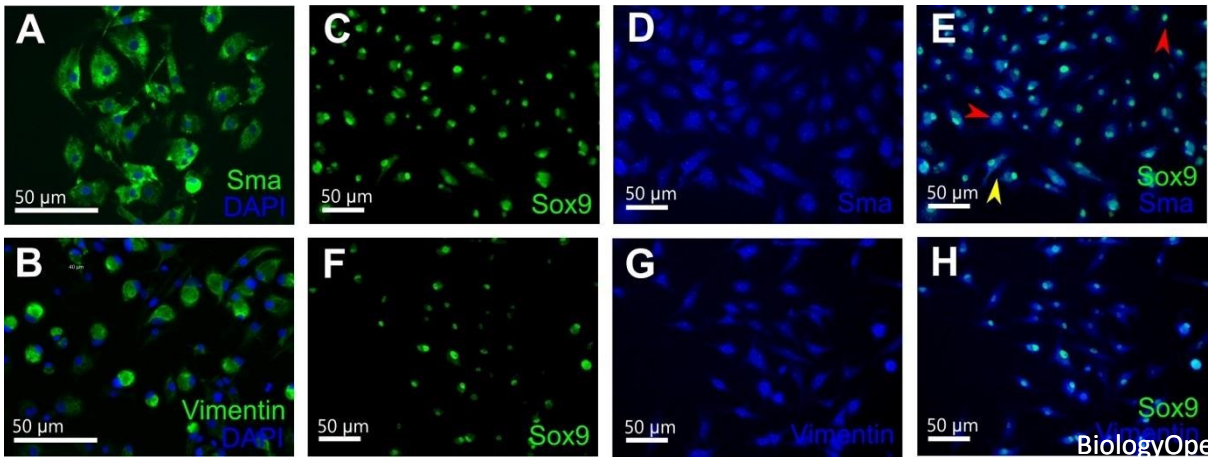

Fig. 3. Immunocytochemistry of *X. tropicalis* testicular cell culture expressing Katushka RFP. Positive staining for Sma (marker of peritubular myoid cells, green) (A) and vimentin (marker of mesenchymal cells and peritubular myoid cells, green) (B). Nuclei were counterstained with DAPI (blue). (C-E) Double staining with Sox9 (marker of Sertoli cells, green) (C) and Sma (blue) (D) antibodies. (E) Merge of C and D. Yellow arrowhead

- cell expressing both antigens, red arrowheads - cells expressing only Sox9 or only Sma. (F-H) Double staining with Sox9 (green) (F) and vimentin (blue) (G) antibodies. (H) - merge of F and G. Scale bar = 50 μm.

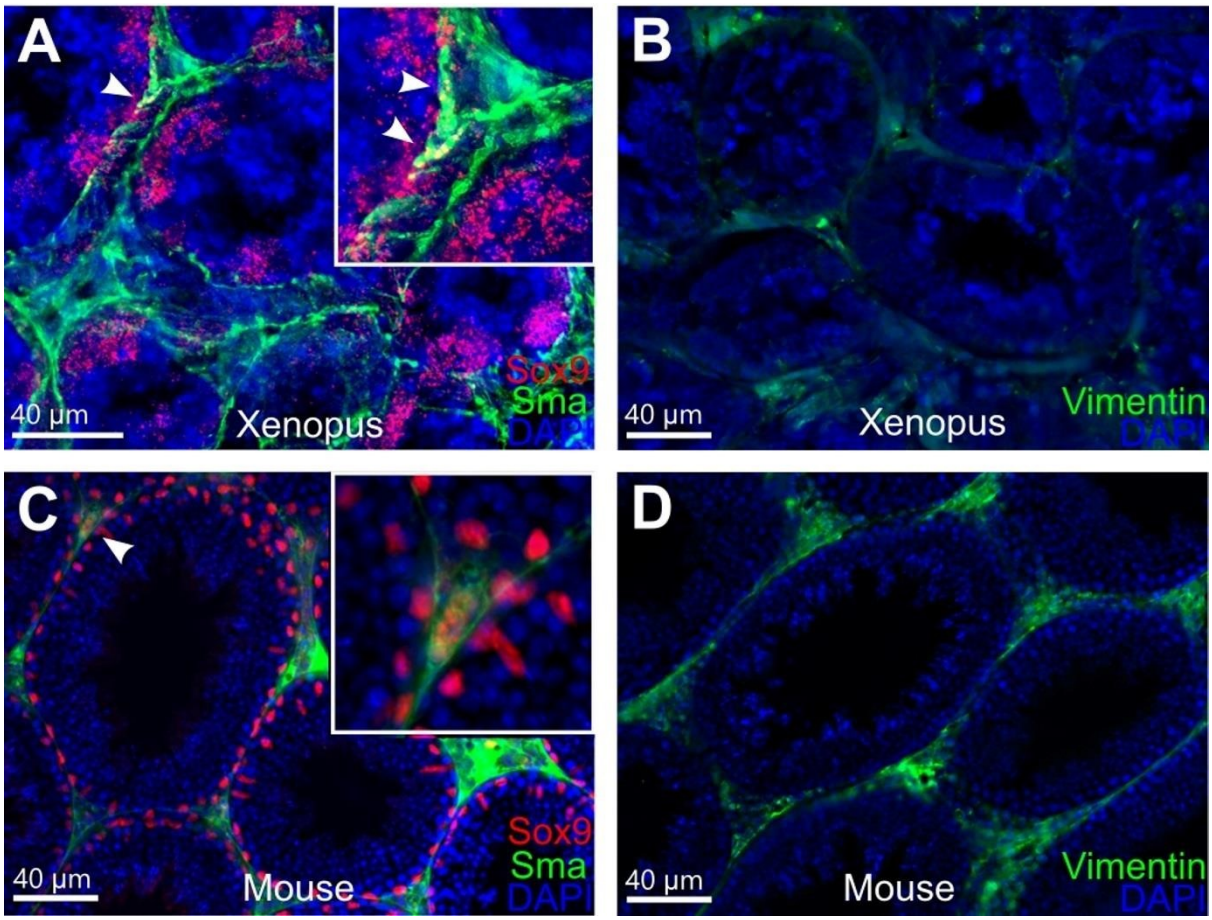

Fig. 4. Immunohistochemistry of agarose embedded testicular sections from *X. tropicalis* and mouse adult males. (A+C) Double staining with Sox9 (red) and Sma (green) antibodies. White arrowheads indicate potential common precursor cells for Sertoli and PTM cell lineages expressing both antigens in *X. tropicalis* (A) and mouse (C) samples. (B+D) Staining with vimentin (green) antibody on *X. tropicalis* (B) and mouse (D) samples. Nuclei were counterstained with DAPI (blue). Scale bar = 40 μm.

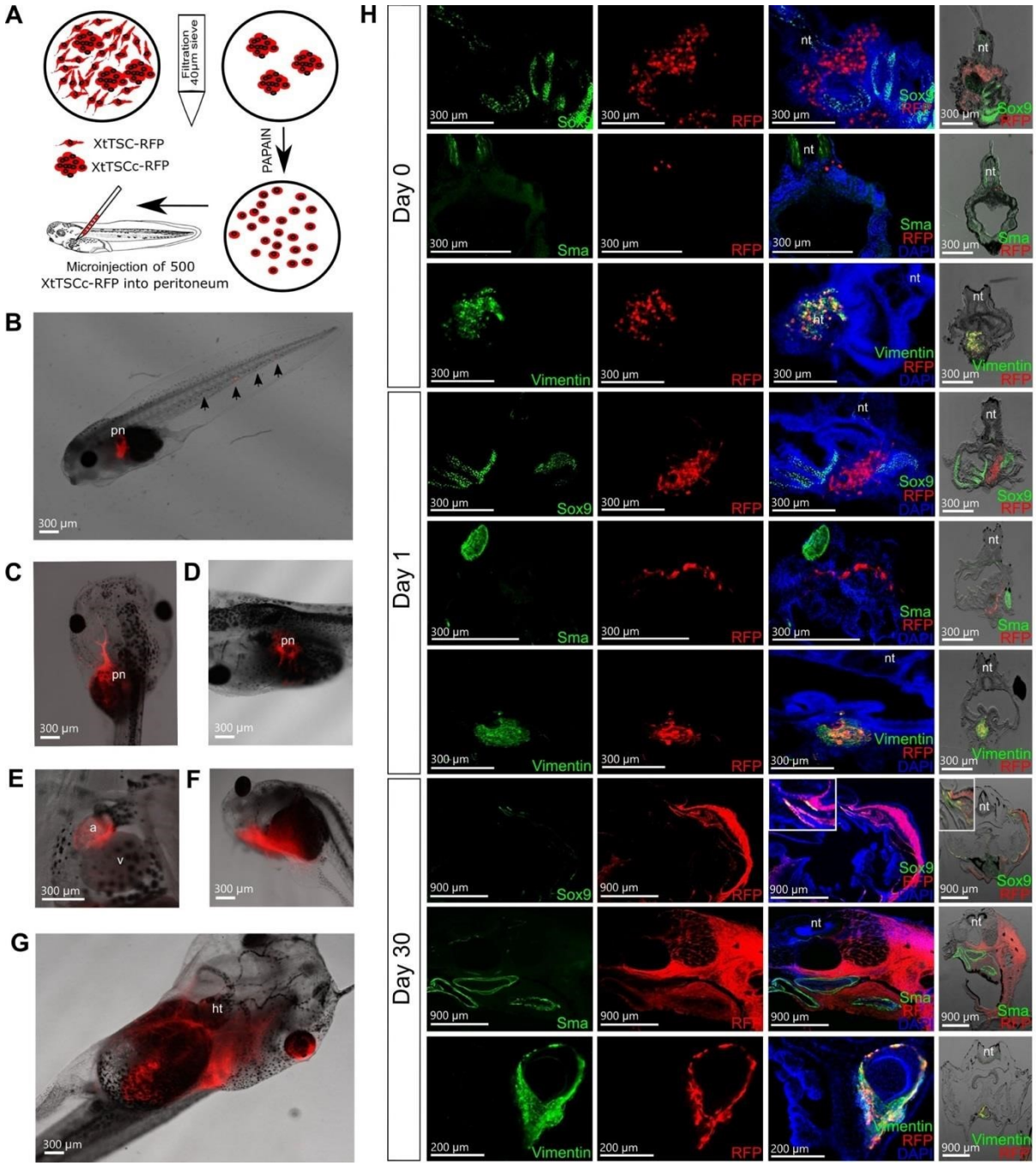

Fig. 5. Migration potential of *X. tropicalis* testicular somatic cells after allogeneic transplantation into peritoneal cavity of tadpoles in st. 41. (A) Scheme of XtTSCc-RFP preparation prior to transplantation employing isolation of cell colonies using 40 µm sieve and subsequent single cell dissociation with papain. 500 cells were microinjected dorsally into peritoneal cavity. (B-G) Observation of RFP positive cells in transplanted tadpoles under stereo microscopy. (B) Cell deposit in pronephros and tail 1day after microinjection. (C-D) Cell deposits in pronephros 13 days after microinjection. (E) Migration of RFP positive cells into heart atrium 15 days after transplantation. (F-G) Cell to cell net growing through the tadpole body observable 30 days after microinjection. (H) Immunohistochemistry of agarose embedded sections of transplanted tadpoles using antibodies against Sox9, Sma and vimentin (green) and Katushka RFP (red) 0, 1 and 30 days after transplantation. RFP positive cells were stained with vimentin antibody but not

Sox9 or Sma even 2 hours after transplantation. 30 days after microinjection few cells start to express Sox9 indicating potential redifferentiation into Sertoli cells or chondrocytes where Sox9 is considered as specific marker. The first three figures in each line were taken under fluorescence microscopy. The figures on the right side were taken under fluorescence stereomicroscopy. Nuclei were counterstained with DAPI (blue). Scale bars in B-G and in H (0 and 1 day after transplantation) = 300 μm. Scale bars in H (30 days after transplantation, staining with Sox9 and Sma antibodies) = 900 μm. Scale bar in H (30 days after transplantation, staining with vimentin antibody) = 200 μm.

Biology Open (2016): doi:10.1242/bio.019265: Supplementary information

Table S1: List of primer sequences for the amplification of *X. tropicalis* cell markers.

X. tropicalis gene symbol	Gene transcript	Primer F Primer R	Size (bp)
acta2	ENSXETT00000020391	ACTGCTGAGCGTGAAATCGT GCCAGCAGATTCCATACCAA	213
cd44	ENSXETT00000016456	CCCTGGGCAATAACGATTCC ATCGGTGACCTCTCCTGGAT	572
cyp11a1	ENSXETT00000011263	GTCACCGGATTGCCCTAAAT CCTTTCCAGAGGCATCTCGT	645
cyp17a1	ENSXETT00000033323	TGCTCTTCTGAAAGCGAAGC TTTGGGAGGGGGTGTAGAG	497
dazl	NM_203748	CAAGCTTTTGTGTTGCCAGA AATGCCATGATCCCAAAGAG	1114
ddx4	ENSXETT00000066339	TGCATGCAATGAGGGATGTTG AGATGAAGGAGCACTGACGTA	899
ddx25	ENSXETT00000064463	AAACGCATCCCAAGCGGAA CGACTCAGCATAGCCAGGAC	435
itgb1	ENSXETT00000048743	CAACTGACGCAGGATTCCATT TCCCCAGTTCCCTTGACTC	400
kitlg	NM_001045596	ACTGAAGGAGGACCATACCCA GGGAGGGATTTGTGGCTGAA	789
klf4	ENSXETT00000012646	TTCCTCACCTCCACCTCCT ACAGTCTCTGCCCATCAGC	556
lif	ENSXETT00000053337	TGTGCAACTGCTGATTCTCC CATTGACTGCTTGGTGGATG	581
myc	ENSXETT00000054171	TGACCCTTCGGTGGTTTTCC CCGCCTCTTGTCGTTCTCTT	454
odc1	ENSXETT00000007603	GCTGCACTGATCCTCAGAC CAAGCTCAATGCCACTCTCC	744
pou5f3.1	NM_001285474	GCAAACAAGAGACGAGCAGG GTGGGCAAAGGAAGGGTAGG	281
pou5f3.2	NM_001129934	ACTCCGACTTATTTGGGTGGAA TCCCTTGTTGGTTGGTCTCC	464
pou5f3.3	NM_001130364	CACTTGCTGGTTTAGGGGGT GGAGGGGGCATTGTAGTTCC	264
sox2	ENSXETT00000004031	GGGCTCCAACAACCAGAGT TAGTGTTGGGACATGTGCAGT	804
sox9	ENSXETT00000048344	AACTCCTCCAACTACCCCC CCTCACTGCTCAGTTCACC	143
tert	ENSXETT00000034113	TGACCAGCCAAAACGGGATG TCGTAGACGAATCCAAGAGCA	484
thy1	ENSXETT00000046686	AAGCCTCACTGCCTGTCTGA AAAGACTGACTCCGCCACAG	350
vim	ENSXETT00000016267	CCTCTTTGGCACGTATTGACTT TCTCCTCCATTTCTCGCATTTG	464

Biology Open (2016): doi:10.1242/bio.019265: Supplementary information

Table S2: Antibodies used in immunofluorescence experiments.

Antigen	Species	Provider	Cat. / Clone No.	Reference / Certificate No.	Dilution
Vimentin	Mouse	DSHB (Developmental Studies Hybridoma Bank)	14h7	Dent et al., 1989	1 µg/ml
Smooth muscle actin	Mouse	Sigma-Aldrich	A2547	Validate by staining on testis section	1:400
Sox9	Rabbit	Sigma-Aldrich	HPA001758	Validate by staining on testis section, similar pattern with previous report (El Jamil et al., 2008)	1:300
Red fluorescence protein	Rabbit	Evrogen	AB233	23301291014	1:5000
Red fluorescence protein	Mouse	Thermo Fisher Scientific	MA5-15257	QB205317	1:500
Mouse IgG- Alexa Fluor®488 conjugate	Goat	Thermo Fisher Scientific	A11001	1664729	1:500
Rabbit IgG- Alexa Fluor®594 conjugate	Goat	Thermo Fisher Scientific	A11012	1678830	1:500
Mouse IgG- Alexa Fluor®594 conjugate	Goat	Thermo Fisher Scientific	A11032	419361	1:500
Rabbit IgG- Alexa Fluor®488 conjugate	Goat	Thermo Fisher Scientific	A11034	870976	1:500

Journal title: Stem Cell International

Article title: Epithelial-mesenchymal transition promotes the differentiation potential of *Xenopus tropicalis* immature Sertoli cells.

Authors:1 Thi Minh Xuan Nguyen1 [1], Marketa Vegrichtova[1], Tereza Tlapakova[1], Magdalena Krulova and Vladimir Krylov

[1]Department of Cell Biology, Charles University, Faculty of Science, Vinicna 7, Prague 2, 128 44, Czech Republic.

Correspondence should be addressed to Vladimir Krylov; vkrylov@natur.cuni.cz

Abstract

Epithelial-mesenchymal transition (EMT) is a fundamental process in embryonic development by which sessile epithelial cells are converted into migratory mesenchymal cells. Our laboratory has been successful in the establishment of ***X****enopus* ***t****ropicalis* **i** mmature **S**ertoli **c**ells (XtiSCs) with the restricted differentiation potential. The aim of this study was the determination of factors responsible for XtiSCs EMT activation and stemness window where cells possess the broadest differentiation potential. For this purpose we tested three potent EMT inducers - GSK-3 inhibitor (CHIR99021), FGF2 and/or TGF-β1 ligands. XtiSCs underwent full EMT after 3-day treatment with CHIR99021 and partial EMT with FGF2, but not with TGF-β1. The morphological change of CHIR-treated XtiSCs to the typical spindle-like cell shape was associated with the upregulation of mesenchymal and downregulation of epithelial markers. Moreover, only CHIR-treated XtiSCs were able to differentiate into chondrocytes *in vitro* and cardiomyocytes *in vivo*. Interestingly, EMT-shifted cells could migrate toward cancer cells *in vitro* and to the injury site *in vivo*. The results provide a better understanding of signaling pathways underlying the generation of testis-derived stem cells.

Introduction

Epithelial-mesenchymal transition (EMT), and its reverse process, mesenchymal-epithelial transition (MET) occur in numerous developmental processes including mesoderm, neural crest, and testicular formation [1]. EMT was characterized by the loss of the apical-basal polarity and cell-cell contacts, and the increase of cell interactions with extracellular matrix (fibronectin, vitronectin) [2,3]. During development, EMT ensures both, high migratory capacity and the cell stemness. Later, EMT-shifted cells can undergo the reciprocal MET to form tissues and organs such as somites [4], kidney [5] and liver [6]. EMT has also been considered to contribute to tissue repair, fibrosis tissue and cancer metastasis [1].

Recently, several groups have tried to generate mesenchymal stem cells (MSCs) by inducing EMT in cultured human epithelial cells. Indeed, the immortalized human mammary epithelial cells were incubated with recombinant TGF-β1 or transduced with vectors expressing EMT key transcription factors, SNAI1 or TWIST. Treated cells have exhibited the characteristics of MSCs, including specific antigenic profile, the capacity to differentiate into mesodermal cell types and to migrate towards cancer cells and wound injury sites [7,8].

Sertoli cells (SCs) in seminiferous tubules, play an essential role in male reproduction. In the early development, anti-Müllerian hormone (AMH) is secreted by SCs to regress Müllerian tract contributing to sex determination and testis formation [9]. In adult testis, SCs regulate sperm cell production via nutritional and scaffolding support.

In spite of their importance, the origin of Sertoli cells is still a question. The insertion of EGFP (enhanced green fluorescent protein) gene under promoter of SRY (sex-determining region Y), a Sertoli cell-specific gene, or Myc-tags upstream the SRY stop codon have visualized mesenchymal morphology of SCs [10,11]. Furthermore, cells labelled with 5′-bromo-2′-deoxyuridine (BrdU) beneath the coelomic epithelium migrating into XY and XX/Sry gonads had positive staining with SF1 (steroidogenic factor 1), another Sertoli cell-specific marker [12,13]. The SCs origin in coelomic epithelium was further suggested in [10,12,14]. Taking together, these results indicate mesenchymal phenotype of pre-Sertoli

cells. Their maturation in seminiferous tubules is coupled with a mesenchymal-epithelial transition (MET). Therefore, we assume that the reverse process, EMT, could convert immature Sertoli cells back to the stem cell-like state with expected broader differentiation potential.

Our laboratory has been successful in the establishing a cell line of ***X****enopus* ***t****ropicalis* **i** mmature **S**ertoli **c**ells (XtiSCs) in a long-term culture [15]. Germ cell markers were not detected in XtiSCs which confirms their somatic origin. Immunocytochemical staining against Sox9 (SC marker, [16]) showed its presence in approx. 90% of cells. On the other hand, XtiSCs formed compact colonies expressing both vimentin and cytokeratin, the mesenchymal and epithelial intermediate filament, respectively. These results indicate that we are dealing with immature Sertoli cells [17,18]. XtiSCs allotransplantation into *X. tropicalis* tadpoles revealed their accumulation in many tissues and organs encompassing heart, intestine, and pronephros. However, immunohistochemistry of tadpole sections showed only the presence of vimentin in transplanted cells, but no expression of tissue or organ-specific markers [15]. XtiSCs *in vitro* differentiation potential was also limited (unpublished results).

TGF-β1, FGF2, and GSK-3β inhibitor are common EMT inducers of epithelial cells *in vitro* [19–21]. We have employed these factors individually to reverse XtiSCs maturation and broaden their differentiation potential. Subsequent evaluation of cell morphology and changes in a gene expression profile after the treatment have been done by reverse transcription polymerase chain reaction (RT-PCR), immunostaining and flow cytometry. Our results showed that XtiSCs underwent full EMT by pharmacological inhibition with GSK-3 (CHIR99021) and partial EMT using FGF2.

Materials and Methods

All chemicals were supplied by Sigma unless otherwise stated.

XtiSCs culture and fluorescent immunostaining

Xenopus tropicalis immature Sertoli cells (XtiSCs) were obtained and cultured as described [15]. To induce epithelial-mesenchymal transition (EMT), cells were cultured in growth medium overnight before its replacement by induction medium supplemented with CHIR99021 (CHIR) (3 μM) (GSK-3 inhibitor) (Sigma), mFGF2 (25 ng/ml), or hTGF-β1 (2.5, 5 or 10 ng/ml) (all from Peprotech) for 3 - 4 days. CHIR9901, FGF2, and TGF-β1 solutions were prepared according to the manufacturer's instructions. CHIR was dissolved in DMSO at 3 mM stock solution. Therefore, the same amount of DMSO (0.1%) was added in growth medium as control. All cell media contained 10% fetal bovine serum (FBS), except medium supplemented with TGF-β1 (only 0.5% FBS).

For immunofluorescence, cells were plated on coverslip glasses coated with collagen type I (2.5 μg/cm^2) or poly-L-lysine (4 μg/cm^2), and cultured in indicated medium for 3-4 days. Cells were then fixed with 2% formaldehyde, permeabilized and incubated with primary antibodies (list and dilution in Supplementary table 2) followed by secondary antibodies conjugated with Alexa Fluor -488 or -594 (1:500, ThermoFisher Scientific). Regarding F-actin staining, fixed cells were incubated with Alexa Fluor 568- conjugated phalloidin (1:100, ThermoFisher Scientific) for 1 hour at room temperature (RT). Cell nuclei were visualized by DAPI.

RNA isolation and RT-PCR

Total RNA was isolated from XtiSCs by RNeasy Plus Mini Kit (Qiagen) followed by the preparation of cDNA using RevertAid First Strand cDNA Synthesis Kit (ThermoFisher, Scientific). This process included on-column DNase treatment step. Target cDNA levels were analyzed by semiquantitative RT-PCR in quadruplicates. Sequences of RT-PCR primers are presented in Supplementary table 1. The relative gene expression was normalized to an endogenous reference gene *actb* (β-actin). ImageJ program was used to measure the intensity of PCR product on figures of electrophoresis gels.

In vitro differentiation

The micromass culture technique as described by [22] was employed to differentiate XtiSCs to chondrocytes using differentiation medium from StemPro™ Chondrogenesis Differentiation Kit (ThermoFisher Scientific) diluted 2:1 with water. Cells were cultured in

growth medium as a control. After 10 days, the pellets were fixed and embedded in OCT for cryostat sectioning. Alcian blue staining was used to assess the formation of extracellular matrix, a hallmark of chondrogenic differentiation. The expression of a chondrogenic marker (collagen type II) was also analyzed by immunofluorescent staining.

For osteogenic differentiation, medium from StemPro™ Osteogenesis Differentiation Kit (ThermoFisher Scientific) diluted 2:1 with water was used. Only half of the medium was changed each 3-4 days. Control cells were cultured in standard growth medium. After 21 days the cells were either stained with alizarin Red. Quantitation of alizarin red staining was done by The Osteogenesis Quantitation Kit (Millipore).

Adipogenic differentiation of XtiSCs was performed by adding 1 µM dexamethasone, 0.2 mM indomethacin, 0.1 mg/ml insulin, 1 mM 3-isobutyl-1-methylxanthine in LB15 and RPMI medium with 10% FBS to a confluent cell culture. The medium was changed every 4 days. Control cells were cultured in standard growth medium. After 21 days, adipogenic differentiation was assessed by staining with oil red-O.

X-gal staining

Cells were fixed with 4% formaldehyde for 5 min at RT, and then incubated with 0.1 % X-gal (Fermentas) in staining solution (5 mM potassium ferrocyanide ($K_4Fe(CN)_6$), 5 mM potassium ferricyanide ($K_3Fe(CN)_6$), 150 mM NaCl, 2 mM $MgCl_2$, 40 mM citric acid in sodium phosphate solution, pH 6.0) at 37°C for 12 hours. Stained (senescent) cells with a blue color were observed and imaged under an inverted microscope (Olympus).

In vitro migration assay

Directed migration ability of induced XtiSCs towards cancer cells was investigated. Paraffin wax was used to fix a collagen-coating cover glass on a superfrost plus slide (ThermoFisher Scientific). The space between both slides was filled with 100 µl suspension of $1.3x10^5$ cells.

This chamber was cultured vertically using indicated medium until reaching confluency (3-4 days). The induction medium was then replaced with 120 µl of standard growth medium (with 0.5% FBS) plus 10% PL-matrix (PL BioScience, Aachen, Germany) to make a detection zone above the cell layer (Fig. 5A). The backside of cell growth area was covered with a white adhesive label to distinguish it from the detection zone. HeLa cell suspension was then added after the complete solidification of PL-matrix (about 1 hour in an incubator). HEK 293 cell suspension was used as a control. After 2 days in the matrix, the number of

cells migrating into the detection zone was counted based on at least five microscopic figures per experimental group. The average of the cell number per mm^2 is depicted in the chart (Fig. 6A).

Cell transplantation and tadpole cultivation

X. tropicalis embryos were produced and cultivated by the standard *in vitro* fertilization procedure [23]. Transgenic Katushka red fluorescent protein (RFP)- positive cells were prepared and sorted as described in [15]. Each tadpole was injected with 1000 RFP expressing cells into peritoneal cavity using the protocol of [15]. After transplantation, the distribution of RFP positive cells was observed under a fluorescence stereomicroscope (Olympus). All experiments with tadpoles were performed following institutional-approved protocols.

In vivo wounding assay

To analyze wound homing capacity of XtiSCs, wounding assay was performed as described [24] with modifications. Briefly, stage 51 or elder (around 3 week-old) *X. tropicalis* larvae were anesthetized with 0.01% tricaine (MS-222) and put into Petri dish with 6% Ficoll, 0.1 x MMR, and 0.1% BSA. Two hundred RFP positive XtiSCs (40 nl) treated or untreated with CHIR99021 had been microinjected into larvae through blood vessels near the abdomen. Just after microinjection, the distal third of the tail was wounded by #55 Forceps (Fine Scientific Tool). Transplanted *X. tropicalis* larvae without wounding were used as a control. The tadpoles were imaged after 6 hours under the fluorescence stereomicroscope (Olympus). Two days later, the wounded tadpoles were collected, fixed, and sectioned for immunohistochemistry employing antibody against fibronectin.

Immunohistochemistry

Testes or transplanted tadpoles at indicated time points were collected, fixed overnight in MEMFA (0.1 M MOPS, 2 mM EGTA, 1 mM $MgSO_4$, and 3.7% formaldehyde) at 4°C, rinsed and immersed into 1% agarose. Vibratome sectioning and immunohistochemistry of fixed tadpoles were performed as described in [15]. Individual sections were mounted on slides with Mowiol/DAPI mounting medium and observed under fluorescence microscopy (Olympus
Cell-R).

Dissociation of tadpoles and flow cytometry analysis

Injected tadpoles at the indicated times were collected, anesthetized with 0.4% tricaine (Sigma-Aldrich), immersed into 0.05% collagenase type 1A for 1 hour, and then into 0.025% trypsin-EDTA at 37°C for 20-30 minutes. Tadpoles were pipetted several times until completely dissociated, and filtered through 20 μm celltrics. Cells were collected by centrifugation and suspended in PBS for flow cytometry analysis.

Cells were washed with PBS, collected by scrapers, fixed with 4% formaldehyde for 10 minutes, rinsed and incubated with primary antibody against CD29 (DSHB 8C8, 2 μg/ml) for one hour at RT, following staining with the Alexa488-conjugated secondary antibody (ThermoFisher Scientific, 1:500) for 30 minutes. Cells incubated only with secondary antibody were used as a control. Stained cells or dissociated tadpoles were analyzed by flow cytometer (BD LSR II) accompanied with BD FACSDIVA™ software for data analysis.

Statistical analysis

All assays were repeated at least in three independent experiments. All data were expressed as mean ± standard deviation (SD). For evaluation of group differences, the unpaired Student's t-test was used assuming equal variance. A P value of <0.05 was accepted as significant.

Results

Cytokeratin as a marker of immature Sertoli cells in X. tropicalis testis

Testicular sections from juvenile (6 month-old) and adult (3-year-old) *X. tropicalis* were stained with two antibodies against cytokeratin/Sox9 or vimentin/Sox9. In the juvenile testes, Sertoli cells with the Sox9 accumulation in the nucleus were observed both inside seminiferous tubules and outside (migrating SC progenitors) (Fig. 1A). Regarding adult frogs, most of SCs were localized inside tubules (Fig. 1B). In contrast to the stable presence of vimentin, the expression of cytokeratin was very dynamic. There was little to no cytokeratin in migrating and adult Sertoli cells. On the other hand, this intermediate

filament was strongly detected in tubular SCs in juvenile testes (Fig. 1AB). These results indicate that cytokeratin accompanied with Sox9 can be used as markers of immature Sertoli cells.

Xenopus tropicalis immature Sertoli cells have been isolated and characterized as described in [15]. Double immunofluorescent staining with two antibodies against cytokeratin and Sox9 showed that most of cells (more than 90%) expressed both proteins indicating their immature status (Fig. 1C). The expression of vimentin was observed as well (Fig. 1C).

Pharmacological inhibition of GSK-3 by CHIR99021 induces EMT in XtiSCs

Three-day incubation of XtiSCs with 3 μM CHIR99021 increased the expression of EMT transcription factors such as Snai1, Zeb1 as revealed by immunofluorescent staining (Fig. 2C, 3A) and *twist* by RT-PCR analysis (Fig. 2D). Spindle-like cell shape (Fig. 2A) and the downregulation of cytokeratin (Fig. 2B) were also observed after the treatment with GSK-3 inhibitor. On the other hand, cell-cell junctions were disrupted altogether with the disappearance of β-catenin on the cell membrane (Fig. 2B). Alternatively, cell-matrix adhesions were facilitated through the increase of fibronectin and its receptor, α5β1 integrin deposited on a collagen-coated surface in the culture medium supplemented with CHIR99021 (Fig. 2C). Other mesenchymal proteins, including vimentin and Cd29, remained unchanged in all groups (Fig. S2).

XtiSCs treated with FGF2 upregulated Zeb1 expression (Fig. 3A) but not other mesenchymal markers nor downregulated epithelial markers, such as cytokeratin (Fig. 2, 3A).

TGF- β1 was also used to induce EMT. However, after 3-day treatment at the concentration of 2.5 ng/ml or 5 ng/ml, XtiSCs turned into bigger and flat shape cells (Fig. S3A) accompanied by the higher activity of β-galactosidase at pH 6.0 (positive staining with X-gal) (Fig. S3B). All cell groups also expressed cytokeratin (Fig. S3C). However, only TGF-β1-treated cells formed the thick and parallel stress fibers as visualized by F-actin staining with phalloidin. These results indicated that XtiSCs became senescent. At the concentration of 10 ng/ml most of cells died after 24 hours (data not shown). The same results were observed after treatment with TGF-β1 at different time-courses (5 days and 7

days) (data not shown). Therefore, results presented in this article include only experiments employing FGF2 and CHIR99021.

Taking together, XtiSCs underwent full EMT after the incubation with GSK-3 inhibitor (CHIR99021) by upregulation of mesenchymal and downregulation of epithelial markers. FGF2 treatment resulted in only partial EMT accompanied with the upregulation of Zeb1.

EMT promotes the XtiSCs stemness and migration potential in vitro

The stemness of wild-type (wt) and CHIR99021 or FGF2 treated XtiSCs was investigated *in vitro*. Interestingly, either full EMT (CHIR99021) or partial EMT (FGF2) led to the upregulation of pluripotent stem cell marker Sox2 and mesenchymal stem cell surface marker *cd44* (Fig. 3AB). Flow cytometry analysis revealed the expression of another mesenchymal stem cell surface marker Cd29 in more than 90% of cells (Fig. S2). However, only CHIR-treated XtiSCs suppressed Smooth muscle actin (Acta2), the earliest marker of mural cells (Fig. 3A). This result indicates that the GSK3 inhibitor has induced XtiSCs reprogramming.

Following, *in vitro* differentiation of untreated and treated XtiSCs into three typical mesenchymal cell lineages was investigated. In all three experimental groups cells could differentiate into osteocytes and adipocytes (Fig. 4, S4). However, CHIR-treated cells showed higher efficiency of differentiation in comparison to the vehicle or FGF2. In the osteogenic induction medium, pretreatment with CHIR99021 increased the number of alizarin red-positive cells as revealed by colorimetric analysis of the cell lysate (Fig. 4AB). For chondrocytes, cells were differentiated by micromass culture technique, and only cells in induction medium could form pellets. After 2 weeks, cell pellets were collected and sectioned for the alcian blue staining and immunofluorescence analysis using antibodies against collagen type II. The size and shape of pellets differed among experimental groups. The biggest and round shaped spheres were characteristic for a CHIR-treated cells. Moreover, they also expressed collagen type II, a cartilage specific marker (Fig. 4B). These data confirmed the mesenchymal origin of XtiSCs, and their reprogramming to stem cell-like cells using GSK3 inhibitor.

Furthermore, directed migration toward cancer cells, another prominent feature of mesenchymal stem cells (MSC) and EMT-shifted cells, was analysed as well. In this study

we employed human cancer cells (HeLa) as an attractant and HEK cells as a negative control. In order to improve the cell leakage of commercial Boyden chambers, we designed *in vitro* migration assay in which cells were cultured vertically and migration inducer (HeLa cell suspension) was placed in the upper layer. XtiSCs and the attractant were separated from each other by the “detection zone” based on a semi-solid cultivation medium (Fig. 5A). Both FGF2 or CHIR99021 enhanced the XtiSCs migration into the detection zone toward HeLa cells during 2-day assay. Interestingly, collective migration of FGF2-treated cells increased their number in the detection zone compared with the individually migrated CHIR99021 counterparts (Fig. 5BC).

EMT promotes the XtiSCs stemness and migration potential in vivo

Approximately 1000 untreated or treated (FGF2 or CHIR99021) RFP expressing XtiSCs were microinjected into the peritoneal cavity of 2 day-old *X. tropicalis* tadpoles (stage 41) (Fig. 6A). Two weeks after injection, 900-1500 transplanted cells were detected in each individual using flow cytometry (Fig. 6A), indicating their high survival rate.

In vivo differentiation potential was demonstrated as the ability of XtiSCs to differentiate into cardiomyocytes after allotransplantation. Vibratome sections of tadpoles at 4, 14 and 30 days post-injection (dpi) were stained with rabbit anti-RFP (red) and mouse-cardiac troponin T (green) antibodies. Staining with cardiomyocyte marker prior to microinjection was negative for both treated and untreated XtiSCs (data not shown). 30 days after transplantation, in 30% tadpoles (3/10) CHIR99021-treated cells expressed cardiac troponin T inside the heart and were included in the myocardium (Fig. 6B). Untreated XtiSCs were distributed around aorta and heart and were negative for cardiac troponin T (Fig. 6B). As for the FGF2 experimental group there was no difference between treated and untreated cells (data not shown).

We also evaluated migration potential of XtiSCs transplanted into 3 week-old tadpoles with a cutaneous injury. The distal third of tail was wounded at 6 mm distance from the injection site using a fine forceps. Non-wounded tadpoles with transplanted cells were used as a control (Fig. 7A). RFP expressing XtiSCs migrated toward injury site and accumulated here 6 hours after the transplantation. In non-wounded tadpoles, XtiSCs were found only in the injection site during the same time period (Fig. 7A). Unexpectedly, untreated XtiSCs migrated significantly faster toward the injury site than CHIR99021 treated cells (Fig. 7AB). We also examined the expression of fibronectin 2 days post-injury. Only XtiSCs aggregated at the injury site were positive but not cells migrated elsewhere (Fig. 7C). This means that

XtiSCs have responded to injury signals and contributed to a wound healing by expressing fibronectin, an essential component of extracellular matrix to recover epidermal layer.

Discussion

The change in the expression of intermediate filament, cytokeratin during Sertoli cell (SC) maturation has been revealed by immunohistochemistry and immunoblotting in human and mouse. Cytokeratin is detected in the basal part of fetal SCs around the well-differentiated seminiferous cords up to the early postnatal period. However, it isn't present in pre-SCs or mature SCs in the adulthood [25,26]. On the contrary, vimentin staining is intense and surrounds nuclei of mature SCs [17]. Even though these changes are poorly understood, co-expression of cytokeratin and vimentin have been considered as the marker of immature SCs [18]. The same results have been obtained on *Xenopus tropicalis* testicular sections using double immunofluorescent staining with two antibodies against cytokeratin and vimentin or cytokeratin and Sox9 (Fig. 1AB). These findings suggest similar mechanisms of Xenopus and human testicular development. Moreover, the same analysis illustrated the incomplete differentiation state of XtiSCs toward SCs via the expression of all three markers (Sox9, cytokeratin, and vimentin) (Fig. 1C).

Signal transducer and activator of transcription 3 (STAT3), plays a dual role during EMT stimulation. Its overexpression enhanced invasion and metastasis of colorectal carcinoma by the downregulation of E-cadherin and by increasing N-cadherin and vimentin expression [27]. However, [28] showed that STAT3 promoted proteasomal degradation of SNAI1 through the activation of GSK3β-mediated phosphorylation leading to its ubiquitination in colorectal cancer cells and subsequent EMT suppression. Moreover, GSK3β also regulates the activation of STAT3. STAT3 DNA binding activity was blocked in GSK3β-knockdown or/and GSK3β inhibitor-treated mouse primary astrocytes and microglial cells [29]. Taking together, STAT3 differentially regulates an EMT regarding its epithelial or mesenchymal shift. STAT3 is required to initiate EMT; however, its inhibition is necessary for a EMT completion. Our results are in agreement with the research of [28] and [29]. Previous study reported that XtiSCs expressed mesenchymal markers including vimentin and alpha-smooth muscle actin, and possessed migration capacity after their transplantation into *X. tropicalis* tadpoles [15]. In spite of that, they still expressed epithelial

markers, such as cytokeratin and β-catenin at the plasma membrane (cell-cell adhesions) (Fig. 2B). These results indicate that XtiSCs attain a hybrid epithelial/mesenchymal state. XtiSCs treatment with GSK3 inhibitor (CHIR99021) reduced Stat3 activity (Fig. 8) and upregulated Snai1 expression (Fig. 2C) to drive XtiSCs to a full mesenchymal state. On the other hand, FGF2 up-regulated Stat3 (Fig. 8) in XtiSCs; hence, these cells still kept their hybrid phenotype. Consequently, the broader differentiation potential of EMT-shifted XtiSCs was evidenced by the higher efficiency in osteogenic and chondrogenic induction *in vitro* and into cardiomyocytes *in vivo*.

In addition, we found that cells treated with GSK-3 inhibitor could grow only on collagen type 1-coated slides or on the gamma-irradiated plastic surface, but not on the non-coated or poly-L-lysine-coated slides (Fig. S1). This observation may correlate with the deposition of fibronectin on collagen or on the positively charged plastic surface to form a ECM supporting the attachment of transiting cells lacking the cell-cell contacts. This result is in the agreement with human epithelial cells, alveolar type II A549s and human bronchial cells. The upregulation of collagen type I accompanied with fibronectin-coated surface induced the production of EMT more effectively than the poly-L-lysine layer [30]. Furthermore, collagen type 1 or fibronectin also promoted the motility of EMT-induced HT29 cells as compared to poly-L-lysine coating
[31].

Depending on the signaling, epithelial cells can undergo both, partial EMT where the cells exhibit the mixture of epithelial and mesenchymal phenotypes or full EMT with down-regulated epithelial markers. The partial EMT enables cells to migrate collectively (as a cell sheet or chain) and maintain a dynamic equilibrium among two phenotypes. Moreover, the stemness of EMT- shifted cells is not relevant to the full mesenchymal state. Rather, a hybrid phenotype is closer to the “stemness window” as defined by [32]. During EMT process, stemness window is close to pure mesenchymal or pure epithelial state correlated to the initiating signaling of EMT and cell context as well. Among the EMT transcription factors, ZEB1 is important to acquire stemness of EMT-shifted cells via miRNA such as miR-200 [33,34]. Despite the thorough investigation of interconnection between different EMT phenotypes and stemness in cancer cells, this research is quite restricted regarding physiological condition. This may correlate to the limitation of available epithelial cell lines able to undergo EMT *in vitro*. Attractively, XtiSCs represent a suitable model with the ability

to exhibit broad spectrum of EMT phenotypes using various growth factors or inhibitors. The range includes the hybrid (more epithelial) state, partial EMT close to the mesenchymal state with FGF2 treatment and the complete EMT with GSK-3 inhibitor. The increase of stem cell markers (Sox2, Cd44) (Fig. 3AB), the upregulation of integrin α5β1 (Fig. 2C) which is absent in SCs [35] but present in mesenchymal stem cells [36], and the suppression of Acta2, an earliest marker of mural cells evidenced the XtiSCs shift back to the stem cell state by the pharmacological inhibitor, CHIR99021. We found out that XtiSCs showed the capacity to differentiate into osteocytes and adipocytes (Fig. 4AB, S4) *in vitro*. The differentiation potential was broadened into chondrocytes and cardiac myocytes after the cell treatment with CHIR99021 (Fig. 4C, 6B).

Mouse mammary epithelial (NMuMG) and mouse cortical tubule (MCT) cells are only two non-transformed cell lines which can undergo EMT *in vitro* [37]. However, their EMT stimulation is restricted rather to TGF-β than other factors. This compromises studies of EMT stimulation via other signaling pathways in non-neoplastic epithelial cells. Interestingly, XtiSCs have shown similar changes in a gene expression level during EMT compared to mammary cells (Fig. 2A, 3A). Therefore, XtiSCs provide an additional model for the investigation of EMT signaling and the stemness of EMT-shifted cells.

The loss of epithelial characteristics is coupled with both, the breakdown of cell-cell contacts and the upregulation of extracellular matrix adhesion to increase the migration capacity. Surprisingly, CHIR99021-induced XtiSCs (full EMT phenotype) migrated slower than cells exhibiting hybrid state (FGF2 treatment) *in vitro*. Cd44 mRNA level of FGF2-treated XtiSCs increased 56 fold, compared to control and 1.27 fold, compared to CHIR-treated cells. The increase of CD44 after FGF2 treatment enhanced the directed migration of several cell types, including periodontal ligament cells [38], endothelial cells and melanoma cells [39].

EMT has been considered to be associated with the re-epithelialization process during wound healing where epithelial sheets of primary keratinocytes are able to migrate to the injury site to form a new epidermal layer [40]. This implies that during the healing process, the epithelial cells undergo partial and reversible EMT as a response to inflammatory cytokines such as tumor necrosis factor alpha (TNF-α) [41]. Nevertheless, the effect of TNF-α on MSCs in injured tissue is more complex. Firstly, TNF-α activates MSCs to secrete the paracrine factors stimulating a homing and angiogenesis of endothelial

progenitors [42,43]. Later on, TNF-α promotes MSC migration toward injury site and induces their differentiation [44,45]. In our study, the response of untreated XtiSCs (hybrid phenotype) to a skin injury was faster and more effective with the expression of fibronectin than in the case of fully mesenchymal XtiSCs induced by CHIR99021 (Fig. 7).

Conclusions

In conclusion, our results suggest the association of EMT with the formation of testicular stem cells. EMT-shifted XtiSCs have brought the similar characteristics of mesenchymal stem cells including the capacity to differentiate to the chondrocytes, osteocytes, and adipocytes, directed migration toward cancer cells in vitro and injury site *in vivo*. XtiSCs can become a potential model for studying EMT signaling.

Data Availability

The experimental data used to support the findings of this study are included within the article and the supplementary information file.

Conflicts of interests

The authors declare no competing financial interests.

Funding statement

The research was funded by the Charles University programs SVV 260435 and 20604315 PROGRES Q43 for T.M.X.N., M.V., T.T., M.K. V.K..

Ethical statement

This study was carried out in strict accordance with the Act No. 246/1992 Coll., on the protection of animals against cruelty. An official permission was issued to the Faculty of Science, Charles University by the Ministry of Education, Youth and Sports of the Czech Republic (No. MSMT-37376/2014-4, date of expiry 3. 3. 2019).

Supplementary material

Supplementary material is available online.

References

[1] Thiery JP, Acloque H, Huang RYJ, Angela Nieto M. Epithelial-Mesenchymal Transitions in Development and Disease. Cell. 2009;139: 871–890.

[2] Kalluri R, Weinberg RA. The basics of epithelial-mesenchymal transition. J Clin Invest. 2009;119: 1420–1428.

[3] Lamouille S, Xu J, Derynck R. Molecular mechanisms of epithelial–mesenchymal transition. Nat Rev Mol Cell Biol. 2014;15: 178–196.

[4] Nakaya Y, Kuroda S, Katagiri YT, Kaibuchi K, Takahashi Y. Mesenchymal-epithelial transition during somitic segmentation is regulated by differential roles of Cdc42 and Rac1. Dev Cell. 2004;7: 425–438.

[5] Plisov SY, Ivanov SV, Yoshino K, Dove LF, Plisova TM, Higinbotham KG, et al. Mesenchymal-epithelial transition in the developing metanephric kidney: gene expression study by differential display. Genesis. 2000;27: 22–31.

[6] Li B, Zheng Y-W, Sano Y, Taniguchi H. Evidence for Mesenchymal−Epithelial Transition Associated with Mouse Hepatic Stem Cell Differentiation. PLoS One. 2011;6: e17092.

[7] Mani SA, Wenjun G, Mai-Jing L, Eaton EN, Ayyakkannu A, Zhou AY, et al. The Epithelial-Mesenchymal Transition Generates Cells with Properties of Stem Cells. Cell. 2008;133: 704–715.

[8] Battula VL, Evans KW, Hollier BG, Shi Y, Marini FC, Ayyanan A, et al. Epithelial-mesenchymal transition-derived cells exhibit multilineage differentiation potential similar to mesenchymal stem cells. Stem Cells. 2010;28: 1435–1445.

[9] Barrionuevo F, Burgos M, Jiménez R. Origin and function of embryonic Sertoli cells. Biomol Concepts. 2011;2: 537–547.

[10] Albrecht KH, Eicher EM. Evidence that Sry is expressed in pre-Sertoli cells and Sertoli and granulosa cells have a common precursor. Dev Biol. 2001;240: 92–107.

[11] Sekido R, Bar I, Narváez V, Penny G, Lovell-Badge R. SOX9 is up-regulated by the transient expression of SRY specifically in Sertoli cell precursors. Dev Biol. 2004;274: 271–279.

[12] Schmahl J, Eicher EM, Washburn LL, Capel B. Sry induces cell proliferation in the mouse gonad. Development. 2000;127: 65–73.

[13] Sekido R, Lovell-Badge R. Sex determination involves synergistic action of SRY and SF1 on a specific Sox9 enhancer. Nature. 2008;456: 824–824.

[14] Karl J, Capel B. Sertoli cells of the mouse testis originate from the coelomic epithelium. Dev Biol. 1998;203: 323–333.

[15] Tlapakova T, Nguyen TMX, Vegrichtova M, Sidova M, Strnadova K, Blahova M, et al. Identification and characterization of Xenopus tropicalis common progenitors of Sertoli and peritubular myoid cell lineages. Biol Open. 2016;5: 1275–1282.

[16] Hemendinger RA, Gores P, Blacksten L, Harley V, Halberstadt C. Identification of a specific Sertoli cell marker, Sox9, for use in transplantation. Cell Transplant. 2002;11: 499–505.

[17] Paranko J, Kallajoki M, Pelliniemi LJ, Lehto VP, Virtanen I. Transient coexpression of cytokeratin and vimentin in differentiating rat Sertoli cells. Dev Biol. 1986;117: 35–44.

[18] Rogatsch H, Hittmair A, Mikuz G, Feichtinger H, Jezek D. Expression of vimentin, cytokeratin, and desmin in Sertoli cells of human fetal, cryptorchid, and tumour-adjacent testicular tissue. Virchows Arch. 1996;427. doi:10.1007/bf00199510

[19] Ciruna B, Rossant J. FGF signaling regulates mesoderm cell fate specification and morphogenetic movement at the primitive streak. Dev Cell. 2001;1: 37–49.

[20] Zhou BP, Deng J, Xia W, Xu J, Li YM, Gunduz M, et al. Dual regulation of Snail by GSK-3beta-mediated phosphorylation in control of epithelial-mesenchymal transition. Nat Cell Biol. 2004;6: 931–940.

[21] Vincent T, Neve EPA, Johnson JR, Kukalev A, Rojo F, Albanell J, et al. A SNAIL1-SMAD3/4 transcriptional repressor complex promotes TGF-beta mediated epithelial-mesenchymal transition. Nat Cell Biol. 2009;11: 943–950.

[22] Greco KV, Iqbal AJ, Rattazzi L, Nalesso G, Moradi-Bidhendi N, Moore AR, et al. High density micromass cultures of a human chondrocyte cell line: A reliable assay system to reveal the modulatory functions of pharmacological agents. Biochem Pharmacol. 2011;82: 1919–1929.

[23] Geach TJ, Zimmerman LB, 2011. Developmental genetics in Xenopus tropicalis. *Methods* Mol Biol. 2011; 770: 77-117.

[24] Paredes R, Ishibashi S, Borrill R, Robert J, Amaya E. Xenopus: An in vivo model for imaging the inflammatory response following injury and bacterial infection. Dev Biol. 2015;408: 213–228.

[25] Stosiek P, Kasper M, Karsten U. Expression of cytokeratins 8 and 18 in human Sertoli cells of immature and atrophic seminiferous tubules. Differentiation. 1990;43: 66–70.

[26] Appert A, Fridmacher V, Locquet O, Magre S. Patterns of keratins 8, 18 and 19 during gonadal differentiation in the mouse: sex- and time-dependent expression of keratin 19. Differentiation. 1998;63: 273.

[27] Xiong H, Hong J, Du W, Lin Y-W, Ren L-L, Wang Y-C, et al. Roles of STAT3 and ZEB1 proteins in E-cadherin down-regulation and human colorectal cancer epithelial-mesenchymal transition. J Biol Chem. 2012;287: 5819–5832.

[28] Lee J, Kim JCK, Lee S-E, Quinley C, Kim H, Herdman S, et al. Signal transducer and activator of transcription 3 (STAT3) protein suppresses adenoma-to-carcinoma transition in Apcmin/+ mice via regulation of Snail-1 (SNAI) protein stability. J Biol Chem. 2012;287: 18182–18189.

[29] Beurel E, Jope RS. Differential regulation of STAT family members by glycogen synthase kinase-3. J Biol Chem. 2008;283: 21934–21944.

[30] Câmara J, Jarai G. Epithelial-mesenchymal transition in primary human bronchial epithelial cells is Smad-dependent and enhanced by fibronectin and TNF-α. Fibrogenesis Tissue Repair. 2010;3: 2.

[31] Przygodzka P, Papiewska-Pajak I, Bogusz H, Kryczka J, Sobierajska K, Kowalska MA, et al. Neuromedin U is upregulated by Snail at early stages of EMT in HT29 colon cancer cells. Biochim Biophys Acta. 2016;1860: 2445–2453.

[32] Jolly MK, Huang B, Lu M, Mani SA, Levine H, Ben-Jacob E. Towards elucidating the connection between epithelial-mesenchymal transitions and stemness. J R Soc Interface.
2014;11: 20140962.

[33] Brabletz S, Bajdak K, Meidhof S, Burk U, Niedermann G, Firat E, et al. The ZEB1/miR-200 feedback loop controls Notch signalling in cancer cells. EMBO J. 2011;30: 770–782.

[34] Zhou C, Jiang H, Zhang Z, Zhang G, Wang H, Zhang Q, et al. ZEB1 confers stem cell-like properties in breast cancer by targeting neurogenin-3. Oncotarget. 2017;8: 54388–54401.

[35] Lustig L, Meroni S, Cigorraga S, Casanova MB, Vianello SE, Denduchis B. Immunodetection of cell adhesion molecules in rat Sertoli cell cultures. Am J Reprod Immunol. 1998;39: 399–405.

[36] Veevers-Lowe J, Ball SG, Shuttleworth A, Kielty CM. Mesenchymal stem cell migration is regulated by fibronectin through α5β1-integrin-mediated activation of PDGFR-β and potentiation of growth factor signals. J Cell Sci. 2011;124: 1288–1300.

[37] Brown KA, Aakre ME, Gorska AE, Price JO, Eltom SE, Pietenpol JA, et al. Induction by transforming growth factor-β1 of epithelial to mesenchymal transition is a rare event in vitro. Breast Cancer Res. 2004;6. doi:10.1186/bcr778

[38] Shimabukuro Y, Terashima H, Takedachi M, Maeda K, Nakamura T, Sawada K, et al. Fibroblast growth factor-2 stimulates directed migration of periodontal ligament cells via PI3K/AKT signaling and CD44/hyaluronan interaction. J Cell Physiol. 2011;226: 809–821.

[39] Baljinnyam E, Umemura M, Chuang C, De Lorenzo MS, Iwatsubo M, Chen S, et al. Epac1 increases migration of endothelial cells and melanoma cells via FGF2-mediated paracrine signaling. Pigment Cell Melanoma Res. 2014;27: 611–620.

[40] Ben Amar M, Wu M. Re-epithelialization: advancing epithelium frontier during wound healing. J R Soc Interface. 2014;11: 20131038.

[41] Yan C, Grimm WA, Garner WL, Qin L, Travis T, Tan N, et al. Epithelial to Mesenchymal Transition in Human Skin Wound Healing Is Induced by Tumor Necrosis Factor-α through Bone Morphogenic Protein-2. Am J Pathol. 2010;176: 2247–2258.

[42] Kwon YW, Heo SC, Jeong GO, Yoon JW, Mo WM, Lee MJ, et al. Tumor necrosis factor-α-activated mesenchymal stem cells promote endothelial progenitor cell homing and angiogenesis. Biochim Biophys Acta. 2013;1832: 2136–2144.

[43] Chen H, Min X-H, Wang Q-Y, Leung FW, Shi L, Zhou Y, et al. Pre-activation of mesenchymal stem cells with TNF-α, IL-1β and nitric oxide enhances its paracrine effects on radiation-induced intestinal injury. Sci Rep. 2015;5: 8718.

[44] Egea V, von Baumgarten L, Schichor C, Berninger B, Popp T, Neth P, et al. TNF-α respecifies human mesenchymal stem cells to a neural fate and promotes migration toward experimental glioma. Cell Death Differ. 2011;18: 853–863.

[45] Croes M, Cumhur Oner F, Kruyt MC, Blokhuis TJ, Bastian O, Dhert WJA, et al. Proinflammatory Mediators Enhance the Osteogenesis of Human Mesenchymal Stem Cells after Lineage Commitment. PLoS One. 2015;10: e0132781.

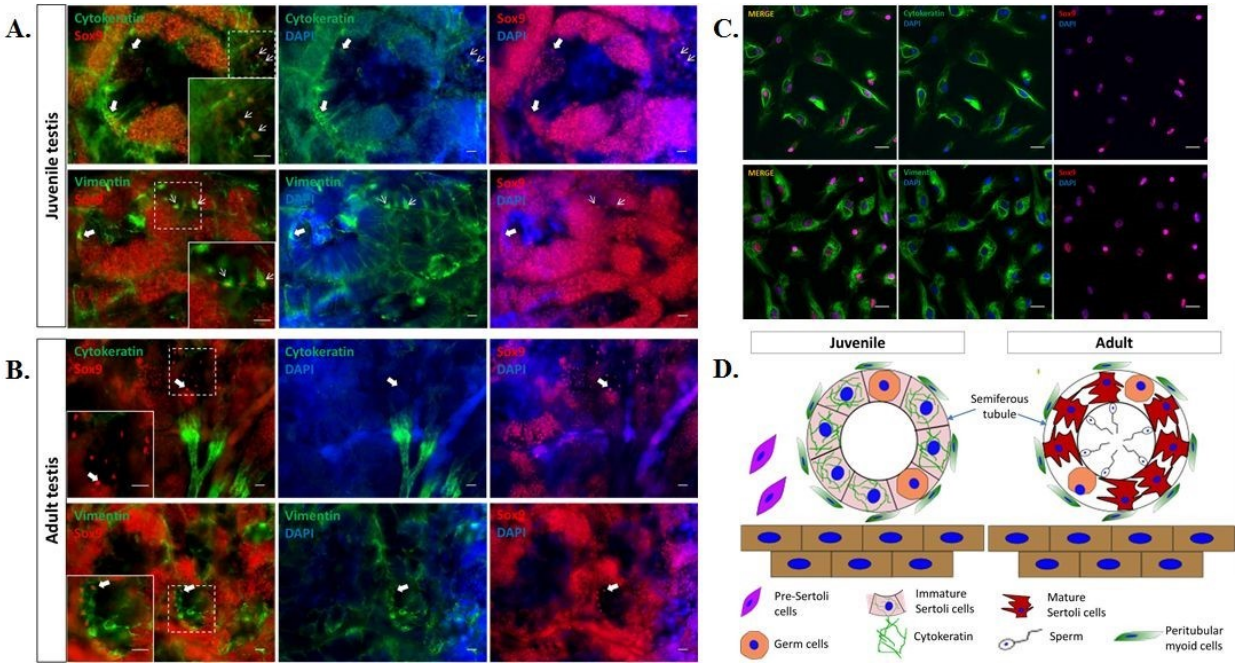

Figure 1. (A) Testicular cross-sections from juvenile *Xenopus tropicalis* stained with two antibodies, Cytokeratin (green)/Sox9 (red, SC marker) or Vimentin (green)/Sox9. Thin arrows show migrating Sertoli cells (SCs) or pre-SCs outside the seminiferous tubules. Thick arrows indicate SCs inside the tubules. Cytokeratin is absent in pre-SCs, in contrast to tubular SCs. On the other hand, Vimentin is present in both types, migrating and tubular SCs. (B) Double staining of testicular cross-sections with two antibodies, Cytokeratin (green)/Sox9 (red) or Vimentin (green)/Sox9 from adult *Xenopus tropicalis.* The only Vimentin is observed in SCs. (C) Immunofluorescent staining of XtiSCs with antibodies against Cytokeratin (green)/Sox9 (red) show that most of XtiSCs expressed both proteins which evidence them as immature Sertoli cells or SC progenitors. The expression of Vimentin was observed in XtiSCs as well. Nuclei were stained with DAPI. Scale bar: 20 μm. (D) The scheme illustrates the development of Sertoli cells in testis.

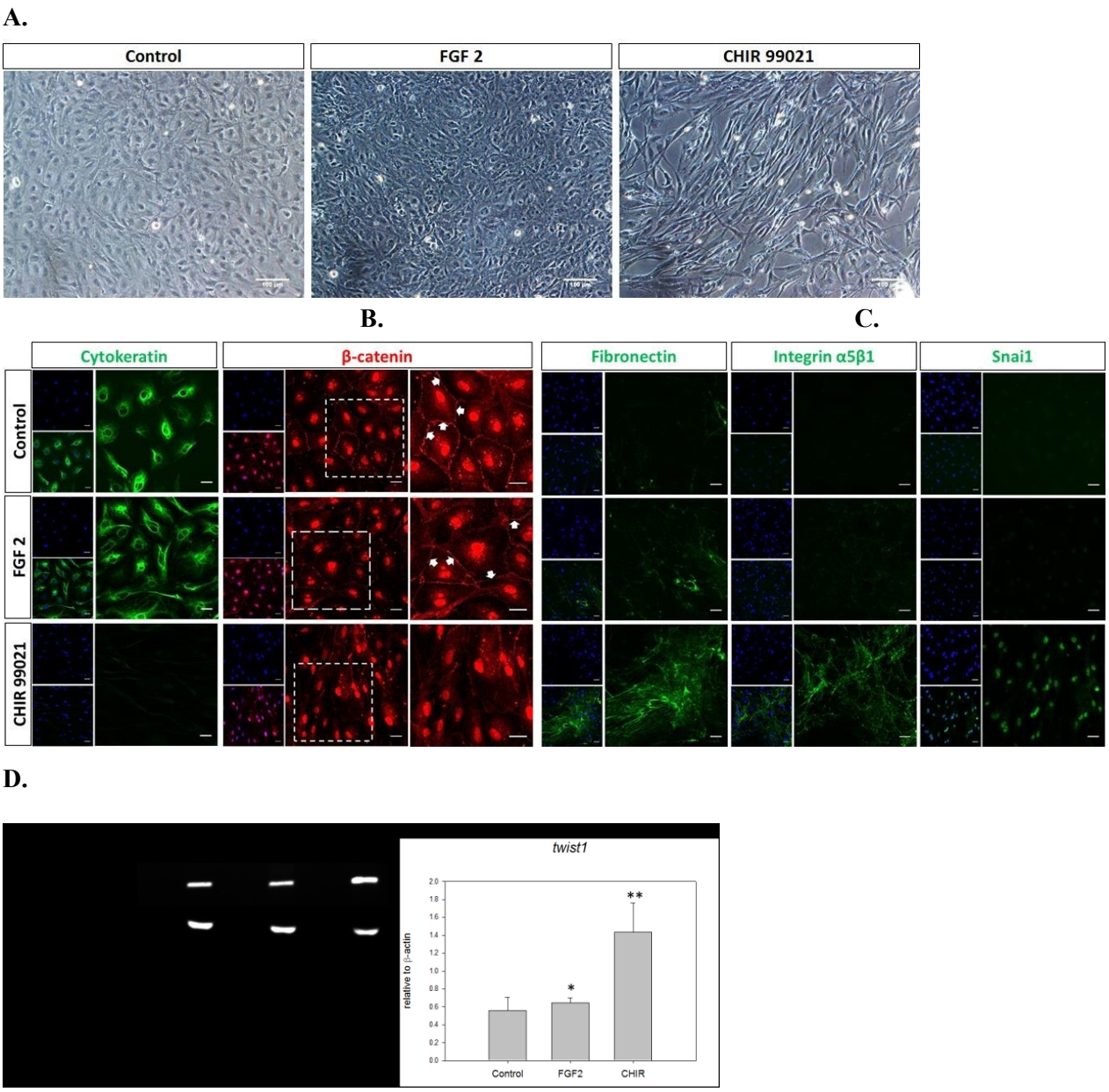

Figure 2. GSK3 inhibitor (CHIR99021) stimulates EMT in XtiSCs cell culture. XtiSCs were cultured in growth medium supplemented with 25 ng/ml FGF2 or 3 μM CHIR99021, or 0.1% DMSO as a control. (A) After three-day treatment, the morphological change of XtiSCs from cobblestone shape to a long-rod shape in medium with CHIR99021 was observed. Scale bar: 100 μm. (B-C) Immunofluorescent staining and RT-PCR analysis showed the downregulation of epithelial markers (Cytokeratin, β-catenin at plasma cell membrane) (B), and the increase of mesenchymal markers (Fibronectin, Integrin α5β1, Snai1, and *twist1*) (C,D). Arrows show the expression of β-catenin at plasma cell membrane. Nuclei stained with DAPI. Scale bar: 20 μm. Results are representative of three biological replicates. *p<0.5, **p<0.001.

A.

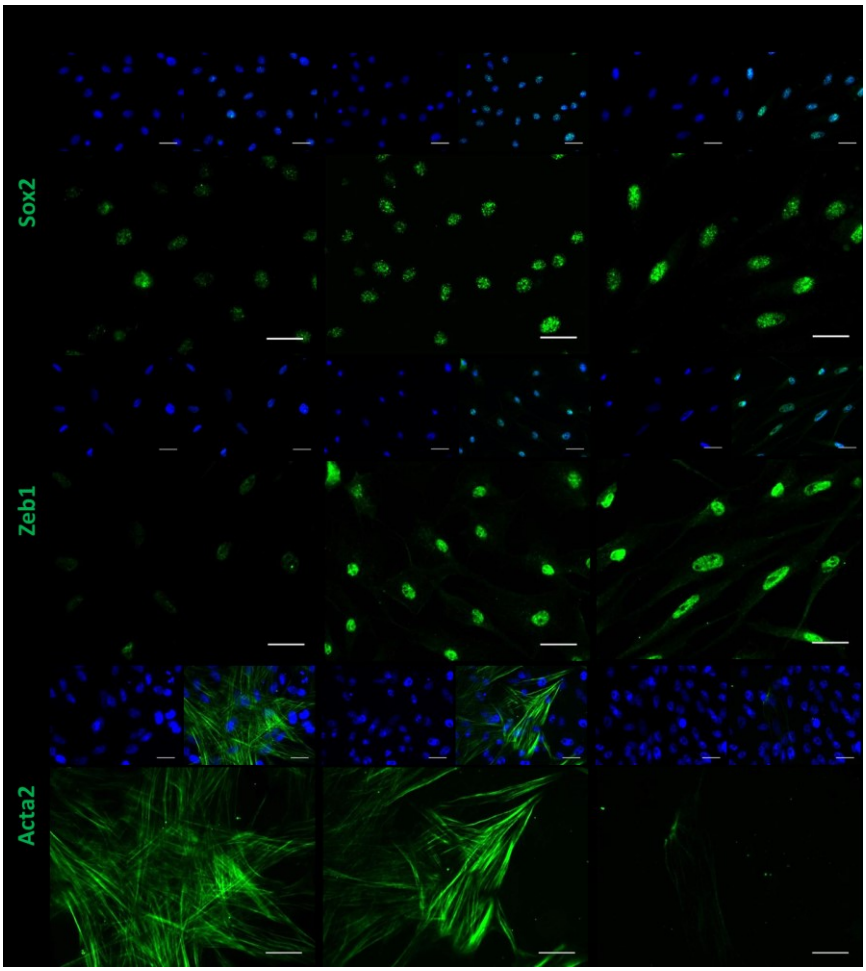

B.

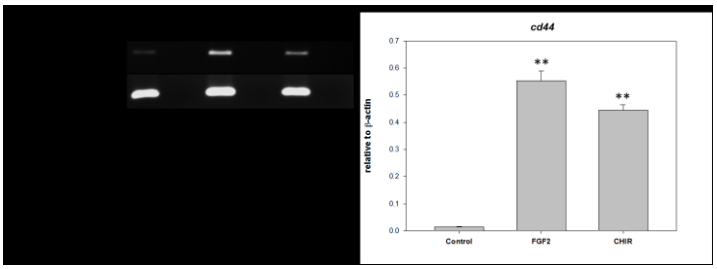

Figure 3. Gene expression of mesenchymal stem cell markers in FGF2 and CHIR99021-treated XtiSCs. Immunofluorescent staining (A) and RT-PCR (B) show the increased expression of stem cell marker Sox2, *cd44* and Zeb1 after FGF2 and CHIR99021 treatment. However, only CHIR-treated XtiSCs suppressed Acta2, the earliest marker of mural cell progenitors. RT, reverse transcriptase. Scale bar: 20 μm. Nuclei stained with DAPI. Results are representative of three biological replicates. **p<0.01.

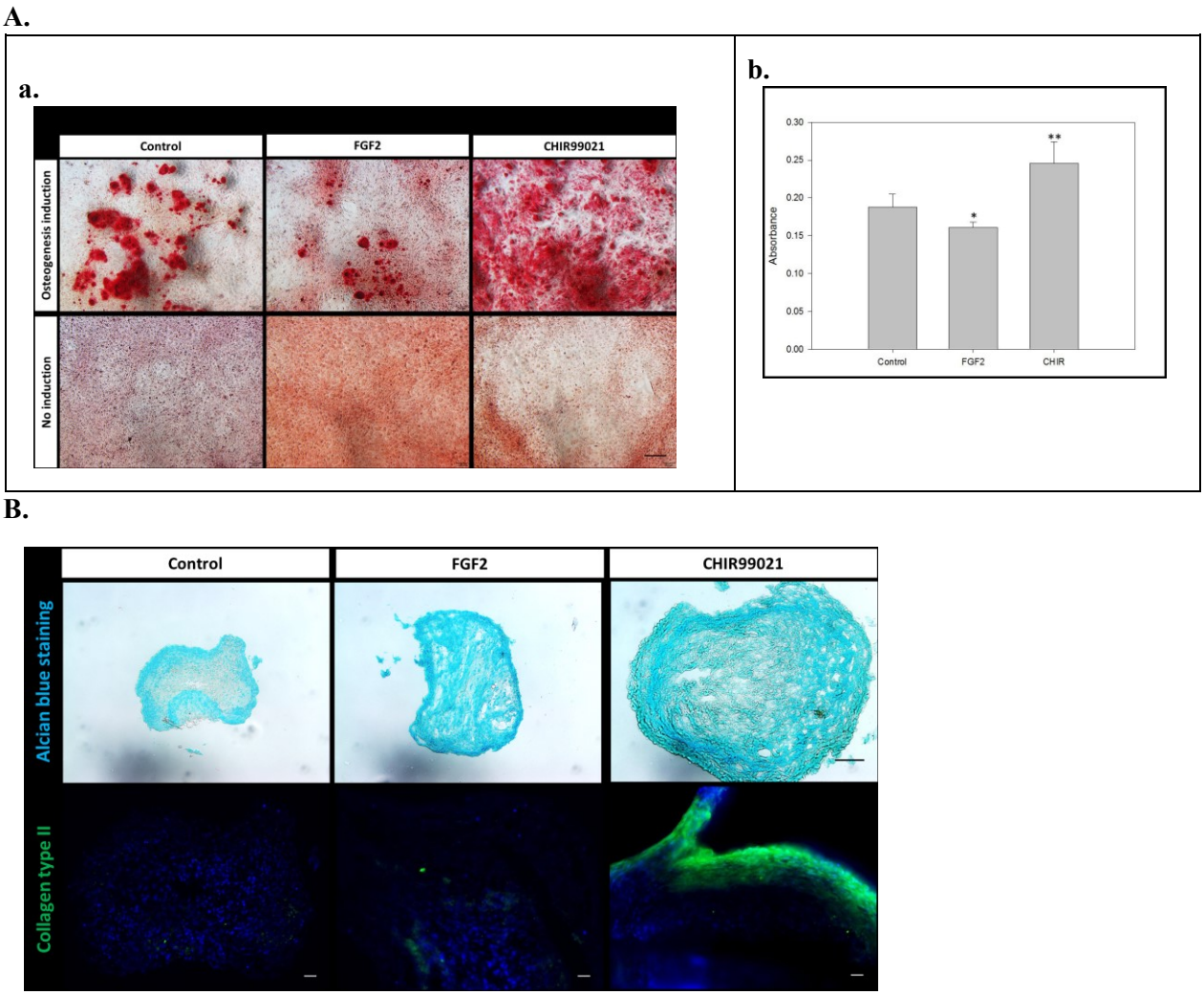

Figure 4: *In vitro* differentiation of XtiSCs. XtiSCs were treated with FGF2, CHIR99021 or 0.1% DMSO as a control for 3-4 days followed by the replacement of medium with osteogenic and chondrogenic induction medium. (A) Osteocyte differentiation of XtiSCs was evidenced as a calcium deposit reacting with alizarin red (a). Cells were lysed at low pH to release alizarin red dye from the stained monolayer for colorimetric test as illustrated in diagram (b). (B) Alcian blue was used to stain glycosaminoglycans in cartilages. In control (untreated cells) the dye reacts only with the periphery of cell clusters. On the other hand, Alcian blue reaction is strong and uniform in XtiSCs clumps after FGF2 and CHIR99021 treatment, indicating the high level of proteoglycan forming the extracellular matrix. Collagen type II, a specific marker of cartilage matrix, were expressed in cells pretreated with CHIR99021 only. Scale bar: 100 µm.*p<0.001, **p<0.005.

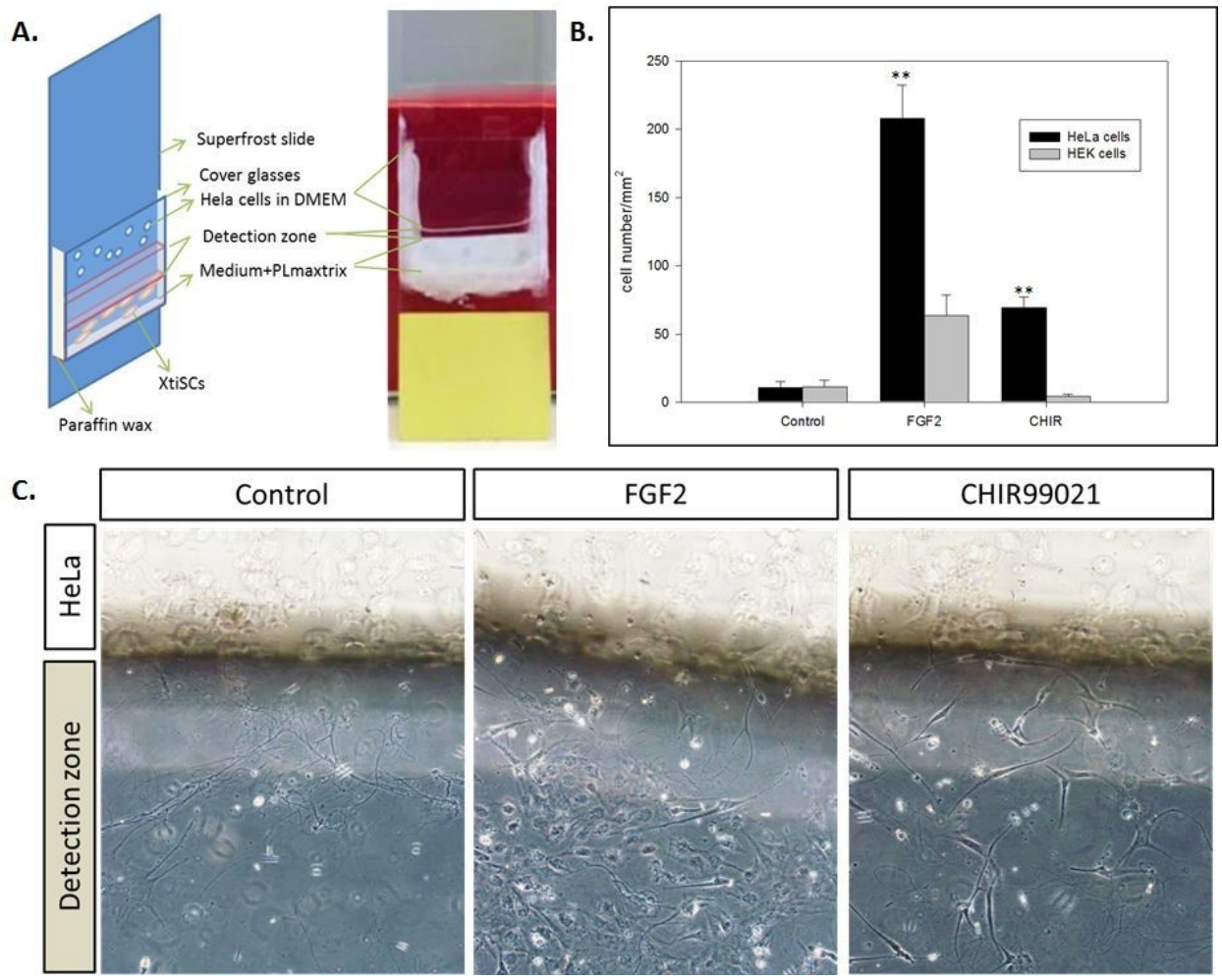

Figure 5. Directed migration of XtiSCs toward cancer cells (HeLa). Scheme (A) illustrates the directed migration assay with XtiSCs in the lower part of incubation chamber containing 100 µl of FGF2, CHIR99021 or 0.1% DMSO enriched media. After three-day treatment, inducing or control (0,1% DMSO) medium was replaced by 120 µl of standard cultivation medium supplemented with PL-matrix. HeLa or HEK cells suspension (control) was added to the upper part after the solidifying of PL-matrix. HeLa cells are separated from XtiSCs by the detection zone. After 36-48 hours, the number of cells in the detection zone was counted and expressed in the chart (B-C). The results are representative of five biological replicates. **$p<0.01$.

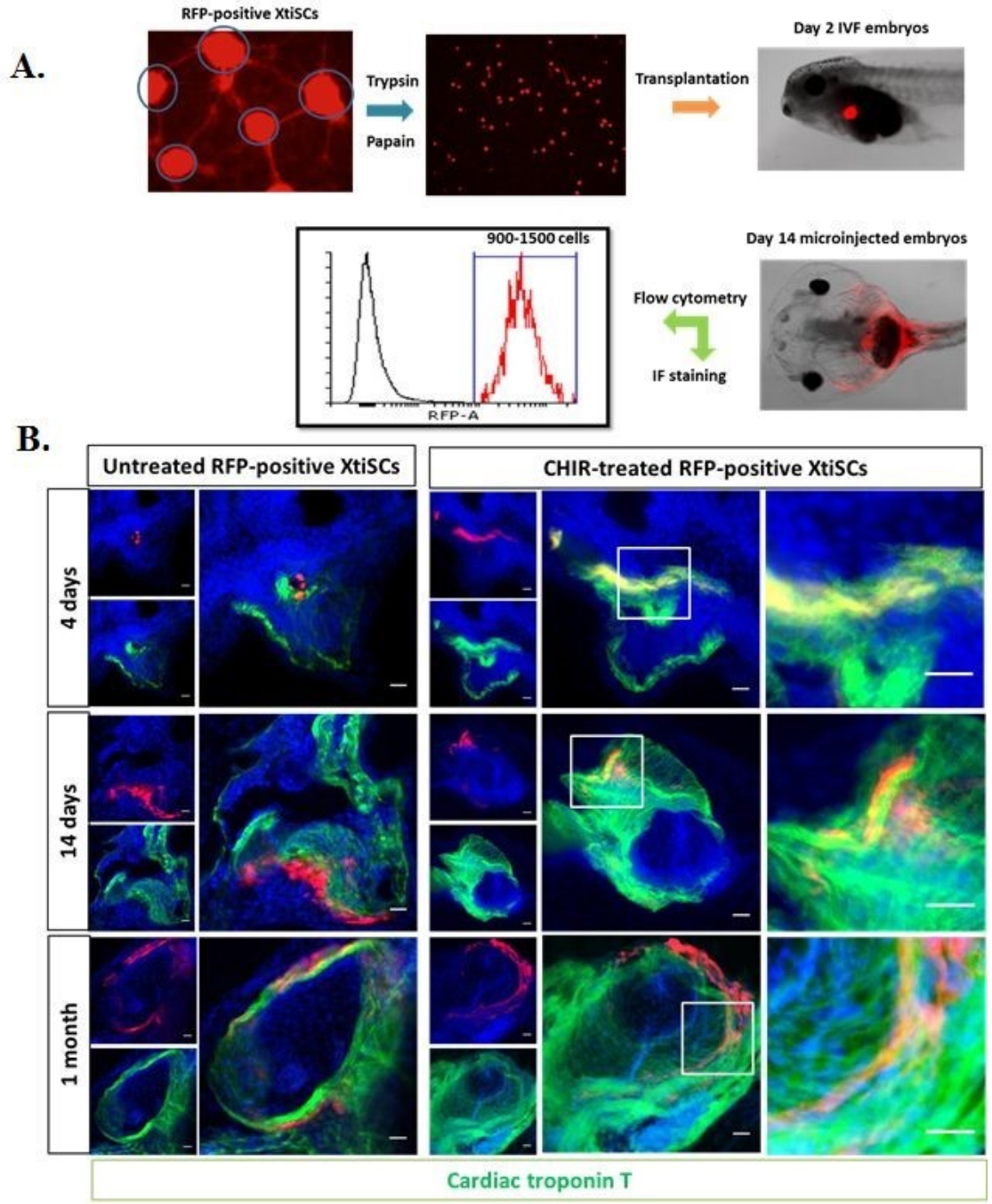

Figure 6. *In vivo* differentiation of EMT- induced XtiSCs into cardiomyocytes. (A) Experimental scheme. RFP- positive XtiSCs were cultured in growth medium supplemented with 3 μM CHIR99021, or 0.1% DMSO as a control for 3-4 days before transplantation into 2 days old tadpoles. (B) At 4, 14 or 30 days post-injection (dpi), tadpoles were fixed and sectioned for double staining with antibodies against red fluorescent protein and cardiac troponin T labeling cardiomyocytes in the heart. Scale bar: 20 μm. Nuclei stained with DAPI. Results are representative of four biological replicates.

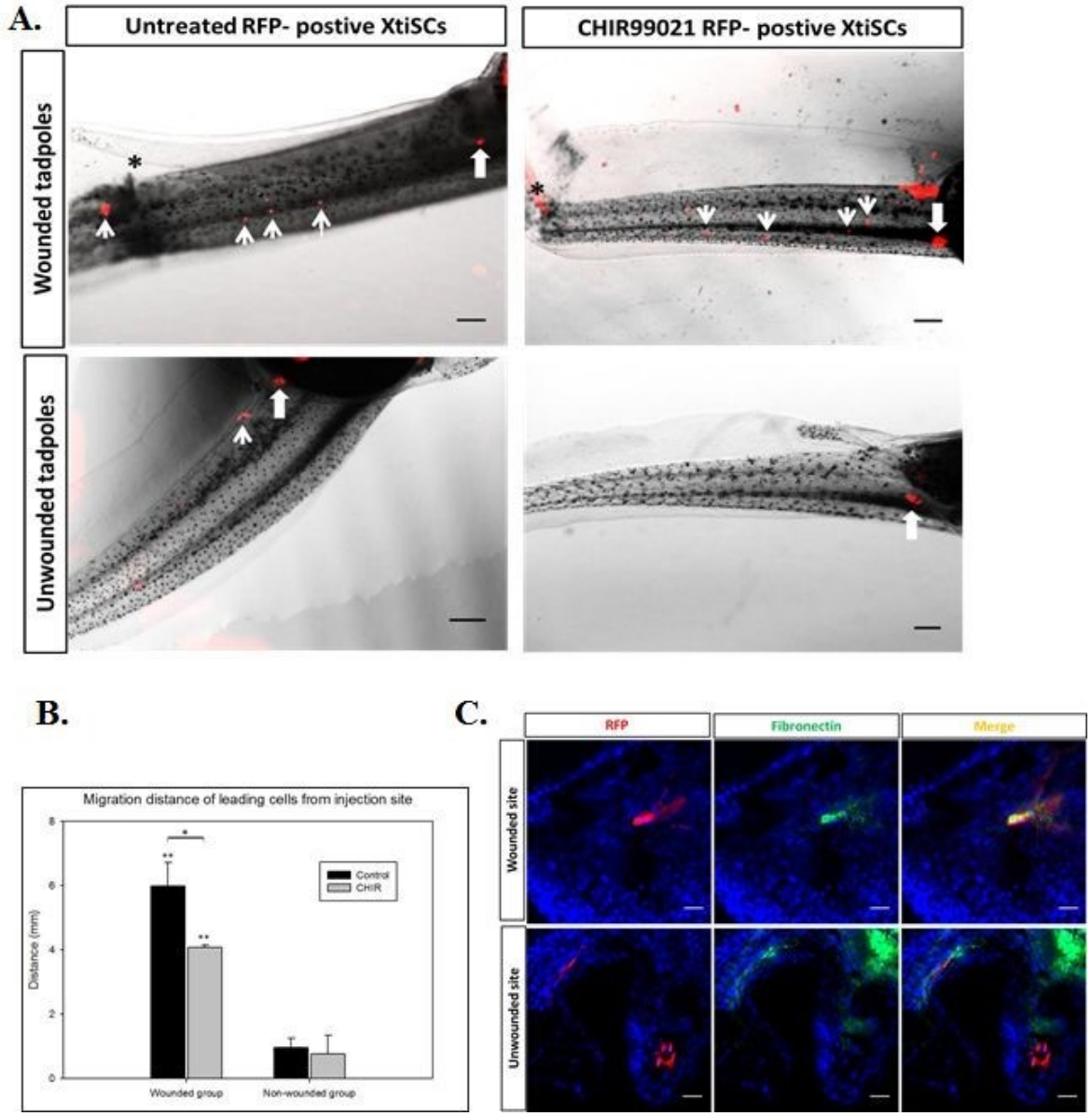

Figure 7. *In vivo* migration of untreated or CHIR99021 treated XtiSCs transplanted into the peritoneal cavity of two days old tadpoles toward skin injury. (A) Differential migration behavior of untreated and treated RFP expressing XtiSCs inside wounded or unwounded tadpoles. Arrows show the migrating RFP positive XtiSCs, thick arrows indicate the injection sites. The injury site is marked by a black asterisk. Scale bar: 500 μm. (B) the distance of leading cells from injection site was measured 6 hours after transplantation by ImageJ and expressed in the chart. (C) Two days after transplantation, fibronectin was detected in untreated XtiSCs at injury site only, but not in cells outside wounded areas in both groups. Nuclei were stained with DAPI. Scale bar: 20 μm. *p<0.05, **p<0.01.

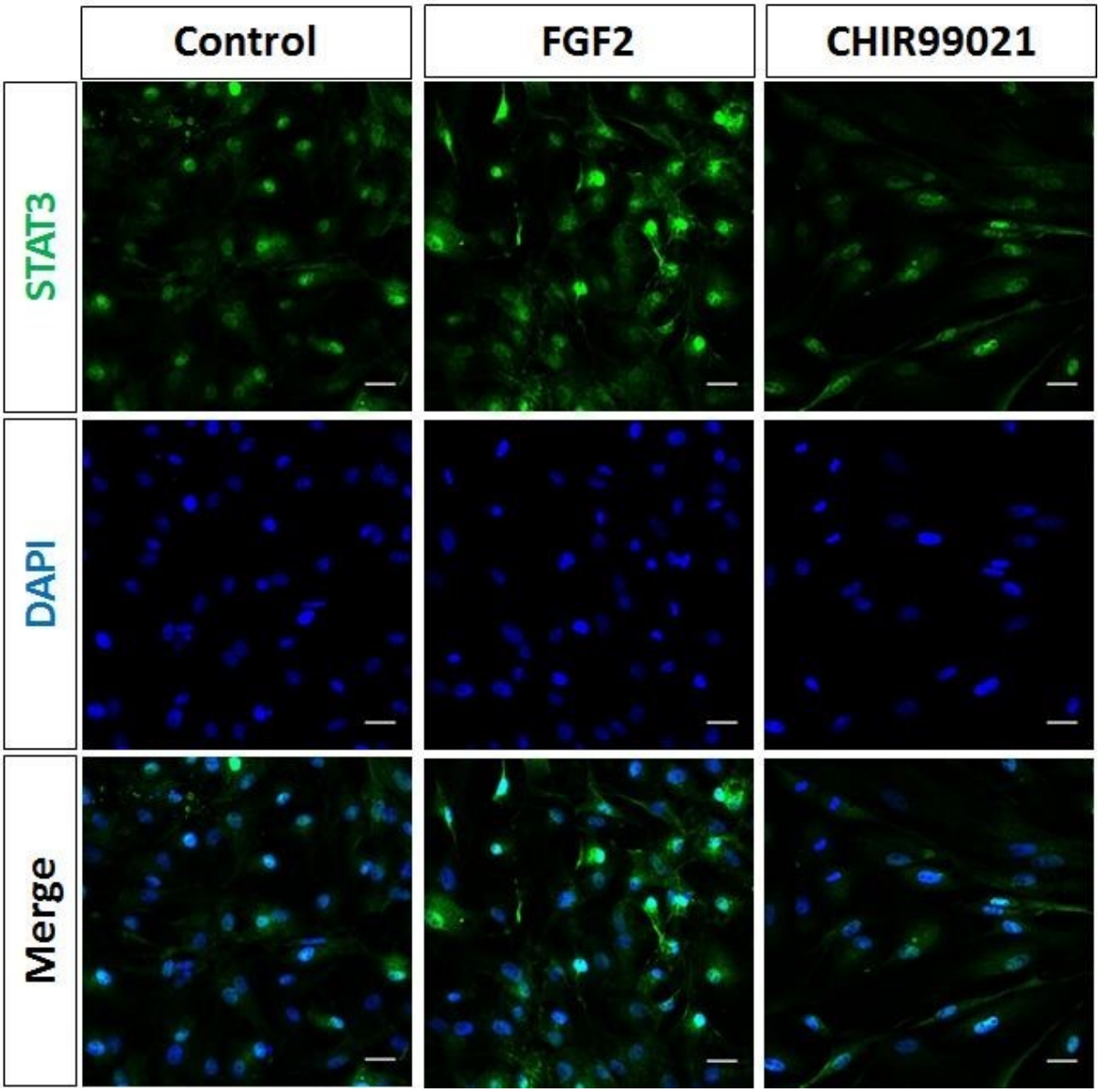

Figure 8. The representative fluorescent images of Stat3 expression in XtiSCs in different medium culture. The Stat3 upregulation is observed in FGF2-treated cells. On the other hand, CHIR99021 is responsible for its downregulation. Nuclei were stained with DAPI. Scale bar: 20 μm.

Title: The interconnection between cytokeratin and cell-cell contact in immature *Xenopus tropicalis* Sertoli cells.

Authors:[a] Thi Minh Xuan Nguyen[a*] [a], Marketa Vegrichtova[a], Tereza Tlapakova[a], Magdalena Krulova and Vladimir Krylov

Thi Minh Xuan Nguyen
Email:
nguyenx@natur.cuni.cz
Marketa Vegrichtova
Email:
marketa.vegrichtova@natur.cuni.cz
Tereza Tlapakova
Email:
tereza.tlapakova@natur.cuni.cz
Magdalena Krulova
Email:
magdalena.krulova@natur.cuni.cz
Vladimir Krylov*
* Corresponding author
Email: vkrylov@natur.cuni.cz
ORCID iD: 0000-0001-8678-7155

Affiliation: [a] Charles University, Faculty of Science, Vinicna 7, 128 44, Prague 2, Czech Republic.

***Corresponding author:**

tel: +420221951773, fax: +420221951758, email: vkrylov@natur.cuni.cz

Keywords:

cytokeratin; adherens junctions; immature Sertoli cells; *Xenopus tropicalis;* testicles

Summary statement:

β-catenin and Cytokeratin are expressed transiently in juvenile testicles and cultivated *Xenopus tropicalis* immature Sertoli cells. Acrylamide and CHIR99021 disrupted CK networks which caused the breakdown of β-catenin-based cell junctions in immature SCs *in vitro* and testicular failure *in vivo*.

ABSTRACT

Sertoli cells (SCs) are of a central importance in connection with the embryonic determination of a male sex and spermatogenesis in adulthood. The failure in SC development leads to a male sterility and testicular cancer. In the juvenile males, SCs are immature and differ considerably from mature cells. The immature SCs proliferate and differentiate until the beginning of puberty when they cease dividing and start to nurture germ cells for the sperm production. These differences between the immature and mature SCs suggest the understanding of the mechanism associated with immature maintenance of SCs until the appropriate time point is a crucial step to identify functional regulation of the mature cells. Concerning intermediate filaments, only Cytokeratin (CK) is transiently observed in immature SCs, but its function in SC differentiation is poorly understood. We examined the relationship between CK and cell junctions during development of *X. tropicalis* testes. Cytokeratin and membrane β-catenin co-expressed in juvenile (5 months) testes and in cultured immature SCs, here called XtiSCs, but they are absent in the adult organ. Suppression of CK by acrylamide in XtiSCs led to breakdown of membrane-bound β-catenin but not F-actin and β-tubulin or cell adhesion proteins (Focal adhesion kinase and integrin β1). In contrast to the obvious dependence of β-catenin appearance in the cell membrane on CK stability, disruption of membrane β-catenin via uncoupling of cadherins with Ca2+ by chelator EGTA had no effect on the cytokeratin stability. Interestingly, CHIR99021, a GSK3 inhibitor, also downregulated CK resulting in the inhibition of cell-to-cell contacts of *in vitro* cultivated immature SCs, XtiSCs and testicular development of juvenile frogs. This study suggests a new role of CK in the retention of β-catenin-based junctions in immature Sertoli cells, and thus serves as a scaffold for the maturation of seminiferous tubules and germ cells.

INTRODUCTION

Sertoli cells (SCs) are localized within seminiferous tubules and play a crucial role in male reproduction. In the early development, anti-Müllerian hormone (AMH) is secreted by SCs to regress female Müllerian tract contributing to determination of somatic male sex (Appert

et al., 1998; Barrionuevo et al., 2011; Lee and Taketo, 1994). Later on, SCs provide nutrients, differentiation factors, appropriate mitogens to nourish the developing germ cells as well as to regulate their maturation in adult testes (de Winter, 1993; Handelsman et al., 1990). Moreover, blood-testis barrier and immunosuppressive molecules produced by SCs protect sperm cells from attacks of immune system and establish the niche for the maturation of spermatogonial stem cells (SSCs) (Mital et al., 2010; Setchell, 2009). The failure in Sertoli cell differentiation results in a male infertility due to a reduced production of sperm cells (Myers et al., 2005; Nistal et al., 1982).

Prior to puberty, SCs are maintained in the immature state with extensively different morphology and biochemical activity in comparison with mature cells. In contrast to constant division of immature SCs, the proliferative activity of the mature cells gradually decline to zero when tight junctions between adjacent SCs are established (Steinberger and Steinberger, 1971). At this point, fully differentiated SCs initiate to produce fluid in to the lumen of seminiferous tubules leading to their expansion and the enlargement of testis. The mature SCs also alter their protein expression, suppressing, e.g., cytokeratin and anti-Müllerian hormone (Sharpe et al., 2003) and starting to produce, e.g., inflammatory cytokine interleukin-1α (Wahab-Wahlgren et al., 2000) and androgen-binding protein to initiate spermatogenesis. Differences between immature and mature SCs are important for the understanding of SCs differentiation and their functional regulation.

Cytokeratins (CK) are the most abundant intermediate filaments (IF) in epithelial cells and the expression of their subsets is highly organ or tissue specific. In the cytoplasm, they form a complex network in association with membrane proteins implying their importance in some aspects of cell morphology and signalling. The transient expression of pair 8/18 (Stosiek et al., 1990), during SC differentiation is described in many species. CK is detected in basal part of SCs from 12.5 d.p.c rat testes with the well-differentiated seminiferous cords to early postnatal period, however, it completely disappears in mature cells (Paranko et al., 1986). In human, CK expression persists in SCs of adult cryptorchid testes or peritumour tubules only (Rogatsch et al., 1996). The examination of CK expression in SCs of juvenile and adult *X. tropicalis* testes was conducted in our laboratory. In agreement with mammalian model only SCs with Sox9 expression in juvenile *X. tropicalis* testes had positive staining with antibodies against CK (data in publishing).

However, even though, CK has been considered as a marker of immature Sertoli cells (Rogatsch et al., 1996), its role in SC development is still poorly understood.

Cell junctions among Sertoli cells and between Sertoli cells and germ cells are crucial for testicular structure and spermatogenesis. In adulthood, blood-testis barrier (BTB) formed by tight junctions between adjacent matured Sertoli cells bisect seminiferous tubules into basal and apical compartments. Spermatogonia from the basal part differentiate and migrate to the apical compartment crossing the dynamic BTB which provides the microenvironment for final differentiation of haploid cells into sperms and prevents spermatids from blood and lymph (Wen et al., 2016). Throughout this process, the immature germ cells are in tight contact with SCs (Wolski et al., 2005). In contrast to the adulthood, spermatogonia of immature males are resting and lying on the basal membrane of seminiferous tubules. This may require different junctions and structure of developing SCs to anchor germ cells to the basement membrane and to protect them against the bloodstream. However, the cell-to-cell contacts in immature seminiferous cords hasn't been analysed yet.

In present study we observed the co-expression of CK and β-catenin involved in SC junctions from young testes. *Xenopus tropicalis* immature Sertoli cells (XtiSCs) have been established and described in the previous report (Tlapakova et al., 2016). *In vitro* treatment of XtiSCs with acrylamide and CHIR99021 showed the potent role of CK in the maintenance of β-catenin-based junctions. The disruption of CK in SCs of developing testis resulted in the failure of testicular maturation.

RESULTS

The role of Cytokeratin in the retention of adherens junctions in immature Sertoli cells

β-catenin, a 92 kDa protein is commonly found in couple with cell-cell junctions (Hartsock and Nelson, 2008) and has a high affinity for a transmembrane glycoprotein, E-cadherin (Huber and Weis, 2001). We examined the expression of Cytokeratin (CK), a marker of immature Sertoli cells (SCs), β-catenin and E-cadherin in juvenile (5-month old) and adult (3-year old) *X. tropicalis* testes. H&E staining of paraffin sections from juvenile testes

showed well-organized seminiferous tubules, however, they were small and narrow due to the incomplete development of tubular lumen compared to testes of 3-year old individuals (Fig. 1A). Interestingly, immunostaining of CK and β-catenin revealed that only juvenile testes (5-month old) exhibited the expression of both proteins in SCs (Fig. 1, B-J). Here, β-catenin was distributed mainly in cell membrane and cytoplasm, but in some SCs we observed also weak nuclear staining (Fig. 1, B-G). Co-expression of β-catenin and E-cadherin surrounding SCs of young testes (Fig. 2, A-C) implies importance of β-catenin in associated with adherens junction of immature SCs. Notably, β-catenin was detected encircling germ cells in young testes as well, but no positive staining with antibodies against CK and E-cadherin was obtained on the germ cells both in young and adult frogs (Fig. 1&2) suggesting different β-catenin-based cell junctions between germ cells to maintain them in undifferentiation stage. The downregulation of β-catenin in matured testes suggest the change in cell-cell junctions of fully functional SCs to provide a structural support for spermatogenesis, even though E-cadherin continued to be presented mainly in the basal compartment of the matured cells (Fig. 2, D-F).

To reveal the role of CK in SC development we employed *in vitro* culture of immature SCs, called ***X****enopus* ***t****ropicalis* **i**mmature **S**ertoli **c**ells (XtiSCs) previously isolated and described in (Tlapakova et al., 2016). Cells expressed SC proteins including Sox9, (Tlapakova et al., 2016), focal adhesion kinase (Fak) and CK (Fig. 3A). XtiSCs revealed strong staining with β-catenin antibody in both, nuclei and cell membrane (Fig. 4A&7C). These results indicate that we are in fact culturing the immature Sertoli cells. Chromosomal analysis showed normal karyotype even after 12 passages (Fig. 3B). In addition, XtiSC didn't form colonies in soft agar, a typical feature of transformed cells (Fig. 3C).

β-catenin has dual biological functions, serving as a component of adherens junction on plasma membrane and as a transcription factor in cell nuclei (Daugherty and Gottardi, 2007). Firstly, we induced the disorganization of CK in XtiSCs to investigate its regulatory effect on membrane-bound β-catenin. The transient negative impact of acrylamide (unpolymerized form) on CK integrity has been well-described in Xenopus and mammals as well (Duncan et al., 2009; Shabana et al., 1994; Sonavane et al., 2017). The serious disruption of CK was also observed in XtiSCs after 75 minutes incubation with 10 mM

acrylamide (Fig. 4B1), leading to the breakdown of β-catenin on the cell membrane (Fig. 4B2). Gradual recovery of membrane β-catenin coincidentally with the CK re-organization was obtained after 90 minutes washing out the acrylamide from the culture medium (Fig. 4C). To examine the reverse process, i.e the effect of the downregulation of a membrane β-catenin on the stability of cytokeratin, we added an Ca2+ chelator EGTA to XtiSC culture to disrupt adherens junction (cadherins) and subsequently destabilize β-catenin on plasma membrane. 15 minutes treatment with 2 mM EGTA caused the disappearance of β-catenin from the cell membrane, and gave rise to the change in XtiSCs' morphology into fibroblast-like cell shape (Fig. 4D). However, the CK network was not affected (Fig. 4,D2&E), resulting in full recovery of β-catenin on the cell membrane after 90 minutes washing out EGTA. Effect of acrylamide and EGTA on other cytoskeletal and cell adhesion proteins was also examined. Cortical actin filaments became predominant to probably enhance the recruitment of β-catenin-based cell-cell adhesions degraded by acrylamide and EGTA (Fig. 5B1&C1) (Engl et al., 2014; Wu et al., 2014). While β-tubulin was not affected by acrylamide (Fig. 5B2), it formed aggregates after the treatment with 2 mM EGTA (Fig. 5C2). No changes in cell-matrix adhesion molecules (FAK and integrin β1) were observed (Fig. 6). Taken together, these results suggest that CK network was required to sustain the β-catenin-based cell junctions in XtiSCs, whereas the CK expression didn't depend on membrane β-catenin stability.

GSK3-mediated phosphorylation causes β-catenin degradation by ubiquitin-proteasome pathway. Interestingly, in the previous study, we observed the suppression of CK in XtiSCs by CHIR99021, a GSK-3 inhibitor (data in publishing). Thus, to determine the relationship between CK expression and β-catenin we added CHIR99021 or lithium chloride (LiCl), another GSK-3 inhibitor (Kramer et al., 2012) to XtiSC culture. Reactivation of cytosolic GSK-3 was achieved by the IWP2 an inhibitor of Wnt secretion (García-Reyes et al., 2018), which subsequently release GSK-3 from the blocking complex, LRP-associated Wnt 'signalosome' (Bilic et al. 2007). XtiSCs didn't respond to 10 mM LiCl after 3-day treatment. In the 20 mM and 40 mM solution, cells died after 24 hours and 6 hours, respectively without any remarkable change in previous time points (data not shown).

Western blot analysis of nuclear fraction revealed little bit higher accumulation of β-catenin in the cell nuclei after 3-day treatment with 3 μM CHIR99021, while no significant

difference in the β-catenin level of control and CHIR99021-treated cells from whole cell lysate was observed (Fig. 7B). Cells cultivated in 2 μM IWP2 showed substantial degradation of β-catenin in the nuclear fraction (Fig. 7B). Expression level and distribution of CK and β-catenin were visualized by immunocytochemistry as well (Fig. 7C). We observed total loss of membrane β-catenin in cells treated with CHIR99021 compared to control. In agreement with the immunoblotting result, the downregulation of nuclear β-catenin was detected in XtiSC incubated with IWP2 only, but not with CHIR99021. Notably, the expression of CK was accompanied by the presence of membrane β-catenin in vehicle control and XtiSCs cultivated with IWP2 (Fig. 6C). This result supports the positive role of CK in the retention of β-catenin in the plasma membrane hence the stabilization of adherens junction in immature SCs. CHIR99021 also induced morphological changes in XtiSCs from cobblestone to long-rod shape associated with the breakdown of cell-to-cell contacts (Fig. 6A&C).

To examine the role of cell junctions in SCs and testicular development, we injected 0, 0.6, 1 and 1.5 μM CHIR99021 into dorsal sac of 5-month old male frogs. 2.5 months after injection, all frogs survived normally. However, no testes were found in individuals injected with 1.5 μM CHIR99021 (Fig. 8A). The testicles obtained from other experimental groups were embedded into paraffin for immunohistochemistry. H&E staining of testicular sections showed impaired morphology and structure of seminiferous tubules in CHIR99021-treated animals. The most serious damage was observed at 1 μM drug concentration, when germinal epithelium extruded away from the basement membrane and the outer myoid layer (Fig. 8B). Lower concentration of CHIR99021 (0.6 μM) resulted in unorganized-seminiferous tubules (Fig. 8B). In comparison with vehicle control individuals, Sox9 protein, a specific maker of Sertoli cells, was almost absent in testes derived from injected frogs as visualized by Western blot analysis (Fig. 8C). Consequently, only few sperm cells were found in testis from 1 μM CHIR99021-injected animals (Fig. 8B).

The data indicate the potential role of CK in SC development via the retention of cell-to-cell contacts mediated by the β-catenin in the adhesion complex. The suppression of CK by CHIR99021 thus inhibited the maturation of SCs leading to a testicular failure.

DISCUSSION

Cytokeratin, like other members of IFs lacks plus and minus ends, thus they have not been thought to be involved in a basic network for intracellular transport. However, several

studies revealed the key role of IF and CK in vesicular trafficking. Depolymerization of IF resulted in the strong inhibition of vesicle transport towards the plasma membrane in astrocytes (Potokar et al., 2007). SNARE proteins are a large protein complex which is essential for docking and fusion of vesicles with cytoplasmic membrane. Delivery of Syntaxin 3, an important component of SNAREs to apical domain of plasma membrane was impaired in CK 8-deficient mice, leading to mistargeted trafficking of a number of apical proteins (Ameen et al., 2001). The mislocalization of GLUT 1 and -3 from apical compartment was identified in embryonic epithelia of CK-null mice (Vijayaraj et al., 2009). Moreover, CK is essential for the retention of proteins at their proper positions. Knockdown of CK caused the Core 2 *N*-acetylglucosaminyltransferase 2/M (C2GnT-M) leaving outside the Golgi complex followed by its ubiquitination and degradation (Petrosyan et al., 2015).

In epithelial cells, β-catenin binds to E-cadherin to form adherens junction in the plasma membrane which maintains cell integrity and is involved in several intracellular signaling pathways. β-catenin can also accumulate in the nucleus and act as a key mediator of Wnt signaling. Using GFP-tagged β-catenin and photobleaching assay displayed high turnover rate and β-catenin transport between nucleus and the plasma membrane in NIH 3T3 cells (Johnson et al., 2009). The balance of β-catenin activity between Wnt signaling and cell-to-cell contacts is regulated by E-cadherin (Fagotto et al., 1996; Heasman et al., 1994) via modulation of the vesicle-associated transport (Chairoungdua et al., 2010). Moreover, transfection of cultured cells with GFP-tagged CK mutant (GFP-CK18 R89C) led to the disruption of CK network. Subsequently, several junction-associated proteins, including β-catenin detached from cell membrane and colocalized with CK aggregates (Hanada et al., 2005). E-cadherin was also mistargeted in these CK mutant-transfected cells. This study shows the association between β-catenin retention at the plasma membrane and CK expression in immature SCs *in vitro* and *in vivo*. Both proteins co-expressed in juvenile testes and *in vitro* cultured immature SCs (Fig. 1&4). The transient disruption of CK network by acrylamide induced the breakdown of membrane-bound β-catenin in XtiSCs (Fig. 4) but not in the opposite manner. The loss of β-catenin-based adherens junctions by EGTA didn't result in the suppression of CK network (Fig. 4). Moreover, experimental observation of CK loss after the stimulation of primary kidney cells and bladder cancer organoids with CHIR99021 has been reported

previously (Francipane and Lagasse, 2015; Yoshida et al., 2018). Our results are in an agreement with these studies. CK was suppressed in XtiSCs (immature SCs) by CHIR99021 and in adult testes (Fig. 1&7). Simultaneously the absence of membrane β-catenin was also observed. CHIR9901 caused the failure of testicular development *in vivo* as the consequence of the dedifferentiation of immature Sertoli cells (Fig. 8). In spite of no direct evidence of CK and β-catenin binding, our experimental data suggests the capacity of CK in the regulation and the maintenance of β-catenin-based junctions in immature SCs.

Glycogen synthase kinase 3 (GSK3), a serine/threonine protein kinase, has over then 100 substrates, including β-catenin and Snail1 resulting in their degradation after phosphorylation. Regarding testicular development, the down-regulation of GSK3β has been reported in non-obstructive azoospermic men (Nazarian et al., 2014). The disruption of GSK3α had a negative effect on the sperm motility of KO mice (Bhattacharjee et al., 2015). In this study we showed that cultivation of immature Sertoli cells derived from the testes of juvenile *X. tropicalis* male with GSK3 inhibitor, CHIR99021, could down-regulate the CK expression and consequently disaggregate β-catenin-based junctions (Fig. 7). This drug was also responsible for the failure of testicular development (Fig. 8). It may indicate the role of GSK3 in the regulation of Sertoli cell maturation. Interestingly, CHIR99021 didn't significantly increase the accumulation of β-catenin in XtiSCs (Fig. 7B). Instead we observed the stability of another nuclear GSK3 substrate, Snail1 (data in publishing) which has been reported to suppress CK expression via the transcription factor Zeb1 and activated STAT3 signalling pathway (Kaufhold and Bonavida, 2014; Wu et al., 2012). XtiSC cultivation in the medium with Wnt inhibitor IWP2 led to the upregulation of the CK expression probably through the Snail1 inhibition by the reactivated GSK-3. As expected, we observed downregulation of the nuclear β-catenin, however, membrane β-catenin wasn´t affected due to the functional CK network (Fig. 7C).

The XtiSCs represents an unique cell model for the identification of key molecules in Sertoli cell maturation. This study revealed a potential role of CK in maintaining immature SC junctions via the retention of plasma membrane β-catenin, contributing to proper testicular development and spermatogenesis.

MATERIAL AND METHODS

All materials were purchased from Sigma-Aldrich, except where noted.

Ethical statement

This study was carried out in strict accordance with the Act No. 246/1992 Coll., on the protection of animals against cruelty. An official permission was issued to the Faculty of Science, Charles University in Prague by the Ministry of Education, Youth and Sports of the Czech Republic (No. MSMT-37376/2014-4, date of expiry 3. 3. 2019).

Histochemistry and immunohistochemistry staining

X. tropicalis testes were collected at indicated time points, fixed overnight in MEMFA (0.1 M MOPS, 2 mM EGTA, 1 mM MgSO4, and 3.7% formaldehyde) at 4°C, rinsed, dehydrated and embedded into paraffin for sectioning by microtome. 8 μm testicular sections were then rinsed in xylene and rehydrated in ascending ethanol gradient. Several sections were stained by H&E following the standard protocol.

For immunofluorescence staining, testes were collected and prepared for vibratome sectioning as described elsewhere (Tlapakova et al., 2016). If the antibody against E-cadherin was used, instead of MEMFA, testes were fixed in freshly prepared Dent's fixative (methanol:DMSO=4:1) overnight at 4°C. 30 μm agarose-embedded sections were permeabilized with 0.2% Triton X-100 for 1 hour and incubated with primary antibodies, including CK (2 μg/ml, 1h5, DSHB), β-Catenin (1:500, C2206), E-cadherin (1:150, 33 4000, Invitrogen) for 3 days at 4°C. Sections were rinsed thoroughly in PBS overnight at 4°C before immersing into secondary antibodies conjugated with Alexa Fluor 488 anti-mouse or Alexa Fluor 594 anti-rabbit (1:500, Thermo Fisher Scientific) for 4 hours at RT. Cell nuclei were visualized by DAPI.

XtiSC culture and fluorescent immunostaining

Xenopus tropicalis immature Sertoli cells (XtiSCs) were obtained and cultured as described (Tlapakova et al. 2016). Cells proliferated in growth medium overnight and then in the induction medium supplemented with acrylamide (10 mM) for 75 minutes, or EGTA (2 mM) for 15 minutes, or LiCl (10 - 40 mM) for 24 hours, or CHIR99021 (CHIR) (3 μM) or IWP2 (2 μM) for 3 days. The CHIR99021 and IWP2 stock solutions were prepared in DMSO according to the manufacturer's instructions. The concentration of DMSO in culture

medium was kept lower than 0.1%. The same concentration of DMSO was kept in the control culture medium.

For immunofluorescence staining, 20 µl drop of 10 000 cells were plated in the center of 12-mm diameter coverslip glasses coated with 0.01% poly-L Lysine or collagen type I (2.5 µg/cm^2). The growth media was added after cells attached on the glass surfaces and exchanged with indicated medium after 24 hours. Cells were collected at indicated time, fixed with 2% formaldehyde for 20 minutes at RT or in Dent's fixative overnight at 4°C (for antibody against Sox9), then permeabilized with 0.1% Triton X-100 for 15 minutes and incubated with primary antibodies, including Cytokeratin type II (2 µg/ml, mouse, 1h5, DSHB), β-catenin (1:500, rabbit, C2206), Sox9 (1:300, rabbit, HPA001758), focal adhesion kinase (FAK) (1:1000, rabbit, F2918), β-tubulin (1:200, mouse, T4026), integrin β1(2 µg/ml, mouse, 8C8, DSHB) followed by secondary antibodies conjugated with Alexa Fluor 488 anti-mouse or Alexa Fluor 594 anti-rabbit (1:500, Thermo Fisher Scientific). F-actin was visualized by Alexa Fluor 647-conjugated phalloidin (1:100, A22287, Thermo Fisher Scientific) for 1 hour at RT. DAPI was used for cell nuclei staining.

Karyotype analysis

0,02 µg/ml colchicine was added into the culture medium with XtiSCs at the exponential growth phase for 4.5 hours to arrest cells at metaphase. Cells were then harvested by trypsin, gently dispersed in amphibian hypotonic solution (0.038 M KCl, 1.9 mM HEPES, 0.038 mM EGTA, 1% Triton X-100, pH = 7.3), followed by the fixation in Carnoy's fixative (methanol: acetic acid ratio 3:1) for 15 mins. The fresh fixative was replaced for three times. The cell suspension was dropped onto clean microscopic slide to spread out metaphase chromosomes. Just before drying out slides were immersed into 50% acetic acid to remove the cell membranes and cytoplasm traces. Slides were then stained with Giemsa and observed under a bright field microscope. A minimum of 15 G-banded metaphase chromosomes were analyzed.

Soft agar colony formation assay

The soft agar colony formation assay allows *in vitro* evaluation of anchorage-independent growth, one of hallmarks of malignant cell transformation. XtiSCs at passage 5 and 12

were harvested by papain to get a single cell suspension, counted using cell counter (Thermo Fisher Scientific), and resuspended in growth medium. 24 000 harvested cells/well of 6-well plate were mixed with medium containing 0.3% agar, and overlaid on the semi-medium containing 0.6% agar in triplicates. The plates were replenished with fresh medium at an interval of two or three days. Colonies were visualized under a stereomicroscope after 3 weeks, and as a positive control, HeLa cells were cultured simultaneously. Colonies greater than 100 microns were considered as a transformed. Three independent assays were done.

Immunoblotting

Cells were cultured in indicated medium for 3 days before nuclear extraction by the amphibian hypotonic solution (0.038 M KCl, 1.9 mM HEPES, 0.038 mM EGTA, 1% Triton X-100, pH = 7.3) and vortexing. The homogenate was centrifuged to separate the nuclear fraction (pellet) from the supernatant (cytoplasmic fraction). For the subsequent immunoblotting analysis the nuclear pellets or whole cells or testes was lysed by RIPA lysis buffer containing cocktail of protease inhibitors (1:100, Promega) following the standard protocol as described (Towbin et al., 1992). They were then dissolved in sample buffer for SDS-PAGE and sonicated using a SONIFER 250 (Branson), followed by boiling for 5 minutes. 10 µg of total proteins were separated by SDS-PAGE in 10% polyacrylamide gels. After electrophoresis, proteins were transferred onto nitrocellulose membranes and incubated with □rst antibodies, including included β-tublin (1:2000, T8328), β-catenin (1:5000, C2206) and Sox9 (0.4 µg/ml, HPA001758). Bound antibodies were then visualized using horseradish peroxidase-conjugated secondary antibody followed by acridan-based chemiluminescent HRP substrate for detection using X-ray film (32132, Thermo Scientific).

In vitro fertilization and *in vivo* CHIR99021 treatment

X. tropicalis embryos were produced and cultivated by the standard *in vitro* fertilization procedure (Geach and Zimmerman, 2011). Young frogs, 4.5-5 months after metamorphosis were injected with 20 µl of CHIR99021 at 0.6, 1, 1.5 µM (in 7.5% DMSO and 92.5% saline) or vehicle (7.5% DMSO and 92.5% saline) into dorsal lymphatic sac

daily for 4 days and monitored 2.5 months after treatment as described on mouse and zebrafish (Chen et al., 2014; Pachenari et al., 2017). The testicles were isolated from experimental frogs at indicated time and sectioned for immunohistochemistry.

Statistics

All assays were repeated at least in three independent experiments.

Competing interests

The authors declare no competing financial interests.

Author contributions

Designing the experiments: T.M.X.N., T.T. and V.K. Experiments carrying out: T.M.X.N., M.V., T.T., M.K. and V.K. Writing the manuscript: T.M.X.N., M.V., T.T., M.K. and V.K.

Funding

The research was funded by the Charles University programs SVV 260435 and 20604315 PROGRES Q43 for T.M.X.N., M.V., T.T., M.K. V.K..

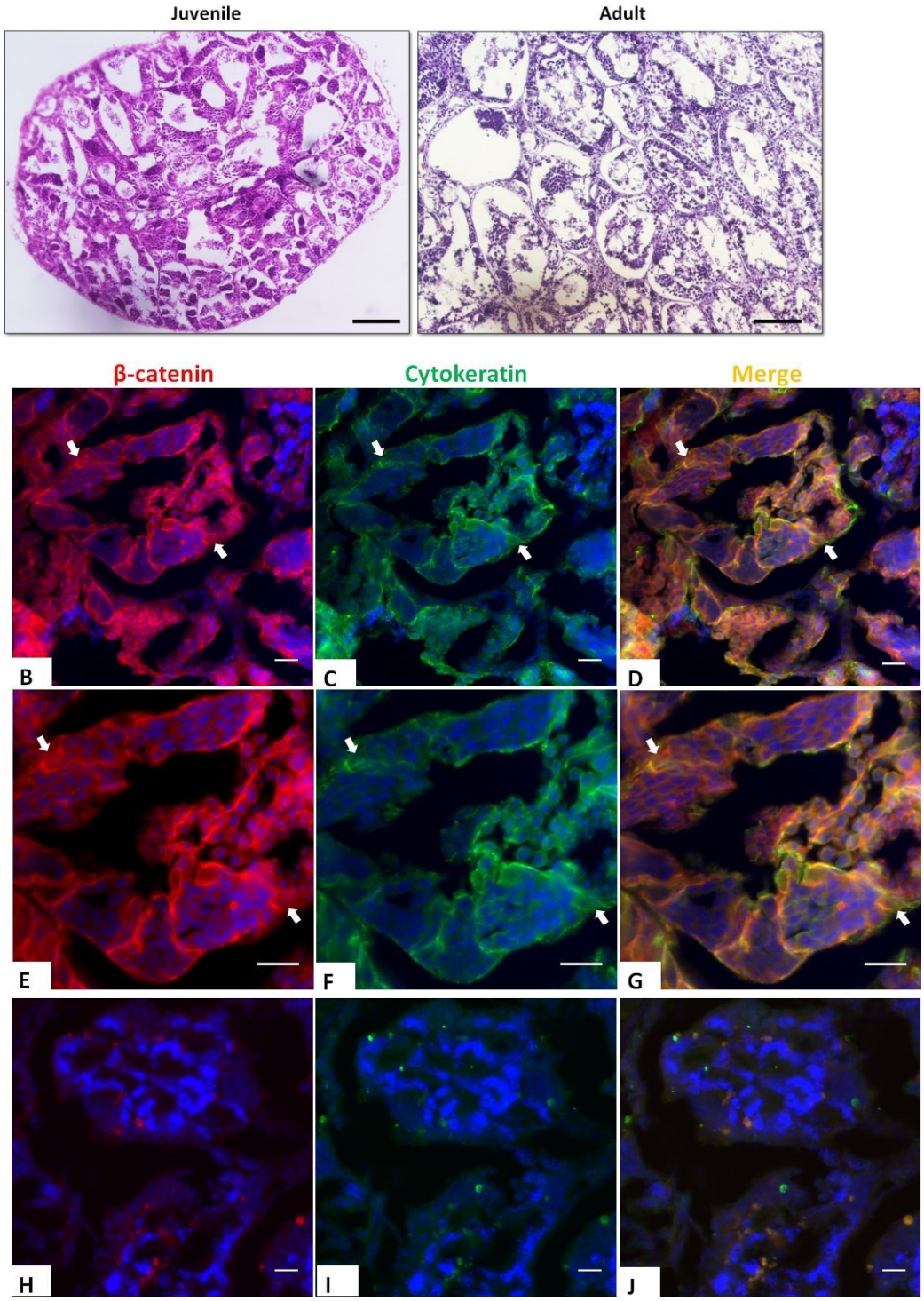

Figure 1. Co-expression of CK and β-catenin during testicular development. A. H&E staining of 5-month and 3-year old *X. tropicalis* testes. Scale bar: 100 μm. Double staining on testicular sections of juvenile (B-G) and adult frogs (H-J) with CK (mouse, green) and β-catenin (rabbit, red) antibodies; (E-G) show higher magnification of young testes' staining. Nuclei were stained with DAPI (blue). Scale bar: 20 μm. Both proteins are presented in the immature testes, but not in the adulthood. In young testes **(B-G)**, β-catenin is expressed mainly in plasma membrane and cytoplasm of Sertoli cells, but weaker staining is also observed in nuclei of some Sertoli cells (see arrow). Arrows represent nuclear accumulation of β-catenin in CK-positive cells.

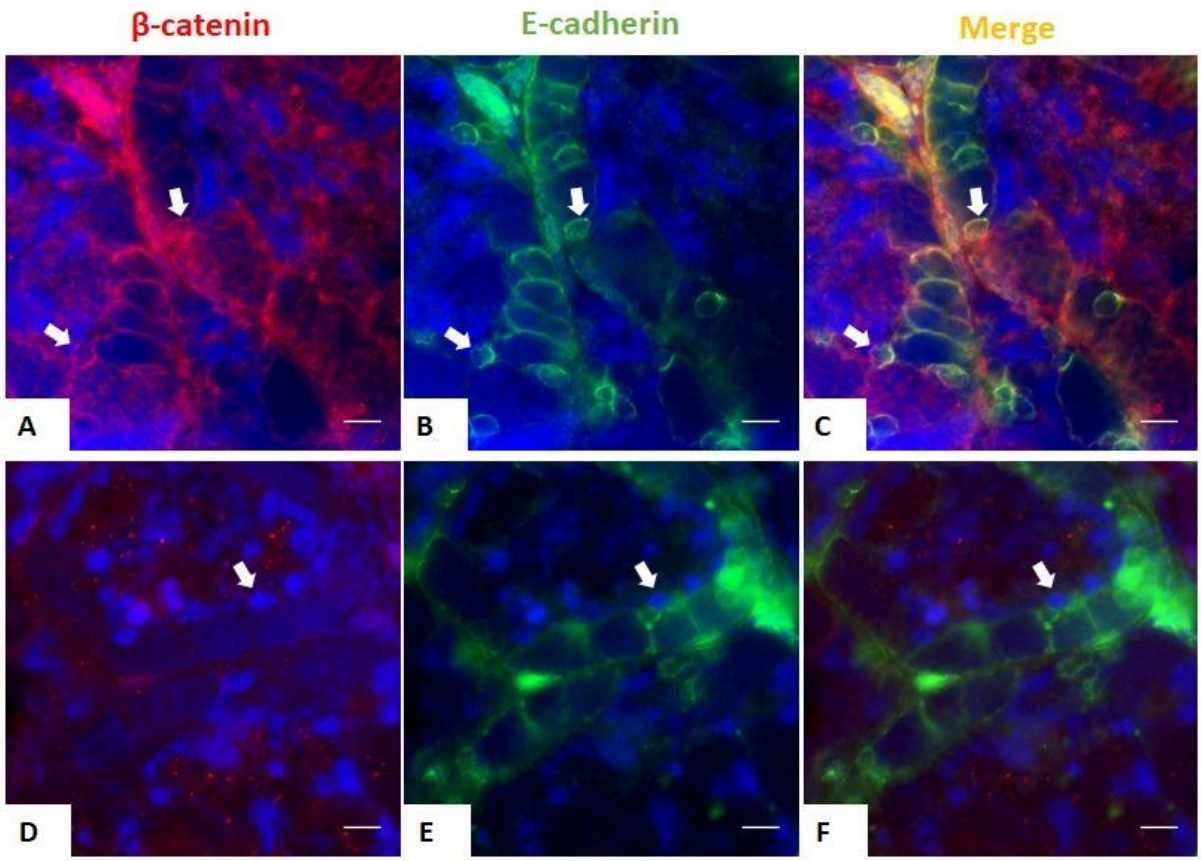

Figure 2. Expression of E-cadherin and β-catenin in Sertoli cells during testicular development. Double staining on testicular sections of juvenile (A-C) and adult frogs (D-F) with E-cadherin (mouse, green) and β-catenin (rabbit, red) antibodies. Nuclei were stained with DAPI (blue). Scale bar: 20 μm. Both proteins surrounded the Sertoli cells of juvenile testes, but only E-cadherin keep to express in the adulthood. Arrows represent Sertoli cells.

A.

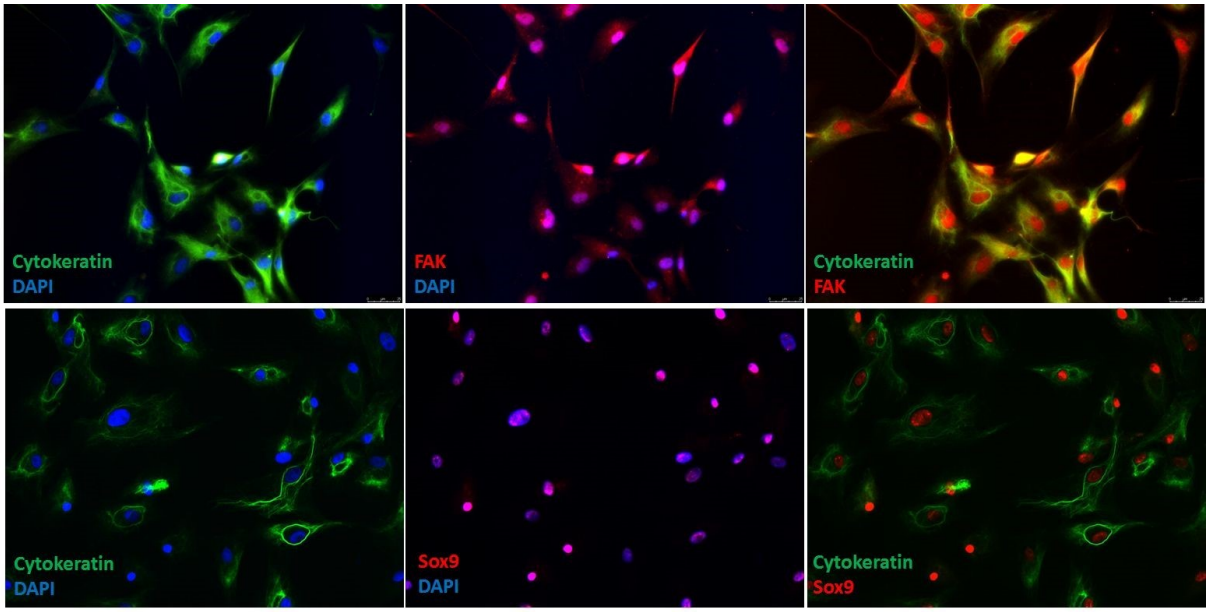

B.

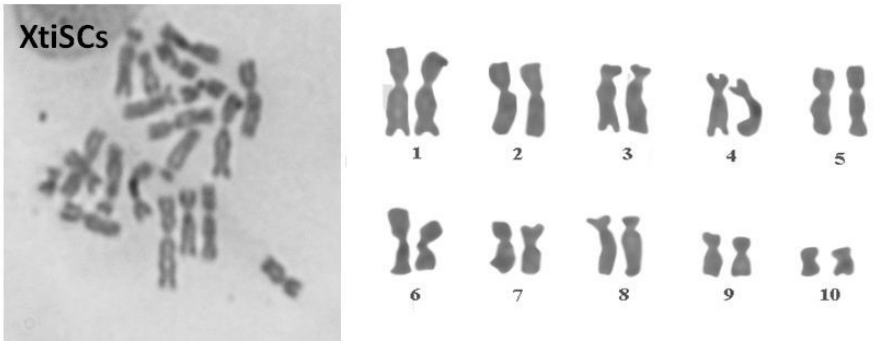

C.

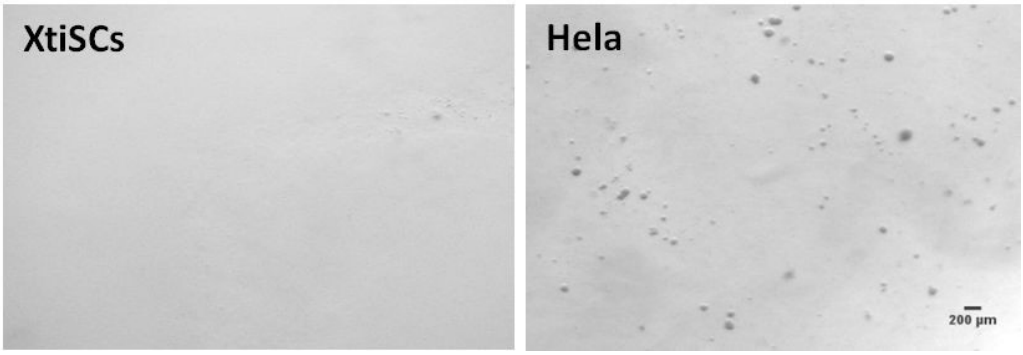

Figure 3. Immunofluorescent, cytogenetic and transformation characteristics of isolated XtiSCs. (A) XtiSCs expressed Sertoli cells' proteins as focal adhesion kinase (FAK, red), Sox9 (red) and CK (green) as a immature Sertoli cell marker. Nuclei were stained with DAPI. Chromosome analysis (B) and soft agar assay (C) showed XtiSCs as a non-transformed cells.

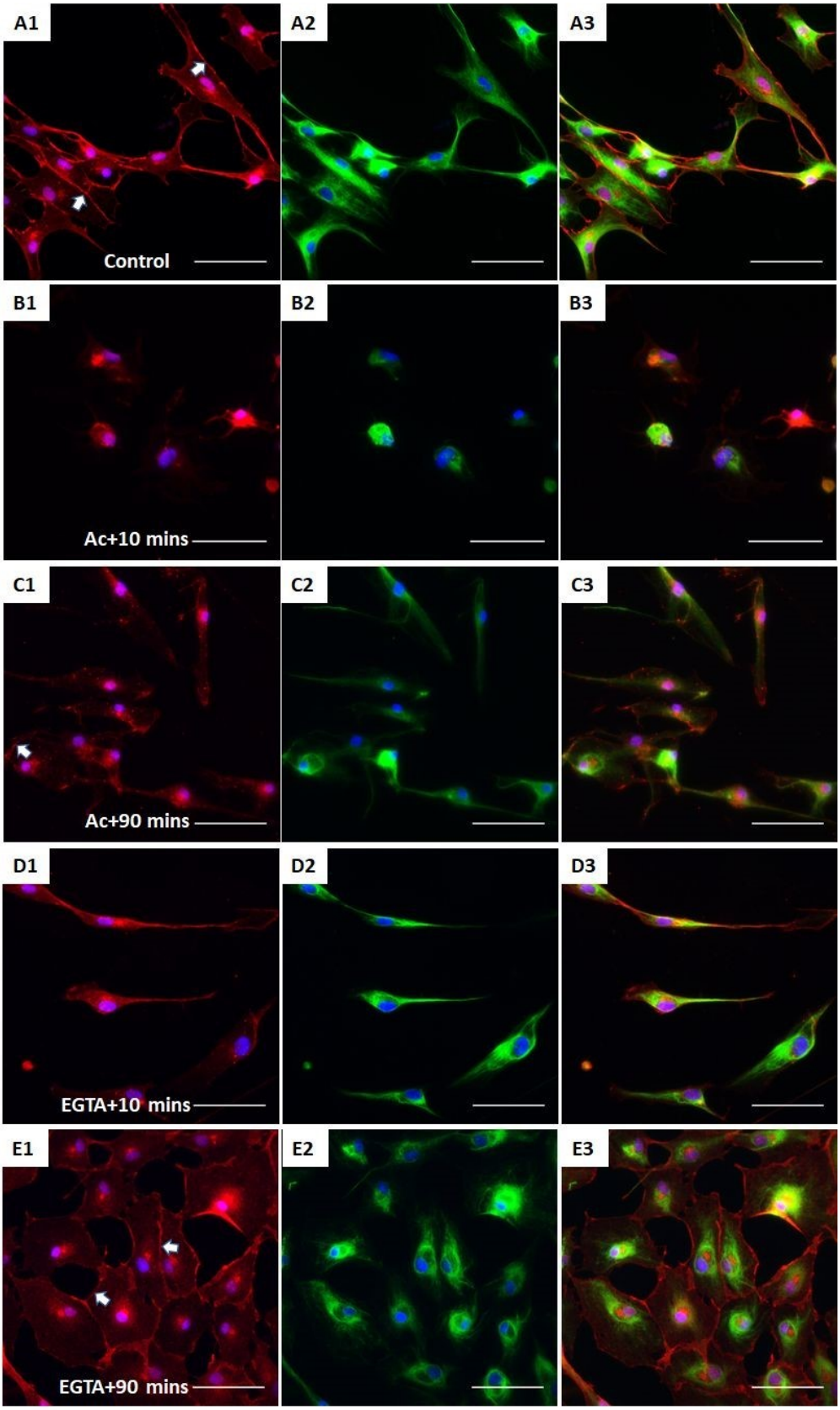

Figure 4. The effect of CK network on the β-catenin-based cell junctions. XtiSCs were treated with vehicles (Control, A) or 10 mM acrylamide (Ac, B&C) or 2 mM EGTA (EGTA, D&E). After treatment, cells were washed and exchange to the fresh medium, and then collected at indicated time points, 10 minutes (B&D) or 90 minutes (C&E) for immunofluorescent staining with antibodies against β-catenin (red, A1-E1), CK (green, A2-

E2), and merge (A3-E3). Arrows show membrane β-catenin. Nuclei were stained with DAPI (blue). Scale bar: 50 μm.

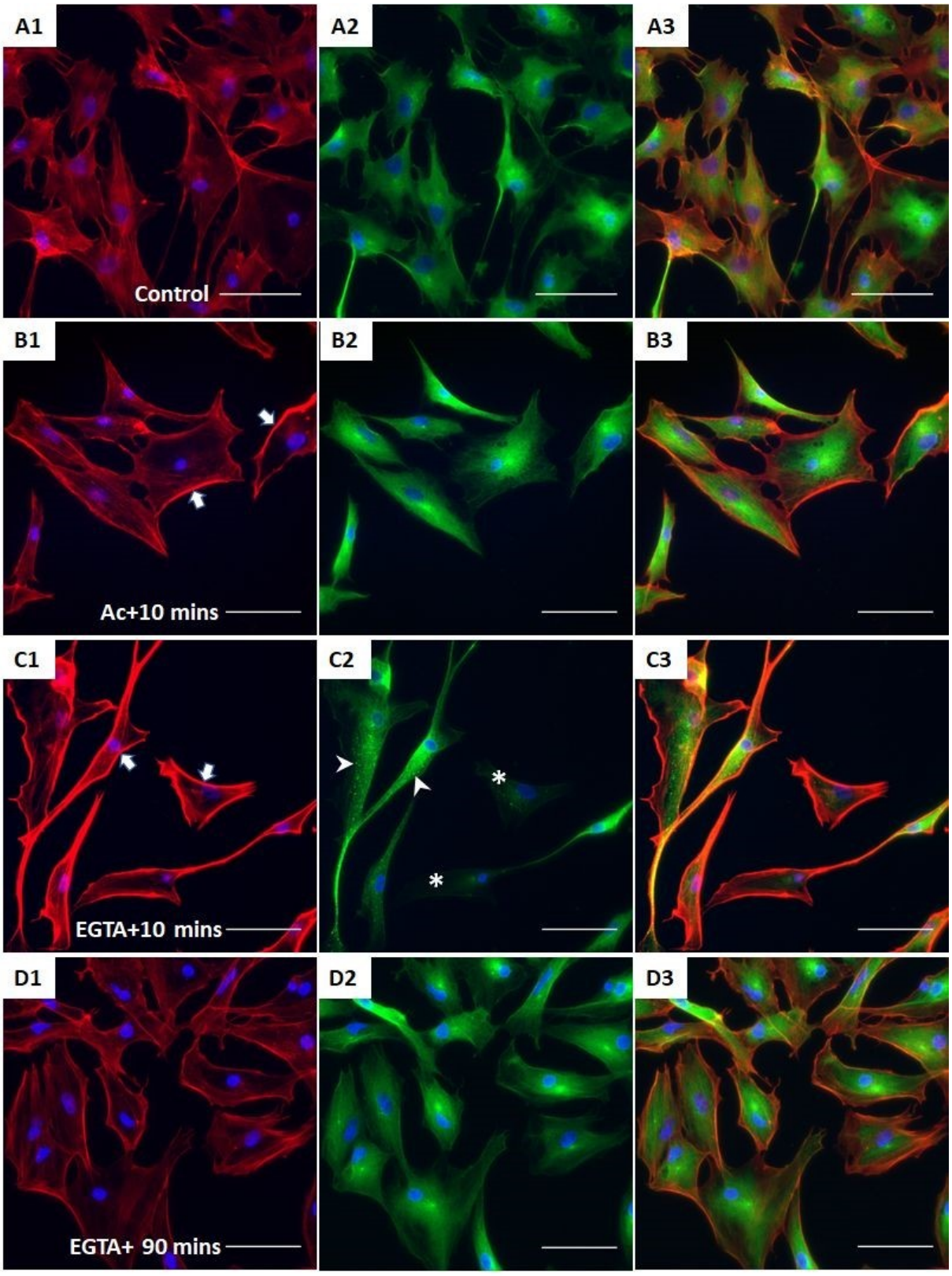

Figure 5. The effect of acrylamide and EGTA on F-actin and tubulin. After treatment, XtiSCs were collected at indicated time points for immunofluorescent staining with antibodies against F-actin (red, A1-D1), β-tubulin (green, A2-D2), and merge (A3-D3).

Arrows show thick membrane F-actin in figure C1 and D1. The aggregates of β-tubulin are marked by arrowheads and asterisks indicate the cells without β-tubulin in figure C2. Nuclei were stained with DAPI (blue). Scale bar: 50 μm.

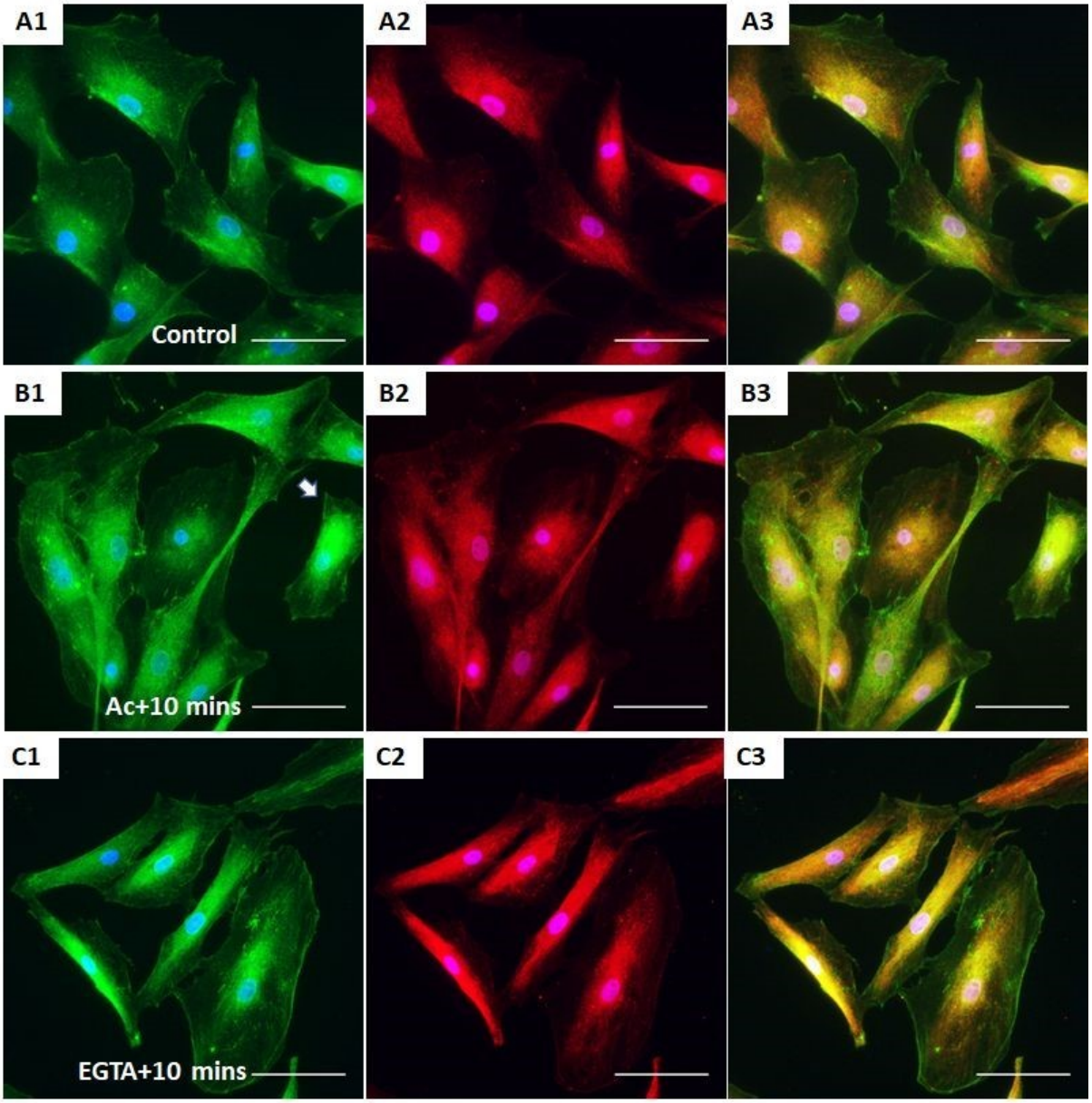

Figure 6. The effect of acrylamide and EGTA on cell adhesions. Immunofluorescent images of XtiSCs 10 minutes after washing out the acrylamide (B) or EGTA (C) staining with antibodies against integrin β1 (CD29, green, A1-C1), Focal adhesion kinase (Fak, red, A2-C2), and merge (A3-C3). Nuclei were stained with DAPI (blue). Scale bar: 50 μm.

Figure 7

A.

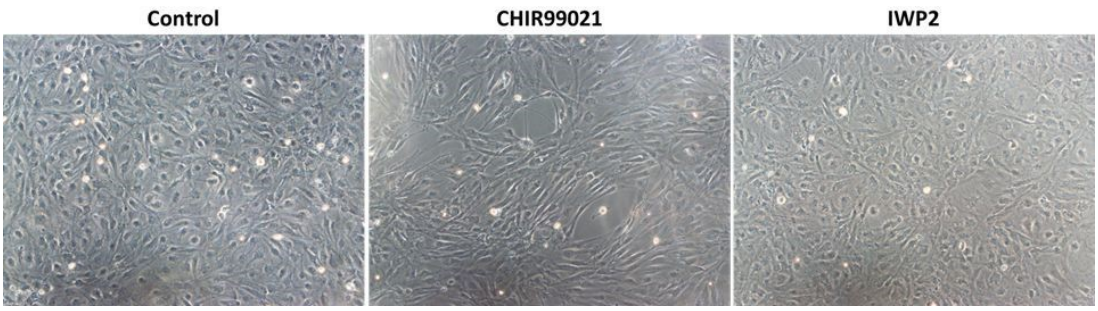

B.

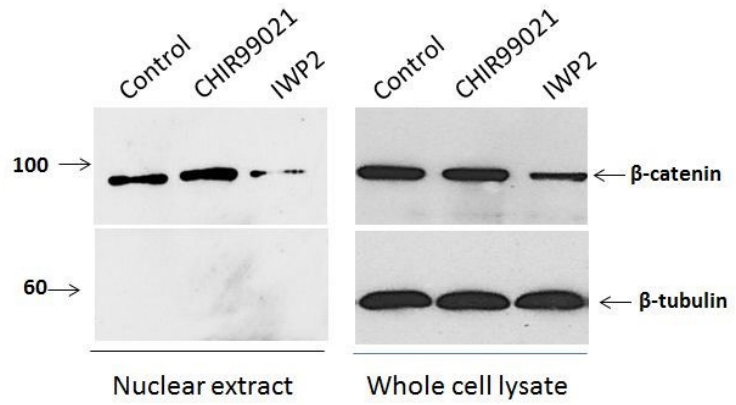

C.

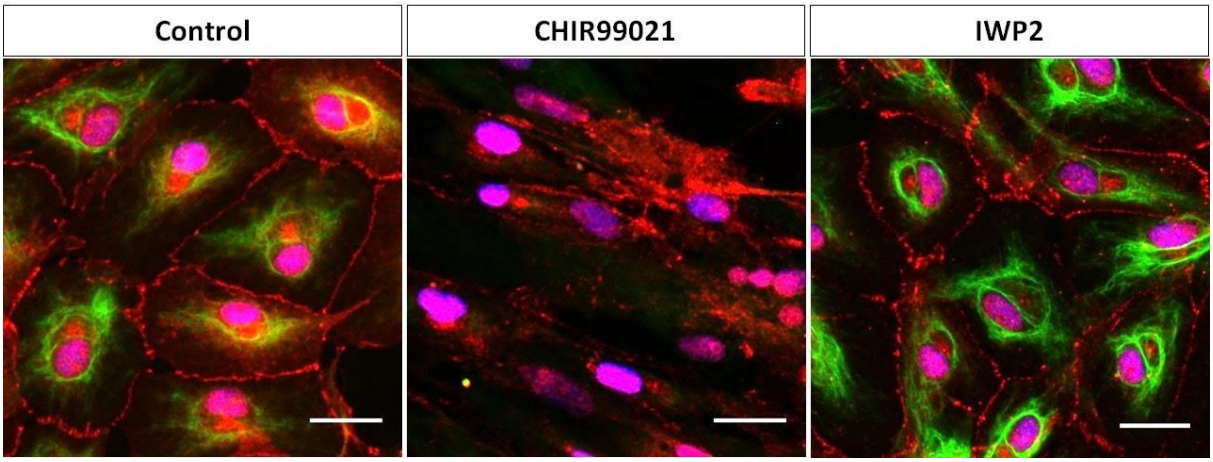

.

Figure 7. CK regulates plasma membrane β-catenin. A. Phase-contrast images of XtiSC after treatment with CHIR99021 and IWP2 for 3 days showed the morphological changes in CHIR99021-treated cells. XtiSCs were collected for blotting (B) or immunofluorescent analysis (C). Nuclear β-catenin was downregulated in media supplemented with IWP2. Immunostaining of CHIR99021-treated XtiSCs against CK (green) and β-catenin (red) revealed the disruption of cytokeratin network and cell-to-cell contact altogether with the disappearance of membrane β-catenin. Nuclei were stained with DAPI (blue). Scale bar: 20 μm.

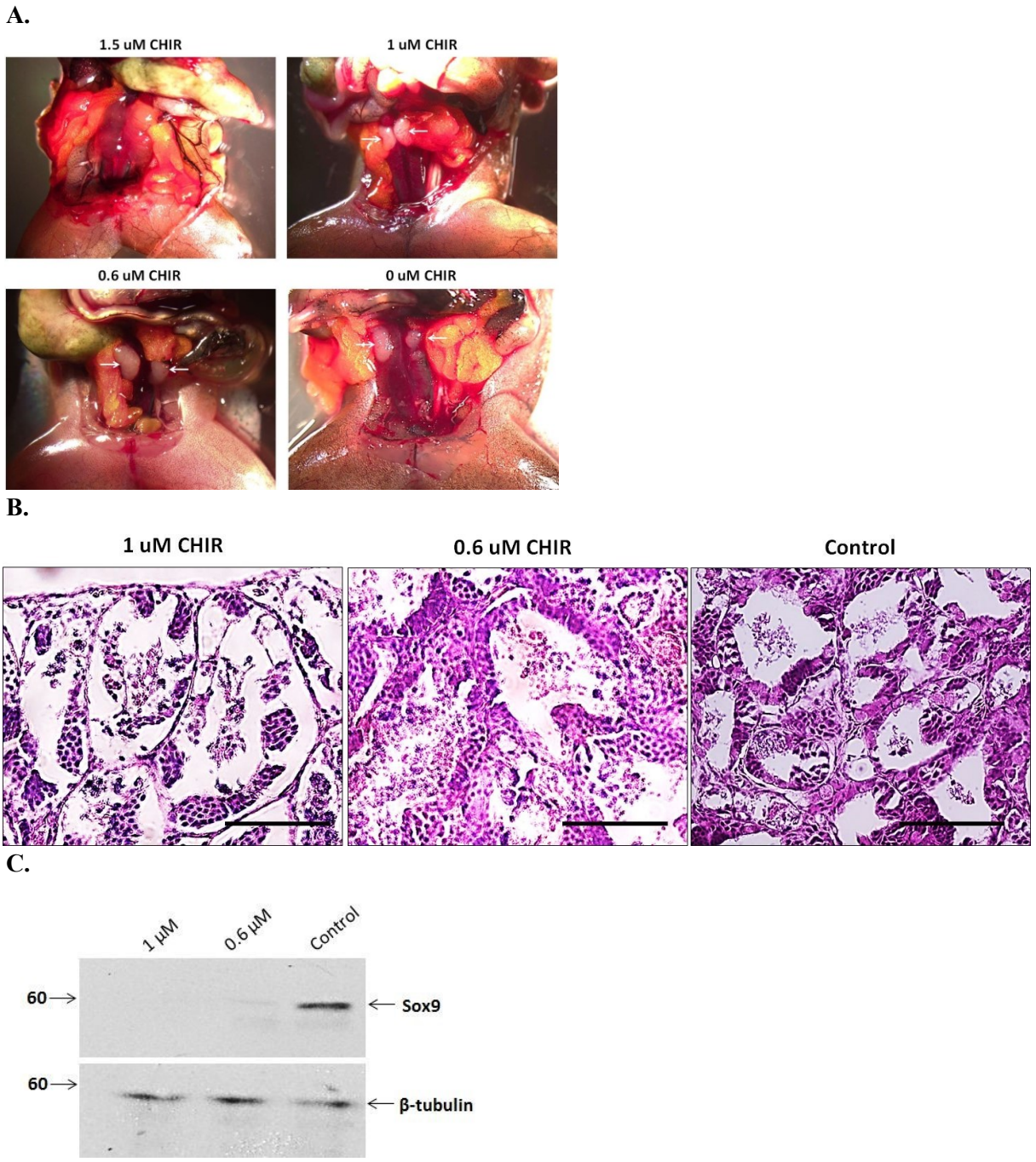

Figure 8. *In vivo* treatment of CHIR99021 led to the failure in testes development. (A) 2.5 months after CHIR99021 injected into dorsal sac, no testes were observed in 1.5 μM injected frogs. Arrows indicate testes. (B) H&E staining of testicular sections from 1, 0.6, 0 μM CHIR-injected *X.tropicalis* frogs. The most serious damage with the detachment of germinal epithelium from tubules was observed in 1 μM group. Testes with 0.6 μM CHIR had unorganized seminiferous tubules. Scale bar: 100 μm. (C) Immunoblotting of testicular extract from 1, 0.6, 0 μM CHIR-injected *X.tropicalis* with antibody against Sox9 (Sertoli cell marker). β-tubulin is as a loading control.

REFERENCES

Ameen, N. A., Figueroa, Y. and Salas, P. J. (2001). Anomalous apical plasma membrane phenotype in CK8-deficient mice indicates a novel role for intermediate filaments in the polarization of simple epithelia. *J. Cell Sci.* **114**, 563–575.

Appert, A., Fridmacher, V., Locquet, O. and Magre, S. (1998). Patterns of keratins 8, 18 and 19 during gonadal differentiation in the mouse: sex- and time-dependent expression of keratin 19. *Differentiation* **63**, 273.

Barrionuevo, F., Burgos, M. and Jiménez, R. (2011). Origin and function of embryoni c Sertoli cells. *Biomol. Concepts* **2**, 537–547.

Bhattacharjee, R., Goswami, S., Dudiki, T., Popkie, A. P., Phiel, C. J., Kline, D. and Vijayaraghavan, S. (2015). Targeted disruption of glycogen synthase kinase 3A (GSK3A) in mice affects sperm motility resulting in male infertility. *Biol. Reprod.* **92**, 65.

Chairoungdua, A., Smith, D. L., Pochard, P., Hull, M. and Caplan, M. J. (2010). Exosome release of β-catenin: a novel mechanism that antagonizes Wnt signaling. *J. Cell Biol.* **190**, 1079–1091.

Chen, E. Y., DeRan, M. T., Ignatius, M. S., Grandinetti, K. B., Clagg, R., McCarthy, K. M., Lobbardi, R. M., Brockmann, J., Keller, C., Wu, X., et al. (2014). Glycogen synthase kinase 3 inhibitors induce the canonical WNT/β-catenin pathway to suppress growth and self-renewal in embryonal rhabdomyosarcoma. *P roc. Natl. Acad. Sci. U. S. A.* **111**, 5349–5354.

Daugherty, R. L. and Gottardi, C. J. (2007). Phospho-regulation of β-Catenin Adhesion and Signaling Functions. *Physiology* **22**, 303–309.

de Winter, J. P. (1993). Activin is produced by rat Sertoli cells in vitro and can act as an autocrine regulator of Sertoli cell function. *Endocrinology* **132**, 975–982.

Duncan, A. R., Forcina, J. J., Tsang, P. C. W. and Townson, D. H. (2009). Disruption of Cytokeratin 18-Containing Intermediate Filaments in Bovine Luteal Cells: Effects of Acrylamide on Progesterone Secretion, Fas Expression, and FasL-Induced Apoptosis. *Biol. Reprod.* **81**, 558–558.

Engl, W., Arasi, B., Yap, L. L., Thiery, J. P. and Viasnoff, V. (2014). Actin dynamics modulate mechanosensitive immobilization of E-cadherin at adherens junctions. *Nat. Cell Biol.* **16**, 587–594.

Fagotto, F., Funayama, N., Gluck, U. and Gumbiner, B. M. (1996). Binding to cadherins antagonizes the signaling activity of beta-catenin during axis formation in Xenopus. *J. Cell Biol.* **132**, 1105–1114.

Francipane, M. G. and Lagasse, E. (2015). The lymph node as a new site for kidney organogenesis. *Stem Cells Transl. Med.* **4**, 295–307.

García-Reyes, B., Witt, L., Jansen, B., Karasu, E., Gehring, T., Leban, J., Henne-Bruns, D., Pichlo, C., Brunstein, E., Baumann, U., et al. (2018). Discovery of Inhibitor of Wnt Production 2 (IWP-2) and Related Compounds As Selective ATP-Competitive Inhibitors of Casein Kinase 1 (CK1) δ/ε. *J. Med. Chem.* **61**, 4087–4102.

Geach, T. J. and Zimmerman, L. B. (2011). Developmental genetics in Xenopus tropicalis. *Methods Mol. Biol.* **770**, 77–117.

Hanada, S., Harada, M., Kumemura, H., Omary, M. B., Kawaguchi, T., Taniguchi, E., Koga, H., Yoshida, T., Maeyama, M., Baba, S., et al. (2005). Keratin-containing inclusions affect cell morphology and distribution of cytosolic cellular components. *E xp. Cell Res.* **304**, 471–482.

Handelsman, D. J., Spaliviero, J. A. and Phippard, A. F. (1990). Highly Vectorial Secretion of Inhibin by Primate Sertoli Cellsin Vitro*. *J. Clin. Endocrinol. Metab.* **71**, 1235–1238.

Hartsock, A. and Nelson, W. J. (2008). Adherens and tight junctions: structure, function and connections to the actin cytoskeleton. *Biochim. Biophys. Acta* **1778**, 660–669.

Heasman, J., Crawford, A., Goldstone, K., Garner-Hamrick, P., Gumbiner, B., McCrea, P., Kintner, C., Noro, C. Y. and Wylie, C. (1994). Overexpression of cadherins and underexpression of beta-catenin inhibit dorsal mesoderm induction in early Xenopus embryos. *Cell* **79**, 791–803.

Huber, A. H. and Weis, W. I. (2001). The structure of the beta-catenin/E-cadherin complex and the molecular basis of diverse ligand recognition by beta-catenin. *Cell* **105**, 391–402.

Johnson, M., Sharma, M., Jamieson, C., Henderson, J. M., Mok, M. T. S., Bendall, L. and Henderson, B. R. (2009). Regulation of β-catenin trafficking to the membrane in living cells. *Cell. Signal.* **21**, 339–348.

Kaufhold, S. and Bonavida, B. (2014). Central role of Snail1 in the regulation of EMT and resistance in cancer: a target for therapeutic intervention. *J. Exp. Clin. Cancer Res.* **33**,.

Kramer, T., Schmidt, B. and Lo Monte, F. (2012). Small-Molecule Inhibitors of GSK-3: Structural Insights and Their Application to Alzheimer's Disease Models. *Int. J Alzheimers. Dis.* **2012**, 1–32.

Lee, C. H. and Taketo, T. (1994). Normal onset, but prolonged expression, of Sry gene in the B6.YDOM sex-reversed mouse gonad. *Dev. Biol.* **165**, 442–452.

Mital, P., Kaur, G. and Dufour, J. M. (2010). Immunoprotective sertoli cells: making allogeneic and xenogeneic transplantation feasible. *Reproduction* **139**, 495–504.

Myers, M., Ebling, F. J. P., Nwagwu, M., Boulton, R., Wadhwa, K., Stewart, J. and Kerr, J. B. (2005). Atypical development of Sertoli cells and impairment of spermatogenesis in the hypogonadal (hpg) mouse. *J. Anat.* **207**, 797–811.

Nazarian, H., Ghaffari Novin, M., Jalili, M. R., Mirfakhraie, R., Heidari, M. H., Hosseini, S. J., Norouzian, M. and Ehsani, N. (2014). Expression of Glycogen synthase kinase 3-β (GSK3-β) gene in azoospermic men. *I ran. J. Reprod. Med.* **1 2**, 313–320.

Nistal, M., Paniagua, R., Abaurrea, M. A. and Santamaría, L. (1982). Hyperplasia and the immature appearance of Sertoli cells in primary testicular disorders. *Hum. Pathol.* **13**, 3–12.

Pachenari, N., Kiani, S. and Javan, M. (2017). Inhibition of glycogen synthase kinase 3 increased subventricular zone stem cells proliferation. *Biomed. Pharmacother.* **93**, 1074–1082.

Paranko, J., Kallajoki, M., Pelliniemi, L. J., Lehto, V. P. and Virtanen, I. (1986). Transient coexpression of cytokeratin and vimentin in differentiating rat Sertoli cells. *Dev. Biol.* **117**, 35–44.

Petrosyan, A., Ali, M. F. and Cheng, P.-W. (2015). Keratin 1 Plays a Critical Role in Golgi Localization of Core 2N-Acetylglucosaminyltransferase M via Interaction with Its Cytoplasmic Tail. *J. Biol. Chem.* **290**, 6256–6269.

Potokar, M., Kreft, M., Li, L., Daniel Andersson, J., Pangrsic, T., Chowdhury, H. H., Pekny, M. and Zorec, R. (2007). Cytoskeleton and vesicle mobility in astrocytes . *Traffic* **8**, 12–20.

Rogatsch, H., Hittmair, A., Mikuz, G., Feichtinger, H. and Jezek, D. (1996). Expression of vimentin, cytokeratin, and desmin in Sertoli cells of human fetal, cryptorchid, and tumour-adjacent testicular tissue. *Virchows Arch.* **427**,.

Setchell, B. P. (2009). Blood-Testis Barrier, Junctional and Transport Proteins and Spermatogenesis. In *Advances in Experimental Medicine and Biology*, pp. 212–233.

Shabana, A. H., Oboeuf, M. and Forest, N. (1994). Cytoplasmic desmosomes and intermediate filament disturbance following acrylamide treatment in cultured rat keratinocytes. *Tissue Cell* **26**, 43–55.

Sharpe, R. M., McKinnell, C., Kivlin, C. and Fisher, J. S. (2003). Proliferation and functional maturation of Sertoli cells, and their relevance to disorders of testis function in adulthood. *Reproduction* **125**, 769–784.

Sonavane, P. R., Wang, C., Dzamba, B., Weber, G. F., Periasamy, A. and DeSimone, D. W. (2017). Mechanical and signaling roles for keratin intermediate filaments in the assembly and morphogenesis of mesendoderm tissue at gastrulation. *Developmen t* **1 44**, 4363–4376.

Steinberger, A. and Steinberger, E. (1971). Replication pattern of Sertoli cells in maturing rat testis in vivo and in organ culture. *Biol. Reprod.* **4**, 84–87.

Stosiek, P., Kasper, M. and Karsten, U. (1990). Expression of cytokeratins 8 and 18 in human Sertoli cells of immature and atrophic seminiferous tubules. *Differentiation* **43**, 66–70.

Tlapakova, T., Nguyen, T. M. X., Vegrichtova, M., Sidova, M., Strnadova, K., Blahova, M. and Krylov, V. (2016). Identification and characterization of Xenopus tropicalis common progenitors of Sertoli and peritubular myoid cell lineages. *Biol. Open* **5**, 1275–1282.

Towbin, H., Staehelin, T. and Gordon, J. (1992). Electrophoretic transfer of proteins from polyacrylamide gels to nitrocellulose sheets: procedure and some applications. 1979. *Biotechnology* **24**, 145–149.

Vijayaraj, P., Kröger, C., Reuter, U., Windoffer, R., Leube, R. E. and Magin, T. M. (2009). Keratins regulate protein biosynthesis through localization of GLUT1 and -3 upstream of AMP kinase and Raptor. *J. Cell Biol.* **187**, 175–184.

Wahab-Wahlgren, A., Holst, M., Ayele, D., Sultana, T., Parvinen, M., Gustafsson, K., Granholm, T. and Söder, O. (2000). Constitutive production of interleukin-1alpha mRNA and protein in the developing rat testis. *Int. J. Androl.* **23**, 360–365.

Wen, Q., Tang, E. I., Xiao, X., Gao, Y., Chu, D. S., Mruk, D. D., Silvestrini, B. and Cheng, C. Y. (2016). Transport of germ cells across the seminiferous epithelium during spermatogenesis-the involvement of both actin- and microtubule-based cytoskeletons. *Tissue Barriers* **4**, e1265042.

Wolski, K. M., Perrault, C., Tran-Son-Tay, R. and Cameron, D. F. (2005). Strength measurement of the Sertoli-spermatid junctional complex. *J. Androl.* **26**, 354–359.

Wu, K., Fan, J., Zhang, L., Ning, Z., Zeng, J., Zhou, J., Li, L., Chen, Y., Zhang, T., Wang, X., et al. (2012). PI3K/Akt to GSK3β/β-catenin signaling cascade coordinates cell colonization for bladder cancer bone metastasis through regulating ZEB1 transcription. *Cell. Signal.* **24**, 2273–2282.

Wu, S. K., Gomez, G. A., Michael, M., Verma, S., Cox, H. L., Lefevre, J. G., Parton, R. G., Hamilton, N. A., Neufeld, Z. and Yap, A. S. (2014). Cortical F-actin stabilization generates apical–lateral patterns of junctional contractility that integrate cells into epithelia. *Nat. Cell Biol.* **16**, 167–178.

Yoshida, T., Sopko, N. A., Kates, M., Liu, X., Joice, G., McConkey, D. J. and Bivalacqua, T. J. (2018). Three-dimensional organoid culture reveals involvement of Wnt/β-catenin pathway in proliferation of bladder cancer cells. *Oncotarget* **9**, 11060–11070.